

**Physiological and phytochemical aspects of ant-plant
mutualism**

Dissertation

in Partial Fulfilment of the Requirements for the Degree of

„doctor rerum naturalium“ (Dr. rer. nat.)

**Submitted to the Council of the Faculty of Biological Sciences
of Friedrich Schiller University Jena**

by Andrea Teresa Müller (M. Sc.)

born on 02.10.1992 in Kulmbach

1. Reviewer: Prof. Dr. Ralf Oelmüller
2. Reviewer: PD Dr. Axel Mithöfer
3. Reviewer: Assist. Prof. Dr. Marcia González Teuber

Hace más una hormiga andando que un gigante parado.

Table of contents

| | | |
|----------|--|------------|
| 1 | Introduction | 1 |
| 1.1 | <i>Plant defense</i> | 1 |
| 1.1.1 | Plant specialized metabolites..... | 2 |
| 1.1.1.1 | Plant volatile organic compounds | 2 |
| 1.1.1.2 | Aldoximes and aldoxime-derived compounds..... | 5 |
| 1.1.1.3 | Plant (poly-)phenolics..... | 7 |
| 1.1.2 | Regulation of plant defense | 10 |
| 1.2 | <i>Ant-plant mutualism</i> | 12 |
| 1.2.1 | Defense in ant-plants | 14 |
| 1.2.2 | The myrmecophytic plant <i>Tococa</i> | 16 |
| 1.3 | <i>Aims of this study</i> | 18 |
| 2 | Manuscripts | 19 |
| 2.1 | <i>Overview</i> | 19 |
| 2.2 | <i>Manuscript I</i> | 21 |
| 2.3 | <i>Manuscript II</i> | 47 |
| 2.4 | <i>Manuscript III</i> | 82 |
| 3 | Discussion | 92 |
| 3.1 | <i>No rose without thorns, no ant-plant without chemical defenses</i> | 92 |
| 3.2 | <i>Ant-colonization affects general and specialized metabolism of ant-plants</i> | 95 |
| 3.3 | <i>Aldoximes go beyond the classical definition of specialized metabolites</i> | 99 |
| 3.4 | <i>The development of new analytical tools like carbon nanotubes for polyphenol detection can facilitate future work and research on non-model organisms</i> | 103 |
| 3.5 | <i>Conclusion and future perspectives</i> | 107 |
| 4 | Summary | 110 |
| 5 | Zusammenfassung | 113 |
| 6 | References | 117 |

| | | |
|-----------|---|------------|
| 7 | Acknowledgements | 135 |
| 8 | Ehrenwörtliche Erklärung | 138 |
| 9 | Curriculum Vitae | 139 |
| 10 | Supplemental information..... | 143 |
| | <i>10.1 Contribution to figures in manuscripts.....</i> | <i>143</i> |
| | 10.1.1 Manuscript No. I | 143 |
| | 10.1.2 Manuscript No. II | 145 |
| | 10.1.3 Manuscript No. III | 148 |
| | <i>10.2 Supplemental data of the manuscripts.....</i> | <i>150</i> |
| | 10.2.1 Supplemental Data – Manuscript I | 150 |
| | 10.2.2 Supplemental Data – Manuscript II | 162 |
| | 10.2.3 Supplemental Data – Manuscript III | 198 |
| | <i>10.3 Supplemental data of the thesis.....</i> | <i>219</i> |

1 Introduction

1.1 Plant defense

As sessile organisms, plants cannot run away from their natural enemies. Instead, the constant struggle for survival against heterotrophic organisms has led to the evolution of a plethora of sophisticated defense mechanisms (Gatehouse, 2002). These strategies include the development of morphological traits like spines, thorns and leaf toughness that deter herbivores from feeding and therefore increase the chances of survival (Hanley et al., 2007). However, an even greater diversity of plant defense strategies is achieved through highly complex plant chemistry, with over 200.000 **specialized metabolites** produced by plants (Pichersky and Lewinsohn, 2011).

Based on their occurrence, plant defenses can be divided into different categories. On one hand, there are so-called *constitutive* defenses, i.e., defensive traits that are always present, such as capsaicin in chili peppers. On the other hand there are *inducible* defenses, which only accumulate in plants under specific circumstances, that is, when a particular aggressor attacks (Mithöfer and Boland, 2012). For instance, infection of rice (*Oryza sativa*) with rice blast fungus (*Pyricularia oryzae*) leads to the production of the antifungal compounds oryzalexin A, B and C (Akatsuka et al., 1985). Similarly, Delphia et al. (2007) found that tobacco plants (*Nicotiana tabacum*) only emit detectable levels of volatiles upon herbivore damage, and that the profile differs depending on whether the tobacco budworm (*Heliothis virescens*) or thrips (*Frankliniella occidentalis*) feed on the plant. These specific responses require recognition of the wounding and the biotic stressor, signal transmission and activation of an appropriate reaction by the plant (Kessler and Baldwin, 2002; Maffei et al., 2007). Phytohormones such as jasmonates play a central role in the **regulation of these defenses** (Erb et al., 2012).

Regarding the mode of action of anti-herbivore defenses, two principle categories can be distinguished: direct and indirect defenses (Kessler and Baldwin, 2002). As implied by the name, direct defenses have a direct effect on the herbivore. These can be antinutritive enzymes like threonine deaminase or arginase, that degrade essential amino acids in the insect gut (Chen et al., 2005) and antinutritive factors like serine protease inhibitors irreversibly inhibiting serine proteases such as trypsin in many lepidopteran pests like *Heliothis zea* and *Spodoptera exigua* (Broadway and Duffey, 1986; Ryan, 1990). Compounds that act as deterrents, like glucosinolates from watercress (*Nasturtium officinale*) for snails and caddisflies (Sachdev-Gupta et al., 1993), and substances that have toxic effects, such as nicotine on *Spodoptera exigua*

(Kumar et al., 2014), are also considered direct defenses. On the other hand, there are compounds that promote attraction of parasitoids or enhanced foraging behavior of natural enemies of the herbivore (Kessler and Heil, 2011). These traits involving a ***third trophic level*** are indirect defenses.

1.1.1 Plant specialized metabolites

Plant specialized metabolites, formerly also called secondary metabolites, are low molecular weight compounds that are not involved in basic metabolism, reproduction or development, but instead play a role in the interaction of plants with their environment (Kroymann, 2011). They can be categorized in three main classes based on their biosynthetic origin: phenolics, nitrogen-containing compounds and terpenoids (Harborne, 1991). In the following paragraphs, the specialized metabolites relevant for this thesis, their biosynthesis, functions, and detection methods, will be described in more detail.

1.1.1.1 Plant volatile organic compounds

Plants emit a wide range of volatile organic compounds (VOCs), which – depending on the context – can fulfill multiple important functions, including defensive ones. Whereas many floral and fruit VOCs aim to attract pollinators and seed dispersers (Dobson et al., 1999; Luft et al., 2003; Cunningham et al., 2004; Raguso, 2008; Rodríguez et al., 2013), VOCs emitted from damaged tissue – so called herbivore-induced plant volatiles (HIPVs) – help the plant to protect itself against biotic stressors and warn neighboring plants (Engelberth et al., 2004; Dicke and Baldwin, 2010; Heil, 2014; Erb et al., 2015; Hammerbacher et al., 2019). In order to study and analyze these VOCs, multiple methods have been developed. The most widespread one is collecting VOCs by enclosing the plant (tissue) of interest with a container or PET bag, and establishing a continuous air flow through the system: either via the closed-loop stripping technique by circulating the same air inside the system, or with a push-pull system where clean air is ‘pushed’ into the system on one side and ‘pulled’ out again on another side by applying a vacuum (Tholl et al., 2006). In both cases, the air flow passes through a carbon-based or organic polymer (e.g. PoraPak) adsorbent, where the VOCs are trapped (Tholl et al., 2006). Elution of the VOCs from the filter trap with an organic solvent then enables the qualitative and quantitative analysis of the volatile profile via gas chromatography coupled to a mass spectrometer (GC-MS) or to a flame-ionization detector (GC-FID), respectively.

The herbivore-induced emission profile of plants is usually comprised of the same four

groups of compounds, categorized based upon their biosynthetic origin (see Dudareva et al. (2006)). Examples for the respective compound classes are given in Figure 1.

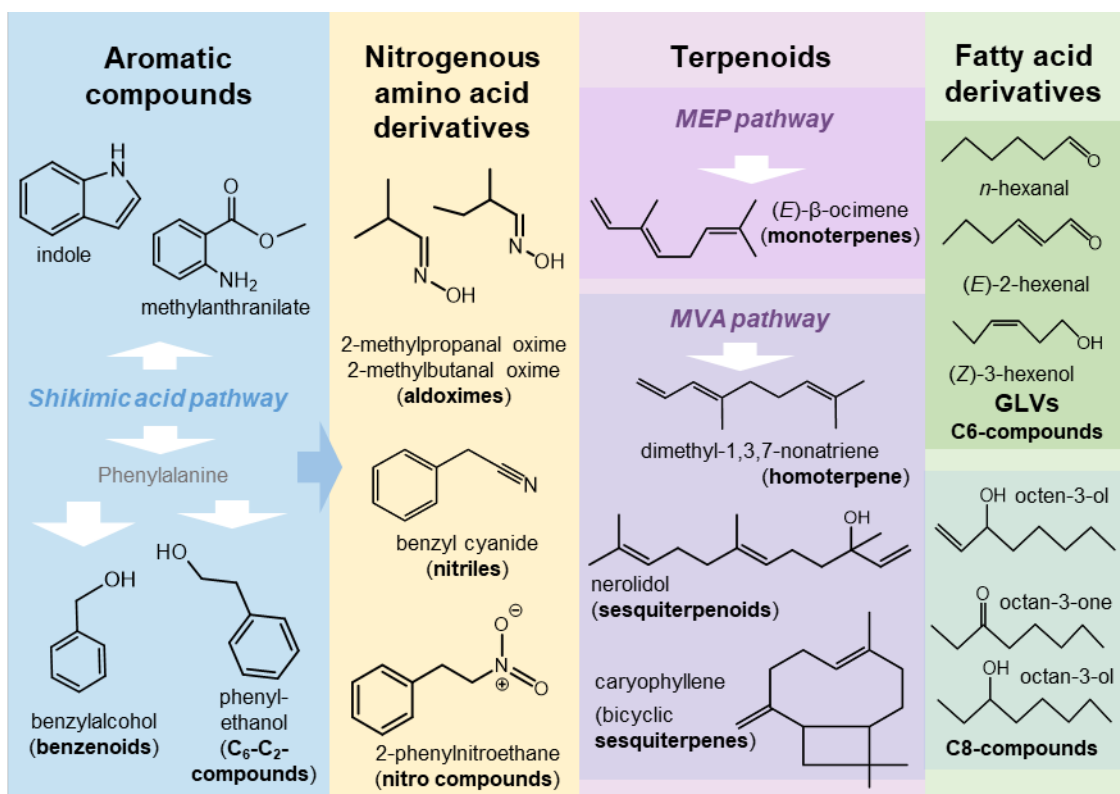


Figure 1: Overview of herbivore-induced plant volatiles (HIPVs). HIPVs can be grouped in four major classes, based on their biosynthetic origin (see Dudareva et al., 2006). I: Aromatic compounds are typically formed along the shikimate and phenylpropanoid biosynthetic route by utilizing pathway intermediates or end products as precursors. II: A number of amino acids including phenylalanine are the biosynthetic origin of many nitrogenous volatile compounds. III: There are two pathways, the mevalonate (MVA) and the methyl-erythritol-phosphate (MEP) pathway that provide plants with the precursors for all terpenoids, isopentenyl diphosphate (IPP) and its isomer dimethylallyl diphosphate (DMAPP) (Rodríguez-Concepción and Boronat, 2002). Condensation of IPP and DMAPP units and subsequent ionization and carbocation-driven rearrangements (Bohlmann et al., 1998) result in a wealth of terpenes, which can be further modified. IV: Fatty acids such as arachidonic acid, linoleic acid, α - and γ -linolenic acid are the precursors for C₆-compounds known as green leaf volatiles (GLVs) (ul Hassan et al., 2015) and volatile C₈-compounds (Wurzenberger and Grosch, 1984) (Wong et al., 2017). Examples are shown for each group of compounds.

Aromatic compounds (Figure 1, blue) are generally formed via the shikimate pathway. An intermediate of the pathway – chorismate – gives rise to (nitrogenous) volatiles such as indole, whereas benzenoids (C₆-C₁), C₆-C₂-compounds and phenylpropanoids (C₆-C₃) are derivatives of one of the pathway's end products: the amino acid phenylalanine (Dudareva et al., 2006; Widhalm and Dudareva, 2015). Nitrogenous compounds (Figure 1, orange) such as aldoximes and nitriles, are derivatives of their respective amino acid precursors (see chapter 1.1.1.2), whereas all terpenoids (Figure 1, purple) are synthesized by condensation (catalyzed by prenyltransferases) of units of isopentenyl diphosphate (IPP) and its isomer dimethylallyl diphosphate (DMAPP) and subsequent ionization and carbocation-driven rearrangements (catalyzed by terpene synthases) (Bohlmann et al., 1998). The universal precursors IPP and DMAPP can thereby be

synthesized via two routes, the plastidic methyl-erythritol-phosphate (MEP) and the cytosolic mevalonate (MVA) pathway (Rodríguez-Concepción and Boronat, 2002). The last group, the fatty acid-derived compounds (Figure 1, green) include the almost ubiquitous green leaf volatiles (GLVs). GLVs are C₆-compounds derived from linoleic acid and α-linolenic acid via the oxylipin pathway (ul Hassan et al., 2015). Noteably, many fungi and a few plant species can also form C₈-compounds from linoleic acid (fungi) (Wurzenberger and Grosch, 1984) or arachidonic acid and γ-linolenic acid (plants) (Wong et al., 2017).

There are three ways in which these HIPVs can help plants defend themselves better against attackers. Firstly, the compounds can directly increase resistance to herbivory. For GLVs like hexanal, 2-hexenol, 3-hexenol and hexanol emitted from damaged tomato or potato leaves, it was shown that they reduced the fecundity of aphids (*Myzus persicae*) (Hildebrand et al., 1993; Vancanneyt et al., 2001). Similarly, many terpenoids can be toxic when ingested, as for instance the sesquiterpene dimer gossypol for *Helicoverpa zea* (Stipanovic et al., 2006), and the sesquiterpene 7-*epi*-zingiberene from wild tomato (*S. habrochaites*) for whiteflies (*Bemisia tabaci*) (Bleeker et al., 2012). Others, like methyl salicylate, are not toxic, but protect the plant by repelling the attacker (Hardie et al., 1994; Glinwood and Pettersson, 2000). In many cases, it is not a single compound that confers the resistance, but a blend of compounds (Hummelbrunner and Isman, 2001; Kessler and Baldwin, 2001; Bruce and Pickett, 2011).

Besides direct effects, HIPVs are often involved in intra-plant signaling. In contrast to phytohormone signaling (see chapter 1.1.2) through the vascular system, HIPVs may trigger responses in distant leaves of the same plant much faster and thus prepare systemic leaves for future attacks (Karban et al., 2006; Heil and Ton, 2008; Meents and Mithöfer, 2020). For instance, Meents et al. (2019) found that the homoterpene (*E*)-4,8-dimethyl-1,3,7-nonatriene (DMNT) emitted by damaged leaves induces the accumulation of sporamin, a trypsin protease inhibitor, in systemic leaves of sweet potato (*Ipomoea batatas*) plants.

Lastly, HIPVs play an important role in the indirect defense against herbivores. The attraction of predators and parasitoids has been thoroughly studied within the last decades and the emission of HIPVs has often been referred to as a “cry for help” (Turlings and Erb, 2018), following the principle of “the enemy of my enemy is my friend”. The HIPVs provide the predator or parasitoid with information about the location of the herbivore, helping the aggressor’s natural enemy to find its prey or host, thus supporting the plant in its defense. This is a very common strategy to attract the herbivore’s

enemies, as an alternative to offering resources (food and/or shelter) to predators (Kessler and Heil (2011), see chapter 1.2). For instance, sesquiterpenes emitted from herbivore-damaged maize serve as cues for female parasitic wasps *Cotesia marginiventris* to find their hosts (Schnee et al., 2006) whereas other parasitic wasps (*Glyptapanteles liparidis*) are attracted to monoterpenes, aldoximes and aldoxime-derived nitriles (3- and 2-methylbutyraldoxime, benzyl cyanide) emitted by herbivore-infested black poplar (*Populus nigra*) (Clavijo McCormick et al., 2014).

1.1.1.2 Aldoximes and aldoxime-derived compounds

Aldoximes ($R_1HC=NOH$, see Figure 2) are nitrogen-containing compounds that occur frequently within the plant kingdom. In plants, they are mostly synthesized from amino acids or modified amino acids and thus reflect these structures (Sorensen et al., 2018). They are well known as important intermediates in the biosynthesis of glucosinolates (Underhill, 1967; Wittstock and Halkier, 2000) and cyanogenic glycosides (Tapper et al., 1967; Andersen et al., 2000). Both types of glycosides are important defense compounds: Glucosinolates can be activated by myrosinases (thio-glycosidases) – the so called mustard oil bomb – and release isothiocyanates and nitriles of the aglycone that are toxic or deterring for many herbivores (Halkier and Gershenzon, 2006). Similarly, cyanogenic glycosides are activated by β -glucosidases and then release toxic hydrogen cyanide to defend the plant (Vetter, 2000). In both cases, the glycosides accumulate constitutively in the plants, and are only activated upon leaf damage.

Apart from being involved in the biosynthesis of defensive glycosides, aldoximes can also be converted into their respective (volatile) nitriles, as has been found for instance in poplar (*P. trichocarpa*, *P. nigra*) (Clavijo McCormick et al., 2014; Irmisch et al., 2014), tea (*Camellia sinensis*) (Liao et al., 2020) and giant knotweed (*Fallopia sachalinensis*) (Yamaguchi et al., 2016). Such nitriles also play a role in direct antiherbivore defense as they act as repellents for generalist caterpillars (Irmisch et al., 2014). However, there is still more to it: yet another metabolic route of aldoximes leads to camalexin, a phytoalexin important in defense against pathogens (Glawischnig, 2007). Furthermore, in some plant species like poplar (Clavijo McCormick et al., 2014), maize (*Zea mays*) (Irmisch et al., 2015) and lima bean (*Phaseolus lunatus*) (Dicke et al., 1999), the free aldoximes accumulate upon herbivore damage as well, with detrimental consequences for the herbivore: the volatile aldoximes like 2- and 3-methylbutyraldoxime act as indirect defense, attracting parasitoids of the gypsy moth (*Lymantria dispar*) (Clavijo McCormick et al., 2014), whereas the semi-volatile phenylacetaldoxime has toxic effects on gypsy

moths (Irmisch et al., 2013). Thus, aldoximes are very versatile products/intermediates of plants' specialized metabolism.

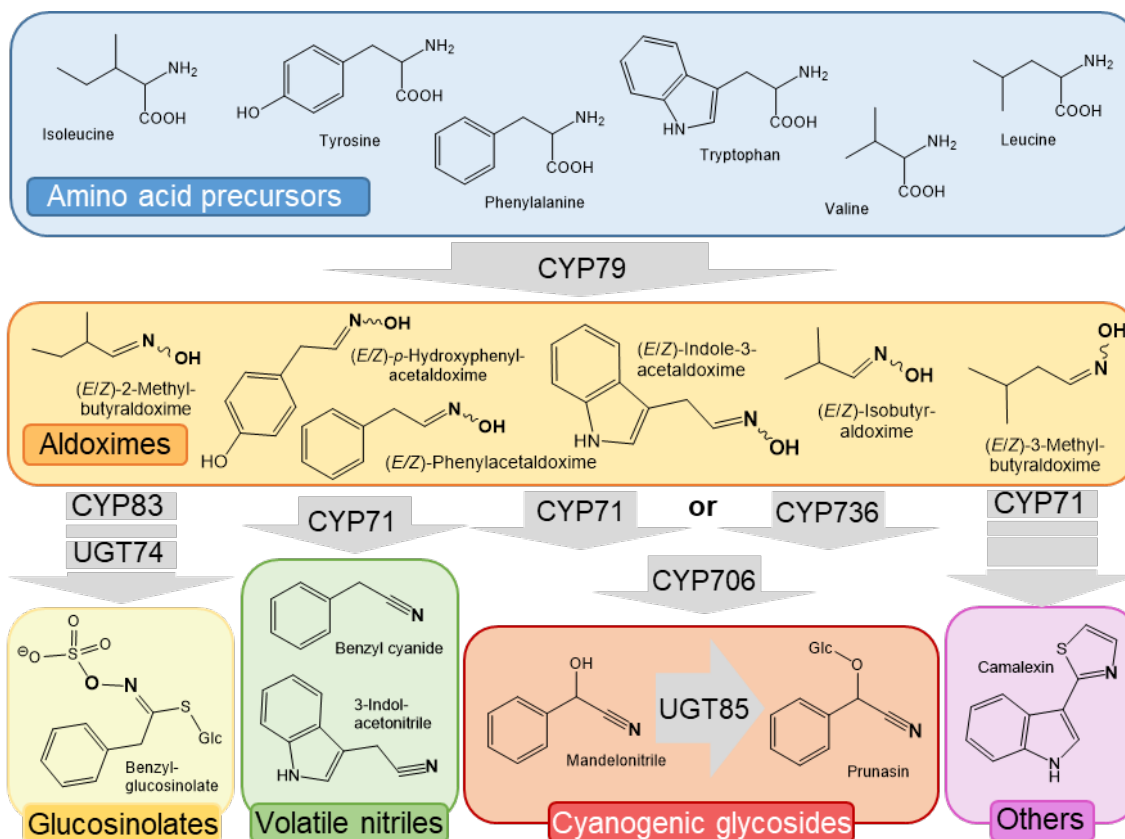


Figure 2: Biosynthesis and metabolism of aldoximes in plant specialized metabolism. In all seed plants, direct conversion of amino acids to their respective aldoximes is catalyzed by cytochrome P450s of the CYP79 subfamily (Sorensen et al., 2018). In contrast, enzymes involved in the downstream metabolism of aldoximes are not that conserved. The oxidation of aldoximes leading to nitriles, hydroxynitriles or thiohydroxamic acids is catalyzed by different cytochrome P450s, e.g. CYP71, CYP706, CYP736, CYP83 enzymes (Bak et al., 1998; Hansen et al., 2001; Takos et al., 2011; Knoch et al., 2016; Yamaguchi et al., 2016; Hansen et al., 2018). For the formation of cyanogenic glycosides, UDP-glycosyltransferases of the subfamilies UGT85 (and UGT94) are typically necessary (Thodberg et al., 2018), whereas UGT74s are involved in the formation of glucosinolates (Grubb et al., 2004).

Except for ferns, where a flavin-dependent monooxygenase is responsible (Thodberg et al., 2020), the direct formation of aldoximes from amino acids is catalyzed by cytochrome P450s of the CYP79 family (see Figure 2), independent of the metabolic fate of the aldoxime (Sorensen et al., 2018). More precisely, these CYP79 enzymes catalyze two N-hydroxylations of amino acids, as well as the subsequent dehydration and decarboxylation of the *N,N*-dihydroxy-intermediate to form the aldoximes (Halkier et al., 1995; Sibbesen et al., 1995). Depending on the precursor amino acid, the resulting aldoximes can be volatile – like Val-, Leu-, Ile-derived aldoximes - and thus are easily detectable by GC-MS, whereas aromatic amino acid- (Trp, Tyr, Phe) derived aldoximes are ‘semi-volatile’ and therefore better detectable by liquid chromatography-tandem mass spectrometry (LC-MS/MS).

1.1.1.3 *Plant (poly-)phenolics*

All plants produce phenolic compounds derived from the shikimate pathway, the subsequent phenylpropanoid pathway and/or the acetate/malonate pathway (see Figures 1,2), including for instance simple phenolic acids, benzenoids, and salicylates, as well as mono- and polymeric structures with more than one phenolic ring ('polyphenolics') like (iso-)flavonoids, hydrolyzable tannins, lignans, lignin, and condensed tannins (Quideau et al., 2011; Cheynier et al., 2013). In total, there are several tens of thousands of specialized metabolites belonging to the structurally very versatile group of plant (poly-)phenolics, with numerous important biological functions, such as serving as cell wall constituents or defensive compounds. However, it is beyond the scope of this introduction to go into all of them. Therefore, the following outline will be limited to an overview of only the most relevant polyphenols for this thesis.

Tannins are a class of polyphenolics that are widespread in higher plants, in trees, shrubs, and herbs, and may occur in various parts of the plants like fruits, bark, wood, seeds, stems, roots and leaves (Sharma et al., 2021). These compounds are well known for forming insoluble complexes with carbohydrates and proteins – in fact, the name is derived from their use as tanning agents that turn animal hides into leather (Bravo, 1998). Plant tannins are divided in two major groups, based on their biosynthetic precursors: condensed tannins (CT) or proanthocyanidins are flavan-3-ol (see Figure 3) oligomers (up to 50 units), whereas hydrolyzable tannins (HT) are esters of polyols (like glucose) and gallic acid-derived acids (Cheynier et al., 2013). The simplest HT have a central glucose moiety, which is esterified with gallic acid molecules. Compounds with one to five galloyl groups are called galloylglucoses, while compounds with more galloyl groups added via depside bonds are called gallotannins (Salminen, 2014). Ellagitannins, on the other hand, are characterized by a hexahydroxydiphenoyl unit (HHDP), which is formed by linking two galloyl moieties via a C-C bond (see Figure 3) (Quideau and Feldman, 1996). Upon enzymatic, acid- or base-catalyzed hydrolysis, this HHDP group is converted to the dilactone ellagic acid, which gave this group its name (Cheynier et al., 2013). Notably, the HHDP group can be further modified during the biosynthesis of ellagitannins so that the characteristic hydrolysis to ellagic acid is not possible anymore (Okuda et al., 1995). Ellagitannins occur in many plant families and are found in many commercial fruits, berries and nuts, like raspberries, strawberries and walnuts (Koponen et al., 2007; Regueiro et al., 2014). They have been in the focus of pharmaceutical studies, as they have potent antibacterial, antimycotic and antiviral activities (Buzzini et

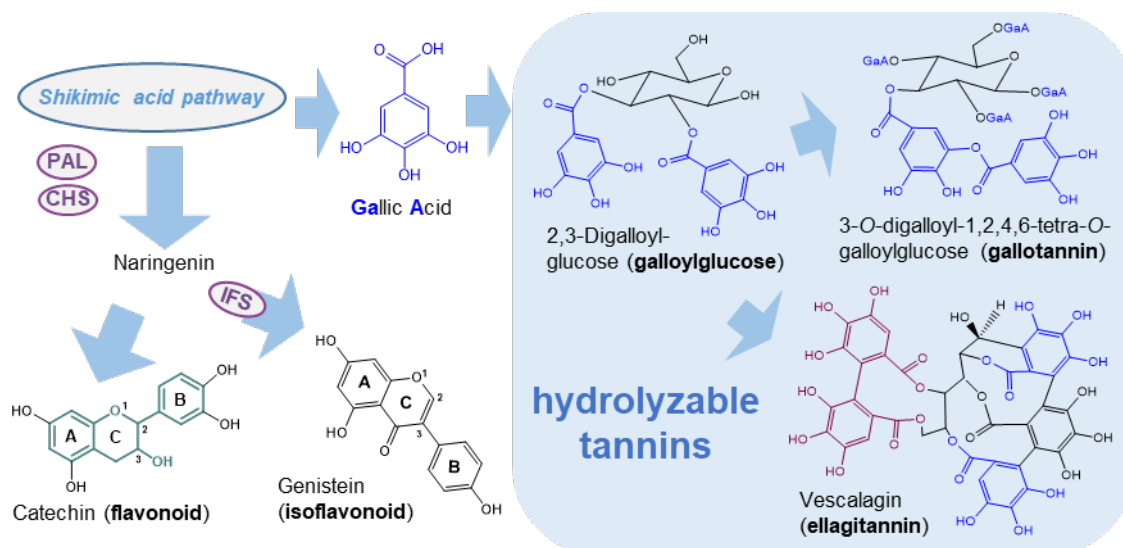


Figure 3: Overview of plant polyphenolics of interest. The shikimate biosynthetic pathway is the starting point of all phenolic compounds. The pathway intermediate 3-dehydroshikimic acid serves as a substrate for the production of gallic acid via NADP⁺ dependent oxidation (Ossipov et al., 2003). The transfer of gallic acid moieties onto sugar units leads to the formation of galloylglucoses and further linking of these gallic acid moieties yields gallotannins or ellagitannins (Salminen, 2014). Another central metabolite of the shikimate pathway is phenylalanine. Its deamination to cinnamic acid and ammonia by a phenylalanine ammonia lyase (PAL) is the entry step in the biosynthesis of phenylpropanoids (Vogt, 2010), whereas two steps downstream of this reaction, coumaroyl-CoA provides the substrate for a chalcone synthase (CHS), a type III polyketide synthase, that uses the substrate and three additional malonyl-CoA units to catalyze the formation a chalcone, the central intermediate for all (iso)-flavonoids (Austin and Noel, 2003). Further isomerization (cyclization), hydroxylation, oxidation and/or reduction steps lead to the formation of (hydroxyl-)flavonones, flavones, (dihydro-)flavonols, anthocyanidins and flavan-(di-)ols such as catechin (Kumar and Pandey, 2013), whereas an isoflavone synthase (IFS) utilizing the cyclized chalcone (= flavanone) as substrate gives rise to isoflavonoids such as genistein (Jung et al., 2000). Gallic acid/ galloyl (GaA) moieties are shown in blue, a hexahydroxydiphenyl-(HHDP) moiety in purple and the flavan-3-ol core in green.

al., 2008; Gontijo et al., 2019). Furthermore, they have antioxidant, antimalarial, and anti-inflammatory properties and therefore provide many health benefits to humans (Adams et al., 2006; Reddy et al., 2007). Surprisingly, whereas their pharmaceutical potential has long been recognized, only recently has the ecological role of ellagitannins in plants become a subject of interest. It has long been assumed that tannins have a protein-binding activity in insect herbivores, as studies with mammals and *in vitro* studies with enzymes showed these effects (Hagerman, 1989). As CT had higher protein-binding activities *in vitro* as compared to HT, further research focused on this compound class. However, newer *in vivo* studies in insects, for instance in the caterpillar *Lymantria dispar*, demonstrated that neither CT nor HT had these effects on insects (Barbehenn et al., 2009; Barbehenn and Constabel, 2011). Instead, tannins are pro-oxidant agents in the alkaline midgut of insects, with ellagitannins being more active than galloyl glucoses, which in turn have a higher activity than CT (Barbehenn et al., 2006; Moilanen and Salminen, 2007). The first studies of the toxicity of HT for insect herbivores have shown that HT indeed reduce performance and survival of generalist and sometimes even specialist caterpillars (Roslin and Salminen, 2008; Moctezuma et al., 2014; Anstett

et al., 2019). Thus, HT and especially ellagitannins are an important class of natural products that are not only able to defend the plant against pathogens, but also against insect herbivores.

Another diverse and important class of polyphenolics are the so-called flavonoids, which are present in all higher plants and of which more than 10.000 structures are reported to date (Williams and Grayer, 2004; Veitch and Grayer, 2008; Veitch and Grayer, 2011). All flavonoids have their biosynthetic origin in the central phenylpropanoid pathway leading from phenylalanine to *p*-coumaryl-CoA, where the first committed step in flavonoid metabolism is the addition of three acetate units from malonyl-CoA to *p*-coumaryl-CoA catalyzed by a type III polyketide chalcone synthase (CHS) (Austin and Noel, 2003; Vogt, 2010). The resulting chalcone with the flavonoid-specific C₆-C₃-C₆ basic skeleton then undergoes intramolecular cyclization by a chalcone isomerase, resulting in a flavanone with the core structure of all flavonoid subgroups: two aromatic rings (A and B) connected by a heterocyclic pyran ring (C) (Figure 3) (Jez et al., 2000; Kumar and Pandey, 2013). Further hydroxylation, oxidation and reduction steps at the C ring result in various subgroups of flavonoids, like flavones, flavonols, anthocyanidins and flavanols, the latter being the monomers of CT (Hahlbrock and Grisebach, 1975). Whereas all of the aforementioned flavonoid groups still have the B ring at the C-2 position, isoflavonoids are defined by having the B ring at the C-3 position, due to an oxidative migration of the B ring catalyzed by an isoflavone synthase, a phenomenon that is mainly restricted to legumes (Jung et al., 2000; Vogt, 2010).

Very similar to HT, flavonoids are of pharmaceutical interest due to their antioxidant, antibacterial, antifungal, antiviral, and anti-inflammatory properties (Kumar and Pandey, 2013). However, they are also recognized as having important functions in the interaction of plants with their environment, including the attraction of pollinators and seed dispersers (especially anthocyanidins due to their color), protection against oxidative stress and UV radiation, as well as protection against insect herbivores and especially against plant pathogens (Mierziak et al., 2014). For instance, catechin and its oligomers (CT) were shown to be inducible in poplar (*P. nigra*) leaves after fungal infection by the biotrophic rust fungus *Melampsora larici-populina*, to reduce hyphal growth and to inhibit rust spore germination (Ullah et al., 2017). Similarly, isoflavonoids accumulating in leaves of the Red Kidney bean (*Phaseolus vulgaris*) after inoculation with *Pseudomonas spp.* were able to inhibit growth of these bacteria (Gnanamanickam and Patil, 1977). Importantly, (iso-)flavonoids do not only fulfill protective functions within the plant tissue, but are also excreted into the rhizosphere - the area around the roots

of plants that is influenced by the roots (Hartmann et al., 2008) – to counteract soil pathogens (Baetz and Martinoia, 2014) or to initiate the symbiosis with nitrogen fixing bacteria (Cooper, 2004).

As pointed out, a common factor in all (poly-)phenols are their antioxidant properties, which can be used for their detection: A colorimetric assay with phosphomolybdic/ phosphotungstic acid complexes, the so called Folin-Ciocalteu reagent, takes advantage of the antioxidant properties of phenolics. The phenolics are oxidized and the reagent is reduced, thereby forming blue complexes, the color intensity (absorbance at 760 nm) of which can be correlated with the antioxidant effect of the phenols and thus indirectly, their quantity (Singleton et al., 1999). For polyphenols, another popular detection and quantification method is based on their own characteristic absorbance: most flavonoids can be detected by a spectrophotometer or LC coupled with a diode array detector (DAD) at 330-380 nm (de Rijke et al., 2006), anthocyani(di)ns at 510-540 nm (Ruiz et al., 2013), and ellagitannins at 270-290 nm (Salminen et al., 1999; Lee et al., 2005; Moilanen et al., 2013). It should be noted, however, that the low absorbance wavelength of ellagitannins is not very reliable for detection, as it can easily interfere with the absorption spectra of other compound classes including flavonoids, so LC-DAD alone can only be applied to previously characterized samples or as a diagnostic tool. For compound identification, a combination of LC-MS/MS and analysis of the absorbance spectra is preferable (de Rijke et al., 2006; Moilanen et al., 2013).

1.1.2 Regulation of plant defense

As mentioned previously (chapter 1.1), plant defense is not a constant, but rather a flexible and adaptive process, and can differ in quantity and quality depending on the circumstances. For one, the ontogeny of a plant does affect its defensive capacities (Bennett and Wallsgrave, 1994; Barton and Koricheva, 2010). On top of that, there are biotic (e.g. herbivores, pathogens) and abiotic (e.g. salt, nutrient, light, temperature, water) stresses that can activate, enhance or reduce certain plant defenses (see i.e. Gershenzon (1984); Kessler and Baldwin (2002); Ballare (2014); Piasecka et al. (2015); Yang et al. (2018)). More precisely, plants have evolved a sophisticated system for perceiving the threat and responding accordingly by adjusting their metabolism to cope with it (Kessler and Baldwin, 2002; Maffei et al., 2007; Howe and Jander, 2008). In this context, plant hormones (or 'phytohormones') are of utmost importance. These are low molecular weight substances that act as chemical messengers influencing many physiological processes of plants including growth and development, but also stress-related metabolism, at low concentrations (Davies, 1995). The most important defensive

phytohormones are abscisic acid (ABA), ethylene (ET), salicylic acid (SA) and jasmonates (JA), with ABA regulating mainly plant defense against abiotic stresses, SA against biotrophic pathogens, JA against necrotrophic pathogens and herbivores and ET fine-tuning the SA and JA mediated responses (Glazebrook, 2005; Bari and Jones, 2009; Gimenez-Ibanez and Solano, 2013; Verma et al., 2016). In particular, the crucial role of JA in regulating plant defense against herbivores has become apparent and was thoroughly studied in recent decades.

Plants perceive tissue damage caused by insect feeding through herbivore- and damage-associated molecular patterns ('HAMPs' and 'DAMPs'). HAMPs are molecules (i.e. volicitin) from the oral secretion of the insect herbivores (Mithöfer and Boland, 2008), while DAMPs are chemical signals (i.e. cell wall fragments) released by the host upon wounding (Heil and Land, 2014). In many cases, these molecules bind to their respective transmembrane receptors ('pattern recognition receptors'), which triggers a series of events to translate the perceived damage signal into an appropriate plant defense response (Erb and Reymond, 2019). Within seconds, the plasma transmembrane potential changes, ion fluxes are modified, an electrical signal starting from the injury travels through the entire plant, and cytosolic calcium ion (Ca^{2+}) levels increase at the site of damage (Maffei and Bossi, 2006; Maffei et al., 2007; Howe et al., 2018). At the same time as the Ca^{2+} levels rise, reactive oxygen species (ROS) are produced and mitogen-activated protein kinases (MAPK) are activated (Maffei et al., 2007; Maffei et al., 2007; Erb and Reymond, 2019). Combined, these signals trigger further downstream events, ultimately leading to the release of α -linolenic acid from membrane lipids by phospholipases and the *de novo* synthesis of JA starting within minutes after wounding (Walling, 2000; Maffei et al., 2007; Wu et al., 2007; Koo, 2017). To put it briefly, jasmonic acid is synthesized via the allene oxide synthase (AOS) branch of the octadecanoid pathway, where oxygenation, epoxidation and cyclization of α -linolenic acid yields first 12-oxophytodienoic acid (OPDA). Further reduction and β -oxidation steps then lead to jasmonic acid (Wasternack, 2007). Conjugation of jasmonic acid with isoleucine by jasmonoyl amino acid conjugate synthase JAR1 eventually results in the bioactive form of JA, JA-Ile (Staswick and Tiryaki, 2004). JA-Ile binds to the F-box protein Coronatine-Insensitive (COI1) of the Skp1/Cullin/F-box complex SCF^{COI1} , an E3 ligase complex that upon binding recognizes the transcriptional repressors Jasmonate ZIM domain proteins (JAZs) as targets and subjects them to ubiquitinylation and proteasomal degradation, thus releasing the transcription factors such as MYC2 to modulate JA-responsive genes (Wasternack and Hause, 2013). As a

result of JA signaling, the biosynthesis of many defensive compounds from all compound classes such as terpene indole alkaloids (van der Fits and Memelink, 2000), HIPVs including terpenoids (e.g. ocimene, linalool, DMNT, farnesene), indole and benzyl cyanide (Rodriguez-Saona et al., 2001; Noge et al., 2011; Clavijo McCormick et al., 2014) and various polyphenols (Gundlach et al., 1992; Xiao et al., 2009) is induced, as well as the expression of genes encoding antinutritive proteins such as protease inhibitors (Thaler et al., 1996; Kessler and Baldwin, 2002; War et al., 2012). Thus, JA is a master regulator of inducible defense against herbivores in all higher plants investigated this far and many studies have made use of jasmonic acid or methyl jasmonate to simulate herbivory (see e.g. Thaler et al. (1996); Heil et al. (2001); Heil et al. (2004); Hernandez-Zepeda et al. (2018)).

1.2 Ant-plant mutualism

As mentioned previously, many plants not only use their chemical and morphological weapons to fight herbivory (direct defenses), but also look for help in the animal kingdom (indirect defenses). In particular, plants often cooperate with ants to fight their attackers. Apart from specialized metabolites like HIPVs, plants such as e.g. cotton (*Gossypium herbaceum*) and lima bean, induce the production of extrafloral nectar (EFN) upon insect feeding damage (Wäckers and Wunderlin, 1999; Choh and Takabayashi, 2006). This lures ants to the plants, which not only feed on the EFN but also fight the herbivores they encounter (Rudgers and Strauss, 2004; Kost and Heil, 2005). While many plants, like the here-mentioned examples, only look for extra help when needed (*facultative interaction*), some recruit their helpers permanently and thus live in a *symbiosis* with the ants. Such plants are called myrmecophytes or ant-plants. In contrast to plants that only occasionally interact with ants and other predators, myrmecophytes form special hollow structures (hollow thorns, stems, leaf pouches or tubers) called “domatia” to host the mutualistic ants permanently and offer them protected nesting sites. Many ant-plants furthermore offer some source of food to the ants, either EFNs like many *Acacia* species (Heil et al., 2004) or so-called food bodies like *Cecropia* or *Macaranga* species (Janzen, 1969; Heil et al., 1998). Sometimes, the nutrient provision is indirect: ants often tend phloem-feeding coccoids and feed on the honeydew they excrete (Davidson and McKey, 1993). Such myrmecophytes have evolved repeatedly, so that to date, more than 600 species of vascular plants from 50 plant families have been described as myrmecophytes, occurring in tropical zones around the world (Chomicki and Renner, 2015). Similarly, so-called plant-ants have adapted to nesting in plants, with more than 110 species from five different subfamilies of Formicidae identified so far (McKey and

Davidson, 1993). While the benefits for the plant-ants (food and shelter) are quite consistent in all of these interactions, the benefits to myrmecophytic plants may vary with geographic location, season, colonizing ant species and plant species. In general, ant-colonization provides some sort of protection to their host. For instance, ant-colonization by *Pheidole bicornis* significantly reduced fungal infection of *Piper sagittifolium* inflorescences which consequently resulted in an increased number of produced seeds (Letourneau, 1998). Similarly, when Heil et al. (1999) tried to infect colonized *Macaranga tribola* plants with fungal hyphae and spores, they observed that symbiotic *Crematogaster* ants actively removed the fungal material from the wounding site, leading to a lower infection rate as compared to ant-deprived conspecifics. More recently, Gonzalez-Teuber et al. (2014) found that colonization by mutualistic ants may also reduce bacterial pathogen load and disease on the leaves of ant-acacia. Importantly, defense against microbes is only one aspect from which ant-plants might benefit. The Neotropical ant-plant *Triplaris americana* is often associated with *Pseudomyrmex* spp., and is easily recognizable in the dense jungle as it grows in the center of a circular area (1-2 m diameter) almost devoid of vegetation (Davidson et al., 1988). These ants not only cut off all leaves at the petiole base that get in contact with their host-plant, but also cut the stems of seedlings, causing the loss of all leaves and ultimately the death of surrounding vegetation and thus can be regarded as a biotic allelopathic agent (Davidson et al., 1988; Larrea-Alcázar and Simonetti, 2007). Such pruning of surrounding vegetation and encroaching vines has been described for various ant-plant interactions including *Acacia* spp. colonized by *Pseudomyrmex* spp. (Janzen, 1966, 1967), *Barteria fistulosa* occupied by *Tetraoponera* spp. (Janzen, 1972), *Macaranga* spp. inhabited by *Crematogaster* spp. (Federle et al., 2002), *Tococa* spp, *Clidemia* spp. or *Duroia* spp. associated with *Myrmelachista* spp. (Morawetz et al., 1992; Renner and Ricklefs, 1998; Frederickson et al., 2005) and *Cecropia* spp. colonized by *Azteca* sp. (Janzen, 1969; Schupp, 1986).

The most prominent role of plant-ants, however – and focus of this thesis – is in defense against insect and mammalian herbivores, including elephants, giraffes, antelopes (Ward and Young, 2002; Palmer and Brody, 2013) as well as beetles, caterpillars, and leaf-cutter ants (Michelangeli, 2003; Dejean et al., 2006). As this exchange – resources versus protection – is beneficial to both partners, this kind of symbiosis is called a *mutualism*.

1.2.1 Defense in ant-plants

The defense of myrmecophytes against herbivores has been studied thoroughly over the last decades, with a focus on the ant-related costs and benefits. Ever since the first report by Janzen (1966), it has been shown many times for various ant-plant species that uncolonized myrmecophytes suffer tremendously from herbivory, with at times lethal consequences for the plants (see e.g. Janzen (1967); Janzen (1972); Vasconcelos (1991); Heil et al. (2001); Michelangeli (2003); Rosumek et al. (2009)). For instance, Michelangeli (2003) found that at some sites, ant-exclusion in *Tococa spp.* led to folivory rates of up to 90% within a month, and Heil et al. (2001) reported similar high rates for ant-deprived *Macaranga spp.* (70%-80% loss of total leaf area within a year). This implied that the indirect defense conferred by the ants is the main defense strategy of myrmecophytes. In agreement with this hypothesis, Janzen (1966) noted an absence of bitter compounds, later identified as cyanogenic glycosides (Seigler and Ebinger, 1987) in ant-acacia as compared to non-myrmecophytic acacia and therefore proposed that, since the ant mediated protection is very efficient, myrmecophytes no longer invest in direct defense mechanisms such as the formation of specialized compounds. The rationale behind this hypothesis was that it is assumed that all defenses are costly to the plant, and therefore spatial and temporal overlap of defense strategies should be avoided (Rhoades, 1979; McKey, 1988; Davidson and Fisher, 1991).

Many studies since then have tried to confirm the proposed trade-off between indirect ant defenses and direct plant produced physical or chemical defenses with mixed results. On the one hand, for instance, Dyer et al. (2001) and Dodson et al. (2000) found higher level of amides in uncolonized *Piper cenocladum*, Heil et al. (1999); (2000) reported lower chitinase activity in myrmecophytic *Macaranga* and *Acacia* species and Moraes and Vasconcelos (2009) measured greater leaf toughness and trichome density in ant-free *Tococa guianensis* plants. On the other hand, when Fincher et al. (2008), Turner (1995) or Heil et al. (2002) compared several myrmecophytic and non-myrmecophytic *Piper*, *Macaranga* or *Acacia* species, they could not find a negative correlation between ant-colonization and chemical defenses. Thus, whether or not there is a trade-off is still a matter of debate.

Notably, not many studies took herbivory as an influencing parameter into account. Little information is available on the regulation and induction of direct defenses in ant-plants in response to herbivory or to the presence/absence of ants. Martin Heil and colleagues initiated studies on the regulation of indirect plant defenses of myrmecophytes. Interestingly, Heil et al. (2004) found that herbivory mimicked by JA spraying could not

induce EFN production in myrmecophytic *Acacia* spp., whereas EFN production increased in non-myrmecophytic *Acacia*. Similarly, a recent study by Hernandez-Zepeda et al. (2018) revealed that ant-colonized *Acacia*, in contrast to non-myrmecophytic *Acacia*, did not transmit JA signaling and consequent EFN induction to distant leaves, nor did these ant-plants emit HIPVs that serve as a plant-plant signal. This data suggests that ant-plants might have reduced inducible plant defenses or impaired JA signaling.

On the other hand, the ants themselves may also be considered as an inducible indirect defense of myrmecophytes. Mutualistic ants usually patrol leaves continuously, however, the appearance of herbivores or plant damage leads to a rapid (within 10 min) accumulation of a large number of ants at the site of danger (Madden and Young, 1992; Agrawal, 1998; Christianini and Machado, 2004). How the ants are recruited to the site has been studied for several plant and ant species with differing results. Sometimes vibrations were enough to attract them (Dejean et al., 2008; Dejean et al., 2009; Hager and Krausa, 2019), in other systems, volatile cues were necessary (Brouat et al., 2000; Mayer et al., 2008; Schatz et al., 2009) whereas the ant behavior observed by Romero and Izzo (2004); Dejean et al. (2008) and Christianini and Machado (2004) suggested that less volatile compounds from plant sap play a role. Of course it is also possible that a mixture of all these signals triggers the response (Agrawal, 1998). Whatever the first cues are, the ants then amplify the signal and recruit nestmates with their own alarm pheromones (Agrawal and Dubin-Thaler, 1999; Bruna et al., 2004; Dejean et al., 2009). This ultimately results in the fast removal of the threat. For instance, Vasconcelos (1991) observed that all of the live termites and 92.5% of the hemipteran eggs placed on *Maieta guianensis* were found and attacked by *Pheidole minutula* until they either jumped off the plant or were killed and fed to larvae. Similarly, *Crematogaster borneensis* took care of 96.6% of trial caterpillars within 1 hour by either driving them off the leaf or killing them (Fiala et al., 1989). As the speed and efficiency of ants finding and removing the herbivore are so high, it may not be necessary for myrmecophytic plants to respond to herbivory and initiate the cascade of JA signaling to induce chemical defenses. Here, the ant-plant *Tococa* was chosen as a model species to study the chemical defense of ant-plants in detail, to investigate the compounds involved, their mode of action and regulation and to determine whether myrmecophytes possess lowered constitutive and inducible defenses.

1.2.2 The myrmecophytic plant *Tococa*

Tococa is a polyphyletic genus of shrubs and small trees belonging to the Melastomataceae family (Michelangeli, 2000). It is widespread throughout the Neotropics, and is best known for the fact that most species – about 2/3 – produce leaf domatia and live in association with mutualistic ants (Michelangeli, 2005, 2010). Typical examples for *Tococa* species are *T. guianensis*, probably the most studied *Tococa* species with the widest geographic distribution, ranging from Mexico to Bolivia, from 0 to 1600 m a.s.l., and *T. quadrialata*, the species of primary interest in this thesis, consisting of 1-4 m tall shrubs that are mainly found in (south-) eastern Peru, in tierra firme forests (Michelangeli, 2005). Several ant species have been found to colonize *Tococa* plants, depending on the geographical location. In general, species of the genera *Azteca* and *Allomerus* are the most common (Cabrera and Jaffe, 1994; Michelangeli, 2003; Dejean et al., 2006; Moraes and Vasconcelos, 2009; Bartimachi et al., 2015), but also ants of the genera *Crematogaster*, *Pheidole*, *Leptothorax*, *Olygomymex*, *Solenopsis*, *Wasmannia* (subfamily: Myrmicinae), *Camponotus*, *Paratrechina*, *Myrmelachista* *Brachymymex*, (subfamily: Formicinae), *Dolichoderus* (subfamily: Dolichoderinae) and *Pseudomyrmex* (subfamily: Pseudomyrmecinae) have been described to inhabit these plants (Cabrera and Jaffe, 1994; Michelangeli, 2005). *Myrmelachista* ants offer special services to *Tococa* plants: in association with ants from this genus, the plants grow in “monocultures” in the jungle (Morawetz et al., 1992) – a phenomena called “devil’s gardens”. The ants attack every non-host plant and inject formic acid into the saplings, causing leaf necrosis (Frederickson et al., 2005). This creates large patches of one or two species of ant-plants (*Tococa*, *Clidemia* and/or *Duroia*) colonized by a single *Myrmelachista* colony in the otherwise species-rich forest (Renner and Ricklefs, 1998; Frederickson et al., 2005). Importantly, this interaction is restricted to *Myrmelachista* ants and has not been observed for other ant genera. Typically, *Tococa*-associated ants defend the plants against insect herbivores: leaf-cutter ants (*Atta* and *Acromymex* spp.) are probably the main defoliator, but also beetles (Coleoptera: Cerambycidae and Chrysomelidae), grasshoppers and bush crickets (Orthoptera: Acrididae and Tettigoniidae) as well as various caterpillars (Lepidoptera: Noctuidae, Pyralidae and Arctiidae) have been identified as herbivores of *Tococa* (Dejean et al., 2006, Alvarez et al., 2001, Morawetz et al., 1992, Michelangeli, 2003). Consequently, ant protection reduces foliar herbivory in *Tococa* compared to unoccupied plants, as has been shown in various ecological studies (see e.g. Alvarez et al. (2001); Michelangeli (2003); Bruna et al. (2004); Dejean et al. (2006)).

While the role of ants in anti-herbivore defense of *Tococa* has been examined by various research groups, very little attention has been paid to plant-derived defenses and

specialized metabolites of *Tococa* in general. Svoma and Morawetz (1992) found phenolic compounds in glandular trichomes and the inner side of the domatia. Spectrophotometric measurements of *Tococa guianensis* suggested that they possess high amounts of hydrolyzable tannins (2.6% dry weight) (Isaza et al., 2007), which is typical for the Melastomataceae family (Serna and Martinez, 2015). On the other hand, Michelangeli and Rodriguez (2005) could not find evidence for alkaloids or cyanogenic glycosides in the tested *Tococa* species, nor in any of the tested plants of the tribe Miconieae (Melastomataceae). To the best of my knowledge, there was no further information published about the phytochemistry of *Tococa*. Ethnobotany hasn't given any further clues about relevant metabolites either: In indigenous cultures, a tea of the leaves or domatia of *Tococa* is consumed to treat infertility or to influence the sex of the fetus, but none of this is attributable to particular compounds or has been scientifically proven to be effective at all (Michelangeli, 2005; De Gazelle, 2014). Thus, possible chemical plant defenses, their biosynthesis, regulation and mode of action remain to be elucidated.

1.3 Aims of this study

Ant-plant mutualism and the importance of ants as biotic defenders for these plants have been well studied in the last decades from an ecological perspective. However, the knowledge about the underlying molecular mechanisms and the phytochemistry of ant-plants is still scarce. Thus, this dissertation aimed to study ant-plant mutualism on a molecular level, with a focus on defense-related metabolism. Because most myrmecophytes are trees, the Neotropical ant-plant *Tococa quadrialata* as a fast growing shrub was chosen as a model species to explore the consequences of the mutualism and to characterize the response of myrmecophytes to herbivory in detail, combining field studies and modern analytical techniques. I aimed to find out about (i) whether *Tococa* plants still possess chemical defenses against herbivores or entirely depend on the protection provided by their mutualistic ants. Special emphasis was placed on herbivore-inducible defenses, their regulation by phytohormones (ii), as well as the biosynthesis and role of the identified compounds (iii). For this purpose, novel analytical methods were developed to detect defensive metabolites and responses. Additionally, to obtain a holistic picture of this mutualism, the general metabolism of ant-plants, and how it is affected by the presence or absence of ants was examined as well.

2 Manuscripts

2.1 Overview

The ant-plant *Tococa quadrialata* and its associated *Azteca cf. tonduzi* ants served as a model system to study the benefits of ant-colonization on a molecular level. Via transcriptome and metabolome analysis, important defense compounds and mechanisms of *T. quadrialata* were identified and additional nutritional benefits of the ants revealed. More specifically, ellagitannins were identified as one of the largest classes of compounds in the generally very polyphenol-rich *Tococa* plant, and insect feeding additionally led to the formation of herbivore-induced volatiles and phenylacetaldoxime glucoside. The results of this study were published in **manuscript I** entitled “Combined –omics framework reveals how ant symbionts benefit the Neotropical ant-plant *Tococa quadrialata* at different levels” (Müller et al., 2022 in *iScience*, 25(10), 105261) and are the keystone of this thesis.

As the accumulation of phenylacetaldoxime glucoside (PAOx-Glc), a previously undescribed natural product, in *T. quadrialata* upon herbivore damage (see **manuscript I**) suggests a role in plant defense for PAOx-Glc, a follow-up project was designed to learn about the biosynthesis and role of this compound and the closely related free phenylacetaldoxime (PAOx). As described in **manuscript II** entitled “The biosynthesis, herbivore induction and defensive role of phenylacetaldoxime glucoside” (Müller et al., 2023, *submitted for publication to Plant Physiology* (25/05/2023)), the genes and corresponding enzymes involved in the biosynthetic pathway of PAOx, benzyl cyanide and PAOx-Glc in *T. quadrialata* were identified, cloned, and characterized biochemically. Experiments on the spatial and temporal accumulation, and induction pattern of these compounds suggest that both PAOx and PAOx-Glc are a strictly local reaction to herbivore damage in *T. quadrialata*, with PAOx-Glc most likely representing a long-term storage form of the toxic PAOx.

For *Tococa spp.* as well as for many other non-model organisms, not all specialized compounds are known nor are standards available for all of the identified ones, and thus, it is often difficult to quantify compounds or compound classes using conventional methods. Therefore, a new method was developed together with cooperation partners to detect and relatively quantify plant polyphenols quickly and easily. Near-infrared (NIR) fluorescent single-wall carbon nanotubes (SWCNTs) were designed as polyphenol sensors that can report changes in total polyphenol content of plants due to biotic stresses. As described in **manuscript III** entitled “Detection and imaging of the plant

pathogen response by near-infrared fluorescent polyphenol sensors” (Nißler et al., 2022 in *Angewandte Chemie, Int. Ed.* 61(2), e202108373), the sensors were not only able to detect the changing polyphenol contents in leaf extracts of *Tococa*, but they also enabled real time imaging of plant responses to pathogens and are therefore an important step towards an easier detection and investigation of (ant-)plants’ reaction towards biotic stress.

2.2 Manuscript I

Manuscript title: Combined –omics framework reveals how ant symbionts benefit the Neotropical ant-plant *Tococa quadrialata* at different levels

Authors: Andrea T. Müller, Michael Reichelt, Eric G. Cosio, Norma Salinas, Alex Nina, Ding Wang, Heiko Moossen, Heike Geilmann, Jonathan Gershenzon, Tobias G. Köllner, Axel Mithöfer

Bibliographic information: iScience (2022), 25(10), 105261.
doi:10.1016/j.isci.2022.105261

The candidate is

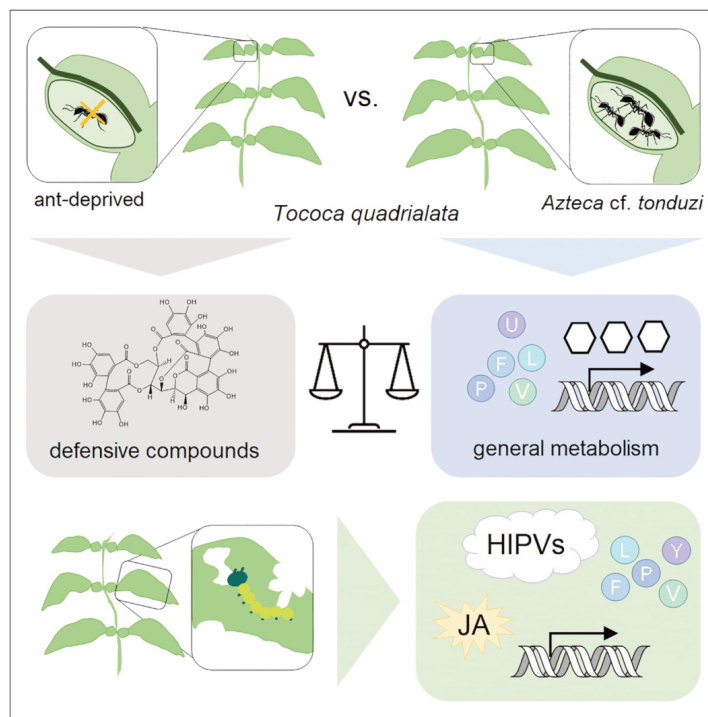
First author, Co-first author, Corresponding author, Co-author

Status: published

Authors' contributions (in %) to the given categories of the publication

| Author | Conceptual | Data analysis | Experimental | Writing the manuscript | Provision of material |
|---------------------|------------|---------------|--------------|------------------------|-----------------------|
| Andrea T. Müller | 30% | 70% | 75% | 70% | - |
| Ding Wang | - | 20% | - | - | - |
| Jonathan Gershenzon | 15% | - | - | 5% | 25% |
| Tobias G. Köllner | 25% | - | - | 10% | 20% |
| Axel Mithöfer | 25% | - | - | 15% | 25% |
| Others | 5% | 10% | 25% | - | 30% |
| Total: | 100% | 100% | 100% | 100% | 100% |

Article

Combined –omics framework reveals how ant symbionts benefit the Neotropical ant-plant *Tococa quadrialata* at different levels

Andrea T. Müller,
Michael Reichelt,
Eric G. Cosio, ...,
Jonathan
Gershenzon,
Tobias G. Köllner,
Axel Mithöfer

amithoef@ice.mpg.de

Highlights

We examine the phytochemistry and transcriptome in myrmecophytic *Tococa* plants

Ant-colonization promotes *Tococa* growth by increasing nitrogen, amino acids, and sugar

Constitutively produced defensive ellagitannin levels increase in the absence of ants

Tococa responds to herbivory by phytohormone signaling and emission of HIPVs

Müller et al., iScience 25,
105261
October 21, 2022 © 2022 The
Authors.
[https://doi.org/10.1016/
j.isci.2022.105261](https://doi.org/10.1016/j.isci.2022.105261)



Article

Combined –omics framework reveals how ant symbionts benefit the Neotropical ant-plant *Tococa quadrialata* at different levels

Andrea T. Müller,^{1,2,3} Michael Reichelt,² Eric G. Cosio,³ Norma Salinas,³ Alex Nina,³ Ding Wang,¹ Heiko Moossen,⁴ Heike Geilmann,⁴ Jonathan Gershenzon,² Tobias G. Köllner,^{5,6} and Axel Mithöfer^{1,6,7,*}

SUMMARY

Ant-plant defensive mutualism is a widely studied phenomenon, where ants protect their host plants (myrmecophytes) against herbivores in return for the provision of nesting sites and food. However, few studies addressed the influence of ant colonization and herbivory on the plant's metabolism. We chose the Amazonian plant *Tococa quadrialata*, living in association with *Azteca cf. tonduzi* ants for an ant-exclusion study to reveal the chemistry behind this symbiosis. We found that colonized plants did not only benefit from protection but also from increased amino acid and nitrogen content, enabling better performance even in an herbivore-free environment. In contrast, ant-deprived *T. quadrialata* plants accumulated more ellagitannins, a major class of constitutive defense compounds. Moreover, herbivory-induced jasmonate-mediated defense responses, including the upregulation of signaling and defense genes and the emission of volatiles irrespective of colonization status. Altogether, we show how ant-colonization can influence the general and defense-related metabolism and performance of myrmecophytes.

INTRODUCTION

Mutualistic relationships between plants and ants have evolved in tropical regions all across the world (Chomicki and Renner, 2015). There are more than 650 plant species classified as obligate ant-plants or myrmecophytes, including species of the genera *Acacia*, *Cecropia*, *Triplaris*, *Macaranga*, and *Tococa* (Chomicki and Renner, 2015). All these myrmecophytic plants offer their mutualistic ants pre-formed nesting spaces (domatia), consisting of hollow structures in thorns, petioles, stems, rhizomes, tubers, or modified leaves. Furthermore, they often provide ants with food like extrafloral nectar (EFN) and/or food bodies. In exchange, the ants protect their hosts against insect and vertebrate herbivores, pathogens, and sometimes prevent the growth of competing plants (Gonzalez-Teuber et al., 2014; Heil and McKey, 2003; Morawetz et al., 1992; Renner and Ricklefs, 1998).

The importance of ants as biotic defenders was revealed by several ant-exclusion studies with various myrmecophytic plants. Ant removal generally causes a dramatic increase in herbivore damage (Rosumek et al., 2009) with occasional lethal consequences for the host plant (Heil et al., 2001a). This high susceptibility of ant-plants to herbivory is assumed to be the result of reduced plant defenses, but this has not been well studied. Direct defense against herbivores can be conferred by physical traits like thorns, prickles, or high levels of lignification as well as by the synthesis and accumulation of certain specialized compounds acting as repellents or toxins (Mithöfer and Boland, 2012). Furthermore, some plant traits may attract enemies of the herbivore and thus provide indirect defense (Clavijo McCormick et al., 2014; Mumm and Dicke, 2010; Turlings and Wäckers, 2004). All these types of defense mechanisms are thought to be costly, so plants should produce defenses only when needed and avoid temporal and spatial overlap of individual defenses (McKey, 1979; Rhoades, 1979). As symbiotic ants confer effective resistance against herbivory, ant-plants may not have been selected to invest in additional anti-herbivore defenses (Janzen, 1966). In accordance with this hypothesis, a classic study by Janzen (1966) showed a reduction of cyanogenic glycosides in myrmecophytic acacia (Seigler and Ebinger, 1987), in comparison to non-myrmecophytic acacia. Other studies found negative correlations between the presence of ants and specific defensive compounds e.g. amides in *Piper* (Dyer et al., 2001), chitinases in *Acacia* and *Macaranga* (Heil et al., 1999, 2000) as well as

¹Max Planck Institute for Chemical Ecology, Research Group Plant Defense Physiology, 07745 Jena, Germany

²Max Planck Institute for Chemical Ecology, Department of Biochemistry, 07745 Jena, Germany

³Pontifical Catholic University of Peru, Institute for Nature Earth and Energy (INTE-PUCP), San Miguel, 15088 Lima, Peru

⁴Max Planck Institute for Biogeochemistry, Stable Isotope Laboratory (BGC-IsotLab), 07745 Jena, Germany

⁵Max Planck Institute for Chemical Ecology, Department of Natural Product Biosynthesis, 07745 Jena, Germany

⁶These authors contributed equally

⁷Lead contact

*Correspondence: amithoef@ice.mpg.de
<https://doi.org/10.1016/j.isci.2022.105261>





morphological defensive traits in *Tococa* (Moraes and Vasconcelos (2009); but see Bartimachi et al. (2015)). Overall, however, a general trade-off between ants and other defenses has not been observed in ant-plants (Del Val and Dirzo (2003); Fincher et al. (2008); Heil et al. (2002); Turner (1995); Ward and Young (2002); but see Koricheva and Romero (2012)). Hence, the factors leading to the reduced performance of myrmecophytes when ants are absent remain to be elucidated.

Direct and indirect defensive traits in plants can either be constitutively expressed or inducible upon herbivory. Many plants accumulate defensive compounds only upon tissue damage as toxic or herbivore-deterrent substances may result in costs to produce or to maintain, in particular, to avoid autotoxicity (Karban et al., 1997). Previous studies on ant-plants have mainly focused on constitutive defenses, with very few studies looking for inducible direct defenses (Frederickson et al., 2013; Moraes and Vasconcelos, 2009). Jasmonates are known to be the hormones primarily responsible for the induction of plant defenses upon insect herbivory (Gatehouse, 2002). However, Heil et al. (2004) showed that unlike in facultative ant-plants, the EFN production of myrmecophytic *Acacia* could not be induced by jasmonic acid (JA). In a more recent study, Hernandez-Zepeda et al. (2018) also found that JA treatment was unable to induce a systemic EFN production in a myrmecophyte and could only induce few number of volatiles, which in turn were unable to propagate the defense reaction further. The lack of an inducible defensive response in myrmecophytes might be an important yet unrecognized factor contributing to their performance when ants are not present.

In recent years, mutualist ants have been studied not only for their roles as protectors but also for their function in plant nutrient acquisition. In epiphytic ant-plants, it has long been known that mutualistic ants serve as nitrogen sources rather than as defenders (Gay, 1993). Now, labeling studies with stable nitrogen isotopes (^{15}N) have shown that in myrmecophytic trees like *Leonardoxa* (Defosse et al., 2011) and *Cecropia* (Dejean et al., 2012), the nutrient flow between ants and myrmecophytes can be bidirectional (reviewed by Mayer et al. (2014)). Especially in the nutrient-poor soils of the Neotropical rainforests, the supply of nitrogen and other nutrients by ants ("myrmecotrophy") may be another important aspect affecting the general performance of myrmecophytes.

Tococa (Melastomataceae) is a genus of shrubs and small trees, found all over the Neotropics, from southern Mexico to Bolivia (Michelangeli, 2005). The majority of species are myrmecophytes forming hollow pouches at the base of the leaf blade or at the apex of the petiole. The ant species associated with *Tococa* vary within its geographic range, with species of the genera *Azteca* and *Allomerus* being the most common (Bartimachi et al., 2015; Cabrera and Jaffe, 1994; Dejean et al., 2006; Michelangeli, 2003; Moraes and Vasconcelos, 2009). The protective effect of ants on *Tococa* species has been demonstrated in several ant-exclusion studies. For instance, in the Canaima National Park in Venezuela, the removal of *Azteca* ants from *Tococa coronata*, *Tococa macrosperma*, or *Tococa guianensis* resulted in an increase in defoliation from 5% to up to 90% (Michelangeli, 2003). However, while the performance of *Tococa* spp. was the subject of many studies, little is known about the phytochemicals of these plants, which could serve as alternative defenses to herbivores when ants are absent. Leaves were reported to contain high concentrations of phenolics, mostly hydrolysable tannins (Serna and Martinez, 2015; Svoma and Morawetz, 1992) and anthocyanins (Dejean et al., 2006), but there is no additional information.

Here, we chose to study the myrmecophytic *Tococa quadrialata* in the Amazonian region of Peru, which associates with *Azteca cf. tonduzi* ants to investigate the influence of ants on the performance and chemistry of these ant-plants in the field. In order to distinguish the effects of mutualism, we monitored the performance of ant-colonized and uncolonized plants in herbivore-free and natural environments. Combined targeted and untargeted metabolomics and transcriptome analyses revealed how ant-plants are affected by the presence or absence of their symbionts. To understand the high susceptibility of these plants toward herbivore damage in the absence of ants, we investigated the constitutive and inducible defense mechanisms of *T. quadrialata*, their regulation, and their impact on plant performance upon herbivore stress. We also addressed the possibility that ants improve *T. quadrialata* performance by enhancing its nutrient supply.

RESULTS

***T. quadrialata* plants colonized by *Azteca cf. tonduzi* ants grow much better than uncolonized plants in their natural environment**

Our field study was centered on a plot of young *T. quadrialata* plants (0.5–1 m tall) (Figure S1Aa–c) colonized by *Azteca cf. tonduzi* ants. The ants were observed to constantly patrol the myrmecophytes' leaves

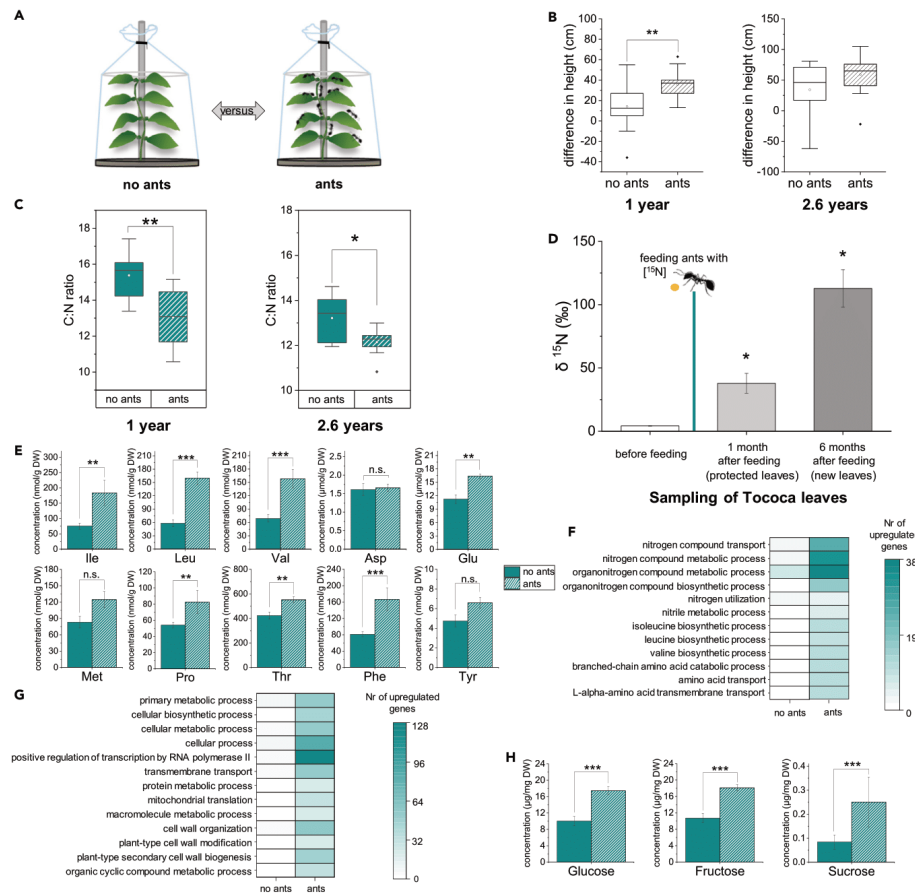


Figure 1. The presence of ants increases nitrogen content and general metabolism in *Tococa quadrialata* plants in the absence of herbivores (A) Experimental design: A set of young *T. quadrialata* plants colonized by *Azteca cf. tonduzi* ants was split into two groups, and ants were removed from one group. Nets were installed around all plants to prevent herbivore damage and recolonization and ensure the same abiotic conditions. The general performance and metabolism of *T. quadrialata* plants with (ants) and without ants (no ants) were measured. (B) Boxplots (25th percentile, median, mean (open circle), and 75th percentile) showing plant growth. 1 year after the start of the experiment, all plants had grown, however, colonized ones had gained more height than their ant-deprived counterparts (**: $p < 0.01$, $df = 33$, Student's t-test, $n = 17-18$). After 2.6 years, both groups of plants had grown taller, but no significant difference between the treatment groups was detectable ($p > 0.05$, $df = 30$, Student's t-test, $n = 13-19$). For further growth parameters, see Figure S2. (C) Boxplots (25th percentile, median, mean (open circle), and 75th percentile) showing carbon-nitrogen (C:N) ratio of the leaves. The C:N ratios of leaves of ant-colonized plants were lower than those of ant-deprived plants at both examined time points (1 year: **: $p < 0.01$, $F_{1,16} = 9.789$, two-way ANOVA, $n = 4-5$; see Figure S3; 2.6 years: *: $p < 0.05$, $df = 14$, Student's t-test, $n = 8$). (D) Feeding ¹⁵N-labelled glycine directly to ants increased the relative amount of ¹⁵N (δ¹⁵N) in *T. quadrialata* leaves even in leaves inaccessible to ants (protected) and in newly grown leaves (new) (*: $p < 0.05$, $df = 2$, one-tailed t-test, $n = 3$). Mean and SE are shown. See Figure S3 for details of the experimental setup.

**Figure 1. Continued**

(E) The presence of ants led to a significantly greater accumulation of several amino acids after 2.6 years (***: $p < 0.001$ **: $p < 0.01$, $df = 14$, Student's t-test, $n = 8$). Mean and SE are shown.

(F) Transcriptome analysis of ant-colonized and ant-deprived plants (1 year) showed that genes involved in nitrogen and amino acid metabolism are upregulated in colonized plants compared to ant-deprived ones (FDR p value ≤ 0.05 , $\log_2FC \geq 1$). Genes were assigned to the corresponding GO terms for biological processes in which they might play a role.

(G) Genes associated with the general metabolism were found to be induced in ant-colonized vs. ant-deprived plants (FDR p value ≤ 0.05 , $\log_2FC \geq 1$). Genes are grouped by their GO terms (see [Data S2](#)).

(H) The presence of ants led to increased amounts of free sugars (2.6 years: ***: $p < 0.001$, $df = 14$, Student's t-test, $n = 8$). Mean and SE are shown.

([Figure S1Ad](#)), quickly discovering any invertebrate or other biological material placed on the plants ([Figure S1Ae and f](#)), and either attacking the intruding object instantly themselves or first recruiting their nestmates for a joint attack ([Data S1](#)). The importance of these aggressive symbionts as biotic defenders was confirmed for this specific interaction when the performances of colonized and uninhabited *T. quadrialata* plants, naturally occurring within the same plot, were monitored over the course of 2.8 years. As expected, uncolonized plants suffered much more herbivory than ant-colonized plants ($p < 0.05$) ([Figure S1B](#)), whereas ant-colonized plants had increased height ([Figure S1C](#)) and gained more leaves ([Figure S1D](#)) and domatia ([Figure S1E](#)) than uncolonized plants, which suffered on average net losses of leaves and domatia over the monitoring period.

Ant colonization enhances nitrogen availability and general metabolism of *T. quadrialata*

Ant-colonization often comes with metabolic costs for the myrmecophytes, which are only compensated by the protection against herbivores ([Frederickson et al., 2012](#); [Stanton and Palmer, 2011](#)). To see which effects the colonization by *A. cf. tonduzi* itself has on the metabolism of *T. quadrialata*, we set up an experiment where we removed ants from half of the young, colonized plants in a plot. To exclude varying levels of herbivory as an influencing factor, all *T. quadrialata*, both with and without ants, were protected from herbivory by covering them with nets, and the performance and metabolism of these plants over time were measured ([Figure 1A](#)). Repeated sampling over a time span of almost 3 years allowed to identify and confirm differences between colonized and ant-deprived plants. Surprisingly, after one year of growing under the nets, ant-colonized plants were taller than ant-deprived plants ($p < 0.01$; [Figure 1B](#)) and had gained more domatia and leaves ($p < 0.05$; [Figure S2](#)). After 2.6 years, there were no longer significant differences between the treatments, likely owing to the fact that the plants reached the maximum height possible below the nets. A possible explanation for the better growth of colonized plants might be that *A. cf. tonduzi* provides *T. quadrialata* with nutrients, as reported for some, but not all, ant-plant mutualisms (see e.g. [Solano and Dejean, 2004](#)). To determine whether colonization brings nutritional benefits, we compared the carbon:nitrogen (C:N) ratio of ant-colonized and ant-deprived plants. Plants growing with ants for 1 and 2.6 years had significantly lower C:N ratios than plants from which ants were excluded throughout the experiment ($p < 0.05$; [Figures 1C and S3A](#)), suggesting that the presence of ants increased nitrogen availability. To confirm the assumption that the additional foliar nitrogen is the result of myrmecotrophy, a labeling experiment was conducted. *T. quadrialata* plants outside the main experimental plot colonized by *Azteca* spp. ants were chosen and a solution of honey mixed with [^{15}N]glycine was fed to the ants (see [Figures S3B–S3E](#) for pictures of the experimental setup). To exclude false positives such as from leaves that had direct contact with the labeled honey mixture or with labeled ant feces, we wrapped the youngest leaves in a bag before the labeling and harvested these samples after 1 month. Additionally, new leaves that emerged after the consumption of honey were collected after 6 months. As shown in [Figure 1D](#), there was a clear enrichment of ^{15}N in protected and newly grown leaves compared to those on the plant before ants were fed with [^{15}N]glycine ($p < 0.05$), demonstrating that *T. quadrialata* plants can indeed take up and transport nitrogen previously consumed by their ant symbionts.

With increased levels of nitrogen, we expected an increased accumulation of nitrogen-containing compounds in *T. quadrialata* and thus quantified the free amino acid contents of ant-colonized compared to ant-deprived plants. Indeed, enhanced levels of Ile, Glu, Pro, and Thr ($p < 0.01$), as well as Leu, Val, and Phe ($p < 0.001$) were found in ant-colonized plants ([Figure 1E](#)). The same trend was observed but without statistical significance for Tyr, Asp, and Met ([Figure 1E](#)). Similar differences in the free amino acid content of ant-colonized vs. ant-deprived plants were seen in the results of the herbivory and JA experiments conducted at about the same time ([Table S1](#)).

On the molecular level, transcriptome analysis of ant-colonized and ant-deprived *T. quadrialata* leaves revealed that many genes associated with nitrogen and amino acid metabolism were expressed at higher levels in ant-colonized plants (Data S2). For example, genes involved in nitrogen compound metabolic processes (GO:0006807), nitrogen compound transport (GO:0071705), nitrile metabolic processes (GO:0050898), and valine/leucine/isoleucine biosynthetic processes (GO:0009099, GO:0009098, GO:0009097) were all upregulated in colonized vs. ant-deprived plants (Figure 1F). Besides nitrogen metabolism, other aspects of general metabolism seemed to be influenced by the colonization status. The upregulation of genes associated with GO terms like cellular biosynthetic processes (GO:0044249), primary metabolic processes (GO:0044238), positive regulation of transcription by RNA polymerase II (GO:0045944), organic cyclic compound metabolic processes (GO:1901360), protein metabolic processes (GO:0019538), amino acid transport (GO:0006865), and mitochondrial translation (GO:0032543) indicates that there is enhanced metabolic activity in ant-colonized plants on many fronts (Figure 1G). In addition, increased amounts of the free sugars glucose, fructose, and sucrose were found in ant-colonized *T. quadrialata* plants compared to ant-deprived plants ($p < 0.001$, Figure 1H).

***T. quadrialata* contains ellagitannin defenses that accumulate to higher levels in plants not colonized by symbiotic ants**

The greater damage suffered by *T. quadrialata* without its *Azteca cf. tonduzi* symbionts might be explained by the lack of other forms of anti-herbivore protection. To search for chemical defenses in this species, we employed untargeted metabolome analysis of methanolic leaf extracts and found high levels of phenolic compounds (Figure 2A). Many of the features detected were tentatively identified as ellagitannins—a class of plant defense compounds (Salminen, 2014)—by the comparison of accurate masses, derived sum formulae, and fragmentation patterns to those in databases and the literature (dos Santos et al., 2012; Fracassetti et al., 2013; Moilanen et al., 2013; Serna and Martinez, 2015; Yoshida et al., 1991) (see Table S4), and an authentic standard for vescalagin (Figures 2B, 2C, and S4). Strikingly, many of these ellagitannins were present in greater amounts in ant-deprived vs. ant-colonized plants (2.6 years after ant removal, Figure 2D). This trend applied not only to ellagitannins, but also to their precursors (digalloylglucose, trigalloylglucose) and related polyphenolics (ellagic acid). Similar differences in ellagitannin content between ant-deprived and ant-colonized plants were obtained from an herbivory experiment (1 year after ant removal, Figure S5).

To determine whether the observed differences between ant-colonized and ant-deprived plants in ellagitannin content, as well as in sugars and amino acids, have an impact on resistance to herbivory, a choice experiment was conducted with larvae of *Spodoptera spp.* These generalist herbivores were allowed to choose whether to feed on leaf discs of ant-colonized or ant-deprived *T. quadrialata* plants, and were found to exhibit a significant preference for leaves from ant-colonized plants ($p < 0.001$, Figure 2E). These results suggest that the greater accumulation of ellagitannins and/or the lower amounts of amino acids and sugars in ant-deprived plants (Figure 1) might reduce herbivore feeding in the absence of symbiotic ants.

Insect herbivory on *T. quadrialata* induces extensive changes in defensive hormones, amino acid content, and volatile emission independent of ant colonization

Beside pre-formed defenses, such as ellagitannins, the resistance of plants against herbivores can also be mediated by induced defenses. To study whether induced defense reactions occur in *T. quadrialata*, we repeatedly (0.5–2.8 years after ant removal, in both rain and dry season) analyzed leaves of ant-colonized and ant-deprived plants after one day of feeding by *S. spp.* caterpillars (Figure 3A). In response to herbivory, the levels of jasmonic acid (JA) and its bioactive conjugate JA-Ile significantly increased in wounded leaves of both ant-deprived and ant-colonized plants (Figure 3B). Colonization status did not affect this response ($p > 0.05$ for colonization and interaction in all experiments). Most JA-derivatives followed the same pattern, but two (Sulfo-JA, OH-JA) decreased under ant colonization regardless of herbivory and the phytohormone salicylic acid (SA) increased in the presence of ants regardless of herbivory. No clear trend was observed for abscisic acid (ABA) (Figure S5A, Table S3).

Untargeted LC-MS analysis of the leaf metabolomes revealed that the features corresponding to ellagitannins were not induced upon herbivory (Figure S5), but those corresponding to amino acids were induced (Figure 3C). Subsequent targeted LC-MS² analyses demonstrated the accumulation of Trp, Phe, Val, Ile, and Leu upon herbivory at all time points, whereas Thr, Pro, and Tyr were only significantly enriched in herbivore-treated leaves at later time points (1 year and 2.7 years after ant-removal, Figure 3D, Table S1). Ant

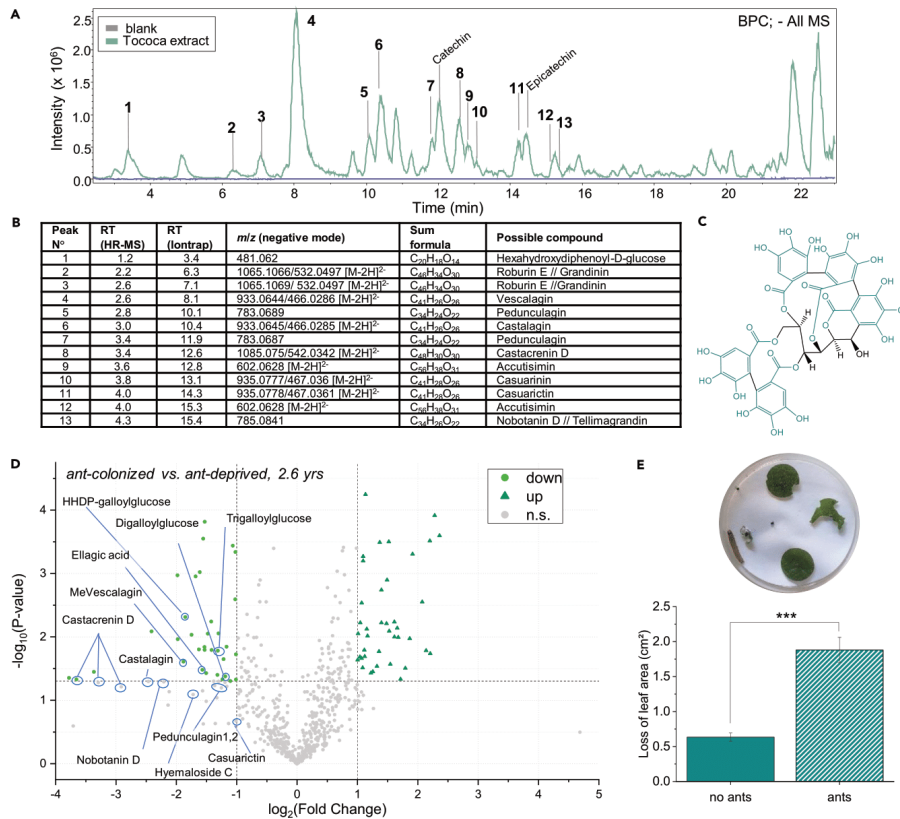


Figure 2. Ellagitannins, a major class of defense compounds in *Tococa quadrialata*, increase when symbiotic ants are not present
 (A) Base peak chromatogram (BPC) of a methanolic leaf extract run in negative ionization mode on an ion-trap LC-MS -showing that ellagitannins and related compounds are some of the main constituents of the extract (peak numbers correspond to lines in panel B).
 (B) Tentative identification of the major peaks of the chromatogram in panel A based on retention time, accurate mass of the most abundant parent ion (usually [M-H]⁻), predicted sum formula, and fragmentation pattern (not shown) (for more details, see Table S4, Figure S4).
 (C) Structure of the ellagitannin vescalagin, derived from 5 gallic acid moieties (highlighted in green) and a central sugar moiety (black).
 (D) Volcano plot of untargeted metabolome analysis of *T. quadrialata* (with MS in negative ionization mode) comparing features of ant-colonized and ant-deprived plants 2.6 years after ant removal. Several features identified as ellagitannins, precursors, and related compounds were found to be more abundant in ant-deprived plants.
 (E) Choice assay with *Spodoptera* larvae offered leaf discs from ant-colonized (ant) and ant-deprived (no ants) plants (2.7–2.8 years after ant-exclusion) in a Petri dish. Larvae allowed to move freely in the Petri dish for 24 h were found to prefer feeding on leaves of ant-colonized plants (***) $p < 0.001$, paired Wilcoxon rank-sum test, $n = 41$). Mean and SE are shown. RT, retention time; HR-MS, high-resolution mass spectrometry; HHDP, hexahydroxydiphenoyl.

colonization did not affect the amount of these herbivory-responsive amino acids 0.5 and 1 year after the initiation of the experiment ($p > 0.05$ for colonization and interaction colonization \times treatment, Table S1), but colonized plants had significantly higher concentrations of Val, Leu, Phe, and Tyr after 2.7 years ($p < 0.01$, Table S1).

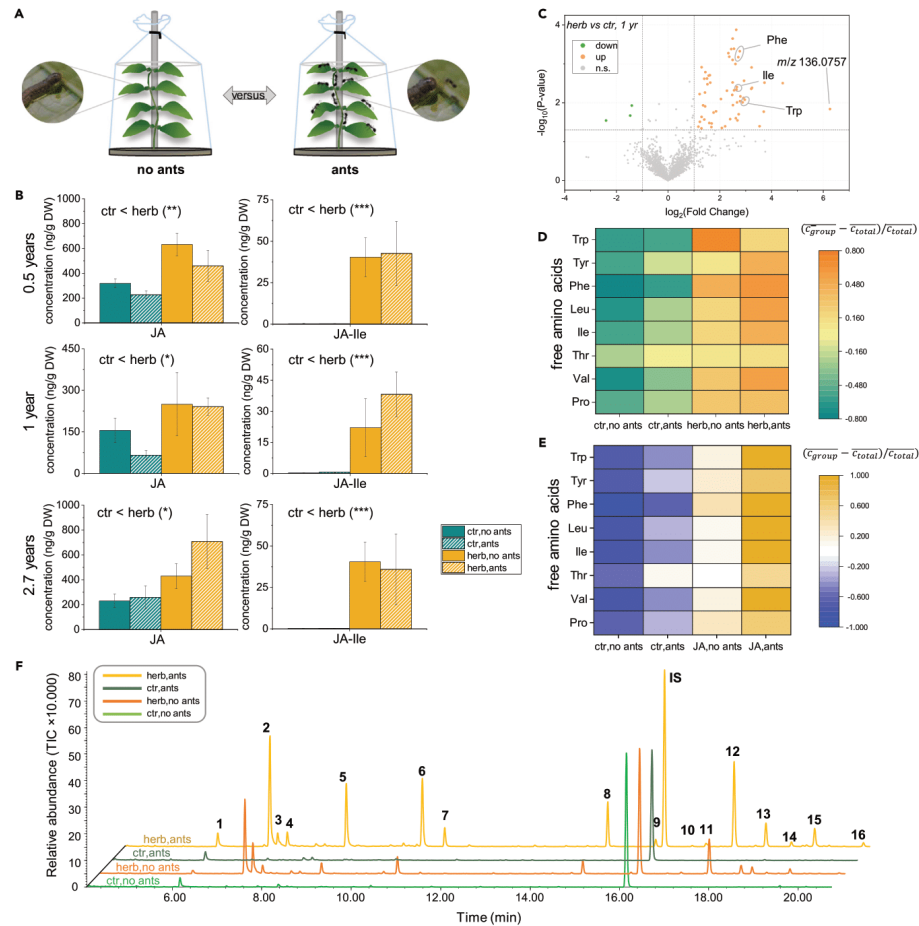


Figure 3. Insect feeding induces changes in defensive hormones, amino acids, and volatile emission of *Tococa quadrialata*
(A) Experimental design; leaves of colonized (ants) and ant-deprived (no ants) plants net-protected from uncontrolled herbivory were exposed to insect feeding 0.5 years (n = 6–8), 1 year (n = 4–5) and 2.7 years (n = 5–6) after the installation of the nets.

(B) In all three repetitions, herbivory led to a significant increase of jasmonic acid (JA) (*: p < 0.001, two-Way ANOVA) and the bioactive conjugate JA-Ile (***: p < 0.001, GLS, log-transformed data). Mean and SE are shown. For information about related compounds and statistics see also Figure S5, Table S3.

(C) Untargeted metabolite analysis comparing methanol extracts of control (ctr) and herbivore-induced (herb) leaves using LC-high resolution MS analysis (MS operating in positive ionization mode). Volcano plot depicts the metabolic features that accumulate upon herbivory (1 year) in orange. Features upregulated in all experiments are annotated.

(D) Targeted analysis revealed additional herbivore-inducible amino acids (2.7 years, $p_{treatment} < 0.05$, two-Way ANOVA, see Table S1).

(E) Treatment of leaves (n = 4–5, 2.7 years) with an aqueous 1 mM solution of jasmonic acid (JA) also induced the accumulation of free amino acids ($p_{treatment} < 0.05$, two-Way ANOVA, see Table S1). Spraying water served as control (ctr).

**Figure 3. Continued**

(F) Representative total ion chromatograms (TIC) of volatiles from each treatment collected for 24 h while insects were feeding. Compounds were identified with GC-MS. IS: internal standard; 1: α -pinene, 2: 1-octen-3-ol, 3: octan-3-one, 4: octan-3-ol, 5: (E)- β -ocimene, 6: (E)-4,8-dimethyl-nonatriene (DMNT), 7: benzyl cyanide, 8: indole, 9: methyl anthranilate, 10: α -copaene, 11: unknown sesquiterpene (fragmentation pattern see [Figure S6](#)), 12: (E)- β -caryophyllene, 13: α -humulene, 14: germacrene D, 15: α -farnesene, 16: nerolidol. All compounds were identified with the NIST17 library, Kovats index (see [Table S2](#)), and, except for 11 and 16, by comparison to authentic standards.

To confirm the hypothesis that the induced response to herbivory in *T. quadrialata* is mediated by jasmonate signaling, 1 mM JA was sprayed onto the leaves of net-covered plants with or without ants (2.8 years after ant removal) and samples were collected after 24 h. Phytohormone analysis showed that levels of the bioactive JA-Ile were increased ($p < 0.001$, generalized least-squares regression, $n = 4-5$) similar to concentrations observed upon insect feeding ([Table S1](#)) ([Figures 3C](#) and [3D](#)). In addition, all of the amino acids found to be inducible by insect feeding—Phe, Trp, Tyr, Val, Thr, Pro, Leu, and Ile—accumulated in leaves after spraying JA ([Figure 3E](#)).

Analysis of the volatile organic compounds (VOCs) emitted in response to herbivory by gas chromatography-mass spectrometry (GC-MS) revealed that the volatile bouquet emitted by *T. quadrialata* plants was significantly altered upon herbivore damage ([Figure 3F](#), [Table S2](#)). The most abundant components of the herbivore-induced blend were 1-octen-3-ol and (E)- β -caryophyllene, followed by (E)- β -ocimene, DMNT, and indole. These compounds were present in only trace amounts or were completely undetectable without herbivory. In addition, the C₈-compounds octan-3-one and octan-3-ol, the N-containing compounds benzyl cyanide and methyl anthranilate, and several sesquiterpenes (α -copaene, α -humulene, α -farnesene, germacrene D, nerolidol, unknown sesquiterpene) were identified as minor herbivore-induced VOCs. Interestingly, the volatile emission of ant-colonized plants often contained further compounds, like 2-heptanone, 2-heptanol, and several iridoids ([Figure S6](#), [Table S2](#)). However, these compounds were only found in substantial amounts when leaves with ants were fed upon by caterpillars ([Figure S6](#)), suggesting that they are not part of the plant's response to herbivory, but actually alarm pheromones of the *A. cf. tonduzi* ants, in accordance with previous findings ([Do Nascimento et al., 1998](#); [Ohmura et al., 2009](#)).

Insect herbivory alters gene expression in *T. quadrialata*

To learn more about the response of ant-plants to feeding damage, we next sequenced the transcriptomes of leaf samples from the herbivory experiment conducted 1 year after ant-removal and assembled the transcriptome *de novo*. Statistical analysis showed that herbivory drastically altered the gene expression profile. In ant-colonized plants, 8928 genes were responsive to herbivore treatment, 3004 of them being upregulated. Similarly, 11,615 genes were differentially expressed in ant-deprived plants upon herbivory. Although there was some overlap of differentially expressed genes (DE-Gs) in herbivore-damaged leaves of plants with and without ants, more genes showed specific activation in one interaction or the other ([Figure 4A](#)). Interestingly, most genes found to differ upon ant colonization were strongly influenced by herbivory as well. Among the genes induced by herbivory were many involved in the biosynthesis of volatile terpenoids, consistent with the herbivore-triggered emission of terpenoid volatiles by insect feeding ([Figure 4B](#)). Similarly, the genes of the tryptophan pathway, associated with the formation of Trp, indole, and methyl anthranilate, were activated by herbivore damage. Several genes involved in the biosynthesis of free amino acids were found to be induced upon herbivory as well, particularly in plants deprived of ants ([Figure 4C](#)). On the other hand, analysis of genes associated with protein degradation, another potential source of free amino acids, did not show a clear pattern of regulation by herbivory.

As the JA spraying experiment showed that JA is responsible for signaling and activating defenses after wounding, we monitored genes associated with JA biosynthesis and metabolism. Many of them were upregulated by herbivory, especially genes classified under the GO term "response to JA," which was among the strongest induced groups of genes ([Figure 4D](#)). As typical responses to JA include cell wall reinforcement, production of protease inhibitors and defensive compounds ([Maag et al., 2015](#); [Wasternack and Hause, 2013](#)), we investigated GO terms that might correspond to such JA responses and found various genes involved in the formation of aromatic compounds like flavonoids and lignins to be induced upon herbivory ([Figure 4E](#)). Strikingly, the expression pattern of protease inhibitors, a major group of defense proteins described in many other plants, was not altered upon herbivory ([Data S2](#)).

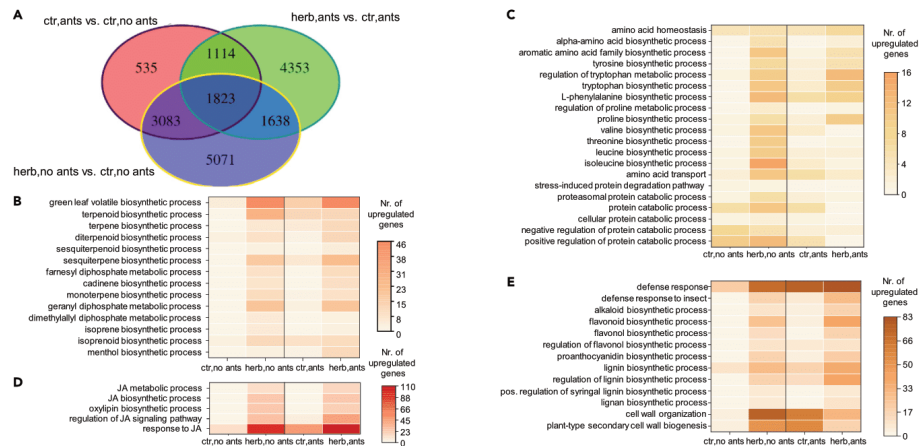


Figure 4. Insect herbivory alters gene expression in *Tococa quadrialata*

(A) Venn diagram showing the numbers of differentially expressed genes (DE-Gs, FDR corrected p value ≤ 0.05 , $|\log_2FC| \geq 1$) in different treatment comparisons, indicating how many DE-Gs were unique to a treatment or common to several treatments. (B–E) Heatmaps showing the number of genes assigned to various gene ontology (GO) terms that are up- or downregulated upon herbivory (herb) in the presence (ants) or absence (no ants) of ants in comparison to the respective control (ctr), see also Data S2. (B) GO terms are associated with the emission of volatile organic compounds. (C) GO terms are associated with the accumulation of free amino acids. D: GO terms linked to jasmonic acid (JA) biosynthesis and signaling. (E) GO terms associated with chemical and physical defense. (B, D, and E) GO terms shown are significantly enriched (FDR corrected p value ≤ 0.05) for at least one comparison (ants or no ants).

DISCUSSION

Ant-plants are frequently reported to suffer from reduced growth and survival in the absence of their mutualist ants (Fonseca, 1994; Heil et al., 2001a; Letourneau, 1998; Rosumek et al., 2009; Schupp, 1986). However, it is not known how the presence/absence of ants affects the plant's metabolism and, thus, if poor plant performance results only from increased herbivory owing to a lack of alternative plant defenses or if the plant misses other ant benefits, such as the provisioning of nutrients, which in turn impairs its metabolism and growth. In this study, we aimed to disentangle the effects of mutualistic ants on a myrmecophytic host plant and characterized the plant's defense strategies. Based on a combination of metabolomics and transcriptomics, we show that the tropical myrmecophyte *T. quadrialata* growing in its natural environment does not rely completely on the ant-mediated defenses but possesses a typical repertoire of responses to herbivory, including phytohormone increases and volatile emission, regardless of ant status, and also increased its investment in ellagitannin chemical defenses in the absence of its *Azteca cf. tonduzi* ants. At the same time, the presence of symbiotic ants makes a significant contribution to the plant nitrogen budget.

Ant colonization provides both protective and nutritional benefits to ant-plants

The absence of ants drastically reduced the performance of *T. quadrialata* in its natural habitat as described for other myrmecophytic species (Fiala et al., 1989; Fonseca, 1994; Janzen, 1966; Michelangeli, 2003; Schupp, 1986). Uncolonized plants suffered from severe folivory indicating that ants had critical functions in protecting plants from herbivores. Interestingly, ant-deprived plants also grew slower than ant-colonized plants in the absence of herbivory. This suggested the possibility that ants contribute to plant nutrition rather than depriving the plant of resources needed for growth—the expected cost of mutualism (Heil et al., 1997; Heil and McKey, 2003; O'Dowd, 1980). We found that *A. cf. tonduzi* were directly providing nitrogen to their host plants, increasing the nitrogen content of *T. quadrialata*, which resulted in higher amounts of free amino acids in ant-colonized plants. An RNA-Seq study revealed that ant-colonized *T. quadrialata* not only expressed genes of general nitrogen, amino acid, and protein metabolism at higher levels than in ant-deprived plants, but were also upregulated in genes of primary metabolism and had



higher levels of free sugars. These differences may well contribute to the greater growth of ant-colonized versus uncolonized *T. quadrialata*, both with and without herbivores.

Not all ant-plant mutualisms follow this pattern. In a study on *Acacia drepanolobium* (Stanton and Palmer, 2011), ant-colonization negatively influenced plant growth in an herbivore-free environment, likely owing to the metabolic costs of ant colony maintenance, which in this case are only partly compensated by the benefits of reduced herbivore pressure (Chamberlain and Holland, 2009; Heil et al., 1997). Similar results were also found for *Cordia nodosa* by Frederickson et al. (2012). The different results can be explained by the varying costs of ant occupancy. *Acacia drepanolobium* and other myrmecophytes are colonized by plant-ants that feed exclusively on the products of the plants, e.g., food bodies or extrafloral nectar, which require a considerable outlay of plant resources (Heil et al., 1997). Azteca ants, on the other hand, forage on the plant and in the surroundings (Sagers et al., 2000; Vasconcelos and Davidson, 2000), reducing the need for a plant-based diet and thus the costs of the relationship for the plant. This study adds to a growing body of evidence (Chanam et al., 2014; Defossez et al., 2011; Dejean et al., 2017; Gay, 1993; Sagers et al., 2000; Solano and Dejean, 2004) that ant symbionts can provide nitrogen to myrmecophytes (but see McNett et al., 2009; Solano and Dejean, 2004). However, whereas the other studies only demonstrate the bidirectional transfer of nutrients, our study shows the importance of this nitrogen source, as we found that ant colonization increased the total foliar nitrogen content, which probably resulted in the observed growth promotion.

Analysis of the metabolome and transcriptome hint toward the molecular mechanisms behind that. A comparison of the leaf metabolomes showed that ant-colonized plants furthermore contained higher amounts of free amino acids and sugars than ant-deprived plants. This together with the results from the RNA-Seq data suggesting an enhanced protein and nitrogen metabolism indicates that the presence of ants enhances the general metabolism in this ant-plant mutualism. The increased nitrogen content together with the reduced danger of herbivore damage permits the plants to focus on growth, which in turn enables the ant-colony to expand as well—a win-win situation.

***T. quadrialata* also produces chemical defenses against herbivory, with increased amounts when ants are absent**

Using untargeted metabolomics, we found that *T. quadrialata* produced a diversity of ellagitannins, a class of hydrolyzable tannins that are characteristic anti-herbivore defense compounds of the plant family Melastomataceae (Serna and Martinez, 2015). Ellagitannins are well-known in human medicine for their anti-inflammatory (Gatis-Carrazzoni et al., 2019), anti-bacterial (Araujo et al., 2021; Gontijo et al., 2019), anti-fungal (Klewicka et al., 2020), and anti-viral (Kesharwani et al., 2017) activities. In the alkaline midgut of insects, these compounds act as strong oxidants (Barbehenn et al., 2006) with negative consequences for herbivores. Vescalagin, for example, which was identified here, was shown to inhibit the growth of two generalist caterpillars (*Acrionicta psi* and *Amphipyra pyramidea*) (Roslin and Salminen, 2008), whereas ellagitannins from Onagraceae reduced survival of *S. spp.* (Anstett et al., 2019). Hence, the ellagitannins identified in this study likely contribute to the direct defense of *T. quadrialata*. Their greater accumulation in ant-deprived versus ant-colonized plants implies compensation for the lack of anti-herbivore protection afforded by ants. Such a trade-off between chemical defense and ant protection in myrmecophytes had originally been proposed by Janzen (1966), who found that non-myrmecophytic *Acacia* produce more cyanogenic glycosides than *Acacia* colonized by ants. As investment in defense is costly, plants should avoid redundancies. Many studies in ant-plants have addressed this hypothesis with mixed results (see: Koricheva and Romero (2012); (Heil et al., 2002), but some studies compared myrmecophytic with non-myrmecophytic species (Heil et al., 2002), or the same species at different life stages (Del Val and Dirzo, 2003). Of the few studies that compared investment in mechanical, chemical, and ant defenses in myrmecophytes of the same species, most of them indicated a trade-off (Dodson et al., 2000; Dyer et al., 2001, 2004; Moraes and Vasconcelos, 2009), but see Frederickson et al. (2013); Letourneau and Barbosa (1999). Hence, we conclude that ant-plants including *T. quadrialata* can adjust their level of constitutive anti-herbivore defense to their colonization status.

The choice assay revealed that indeed leaves of ant-deprived plants are less attractive to a generalist herbivore, most likely a combined effect of the higher nutritional value of ant-colonized leaves (higher sugar and amino acid content) and increased defenses in ant-free *T. quadrialata* plants. Roslin and Salminen (2008) already demonstrated with performance assays on the artificial diet that vescalagin is a strong feeding deterrent for generalist caterpillars, whereas Moraes and Vasconcelos (2009) found enhanced

mechanical defenses like leaf toughness and trichome density in ant-free *T. guianensis*, defensive traits we haven't analyzed, but may add to the observed feeding preference. Taking into account all the results from the long-term experiment, it can be concluded that ant-deprived plants adjust to their situation over time by the upregulation of their direct defenses and are therefore better defended against insect herbivory than a colonized plant without ant protection.

Ant-plants still possess some inducible defense mechanisms, such as the emission of volatiles

Based on our observations and numerous literature reports, symbiotic ants can be very effective at preventing herbivory. Hence, we hypothesized that myrmecophytes colonized by ants do not require inducible defense mechanisms. However, we found that insect feeding led to increases in jasmonate levels and the emission of HIPVs. These responses occurred regardless of the status of colonization, suggesting that the presence or absence of ants does not influence such defense reactions. Similar results were found for the myrmecophyte *C. nodosa*, where herbivory increased leaf toughness, total phenolics, and trichomes, whether or not ants were present (Frederickson et al., 2013). The presence of herbivore-induced defenses in ant-colonized plants is curious as they will never match the reaction speed of the ants. Although ants need only a few minutes to attack intruders (Agrawal, 1998; Agrawal and Dubin-Thaler, 1999; Bruna et al., 2004; Christianini and Machado, 2004; Dejean et al., 2008; Schatz et al., 2009), the JA-mediated production of defensive natural products takes hours to days (Joo et al., 2018; Maffei et al., 2007; McCormick et al., 2014; Schaub et al., 2010). Perhaps ant protection is not sufficiently reliable under all conditions.

The induction of volatiles by herbivory may have several functions in myrmecophytes. For various ant-plant mutualisms, it was demonstrated that volatile cues can attract mutualistic ants to the site of damage within a few minutes (Agrawal, 1998; Agrawal and Dubin-Thaler, 1999; Bruna et al., 2004; Christianini and Machado, 2004; Dejean et al., 2008; Schatz et al., 2009). Thus, any ant-attracting volatile should be released immediately upon wounding, as for instance methyl salicylate or hexanal (McCormick et al., 2014) emitted by *Leonardoxa africana* to recruit *Petalomyrmex phylax* ants (Schatz et al., 2009), and *Cecropia obtusifolia* to attract *Azteca* spp. ants (Agrawal, 1998). In *T. quadrialata*, however, only octen-3-ol and its derivatives would qualify as potential wounding signals for ants, as the other released volatiles, including terpenoids and nitrogen-containing compounds, are only emitted hours after induction (Erb et al., 2015; McCormick et al., 2014). The damage-induced emission of octen-3-ol is particularly interesting as it is mainly known as a fungal volatile and, in plants, has only been described in legumes so far (Kigathi et al., 2009). Ants also produce their own volatile alarm pheromones to attract nestmates (Agrawal and Dubin-Thaler, 1999; Bruna et al., 2004; Christianini and Machado, 2004; Dejean et al., 2008), as we observed in our volatile collections (Figure S6).

Many of the herbivore-inducible terpenoids we measured from *T. quadrialata* have been reported to be emitted upon simulated herbivory in myrmecophytic *Piper* spp. (α -pinene, β -ocimene, α -copaene, β -caryophyllene, α -humulene, α -farnesene, germacrene D) (Mayer et al., 2018) and from the non-myrmecophytic *Acacia cochliacantha* (β -ocimene, β -caryophyllene, α -farnesene, germacrene D) (Hernandez-Zepeda et al., 2018). In the latter, this blend was able to induce the secretion of extrafloral nectar in systemic leaves, implying a role for these compounds in intra-plant signaling and induction of plant defense (Hernandez-Zepeda et al., 2018). In non-myrmecophytes, studies have shown that DMNT induces direct defenses in sweet potato (Meents et al., 2019), indole primes defense induction in neighboring maize plants (Erb et al., 2015), and octen-3-ol activates JA-dependent defenses in *Arabidopsis* (Kishimoto et al., 2007). Hence, one could speculate that ant-plants might use these HIPVs as signals to warn systemic leaves or neighboring plants that ant protection is failing and activate direct plant defenses. Other HIPVs released from *T. quadrialata* plants may serve as herbivore repellents, as has been shown for (*E*)- β -caryophyllene with leaf cutter ants (North et al., 2000), for benzyl cyanide with *Lymantria dispar* caterpillars (Irmisch et al., 2014), and for methyl anthranilate with sparrows (Ahmad et al., 2018).

Besides altering the emission of volatiles, herbivory on *T. quadrialata* also enhanced the accumulation of free amino acids. Our transcriptome data suggest that this amino acid enrichment is the result of *de novo* synthesis rather than protein degradation. This response may help provide substrate for other defense reactions.

The response of *T. quadrialata* to herbivory is mediated by JA signaling

To better understand the inducible defense responses of *T. quadrialata*, we examined defense hormone levels in response to *Spodoptera* spp. herbivory. Caterpillar feeding led to the accumulation of JA and



its bioactive conjugate JA-Ile as well as increased expression of the respective genes for JA biosynthesis and response to JA, implying that the inducible responses in herbivore-damaged leaves were mainly caused by JA signaling. Indeed, the treatment of *T. quadrialata* leaves with JA resulted in the accumulation of the same amino acids that were found to be induced upon herbivory. However, not all ant-plants regulate herbivore responses in the same fashion. Myrmecophytic *Acacia* did not respond to JA treatment at all (Heil et al., 2004), or responded only in a limited way by inducing the enhanced secretion of extrafloral nectar (Heil et al., 2001b; Hernandez-Zepeda et al., 2018) and emission of volatiles (Hernandez-Zepeda et al., 2018) only in the absence of ants and only locally. The effect of JA on direct defenses has not been investigated in ant-plants at all to the best of our knowledge. Typical responses to JA signaling in non-myrmecophytes include increased glucosinolate levels (Wasternack and Hause, 2013), alkaloid biosynthesis (Wasternack and Hause, 2013), and protease inhibitor accumulation (Farmer et al., 1992). Increases in protease inhibitors triggered at the transcript level (Koiwa et al., 1997) seem to be a common JA-inducible defense across the plant kingdom (Habib and Fazili, 2007). However, unlike in other plant species (Eberl et al., 2021), herbivory and subsequent JA signaling in *T. quadrialata* did not result in a strong upregulation of protease inhibitor genes. The absence of this defense strategy might contribute to the observed high susceptibility of *T. quadrialata* to herbivory, as protease inhibitors not only have a negative impact on the digestive enzymes of insects but also protect other plant defensive proteins like peroxidases or chitinases from degradation (Mithöfer and Boland, 2012). Nevertheless, the finding that herbivory on *T. quadrialata* can induce jasmonate biosynthesis and accumulation and downstream JA-mediated defense responses demonstrates that this well-protected myrmecophyte still is able to activate typical plant defense reactions. *T. quadrialata* neither depends completely on the ant-provided protection nor lost its ability to activate chemical defenses during evolution. However, the obvious loss of protease inhibitor induction might be interpreted as the first step in that direction.

Limitations of the study

We investigated the interaction between the myrmecophytic plant *T. quadrialata* and *Azteca cf. tonduzi* on different levels, from ecological to molecular and phytochemical points of view. This included field studies in combination with metabolomics for the identification of defense compounds and RNA-Seq to analyze gene regulation. The protective role of ants and the phenomenon of myrmecotrophy have been shown for other ant-plant mutualisms but needed to be confirmed for this particular system as well. However, the chemical and molecular characterization of the plants in response to the presence/absence of ants on one hand and to herbivory, on the other hand, is a first important step toward a deeper understanding of the underlying molecular mechanisms driving this symbiosis. Combining the chemical and transcriptomic analysis, we were able to draw correlations between ecological observations and metabolic findings; nevertheless, we are still not able to fully explain how the accumulation of certain compounds or genes results in a certain phenotype. Future research will be necessary to fully understand the molecular basis and physiology of ant-plant symbiosis. Conclusive evidence for specific metabolic pathways and their impact on the plant's performance requires genetic modifications of ant-plants, which hopefully will be possible in the future.

STAR★METHODS

Detailed methods are provided in the online version of this paper and include the following:

- KEY RESOURCES TABLE
- RESOURCE AVAILABILITY
 - Lead contact
 - Materials availability
 - Data and code availability
- EXPERIMENTAL MODEL AND SUBJECT DETAILS
 - Study site and system
 - Ant-exclusion
 - ¹⁵N-labeling study
- METHOD DETAILS
 - Long-term monitoring
 - Herbivory experiment
 - Volatile collection
 - Analysis of herbivore induced volatiles

- Treatment with jasmonic acid
- Choice assay
- Plant tissue for chemical and elemental analysis
- ¹⁵N pulse-chase experiment
- Isotope analysis
- Plant defense hormone analysis
- Free amino acid analysis
- Free sugar analysis
- Full scan LC-MS analysis of ellagitannins
- Untargeted metabolomics and HRMS
- RNA extraction and illumina sequencing
- RNA-seq data analysis
- **QUANTIFICATION AND STATISTICAL ANALYSIS**

SUPPLEMENTAL INFORMATION

Supplemental information can be found online at <https://doi.org/10.1016/j.isci.2022.105261>.

ACKNOWLEDGMENTS

We thank the Explorer's Inn for accommodation, especially during the pandemic, Rudi Saul, Fabian Limonchi, and Eliana Esparza (INTE-PUCP) for help with the organization and logistics of the field work, Alfredo Ibañez (ICOPA-PUCP) for lab space and equipment, Daniel Veit and Saskia Gablenz (MPI-CE) for technical equipment, Abel Bernadou and Lina Pedraza (University of Regensburg) for the identification of the ant species, Grit Kunert for statistical advice, AIDER for assistance with the permits, SERNANP and SERFOR for the authorization of this research.

The research was funded by the Max Planck Society, and fellowships of the Friedrich Schiller University Jena as part of the IMPRS, and the German Academic Exchange Service (DAAD) to ATM.

AUTHOR CONTRIBUTIONS

AM, TGK, JG, EGC, and ATM designed the research. ATM, MR, EGC, AN, and NS performed the research. HM and HG carried out the elemental analysis. ATM, MR, and DW analyzed the data. ATM and AM wrote the article with input from all other authors.

DECLARATION OF INTERESTS

The authors declare no competing interests.

Received: July 29, 2022

Revised: September 6, 2022

Accepted: September 26, 2022

Published: October 21, 2022

REFERENCES

- Agrawal, A.A. (1998). Leaf damage and associated cues induced aggressive and recruitment in a neotropical ant-plant. *Ecology* 79, 2100–2112. <https://doi.org/10.2307/176713>.
- Agrawal, A.A., and Dubin-Thaler, B.J. (1999). Induced responses to herbivory in the Neotropical ant-plant association between Azteca ants and Cecropia trees: response of ants to potential inducing cues. *Behav. Ecol.* 45, 47–54. <https://doi.org/10.1007/s002650050538>.
- Ahmad, S., Saleem, Z., Jabeen, F., Hussain, B., Sultana, T., Sultana, S., Al-Ghanim, K.A., Al-Mulhim, N.M.A., and Mahboob, S. (2018). Potential of natural repellents methylanthranilate and anthraquinone applied on maize seeds and seedlings against house sparrow (*Passer domesticus*) in captivity. *Braz. J. Biol.* 78, 667–672. <https://doi.org/10.1590/1519-6984.171686>.
- Anstett, D.N., Cheval, I., D'Souza, C., Salminen, J.P., and Johnson, M.T.J. (2019). Ellagitannins from the Onagraceae decrease the performance of generalist and specialist herbivores. *J. Chem. Ecol.* 45, 86–94. <https://doi.org/10.1007/s10886-018-1038-x>.
- Araújo, A.R., Araújo, A.C., Reis, R.L., and Pires, R.A. (2021). Vesicalagin and castalagin present bactericidal activity toward methicillin-resistant bacteria. *ACS Biomater. Sci. Eng.* 7, 1022–1030. <https://doi.org/10.1021/acsbomaterials.0c01698>.
- Barbehenn, R.V., Jones, C.P., Hagerman, A.E., Karonen, M., and Salminen, J.-P. (2006). Ellagitannins have greater oxidative activities than condensed tannins and Galloyl glucoses at high pH: potential impact on caterpillars. *J. Chem. Ecol.* 32, 2253–2267. <https://doi.org/10.1007/s10886-006-9143-7>.
- Bartimachi, A., Neves, J., and Vasconcelos, H.L. (2015). Geographic variation in the protective effects of ants and trichomes in a Neotropical ant-plant. *Plant Ecol.* 216, 1083–1090. <https://doi.org/10.1007/s11258-015-0491-7>.
- Boeckler, G.A., Towns, M., Unsicker, S.B., Mellway, R.D., Yip, L., Hilke, I., Gershenson, J., and Constabel, C.P. (2014). Transgenic upregulation of the condensed tannin pathway in



- poplar leads to a dramatic shift in leaf palatability for two tree-feeding Lepidoptera. *J. Chem. Ecol.* **40**, 150–158. <https://doi.org/10.1007/s10886-014-0383-7>.
- Bruna, E.M., Lapola, D.M., and Vasconcelos, H.L. (2004). Interspecific variation in the defensive responses of obligate plant-ants: experimental tests and consequences for herbivory. *Oecologia* **138**, 558–565. <https://doi.org/10.1007/s00442-003-1455-5>.
- Cabrera, M., and Jaffe, K. (1994). A trophic Mutualism between the myrmecophytic Melastomataceae *Tococa guianensis* and an Azteca ant species. *Ecotropicos* **7**, 1–10.
- Chamberlain, S.A., and Holland, J.N. (2009). Quantitative synthesis of context dependency in ant-plant protection mutualisms. *Ecology* **90**, 2384–2392. <https://doi.org/10.1890/08-1490.1>.
- Chanam, J., Sheshshayee, M.S., Kasinathan, S., Jagdeesh, A., Joshi, K.A., Borges, R.M., and Kay, A. (2014). Nutritional benefits from domatia inhabitants in an ant-plant interaction: interlopers do pay the rent. *Funct. Ecol.* **28**, 1107–1116. <https://doi.org/10.1111/1365-2435.12251>.
- Chomicki, G., and Renner, S.S. (2015). Phylogenetics and molecular clocks reveal the repeated evolution of ant-plants after the late Miocene in Africa and the early Miocene in Australasia and the Neotropics. *New Phytol.* **207**, 411–424. <https://doi.org/10.1111/nph.13271>.
- Christianini, A.V., and Machado, G. (2004). Induced biotic responses to herbivory and associated cues in the Amazonian ant-plant *Maieta poeppigii*. *Entomol. Exp. Appl.* **112**, 81–88. <https://doi.org/10.1111/j.0013-8703.2004.00188.x>.
- Clavijo McCormick, A., Irmisch, S., Reinecke, A., Boeckler, G.A., Veit, D., Reichelt, M., Hansson, B.S., Gershenzon, J., Köllner, T.G., and Unsicker, S.B. (2014). Herbivore-induced volatile emission in black poplar: regulation and role in attracting herbivore enemies. *Plant Cell Environ.* **37**, 1909–1923. <https://doi.org/10.1111/pce.12287>.
- Defosse, E., Djéto-Lordon, C., McKey, D., Seloze, M.A., and Blatrix, R. (2011). Plant-ants feed their host plant, but above all a fungal symbiont to recycle nitrogen. *Proc. Biol. Sci.* **278**, 1419–1426. <https://doi.org/10.1098/rspb.2010.1884>.
- Dejean, A., Delabie, J.H.C., Cerdan, P., Gibernau, M., and Corbara, B. (2006). Are myrmecophytes always better protected against herbivores than other plants? *Biol. J. Linn. Soc. Lond.* **89**, 91–98. <https://doi.org/10.1111/j.1095-8312.2006.00660.x>.
- Dejean, A., Grangier, J., Leroy, C., and Orivel, J. (2008). Host plant protection by arboreal ants: looking for a pattern in locally induced responses. *Evol. Ecol. Res.* **10**, 1217–1223.
- Dejean, A., Petitclerc, F., Compin, A., Azémar, F., Corbara, B., Delabie, J.H.C., and Leroy, C. (2017). Hollow internodes permit a neotropical understory plant to shelter multiple mutualistic ant species, obtaining protection and nutrient provisioning (myrmecotrophy). *Am. Nat.* **190**, E124–E131. <https://doi.org/10.1086/693782>.
- Dejean, A., Petitclerc, F., Roux, O., Orivel, J., and Leroy, C. (2012). Does exogenous food benefit both partners in an ant-plant mutualism? The case of *Cecropia obtusa* and its guest *Azteca* plant-ants. *C. R. Biol.* **335**, 214–219. <https://doi.org/10.1016/j.crvi.2012.01.002>.
- Del Val, E., and Dirzo, R. (2003). Does ontogeny cause changes in the defensive strategies of the myrmecophyte *Cecropia peltata*? *Plant Ecol.* **169**, 35–41. <https://doi.org/10.1023/A:1026227811685>.
- Do Nascimento, R.R., Billen, J., Sant'ana, A.E.G., Morgan, E.D., and Harada, A.Y. (1998). Pygidial gland of *Azteca* nr. *bicolor* and *Azteca chartifex*: morphology and chemical identification of volatile components. *J. Chem. Ecol.* **24**, 1629–1637. <https://doi.org/10.1023/a:1020864427854>.
- Dodson, C.D., Dyer, L.A., Searcy, J., Wright, Z., and Letourneau, D.K. (2000). Cencoladamide, a dihydropyridone alkaloid from *Piper cenocladum*. *Phytochemistry* **53**, 51–54. [https://doi.org/10.1016/S0031-9422\(99\)00446-X](https://doi.org/10.1016/S0031-9422(99)00446-X).
- dos Santos, A.P.M., Fracasso, C.M., Luciene dos Santos, M., Romero, R., Sazima, M., and Oliveira, P.E. (2012). Reproductive biology and species geographical distribution in the Melastomataceae: a survey based on New World taxa. *Ann. Bot.* **110**, 667–679. <https://doi.org/10.1093/aob/mcs125>.
- Dyer, L.A., Dodson, C.D., Beiloffer, J., and Letourneau, D.K. (2001). Trade-offs in ant/herbivore defenses in *Piper cenocladum*: ant mutualists versus plant secondary metabolites. *J. Chem. Ecol.* **27**, 581–592. <https://doi.org/10.1023/A:1010345123670>.
- Dyer, L.A., Letourneau, D.K., Dodson, C.D., Tobler, M.A., Stireman, J.O., III, and Hsu, A. (2004). Ecological causes and consequences of variation in defensive chemistry of a neotropical shrub. *Ecology* **85**, 2795–2803. <https://doi.org/10.1890/03-0233>.
- Eberl, F., Fabisch, T., Luck, K., Köllner, T.G., Vogel, H., Gershenzon, J., and Unsicker, S.B. (2021). Poplar protease inhibitor expression differs in an herbivore specific manner. *BMC Plant Biol.* **21**, 170. <https://doi.org/10.1186/s12870-021-02936-4>.
- Erb, M., Veyrat, N., Robert, C.A.M., Xu, H., Frey, M., Ton, J., and Turlings, T.C.J. (2015). Indole is an essential herbivore-induced volatile priming signal in maize. *Nat. Commun.* **6**, 6273. <https://doi.org/10.1038/ncomms7273>.
- Farmer, E.E., Johnson, R.R., and Ryan, C.A. (1992). Regulation of expression of proteinase inhibitor genes by methyl jasmonate and jasmonic Acid. *Plant Physiol.* **98**, 995–1002. <https://doi.org/10.1104/pp.98.3.995>.
- Fiala, B., Maschwitz, U., Pong, T.Y., and Helbig, A.J. (1989). Studies of a south East Asian ant-plant association: protection of *Macaranga* trees by *Crematogaster borneensis*. *Oecologia* **79**, 463–470. <https://doi.org/10.1007/BF00378662>.
- Fincher, R.M., Dyer, L.A., Dodson, C.D., Richards, J.L., Tobler, M.A., Searcy, J., Mather, J.E., Reid, A.J., Rolig, J.S., and Pidcock, W. (2008). Inter- and intraspecific comparisons of ant/herbivore defenses in three species of rainforest understory shrubs. *J. Chem. Ecol.* **34**, 558–574. <https://doi.org/10.1007/s10886-008-9432-4>.
- Fonseca, C.R. (1994). Herbivory and the long-lived leaves of an Amazonian ant-tree. *J. Ecol.* **82**, 833–842. <https://doi.org/10.2307/2261447>.
- Fracassetti, D., Costa, C., Moulay, L., and Tomás-Barberán, F.A. (2013). Ellagic acid derivatives, ellagitannins, proanthocyanidins and other phenolics, vitamin C and antioxidant capacity of two powder products from camu-camu fruit (*Myrciaria dubia*). *Food Chem.* **139**, 578–588. <https://doi.org/10.1016/j.foodchem.2013.01.121>.
- Frederickson, M.E., Ravenscraft, A., Arcila Hernández, L.M., Booth, G., Astudillo, V., Miller, G.A., and Kitzberger, T. (2013). What happens when ants fail at plant defence? *Cordia nodosa* dynamically adjusts its investment in both direct and indirect resistance traits in response to herbivore damage. *J. Ecol.* **101**, 400–409. <https://doi.org/10.1111/1365-2745.12034>.
- Frederickson, M.E., Ravenscraft, A., Miller, G.A., Arcila Hernández, L.M., Booth, G., and Pierce, N.E. (2012). The direct and ecological costs of an ant-plant symbiosis. *Am. Nat.* **179**, 768–778. <https://doi.org/10.1086/665654>.
- Gatehouse, J.A. (2002). Plant resistance towards insect herbivores: a dynamic interaction. *New Phytol.* **156**, 145–169. <https://doi.org/10.1046/j.1469-8137.2002.00519.x>.
- Gatis-Carrazoni, A.S.S.G., Mota, F.V.B., Leite, T.C.C., de Oliveira, T.B., da Silva, S.C., Bastos, I.V.A., de Souza Maia, M.B., Pereira, P.S., Neto, P.P.M., de Oliveira Chagas, E.C., et al. (2019). Anti-inflammatory and antinociceptive activities of the leaf methanol extract of *Miconia minutiflora* (Bonpl.) DC. and characterization of compounds by UPLC-DAD-QTOF-MS/MS. *Naturyn-Schmiedberg's Arch. Pharmacol.* **392**, 55–68. <https://doi.org/10.1007/s00210-018-1561-x>.
- Gay, H. (1993). Animal-fed plants: an investigation into the uptake of ant-derived nutrients by the far-eastern epiphytic fern *Lecanopteris Reinw.* (Polypodiaceae). *Biol. J. Linn. Soc. Lond.* **50**, 221–233. <https://doi.org/10.1111/j.1095-8312.1993.tb00928.x>.
- Gontijo, D.C., Gontijo, P.C., Brandão, G.C., Diaz, M.A.N., de Oliveira, A.B., Fietto, L.G., and Leite, J.P.V. (2019). Antioxidant study indicative of antibacterial and antimutagenic activities of an ellagitannin-rich aqueous extract from the leaves of *Miconia latecrenata*. *J. Ethnopharmacol.* **236**, 114–123. <https://doi.org/10.1016/j.jep.2019.03.007>.
- González-Teuber, M., Kaltenpoth, M., and Boland, W. (2014). Mutualistic ants as an indirect defence against leaf pathogens. *New Phytol.* **202**, 640–650. <https://doi.org/10.1111/nph.12664>.
- Habib, H., and Fazili, K.M. (2007). Plant protease inhibitors: a defense strategy in plants. *Biotechnol. Mol. Biol. Rev.* **2**, 68–85.
- Heil, M., Delsinne, T., Hilpert, A., Schürkens, S., Andary, C., Linsenmair, K.E., Sousa, S. M., and McKey, D. (2002). Reduced chemical defence in ant-plants? A critical re-evaluation of a widely accepted hypothesis. *Oikos* **99**, 457–468. <https://doi.org/10.1034/j.1600-0706.2002.11954.x>.

- Heil, M., Fiala, B., Linsenmair, K.E., and Boller, T. (1999). Reduced chitinase activities in ant plants of the genus *Macaranga*. *Naturwissenschaften* 86, 146–149. <https://doi.org/10.1007/s001140050589>.
- Heil, M., Fiala, B., Linsenmair, K.E., Zotz, G., and Menke, P. (1997). Food body production in *Macaranga triloba* (Euphorbiaceae): a plant investment in anti-herbivore defence via symbiotic ant partners. *J. Ecol.* 85, 847–861. <https://doi.org/10.2307/2960606>.
- Heil, M., Fiala, B., Maschwitz, U., and Linsenmair, K.E. (2001a). On benefits of indirect defence: short- and long-term studies of ant-herbivore protection via mutualistic ants. *Oecologia* 126, 395–403. <https://doi.org/10.1007/s004420000532>.
- Heil, M., Greiner, S., Meimberg, H., Krüger, R., Noyer, J.-L., Heubl, G., Linsenmair, K.E., and Boland, W. (2004). Evolutionary change from induced to constitutive expression of an indirect plant resistance. *Nature* 430, 205–208. <https://doi.org/10.1038/nature02703>.
- Heil, M., Koch, T., Hilpert, A., Fiala, B., Boland, W., and Linsenmair, K. (2001b). Extrafloral nectar production of the ant-associated plant, *Macaranga tanarius*, is an induced, indirect, defensive response elicited by jasmonic acid. *Proc. Natl. Acad. Sci. USA* 98, 1083–1088. <https://doi.org/10.1073/pnas.031563398>.
- Heil, M., and McKey, D. (2003). Protective ant-plant interactions as model systems in ecological and evolutionary research. *Annu. Rev. Ecol. Syst.* 34, 425–553. <https://doi.org/10.1146/annurev.ecolsys.34.011802.132410>.
- Heil, M., Staehelin, C., and McKey, D. (2000). Low chitinase activity in *Acacia* myrmecophytes: a potential trade-off between biotic and chemical defences? *Naturwissenschaften* 87, 555–558. <https://doi.org/10.1007/s001140050778>.
- Hernández-Zepeda, O.F., Razo-Belman, R., and Heil, M. (2018). Reduced responsiveness to volatile signals creates a modular reward provisioning in an obligate food-for-protection mutualism. *Front. Plant Sci.* 9, 1076. <https://doi.org/10.3389/fpls.2018.01076>.
- Heyer, M., Reichelt, M., and Mithöfer, A. (2018). A holistic approach to analyze systemic jasmonate accumulation in individual leaves of *Arabidopsis* rosettes upon wounding. *Front. Plant Sci.* 9, 1569. <https://doi.org/10.3389/fpls.2018.01569>.
- Irmisch, S., Clavijo McCormick, A., Günther, J., Schmidt, A., Boeckler, G.A., Gershenzon, J., Unsicker, S.B., and Köllner, T.G. (2014). Herbivore-induced poplar cytochrome P450 enzymes of the CYP71 family convert aldoximes to nitriles which repel a generalist caterpillar. *Plant J.* 80, 1095–1107. <https://doi.org/10.1111/tpj.12711>.
- Jander, G., Norris, S.R., Joshi, V., Fraga, M., Rugg, A., Yu, S., Li, L., and Last, R.L. (2004). Application of a high-throughput HPLC-MS/MS assay to *Arabidopsis* mutant screening: evidence that threonine aldolase plays a role in seed nutritional quality. *Plant J.* 39, 465–475. <https://doi.org/10.1111/j.1365-3113X.2004.02140.x>.
- Janzen, D.H. (1966). Coevolution of mutualism between ants and acacias in central America. *Evolution* 20, 249–275. <https://doi.org/10.2307/2406628>.
- Joo, Y., Schuman, M.C., Goldberg, J.K., Kim, S., Yon, F., Brütting, C., and Baldwin, I.T. (2018). Herbivore-induced volatile blends with both “fast” and “slow” components provide robust indirect defence in nature. *Funct. Ecol.* 32, 136–149. <https://doi.org/10.1111/1365-2435.12947>.
- Karban, R., Agrawal, A.A., and Mangel, M. (1997). The benefits of induced defenses against herbivores. *Ecology* 78, 1351–1355. [https://doi.org/10.1890/0012-9658\(1997\)078\[1351:TBODIA\]2.0.CO;2](https://doi.org/10.1890/0012-9658(1997)078[1351:TBODIA]2.0.CO;2).
- Kesharwani, A., Polachira, S.K., Nair, R., Agarwal, A., Mishra, N.N., and Gupta, S.K. (2017). Anti-HSV-2 activity of *Terminalia chebula* Retz extract and its constituents, chebulagic and chebulinic acids. *BMC Compl. Alternative Med.* 17, 110. <https://doi.org/10.1186/s12906-017-1620-8>.
- Kigathi, R.N., Unsicker, S.B., Reichelt, M., Kesselmeier, J., Gershenzon, J., and Weisser, W.W. (2009). Emission of volatile organic compounds after herbivory from *Trifolium pratense* (L.) under laboratory and field conditions. *J. Chem. Ecol.* 35, 1335–1348. <https://doi.org/10.1007/s10886-009-9716-3>.
- Kishimoto, K., Matsui, K., Ozawa, R., and Takabayashi, J. (2007). Volatile 1-octen-3-ol induces a defensive response in *Arabidopsis thaliana*. *J. Gen. Plant Pathol.* 73, 35–37. <https://doi.org/10.1007/s10327-006-0314-8>.
- Klewicka, E., Sójka, M., Ścieszka, S., Klewicki, R., Młczarek, A., Lipińska, L., and Kolodziejczyk, K. (2020). The antimicrobial effect of ellagitannins from raspberry (*Rubus idaeus* L.) on *Alternaria alternata* LOCK 0409. *Eur. Food Res. Technol.* 246, 1341–1349. <https://doi.org/10.1007/s00217-020-03493-0>.
- Koivi, H., Bressan, R.A., and Hasegawa, P.M. (1997). Regulation of protease inhibitors and plant defense. *Trends Plant Sci.* 2, 379–384. [https://doi.org/10.1016/S1360-1385\(97\)90052-2](https://doi.org/10.1016/S1360-1385(97)90052-2).
- Koricheva, J., and Romero, G.Q. (2012). You get what you pay for: reward-specific trade-offs among direct and ant-mediated defences in plants. *Biol. Lett.* 8, 628–630. <https://doi.org/10.1098/rsbl.2012.0271>.
- Lackus, N.D., Müller, A., Kröber, T.D.U., Reichelt, M., Schmidt, A., Nakamura, Y., Paetz, C., Luck, K., Lindroth, R.L., Constabel, C.P., et al. (2020). The occurrence of sulfated salicinoids in poplar and their formation by Sulfotransferase1. *Plant Physiol.* 183, 137–151. <https://doi.org/10.1104/pp.19.01447>.
- Letourneau, D.K. (1998). Ants, stem-borers, and fungal pathogens: experimental tests of a fitness Advantage in *piper* ant-plants. *Ecology* 79, 593–603. <https://doi.org/10.2307/176956>.
- Letourneau, D.K., and Barbosa, P. (1999). Ants, stem borers, and pubescence in *Endospermum* in Papua New Guinea. *Biotropica* 31, 295–302. <https://doi.org/10.1111/j.1744-7429.1999.tb00141.x>.
- Maag, D., Erb, M., Köllner, T.G., and Gershenzon, J. (2015). Defensive weapons and defense signals in plants: some metabolites serve both roles. *Bioessays* 37, 167–174. <https://doi.org/10.1002/bies.201400124>.
- Madsen, S.R., Kunert, G., Reichelt, M., Gershenzon, J., and Halkier, B.A. (2015). Feeding on leaves of the glucosinolate transporter mutant *gtr1gtr2* reduces fitness of *Myzus persicae*. *J. Chem. Ecol.* 41, 975–984. <https://doi.org/10.1007/s10886-015-0641-3>.
- Maffei, M.E., Mithöfer, A., and Boland, W. (2007). Before gene expression: early events in plant-insect interaction. *Trends Plant Sci.* 12, 310–316. <https://doi.org/10.1016/j.tplants.2007.06.001>.
- Mayer, V.E., Frederickson, M.E., McKey, D., and Blatrix, R. (2014). Current issues in the evolutionary ecology of ant-plant symbioses. *New Phytol.* 202, 749–764. <https://doi.org/10.1111/nph.12690>.
- Mayer, V.E., Nepel, M., Blatrix, R., Oberhauser, F.B., Fiedler, K., Schönenberger, J., and Voglmayr, H. (2018). Transmission of fungal partners to incipient *Cecropia*-tree ant colonies. *PLoS One* 13, e0192207. <https://doi.org/10.1371/journal.pone.0192207>.
- McCormick, A.C., Boeckler, G.A., Köllner, T.G., Gershenzon, J., and Unsicker, S.B. (2014). The timing of herbivore-induced volatile emission in black poplar (*Populus nigra*) and the influence of herbivore age and identity affect the value of individual volatiles as cues for herbivore enemies. *BMC Plant Biol.* 14, 304. <https://doi.org/10.1186/s12870-014-0304-5>.
- McKey, D. (1979). The distribution of plant secondary compounds within plants. In *Herbivores: their interaction with secondary plant metabolites*, G.A. Rosenthal and D.H. Janzen, eds. (Academic Press), pp. 55–133.
- McNett, K., Longino, J., Barriga, P., Vargas, O., Phillips, K., and Sagers, C.L. (2009). Stable isotope investigation of a cryptic ant-plant association: *myrmelachista flavocotea* (Hymenoptera, Formicidae) and *Ocotea* spp. (Lauraceae). *Insectes Soc.* 57, 67–72. <https://doi.org/10.1007/s00040-009-0051-z>.
- Meents, A.K., Chen, S.P., Reichelt, M., Lu, H.H., Bartram, S., Yeh, K.W., and Mithöfer, A. (2019). Volatile DMNT systemically induces jasmonate-independent direct anti-herbivore defense in leaves of sweet potato (*Ipomoea batatas*) plants. *Sci. Rep.* 9, 17431. <https://doi.org/10.1038/s41598-019-53946-0>.
- Michelangeli, F.A. (2003). Ant protection against herbivory in three species of *Tococa* (Melastomataceae) occupying different environments. *Biotropica* 35, 181–188. <https://doi.org/10.1111/j.1744-7429.2003.tb00277.x>.
- Michelangeli, F.A. (2005). *Tococa* (Melastomataceae). *Flora Neotrop.* 98, 1–114. <https://doi.org/10.2307/4393950>.
- Mithöfer, A., and Boland, W. (2012). Plant defense against herbivores: chemical aspects. *Annu. Rev. Plant Biol.* 63, 431–450. <https://doi.org/10.1146/annurev-arplant-042110-103854>.
- Moilanen, J., Sinkkonen, J., and Salminen, J.-P. (2013). Characterization of bioactive plant ellagitannins by chromatographic, spectroscopic and mass spectrometric methods.



- Chemoecology 23, 165–179. <https://doi.org/10.1007/s00049-013-0132-3>.
- Moraes, S.C., and Vasconcelos, H.L. (2009). Long-term persistence of a Neotropical ant-plant population in the absence of obligate plant-ants. *Ecology* 90, 2375–2383. <https://doi.org/10.1890/08-1274.1>.
- Morawetz, W., Henzl, M., and Wallnöfer, B. (1992). Tree killing by herbicide producing ants for the establishment of pure *Tococa occidentalis* populations in the Peruvian Amazon. *Biodivers. Conserv.* 1, 19–33. <https://doi.org/10.1007/BF00700248>.
- Mumm, R., and Dicke, M. (2010). Variation in natural plant products and the attraction of bodyguards involved in indirect plant defense. *Can. J. Zool.* 88, 628–667. <https://doi.org/10.1139/z10-032>.
- North, R.D., Howse, P.E., and Jackson, C.W. (2000). Agonistic behavior of the leaf-cutting ant *Atta sexdens rubropilosa* elicited by carophyllene. *J. Insect Behav.* 13, 1–13. <https://doi.org/10.1023/A:1007749723868>.
- O'Dowd, D.J. (1980). Pearl bodies of a neotropical tree, *Ochroma pyramidale*: ecological implications. *Am. J. Bot.* 67, 543–549. <https://doi.org/10.2307/2442294>.
- Ohmura, W., Hishiyama, S., Nakashima, T., Kato, A., Makihara, H., Ohira, T., and Irei, H. (2009). Chemical composition of the defensive secretion of the longhorned beetle, *Chloridolum lochooanum*. *J. Chem. Ecol.* 35, 250–255. <https://doi.org/10.1007/s10886-009-9591-y>.
- Pang, Z., Chong, J., Zhou, G., de Lima Moraes, D.A., Chang, L., Barrette, M., Gauthier, C., Jacques, P.E., Li, S., and Xia, J. (2021). MetaboAnalyst 5.0: narrowing the gap between raw spectra and functional insights. *Nucleic Acids Res.* 49, W388–W396. <https://doi.org/10.1093/nar/gkab382>.
- Renner, S.S., and Ricklefs, R.E. (1998). Herbicidal activity of domatia-inhabiting ants in patches of *Tococa guianensis* and *Clidemia heterophylla*. *Biotropica* 30, 324–327. <https://doi.org/10.1111/j.1744-7429.1998.tb00067.x>.
- Rhoades, D.F. (1979). Evolution of plant defense against herbivores. In *Herbivores: their interaction with secondary metabolites*, G.A. Rosenthal and D.H. Janzen, eds. (Academic Press), pp. 1–55.
- Risso, D., Ngai, J., Speed, T.P., and Dudoit, S. (2014). Normalization of RNA-seq data using factor analysis of control genes or samples. *Nat. Biotechnol.* 32, 896–902. <https://doi.org/10.1038/nbt.2931>.
- Robinson, M.D., McCarthy, D.J., and Smyth, G.K. (2010). edgeR: a Bioconductor package for differential expression analysis of digital gene expression data. *Bioinformatics* 26, 139–140. <https://doi.org/10.1093/bioinformatics/btp616>.
- Roslin, T., and Salminen, J.P. (2008). Specialization pays off: contrasting effects of two types of tannins on oak specialist and generalist moth species. *Oikos* 117, 1560–1568. <https://doi.org/10.1111/j.2008.0030-1299.16725.x>.
- Rosumek, F.B., Silveira, F.A.O., de S Neves, F., de U Barbosa, N.P., Diniz, L., Oki, Y., Pezzini, F., Fernandes, G.W., and Cornelissen, T. (2009). Ants on plants: a meta-analysis of the role of ants as plant biotic defenses. *Oecologia* 160, 537–549. <https://doi.org/10.1007/s00442-009-1309-x>.
- RStudio_Team (2021). RStudio: Integrated Development Environment for R (RStudio PBC). <http://www.rstudio.com/>.
- Sagers, C.L., Ginger, S.M., and Evans, R.D. (2000). Carbon and nitrogen isotopes trace nutrient exchange in an ant-plant mutualism. *Oecologia* 123, 582–586. <https://doi.org/10.1007/PL00008863>.
- Salminen, J.P. (2014). The chemistry and chemical ecology of ellagitannins in plant–insect interactions: from underestimated molecules to bioactive plant constituents. In *Recent Advances in Polyphenol Research*, A. Romani, V. Lattanzio, and S. Quideau, eds. (Wiley-Blackwell), pp. 83–113.
- Schatz, B., Djieto-Lordon, C., Dormont, L., Bessi re, J.M., McKey, D., and Blatrix, R. (2009). A simple non-specific chemical signal mediates defence behaviour in a specialised ant-plant mutualism. *Curr. Biol.* 19, R361–R362. <https://doi.org/10.1016/j.cub.2009.03.026>.
- Schaub, A., Blande, J.D., Graus, M., Oksanen, E., Holopainen, J.K., and Hansel, A. (2010). Real-time monitoring of herbivore induced volatile emissions in the field. *Physiol. Plant.* 138, 123–133. <https://doi.org/10.1111/j.1399-3054.2009.01322.x>.
- Schneider, C.A., Rasband, W.S., and Eliceiri, K.W. (2012). NIH Image to ImageJ: 25 years of image analysis. *Nat. Methods* 9, 671–675. <https://doi.org/10.1038/nmeth.2089>.
- Schupp, E.W. (1986). Azteca protection of Cecropia: ant occupation benefits juvenile trees. *Oecologia* 70, 379–385. <https://doi.org/10.1007/BF00379500>.
- Seigler, D.S., and Ebinger, J.E. (1987). Cyanogenic glycosides in ant-acacias of Mexico and Central America. *SW. Nat.* 32, 499–503. <https://doi.org/10.2307/3671484>.
- Serna, D.M.O., and Martinez, J.H.I. (2015). Phenolics and polyphenolics from Melastomataceae species. *Molecules* 20, 17818–17847. <https://doi.org/10.3390/molecules201017818>.
- Simão, F.A., Waterhouse, R.M., Ioannidis, P., Kriventseva, E.V., and Zdobnov, E.M. (2015). BUSCO: assessing genome assembly and annotation completeness with single-copy orthologs. *Bioinformatics* 31, 3210–3212. <https://doi.org/10.1093/bioinformatics/btv351>.
- Solano, P.J., and Dejean, A. (2004). Ant-fed plants: comparison between three geophytic myrmecophytes. *Biol. J. Linn. Soc. Lond.* 83, 433–439. <https://doi.org/10.1111/j.1095-8312.2004.00381.x>.
- Stanton, M.L., and Palmer, T.M. (2011). The high cost of mutualism: effects of four species of East African ant symbionts on their myrmecophyte host tree. *Ecology* 92, 1073–1082. <https://doi.org/10.1890/0012-9658-92-5-1073>.
- Svoma, E., and Morawetz, W. (1992). Drüsenhaare, Emergenzen und Blattdomatien bei der Ameisenpflanze *Tococa occidentalis* (Melastomataceae). *Bot. Jahrb. Syst.* 114, 185–200.
- Turlings, T.C.J., and Wäckers, F. (2004). Recruitment of predators and parasitoids by herbivore-injured plants. In *Advances in Insect Chemical Ecology*, J.G. Millar and R.T. Cardé, eds. (Cambridge University Press), pp. 21–75. <https://doi.org/10.1017/CBO9780511542664.003>.
- Turner, I.M. (1995). Foliar defences and habitat adversity of three Woody plant communities in Singapore. *Funct. Ecol.* 9, 279–284. <https://doi.org/10.2307/2390574>.
- Vasconcelos, H.L., and Davidson, D.W. (2000). Relationship between plant size and ant associates in two Amazonian ant-plants. *Biotropica* 32, 100–111. <https://doi.org/10.1111/j.1744-7429.2000.tb00452.x>.
- Ward, D., and Young, T.P. (2002). Effects of large mammalian herbivores and ant symbionts on condensed tannins of *Acacia drepanolobium* in Kenya. *J. Chem. Ecol.* 28, 921–937. <https://doi.org/10.1023/A:1015249431942>.
- Wastermack, C., and Hause, B. (2013). Jasmonates: biosynthesis, perception, signal transduction and action in plant stress response, growth and development. An update to the 2007 review. *Ann. Bot.* 111, 1021–1058. <https://doi.org/10.1093/aob/mct067>.
- Werner, R.A., and Brand, W.A. (2001). Referencing strategies and techniques in stable isotope ratio analysis. *Rapid Commun. Mass Spectrom.* 15, 501–519. <https://doi.org/10.1002/rcm.258>.
- Yoshida, T., Ohbayashi, H., Ishihara, K., Ohwashi, W., Haba, K., Okano, Y., Shingu, T., and Okuda, T. (1991). Tannins and related polyphenols of melastomataceous plants. I. Hydrolyzable tannins from *Tibouchina semidecandra* COGN. *Chem. Pharm. Bull.* 39, 2233–2240. <https://doi.org/10.1248/cpb.39.2233>.
- Yu, G., Wang, L.-G., Han, Y., and He, Q.-Y. (2012). clusterProfiler: an R Package for comparing biological themes among gene clusters. *OMICS* 16, 284–287. <https://doi.org/10.1089/omi.2011.0118>.

STAR★METHODS

KEY RESOURCES TABLE

| REAGENT or RESOURCE | SOURCE | IDENTIFIER |
|--|---------------------------------------|-------------------------------------|
| Biological samples | | |
| <i>Tococa quadrialata</i> leaves | this paper | NCBI:txid427262 |
| Chemicals, peptides, and recombinant proteins | | |
| n-bromodecane | Sigma-Aldrich | 145785, CAS:112-29-8 |
| Jasmonic acid (JA) | synthesized by Anja David, MPI-CE | adavid@ice.mpg.de, CAS: 77026-92-7 |
| ¹⁵ N-Glycine | Eurisotope | NLM-202-1 |
| D ₆ -JA | HPC Standards GmbH | 674797 |
| D ₆ -ABA | Toronto Research Chemicals | A110002 |
| D ₄ -5A | Santa Cruz Biotechnology | sc-212908 |
| D ₆ -JA-Ile | HPC Standards GmbH | 674798 |
| algal labelled amino acid mix | Isotec | T81-11001, Sigma-Aldrich:487910 |
| ¹³ C ₆ -glucose | Sigma-Aldrich | 389374 |
| ¹³ C ₆ -fructose | Toronto Research Chemicals | F792546 |
| DNaseI | ZymoResearch | E1010 |
| vescalagin | Sigma-Aldrich | 76418-5MG, CAS: 36001-47-5 |
| α-pinene | Fluka | 80604, CAS: 7785-70-8 |
| (E)-β-cimene | Firmenich | 948840, CAS: 3779-61-6 |
| (E)-DMNT | synthesized by Stefan Bartram, MPI-CE | bartram@ice.mpg.de, CAS: 19945-61-0 |
| α-copaene | Fluka | 27814, CAS: 3856-25-5 |
| (E)-β-caryophyllene | Sigma-Aldrich | C9653, CAS: 87-44-5 |
| α-humulene | Sigma-Aldrich | 53675, CAS: 6753-98-6 |
| germacrene D | Isolated by Stefan Bartram, MPI-CE | bartram@ice.mpg.de, CAS: 37839-63-7 |
| α-farnesene | Sigma-Aldrich | W383902, CAS: 502-61-4 |
| indole | Sigma-Aldrich | I3408, CAS: 120-72-9 |
| methyl anthranilate | Sigma-Aldrich | M29703, CAS: 134-20-3 |
| 2-heptanone | Sigma-Aldrich | 537683, CAS: 110-43-0 |
| 2-heptanol | Fluka | 51800, CAS: 543-49-7 |
| oct-1-en-3-ol | Fluka | 74950, CAS: 3391-86-4 |
| 3-octanone | Merck | 821860, CAS: 106-68-3 |
| octan-3-ol | Sigma-Aldrich | 218405, CAS: 589-98-0 |
| benzyl cyanide | Merck | 8.01811, CAS: 140-29-4 |
| Critical commercial assays | | |
| Spectrum Plant Total RNA Kit | Sigma-Aldrich | STRN50 |
| One-Step PCR Inhibitor Removal Kit | ZymoResearch | D6030 |
| Deposited data | | |
| Raw reads (transcriptome sequencing) | this paper | PRJNA865704 |
| Experimental models: Organisms/strains | | |
| <i>Tococa quadrialata</i> | this paper | NCBI:txid427262 |
| <i>Azteca</i> spp. | this paper | NCBI:txid121511 |
| <i>Spodoptera</i> spp. | this paper | NCBI:txid7106 |

(Continued on next page)

| <i>Continued</i> | | |
|---|---|---|
| REAGENT or RESOURCE | SOURCE | IDENTIFIER |
| Software and algorithms | | |
| ImageJ | Schneider et al. (2012) | https://imagej.nih.gov/ij/ |
| NIST/EPA/NIH EI Mass Spectral Library | National Institute of Standards and Technology | https://chemdata.nist.gov/dokuwiki/doku.php?id=chemdata%3Adownloads%3Astart#nist_epa_nih_mass_spectral_database |
| Analyst 1.6.3 | Applied Biosystems | https://sciex.com/products/software/analyst-software |
| Metaboscape software | Bruker Daltonics | https://www.bruker.com/en/products-and-solutions/mass-spectrometry/ms-software/metaboscape.html |
| CLC Genomics Workbench | Qiagen Bioinformatics | https://www.qiagen.com/us/products/discovery-and-translational-research/next-generation-sequencing/informatics-and-data/analysis-and-visualization/clc-genomics-workbench/ |
| OmicsBox software | biobam | https://www.biobam.com/omicsbox/ |
| R | RStudio Team (2021) | http://www.rstudio.com/ |
| OriginPro | OriginLab Corporation | https://www.originlab.com/ |
| SciFinder | CAS | https://scifinder.cas.org |
| Other | | |
| PoraPak filter | Material: Alltech, packed filters bought from http://www.volatilecollectiontrap.com/main.sc | VCT-1/4-3-POR-Q-25MG |
| GC-MS | Agilent Technologies | Agilent 6890 GC & 5973 MS |
| Optima-5 column | Macherey-Nagel | 726056.30 |
| PET bags | Toppits® | Bratschlauch |
| HPLC | Agilent Technologies | Agilent 1260 & Agilent 1100 |
| Zorbax Eclipse XDB-C18 column (API6500) | Agilent Technologies | 927975-902 |
| Zorbax Eclipse XDB-C18 column (timsToF) | Agilent Technologies | 981758-902 |
| QTRAP 6500 tandem mass spectrometer | AB Sciex | https://sciex.com/products/mass-spectrometers |
| HILIC column | Supelco | 56401AST |
| ESI iontrap mass spectrometer | Bruker Daltonics | Esquire 6000 https://www.bruker.com/en/products-and-solutions/mass-spectrometry/esi-ion-trap.html |
| Phenyl-Hexyl column | Phenomenex | 00F-4257-E0 |
| Dionex Ultimate 3000 series UHPLC | Thermo Scientific | https://www.thermofisher.com/de/en/home.html |
| Bruker timsToF mass spectrometer | Bruker Daltonics | timsTOF https://www.bruker.com/en/products-and-solutions/mass-spectrometry/timstof/timstof.html |
| isotope ratio mass spectrometer | Thermo Finnigan | Delta + XL |
| elemental analyzer | CE Instruments | NA1110 (now EA1110, part N° 112 110 52) |

RESOURCE AVAILABILITY

Lead contact

Further information and requests for resources and reagents should be directed to and will be fulfilled by the lead contact, Axel Mithöfer (amithoef@ice.mpg.de).

Materials availability

This study did not generate new unique reagents.

Data and code availability

- The RNA-Seq data generated in this study were deposited at NCBI SRA and are publicly available as of the date of publication. The accession number is listed in the [key resources table](#).
- The paper does not report original code.
- Any additional information required to reanalyze the data reported in this paper is available from the [lead contact](#) upon request.

EXPERIMENTAL MODEL AND SUBJECT DETAILS**Study site and system**

The experiments were conducted in the Tambopata Reserve [12° 50' 10" S, 69° 17' 34" W] close to the Explorer's Inn lodge in the lowland Amazon basin of Peru (Madre de Dios province) at an elevation a.s.l. of 210 m. The average annual rainfall is 2377 mm with a dry season from June until October. The maximum monthly temperature is around 30°C whereas the monthly minimum was found to be around 19°C.

For the individual experiments, we worked with several subpopulations of *T. quadrialata* found at different spots in the reserve and inhabited by distinct ant colonies and/or species. The *Tococa* species was determined following [Michelangeli \(2005\)](#). All mutualistic ants belonged to the genus *Azteca* (pers. comm. P.-J. Malé), and the species was identified based on morphological features, following the key for Neotropical *Azteca* species: <https://ants.biology.utah.edu/GENERA/AZTECA/key.html#BM110> (accessed: 22.03.2022).

Spodoptera spp. are well-studied generalist herbivores. Larvae were collected from local fields and starved for 24 h before the experiments. For volatile collections and herbivory treatments, larvae of the 4th and 5th instar were used, whereas choice experiments were conducted with larvae of the 2nd and 3rd instar. All larvae were removed immediately after the respective experiment.

Ant-exclusion

The subpopulation of *T. quadrialata* used for the ant-exclusion study was found alongside a small path. All individuals were colonized by *Azteca* cf. *tonduzi* (subfamily Dolichoderinae), which are obligate plant-ants. It's noteworthy that *Azteca* is a polygynous genus so even though multiple ant queens were found within the plot, the whole subpopulation of *T. quadrialata* seemed to be colonized by a single, large ant colony. The ants mainly lived inside the domatia of the plants, however, in some cases, they also formed carton nests around the stem.

The *T. quadrialata* population consisted of 70 very young plants, the tallest one measuring 80 cm in height and the largest one having 21 leaves with domatia. Some of the population were transplanted within the plot in May 2018 to assure enough space for each individual. In October 2018, all plants with a minimum height of 20 cm and a minimum number of four domatia were randomly assigned to two groups: ant-colonized and ant-deprived. Ant exclusion from 20 plants was achieved by flushing every domatium several times with water and carefully squeezing the flushed domatia to guarantee complete ant removal. Additional ants found on the leaves and stem were removed manually using forceps. As a control treatment, domatia of colonized plants were squeezed, but not flushed, although this was reported to not cause any effect in previous ant-exclusion experiments. To prevent recolonization and herbivore damage, rain and light permeable nets were put around the plants and dug into the ground to block any access. In addition, plastic fences painted with Tanglefoot, a non-toxic, sticky resin serving as a mechanical barrier, were installed around the individuals.

Both 4 days and 6 weeks after ant removal, all domatia were flushed again and any remaining ants were removed. In the course of the experiment, plants were repeatedly checked for recolonization and whenever it occurred, the ant-removal procedure was repeated, and the individual was excluded from any experiment for the next 6 months.

The 20 ant-colonized plants in this experiment were covered with nets as well to ensure the same light conditions. However, nets were open to the ground allowing free movement of the ants along the plants.



¹⁵N-labeling study

For the labeling study, we used isolated individuals from three distinct subpopulations of *T. quadrialata* associated with *Azteca* spp. in the same area. The selected plants were 60–120 cm in size with 10–20 leaves. In two of the plants, the ants were living exclusively inside the plant whereas in the other, the colony also formed carton nests.

METHOD DETAILS

Long-term monitoring

To investigate the effect of the presence or absence of ants on the performance of *T. quadrialata*, the height, leaf and domatium number as well as the herbivore damage of all plants and treatments from the main plot were monitored over time. Data were collected over a time span of three yrs from 2018–2021, but no data could be obtained in 2020 due to the COVID-19 pandemic. Herbivore damage was estimated by two experimenters on a scale of 0–10, where 0 is no leaf damage and 10 no remaining leaf tissue. Only fully opened leaves and domatia with a minimum diameter of 0.5 cm were considered. Since leaves of the protected plants were collected for several experiments, this additional leaf loss was taken into account for growth measurements. These removed leaves appear in the statistics as still belonging to the plants, without considering the possibility of natural loss.

Herbivory experiment

The reaction to herbivory was studied using 10–16 ant-inhabited and 10–16 non-colonized individuals from the ant-exclusion experiment. The plants of each group were divided in half and randomly assigned to the herbivory or control groups. One leaf of the second pair of fully expanded leaves was enclosed with a PET bag (Toppits® Bratschlauch, Minden, Germany) to avoid herbivore escape. Two *Spodoptera*, spp. larvae were released on all leaf samples of the herbivory group and allowed to feed for 24 hours, whereas the control leaves were enclosed with an empty bag for 24 h. At the end of the experiment, all leaves were excised and photographed to determine the leaf damage, the midrib and domatium were removed and both halves of the leaf lamina were immediately but separately flash-frozen in liquid nitrogen. One half of each leaf sample was stored at -80°C until further processing to extract RNA, the other half was lyophilized for subsequent chemical analysis. *Spodoptera* larvae were conserved in ethanol. The experiment was conducted 6 months, 12 months, and 33 months after ant-exclusion.

Volatile collection

Simultaneously to the herbivore treatment, volatiles were collected over 24 h hours using a push-pull system, where charcoal purified air was pumped into the bag at a flow rate of 0.4 L min⁻¹ while 0.3 L min⁻¹ were pumped from the plant headspace out of the system passing through a 20 mg PoraPak (Alltech, Deerfield, IL, USA) filter that absorbed the volatiles. As controls, volatiles found in PET bags containing only *Spodoptera*, only *Azteca* ants or just purified air were collected in the same way. The experiment was performed in October 2019, 1 y after the ant-exclusion. As the feeding behavior of the larvae, the temperature, and hence the volatile production varied widely, the experiment was repeated in June, July and August 2021. Photographs of the wounded and controlled leaves allowed the determination of leaf size and feeding damage. Herbivory samples with a damage smaller than 1% of leaf area were excluded from further statistical analyses.

Analysis of herbivore induced volatiles

Volatiles were eluted from PoraPak filters using 200 µL dichloromethane containing 10 ng/µL n-bromodecane (Sigma-Aldrich, Taufkirchen, Germany) as an internal standard. Samples were analyzed using a Hewlett-Packard model 6890 gas chromatograph (Agilent Technologies, Santa Clara, CA, USA) equipped with a 30 m × 0.25 mm × 0.25 µm Optima-5 column (Macherey-Nagel, Düren, Germany) with 1 µL splitless injection. The injector was held at 220°C and helium (MS) or H₂ (FID) was used as a carrier gas at 2 mL/min. The oven temperature of the GC-MS was held at 45°C for 2 min, then increased to 200°C at a rate of 6°C/min and further increased to 300°C at a rate of 60°C/min where it was hold again for 2 min.

For the identification of the volatiles, the GC was coupled to an Agilent model 5973 mass spectrometer with a quadrupole mass selective detector (transfer line temperature, 270°C; source temperature, 230°C; quadrupole temperature, 150°C; ionization potential, 70 eV; scan range of 50–400 amu). Compounds were identified using the NIST Mass Spectral Search Program (National Institute of Standards and Technology,

Gaithersburg, MD, USA) to search the NIST/EPA/NIH EI Mass Spectral Library (NIST 17) and/or authentic standards.

Quantification was performed with the trace of a flame ionization detector (FID) operated at 300°C. Peak areas of the compounds were compared to the peak area of the internal standard *n*-bromodecane applying equal response factors on a weight basis.

Treatment with jasmonic acid

The role of jasmonic acid (JA, synthesized by Anja David, MPI-CE) in *Tococa* was studied on 8 ant-inhabited and 8 uninhabited individuals from the ant-exclusion experiment. Plants of each group were divided in half and randomly assigned to the JA or the control group. One leaf per plant was sprayed with approx. 1 mL 1 mM JA aq. (1/200 (v/v) EtOH/H₂O) or water (1/200 (v/v) EtOH/H₂O). Leaves were allowed to dry for 1 h and then were enclosed with PET bags (Toppits Bratschlauch, Minden, Germany). After 24 h, all leaves were excised, midrib and domatium removed, the lamina flash-frozen in liquid nitrogen and later on lyophilized for subsequent chemical analyses. This experiment was conducted 34 months after ant-removal.

Choice assay

Leaf discs (22 mm diameter) were excised from undamaged leaves of ant-colonized and ant-deprived plants and offered to individual 2nd-3rd instar *Spodoptera* larvae (n = 41) in custom-made petri dishes (see Figure S6B; for more detail (Boeckler et al., 2014)). After 24 h, the remaining leaf tissue was photographed and the consumed leaf area was determined using ImageJ (Schneider et al., 2012).

Plant tissue for chemical and elemental analysis

After 2.5 yrs following ant exclusion (May 2021), 8 colonized and 8 ant-deprived plants were chosen and one leaf of the second pair of fully expanded leaves of each plant collected. After the removal of midrib and domatia, both halves of the leaf lamina were immediately but separately flash-frozen in liquid nitrogen. One half of each leaf sample was stored at -80°C until further processing to extract RNA, while the other half was lyophilized for chemical analysis.

To analyze the impact of Azteca ants on the plant's nutrient supply, a part of the lyophilized leaf samples from this sampling and from the herbivory experiments were used for C:N-ratio analysis.

¹⁵N pulse-chase experiment

Aqueous solutions of 20 mg of 98% ¹⁵N-Glycine (Eurisootope, Saint-Aubin, France) mixed with honey 1:4 (v/v) were prepared. Eppendorf tubes with the ¹⁵N-labeled glycine-honey mix were attached at the stem beneath the youngest pair of fully expanded leaves of each plant. As control, 5 cm² leaf samples of the plants were collected immediately before the start of the experiment. Furthermore, one of the youngest leaves was wrapped into a perforated plastic bag to ensure that no ant could contact the leaf after feeding on the sugar enriched with [¹⁵N]glycine and thereby contaminate it. The honey mixtures were consumed by the ants within a few days. Samples of the protected leaves as well as the unprotected neighboring leaves were taken 30 days after the pulse. After 6 and 24 months, newly grown leaves were collected. Leaf samples were dried in the field using silica gel and later in an oven at 60°C for 3 days.

Isotope analysis

1 mg of homogenous leaf powder was weighted in a tin capsule. $\delta^{13}\text{C}$ and $\delta^{15}\text{N}$ isotope analyses were conducted on an elemental analyzer (NA1110, CE Instruments, Milan, Italy) coupled to a Delta+XL isotope ratio mass spectrometer (Thermo Finnigan, Bremen, Germany) via a ConFlow III. Sample element amounts were scaled against an in house standard "Ali-j3" (acetanilide) with $\delta^{13}\text{C}$ and $\delta^{15}\text{N}$ values of $-30.06 \pm 0.1\text{‰}$ and $-1.51 \pm 0.1\text{‰}$ on the $\delta^{13}\text{C}_{\text{VPDB-LSVEC}}$ and $\delta^{15}\text{N}_{\text{AIR-N2}}$ scales, respectively. A caffeine "caf-j3" sample was analyzed multiple times per sequence as quality control with values of $-40.46 \pm 0.1\text{‰}$ and $-15.46 \pm 0.1\text{‰}$ on the $\delta^{13}\text{C}_{\text{VPDB-LSVEC}}$ and $\delta^{15}\text{N}_{\text{AIR-N2}}$ scales, respectively. Linearity, blank and drift corrections were done for each sequence according to Werner and Brand, 2001 (Werner and Brand, 2001).

Plant defense hormone analysis

Hormones were extracted from 20 mg of freeze-dried ground leaf powder with 0.5 mL of methanol (MeOH) containing the internal standards: 40 ng/mL D₆-JA (HPC Standards GmbH, Germany), D₆-ABA (Toronto



Research Chemicals, Toronto, Canada), D₄-SA (Santa Cruz Biotechnology, USA), and 8 ng/mL D₆-JA-Ile (HPC Standards GmbH, Germany)]. The homogenate was mixed for 30 min and centrifuged at 16,000 g for 10 min. The filtrated supernatant was used for hormone analysis. Compound separation was achieved by liquid chromatography (Agilent 1260; Agilent Technologies, Waldbronn, Germany) on a Zorbax Eclipse XDB-C18 column (50 mm × 4.6 mm, 1.8 μm, Agilent Technologies). Column temperature was maintained at 20°C, the flow rate was constant at 1.1 mL/min. Both 0.05% formic acid in H₂O (A) and 100% acetonitrile (B) were employed as mobile phases A and B. The elution profile was: 0–0.5 min, 5% B; 0.5–6.0 min, 5–37.4% B; 6.02–7.5 min, 80–100% B; 7.5–9.5 min, 100% B; 9.52–12 min, 5% B. An QTRAP 6500 tandem mass spectrometer (AB Sciex, Framingham, MA, USA) was operated in the negative ionization mode, using scheduled multiple reaction monitoring (MRM) to monitor analyte parent ion → product ion formation for detection of JA, JA-Ile, ABA, SA and the respective labeled standards see [Heyer et al. \(2018\)](#). For SO₄-JA: *m/z* 305.0 → 97.0 (CE -55 V; DP -30 V). For OH-JA: *m/z* 225.1 → 59.0 (CE -24 V; DP -30 V). For OH-JA-Ile: *m/z* 338.1 → 130.1 (CE -30 V; DP -30 V). For COOH-JA-Ile: *m/z* 352.1 → 130.1 (CE -30 V; DP -30 V). Chromatograms were analyzed using the software Analyst 1.6.3 (Applied Biosystems, Bedford, MA, USA) with automated peak integration. The quantification was realized by comparing the sample peak areas with the peak area of the internal standards. The concentrations of OH-JA and SO₄-JA were quantified relative to D₆-JA applying a theoretical response factor of 1.0 and the determined response factor 6.0, respectively. The levels of 12-hydroxy-JA-Ile (OH-JA-Ile) and 12-carboxy-JA-Ile (COOH-JA-Ile) were determined relative to D₆-JA-Ile applying a theoretical response factor of 1.0.

Free amino acid analysis

For the quantification of free amino acids, the raw extracts used for phytohormone analysis were diluted 1:10 with water containing an algal amino acid mix (10 μg mL⁻¹ U-¹³C, U-¹⁵N isotopically labelled amino acid mix; Isotec, Miamisburg, OH, USA) as internal standard. The extracts were analyzed on an Agilent 1260 Infinity high-performance liquid chromatography system (Agilent Technologies) coupled to an API 6500 ESI-Triple Quad mass spectrometer (AB Sciex, Darmstadt, Germany). Separation was achieved on a Zorbax Eclipse XDB-C18 column (50 mm × 4.6 mm, 1.8 μm, Agilent Technologies). Both 0.05% formic acid in H₂O and acetonitrile were employed as mobile phases A and B, respectively. The elution profile was 0–1 min 3% B; 1.0–2.7 min 3–100% B; 2.7–3.0 min 100% B; 3.1–6.0 min 3% B. Column temperature was maintained at 20°C, the flow rate was constant at 1.1 mL/min. The mass spectrometer was operated in the positive ionization mode with multiple reaction monitoring (MRM) as described by [Jander et al. \(2004\)](#). The Analyst 1.6.3 software (Applied Biosystems) was used for data acquisition and processing. Individual amino acids in the sample were quantified by the respective ¹³C, ¹⁵N-labelled amino acid internal standard, except for tryptophan that was quantified using ¹³C, ¹⁵N-Phe applying a response factor of 0.42.

Free sugar analysis

Soluble sugars were analyzed from the methanol extracts (at 1:10 dilution in water containing 5 μg/mL ¹³C₆-glucose (Sigma-Aldrich), and 5 μg/mL ¹³C₆-fructose (Toronto Research Chemicals, Toronto, Canada), by LC-MS/MS as described in ([Madsen et al., 2015](#)). The diluted extracts were analyzed on an Agilent 1200 Infinity high-performance liquid chromatography system (Agilent Technologies) coupled to an API 3200 ESI-Triple Quad mass spectrometer (AB Sciex). Separation was achieved on a HILIC column (apHera NH2 Polymer; Supelco, Bellefonte, PA, USA; 150 mm × 4.6 mm, 5 μm). H₂O and acetonitrile were employed as mobile phases A and B, respectively. The elution profile was 0–0.5 min 80% B; 0.5–13 min 80–55% B; 13–14 min 80% B; 14–18 min 80% B. Column temperature was maintained at 20°C, the flow rate was constant at 1.0 mL/min. The mass spectrometer was operated in the negative ionization mode with multiple reaction monitoring (MRM) to monitor analyte parent ion → product ion: glucose (*m/z* 178.8 → 89.0), fructose (*m/z* 178.8 → 89.0), ¹³C₆-glucose (*m/z* 185.0 → 92.0), ¹³C₆-fructose (*m/z* 185.0 → 92.0), sucrose (*m/z* 340.9 → 59.0). The Analyst 1.6.3 software (Applied Biosystems) was used for data acquisition and processing. The concentrations of glucose and fructose were determined relative to the internal standards of ¹³C₆-glucose and ¹³C₆-fructose, respectively. The content of sucrose (Sigma-Aldrich) was calculated based on an external standard curve.

Full scan LC-MS analysis of ellagitannins

MS experiments were carried out using an Esquire 6000 electrospray iontrap mass spectrometer (ESI-MS; Bruker Daltonics, Bremen, Germany) after separation by Agilent 1100 HPLC (Agilent Technologies) using a Luna Phenyl-Hexyl 100 Å column (4.6 × 150 mm, 5 μm; Phenomenex, Aschaffenburg, Germany). The binary mobile phase consisted of 0.2% formic acid in H₂O (A) and acetonitrile (B) at the flow rate of 1 mL min⁻¹. The

elution profile was: 0–20 min, 5–25% B; 20–20.1 min, 25–100% B; 20.1–23 min 100% B; 23–23.1 min 100–5% B; 23.1–28 min 5% B. The ESI-MS was operated in negative ionization mode, scanning m/z between 100 and 1400, and with an optimal target mass adjusted to m/z 550. The mass spectrometer was operated at the following specifications: capillary exit voltage, -132 eV; capillary voltage, $-3,000$ V; nebulizer pressure, 35 psi; drying gas, 11 L min^{-1} ; gas temperature, 330°C . The instrument was further coupled to a diode array detector, which enabled measurement of the absorption spectra of the ellagitannins.

Untargeted metabolomics and HRMS

The methanolic extracts of *T. quadrialata* leaves were analyzed in an untargeted metabolomic approach as described by Lackus et al. (2020) with a randomized sample order. Ultra-high-performance liquid chromatography–electrospray ionization–high resolution mass spectrometry (UHPLC–ESI–HRMS) was performed with a Dionex Ultimate 3000 series UHPLC (Thermo Scientific) and a Bruker timsToF mass spectrometer (Bruker Daltonics, Bremen, Germany). UHPLC was used applying a reversed-phase Zorbax Eclipse XDB-C18 column (100 mm \times 2.1 mm, 1.8 μm , Agilent Technologies, Waldbronn, Germany) with a solvent system of 0.1% formic acid (A) and acetonitrile (B) at a flow rate of 0.3 mL/min. The elution profile was the following: 0 to 0.5 min, 5% B; 0.5 to 11.0 min, 5% to 60% B in A; 11.0 to 11.1 min, 60% to 100% B, 11.1 to 12.0 min, 100% B and 12.1 to 15.0 min 5% B. Electrospray ionization (ESI) in negative/positive ionization mode was used for the coupling of LC to MS. The mass spectrometer parameters were set as follows: capillary voltage 4.5 KV/3.5KV, end plate offset of 500V, nebulizer pressure 2.8 bar, nitrogen at 280°C at a flow rate of 8L/min as drying gas. Acquisition was achieved at 12 Hz with a mass range from m/z 50 to 1500, with data-dependent MS/MS and an active exclusion window of 0.1 min, a reconsideration threshold of 1.8-fold change, and an exclusion after 5 spectra. Fragmentation was triggered on an absolute threshold of 50 counts and acquired on the two most intense peaks with MS/MS spectra acquisition of 12 Hz. Collision energy was alternated between 20 and 50V. At the beginning of each chromatographic analysis 10 μL of a sodium formate-isopropanol solution (10 mM solution of NaOH in 50/50 (v/v%) isopropanol water containing 0.2% formic acid) was injected into the dead volume of the sample injection for re-calibration of the mass spectrometer using the expected cluster ion m/z values. Peak detection was carried out using Metaboscape software (Bruker Daltonik, Bremen, Germany) with the T-Rex 3D algorithm for qTOF data. For peak detection the following parameters were used: intensity threshold of 300 with a minimum of 10 spectra, time window from 0.4 to 11.8 min, peaks were kept if they were detected in at least all replicates of one sample group. Adducts of $[\text{M}+\text{H}]^+$, $[\text{M}+\text{Na}]^+$, and $[\text{M}+\text{K}]^+$ (for positive mode) or $[\text{M}-\text{H}]^-$, $[\text{M}-\text{Cl}]^-$, and $[\text{M}-\text{COOH}]^-$ (for negative mode) were grouped as a single bucket if they had an EIC correlation of 0.8. SciFinder (<https://scifinder.cas.org>) served to predict structures and identify unknown compounds.

RNA extraction and illumina sequencing

The half of the leaf samples that was stored at -80°C was ground in liquid nitrogen. RNA was isolated from 100 mg ground leaf powder utilizing the Spectrum™ Plant Total RNA Kit (50) (Sigma-Aldrich) following the manufacturer's instructions with an on-column DNA digestion using DNaseI (ZymoResearch, Freiburg/Brsq., Germany). After a further purification step (OneStep PCR Inhibitor Removal Kit, ZymoResearch), RNA concentration, purity, and quality were assessed using a spectrophotometer (NanoDrop, 2000c; Thermo Scientific) and an Agilent 2100 bioanalyzer (Agilent Technologies).

The isolated RNA was sent to Novogene Europe, Cambridge, UK for analysis on an Illumina NovaSeq 6000 instrument (San Diego, CA, USA). There, 20 M paired end reads of 150 bp per sample were generated from the leaf transcriptome libraries of ant-colonized and ant-deprived plants that were subjected to herbivore or control treatment.

RNA-seq data analysis

Trimming of the sequences, quality control, and *de novo* assembly were performed using CLC Genomics Workbench (Qiagen Bioinformatics). A representative sample per treatment was selected, pooled, and reads randomly reduced by 50%. A total of 145×10^6 paired-end reads were used to generate the transcriptome library (word size 30, bubble size 1200). The consensus assembly contained 67,140 contigs with a N50 value of 1,304. BUSCO (Benchmarking Universal Single-Copy Orthologs) assessment (<https://busco.ezlab.org/>, last accessed on 04.02.2022 (Simao et al., 2015)), resulted in 66.6% complete BUSCOs and 14.1% missing BUSCOs when comparing our assembled transcripts to the Embryophyta lineage data set. Gene abundances were quantified for each individual sample using RSEM (version 1.2.22). To adjust nuisance technical effects, RNA-Seq data was normalized by R package RUV (remove unwanted variation (Risso



et al., 2014)). EdgeR (Robinson et al., 2010) (<https://bioconductor.org>) was carried out to identify the differentially expressed genes (DEGs) with a cut off p-value ≤ 0.05 and FDR ≤ 0.05 . All DEGs were annotated against Swiss-Prot and GO (Gene Ontology) using OmicsBox software (biobam, Valencia, Spain). GO enrichment analysis of DEGs was performed using R package clusterProfiler (Yu et al., 2012). Contigs potentially encoding for protease inhibitors were identified by GO terms associated with peptidase inhibitor activity (GO:0004866, GO:0004867, GO:0004869, GO:008191, GO:0019828, GO:0030414, GO:0010859) and a positive BLAST hit against a known plant protease inhibitor in the NCBI nr.

QUANTIFICATION AND STATISTICAL ANALYSIS

The statistical analyses were performed with R (RStudio_Team, 2021): defense hormone, amino acid and C:N data (Figures 1C (1 year), 3B, 3D, 3E, 53A, and 55A; Tables S1 and S3) after herbivore and JA treatments were tested with Two-Way ANOVA or fitted to a linear model (generalized least squares) as a function of treatment \times colonization. Whenever possible, the respective model was reduced to the minimal model. All data were tested for statistical assumptions (normal distribution and homogeneity of variances) using diagnostic plots and were log-transformed, if necessary. For the amino acid analysis, outliers were removed if $c < (Q1 - 1.5 \times IQR)$ or $c > (Q3 + 1.5 \times IQR)$ with Q as quartile and IQR as interquartile range. Differences in growth (Figures 1B, S1B–S1E, and S2), nutritional value (Figures 1E and 1H) and nitrogen content (Figure 1C, 2.6 yrs) were evaluated by Student's t-tests or Wilcoxon rank sum tests, whenever the data was not normally distributed. For the ^{15}N -labeling data, one-tailed t-tests were performed, whereas a paired Wilcoxon signed rank test was used to analyze data from the choice assay. As the data from the volatile collections were not normally distributed, nonparametric Kruskal-Wallis tests were utilized to analyze this data (Table S2). Statistical details can be found in the figures (mean \pm SE; significance (*: $p < 0.05$; **: $p < 0.01$, ***: $p < 0.001$)), figure legends and results (n, test, significance) and SI tables (n, test, F-value/L-ratio/ χ^2 , p value). Data for volcano plots (Figure 2D) and heatmaps (Figures 3C and 55B) displaying untargeted metabolomics results were calculated with R using the package MetaboAnalyst (Pang et al., 2021) after preprocessing the data with MetaboScape (Bruker Daltonics). More precisely, the preprocessed data was normalized by weight, filtered by interquartile range and auto scaled. The results of the statistical analysis were visualized with OriginPro, Version 2019 (OriginLab Corporation, Northampton, MA, USA) or R.

2.3 Manuscript II

Manuscript title: The biosynthesis, herbivore induction and defensive role of phenylacetaldoxime glucoside

Authors: Andrea T. Müller, Yoko Nakamura, Michael Reichelt, Katrin Luck, Eric G. Cosio, Nathalie D. Lackus, Jonathan Gershenzon, Axel Mithöfer, Tobias G. Köllner

Bibliographic information: *not available*

The candidate is

First author, Co-first author, Corresponding author, Co-author

Status: submitted for publication to Plant Physiology

Authors' contributions (in %) to the given categories of the publication

| Author | Conceptual | Data analysis | Experimental | Writing the manuscript | Provision of material |
|---------------------|-------------|---------------|--------------|------------------------|-----------------------|
| Andrea T. Müller | 30% | 75% | 75% | 65% | - |
| Jonathan Gershenzon | 10% | - | - | - | 20% |
| Tobias G. Köllner | 35% | 5% | - | 30% | 20% |
| Axel Mithöfer | 25% | - | - | - | 45% |
| Others | - | 20% | 25% | 5% | 15% |
| Total: | 100% | 100% | 100% | 100% | 100% |

Note: This manuscript was submitted to Plant Physiology (Plant Phys) for possible open access publication on May 25 (2023) and is incorporated in this thesis under the terms of the Creative Commons Attribution (CC-BY) license.

Short title: Formation and role of phenylacetaldoxime glucoside

The biosynthesis, herbivore induction, and defensive role of phenylacetaldoxime glucoside

Andrea T. Müller^{a,b,c}, Yoko Nakamura^{d,e}, Michael Reichelt^b, Katrin Luck^b, Eric Cosio^c, Nathalie Lackus^{b,f}, Jonathan Gershenzon^b, Axel Mithöfer^{a,#} and Tobias G. Köllner^{e,#,*}

^a Max Planck Institute for Chemical Ecology, Research Group Plant Defense Physiology, D-07745 Jena, Germany

^b Max Planck Institute for Chemical Ecology, Department of Biochemistry, D-07745 Jena, Germany

^c Pontifical Catholic University of Peru, Institute for Nature Earth and Energy (INTE-PUCP), San Miguel 15088, Lima, Peru

^d Max Planck Institute for Chemical Ecology, Research group Biosynthesis/NMR, D-07745 Jena, Germany

^e Max Planck Institute for Chemical Ecology, Department of Natural Product Research, D-07745 Jena, Germany

^f Present address: Julius-Maximilians-Universität Würzburg, Faculty of Biology, Julius-von-Sachs-Institute for Biosciences, Chair of Pharmaceutical Biology, Julius-von-Sachs-Platz 2, D-97082 Würzburg, Germany

*corresponding author: koellner@ice.mpg.de

#equal contribution

ATM: amueller@ice.mpg.de

YN: ynakamura@ice.mpg.de

MR: reichelt@ice.mpg.de

KL: kluck@ice.mpg.de

EC: ecosio@pucp.pe

NL: nlackus@ice.mpg.de

JG: gershenzon@ice.mpg.de

AM: amithoefer@ice.mpg.de

TGK: koellner@ice.mpg.de

Summary

Aldoximes are well-known metabolic precursors for plant defense compounds such as cyanogenic glycosides, glucosinolates, and volatile nitriles. They are also defenses themselves produced in response to herbivory; however, it is unclear whether aldoximes can be stored over a longer term as defense compounds and how plants protect themselves against the potential autotoxic effects of aldoximes. Here, we show that the Neotropical myrmecophyte *tococa* (*Tococa quadrialata*) accumulates phenylacetaldoxime glucoside (PAOx-Glc) in response to leaf herbivory. Sequence comparison, transcriptomic analysis, and heterologous expression revealed that two cytochrome P450 enzymes CYP79A206 and CYP79A207 and the UDP-glucosyltransferase UGT85A123 are involved in the formation of PAOx-Glc in *tococa*. Another P450, CYP71E76, was shown to convert phenylacetaldoxime (PAOx) to the volatile defense compound benzyl cyanide. The formation of PAOx-Glc and PAOx in leaves is a very local response to herbivory, but does not appear to be regulated by jasmonic acid signaling. In contrast to PAOx, which was only detectable during herbivory, PAOx-Glc levels remained high for at least three days after insect feeding. This, together with the fact that gut protein extracts of three insect herbivore species exhibited hydrolytic activity toward PAOx-Glc, suggests that the glucoside is a stable storage form of a defense compound that may provide rapid protection against future herbivory. Moreover, the finding that herbivory or pathogen elicitor treatment also led to the accumulation of PAOx-Glc in three other phylogenetically distant plant species suggests that the formation and storage of aldoxime glucosides may represent a widespread plant defense response.

Key words:

aldoximes, nitriles, cytochrome P450, CYP71, CYP79, glycosyltransferase, UGT, herbivory

Introduction

Aldoximes are widely distributed in plants and function as biosynthetic precursors for several classes of defense compounds. They have long been described as precursors of cyanogenic glycosides (Tapper et al., 1967; Andersen et al., 2000) and glucosinolates (Underhill, 1967; Wittstock and Halkier, 2000), two classes of phytoanticipins that can be activated during leaf damage to release hydrogen cyanide, isothiocyanates, thiocyanates, nitriles, and other toxic products (Dewick, 1984). In addition, aldoximes act as precursors for the formation of the phytoalexin camalexin (Glawischnig, 2007) and volatile nitriles (Irmisch et al., 2014). Such nitriles are often important constituents of the volatile blend of herbivore-damaged leaves and contribute to direct and indirect plant defense against insect herbivores (Clavijo McCormick et al., 2014; Irmisch et al., 2014). In addition to being rapidly metabolized to other defense compounds, some semi-volatile aldoximes, such as (*E*)- and (*Z*)-phenylacetaldoxime (PAOx), can accumulate as toxins during herbivory (Irmisch et al., 2013), while other more volatile aldoximes such as 2- and 3-methylbutyraldoxime or (*E*)- and (*Z*)-isobutyraldoxime are released from herbivore-damaged plants to attract natural enemies of herbivores (Clavijo McCormick et al., 2014).

Several cytochrome P450s (CYPs) have been described to mediate the formation and metabolism of aldoximes in angiosperms and gymnosperms (Sorensen *et al.*, 2018). P450s from the CYP79 family have been shown to catalyze the formation of aldoximes from amino acids or amino acid derivatives such as phenylalanine, tyrosine, tryptophan, valine, leucine, isoleucine, and chain-elongated forms of methionine (Sorensen et al., 2018). Mechanistically, this reaction involves two consecutive N-hydroxylations, followed by a dehydration and a decarboxylation step to release the corresponding oxime (Halkier et al., 1995; Sibbesen et al., 1995). In Brassicales, CYP83 enzymes convert aldoximes to S-alkylthiohydroximates, resulting eventually in glucosinolates (Naur et al., 2003; Zhu et al., 2012). Alternatively, CYP71/736 enzymes found in different plant families use aldoximes as substrates to form nitriles (Irmisch et al., 2014; Yamaguchi et al., 2016; Hansen et al., 2018) or hydroxynitriles (Bak et al., 1998; Jørgensen et al., 2011; Takos et al., 2011; Yamaguchi et al., 2014; Knoch et al., 2016). The latter are further converted to cyanogenic glycosides (α -hydroxynitriles) or, in rare cases, to non-cyanogenic glycosides (β - or γ -hydroxynitrile glycosides) via a glycosylation reaction catalyzed by UDP-glycosyltransferases of the family 85 (UGT85) (Jones et al., 1999; Takos et al., 2011; Knoch et al., 2016). Nitriles, on the other hand, are either emitted as volatiles or further metabolized to their respective acids or amides

by the action of nitrilases (Irmisch et al., 2014; Gunther et al., 2018). Unlike glucosinolates and cyanogenic glycosides, which are preformed and activated only upon herbivory or pathogen infection, volatile aldoximes and nitriles are often formed in response to biotic stressors, and their formation is closely linked to the expression of the corresponding P450 enzymes (Irmisch et al., 2013; Irmisch et al., 2014; Luck et al., 2016).

Tococa (*Tococa quadrialata*, recently renamed *Miconia microphysca* (Michelang.)), is a Neotropical shrub species that lives in close association with symbiotic ants. As a so-called ant-plant, tococa provides ants with preformed nesting sites - hollow structures at the base of the leaf blade called domatia - and in return is defended by the ants against herbivores, pathogens, and encroaching vines (Gonzalez-Teuber et al., 2014; Morawetz et al., 1992; Michelangeli, 2003; Dejean et al., 2006). While the role of the ants in this symbiotic plant-insect system has been extensively studied, not much is known about the chemical defenses of tococa. Knowledge about natural predators of tococa is also limited. Only leafcutter ants and unspecified beetle and caterpillar species are mentioned in the literature (Michelangeli, 2003; Alvarez et al., 2001; Dejean et al., 2006). In a recent study (Müller et al., 2022), we investigated the response of tococa to herbivory by a generalist *Spodoptera* species under field conditions. A number of herbivore-induced metabolites were detected, including benzyl cyanide, and a previously unknown metabolite, identified in the present study as phenylacetaldoxime glucoside (PAOx-Glc). Here, we aimed to investigate the biosynthesis and biological role of phenylacetaldoxime (PAOx) and PAOx-Glc in tococa. We used transcriptomics and heterologous expression in *Escherichia coli*, *Saccharomyces cerevisiae*, and *Nicotiana benthamiana* to identify enzymes involved in the formation and metabolism of aldoximes. Our studies on the occurrence, inducibility, and turnover of PAOx-Glc and PAOx suggest that the formation of these compounds is a very local response to tissue damage. These findings, together with the results from glucosidase assays with insect gut protein extracts and growth inhibition assays with various pathogens, suggest that aldoximes are involved in protecting the wound site. In addition, PAOx-Glc as a stable storage form of PAOx may provide rapid protection against subsequent herbivory.

Results

Identification of PAOx-Glc in wounded tocooca leaves

Targeted and untargeted metabolome analyses of herbivore-damaged and undamaged leaves of *T. quadrialata* plants grown either in the field or in the greenhouse showed that herbivory by *Spodoptera spp.* led to an induced emission of volatiles and the accumulation of a number of non-volatile polar compounds (Müller et al. (2022), Figure 1A,B; Fig. S1). Among the latter metabolites, one of the highest fold changes was repeatedly found for a feature with m/z 136.0757 $[M+H]^+$. The accurate mass allowed the prediction of the sum formula C_8H_9NO (exact mass $[M+H]^+$ 136.0757). This formula corresponds, among others, to the molecular formulae of PAOx and phenylacetamide. However, a more detailed analysis of the mass spectrum revealed that this feature likely represents an in-source fragment of a compound with a mass of 297 (m/z 298.1284 $[M+H]^+$) (Figure 1C). The mass difference of 162 corresponds to $C_6H_{10}O_5$, a neutral loss typical for glucosides (Cabrera, 2006). Indeed, incubation of the methanol-extractable fraction of tocooca leaf metabolites with a commercially available β -glucosidase resulted in a decrease of the unknown compound and an increase of PAOx (Fig. S2C), suggesting that the unknown compound is likely a glucoside of PAOx. Synthesis of PAOx-Glc (Fig. S3-12) and a comparison of its retention time and fragmentation pattern with those of the unknown compound (Fig. S2A,B) confirmed the latter as PAOx-Glc, a previously undescribed natural product. The synthetic standard further allowed the quantification of PAOx-Glc in herbivore-damaged and undamaged tocooca leaves. The amount of PAOx-Glc in *Spodoptera littoralis*-damaged leaves was about ten times higher than that of PAOx, with concentrations of up to 10 $\mu\text{g/g}$ fresh weight (Figure 2A). In contrast, undamaged leaves contained only trace amounts of PAOx and of PAOx-Glc.

Tococa CYP79A206 and CYP79A207 produce PAOx *in vitro* from phenylalanine

The biosynthesis of PAOx from phenylalanine in plants is usually catalyzed by CYP79 enzymes and a TBLASTN search with CYP79A1 from sorghum (*Sorghum bicolor*) against the transcriptome of herbivore-damaged tocooca leaves revealed two full-length genes with high similarity to CYP79A and CYP79B genes from other plants (Figure 2D). The full-length genes were designated CYP79A206 and CYP79A207 according to the P450 nomenclature rules (David Nelson). Both CYP79A206 and CYP79A207 were

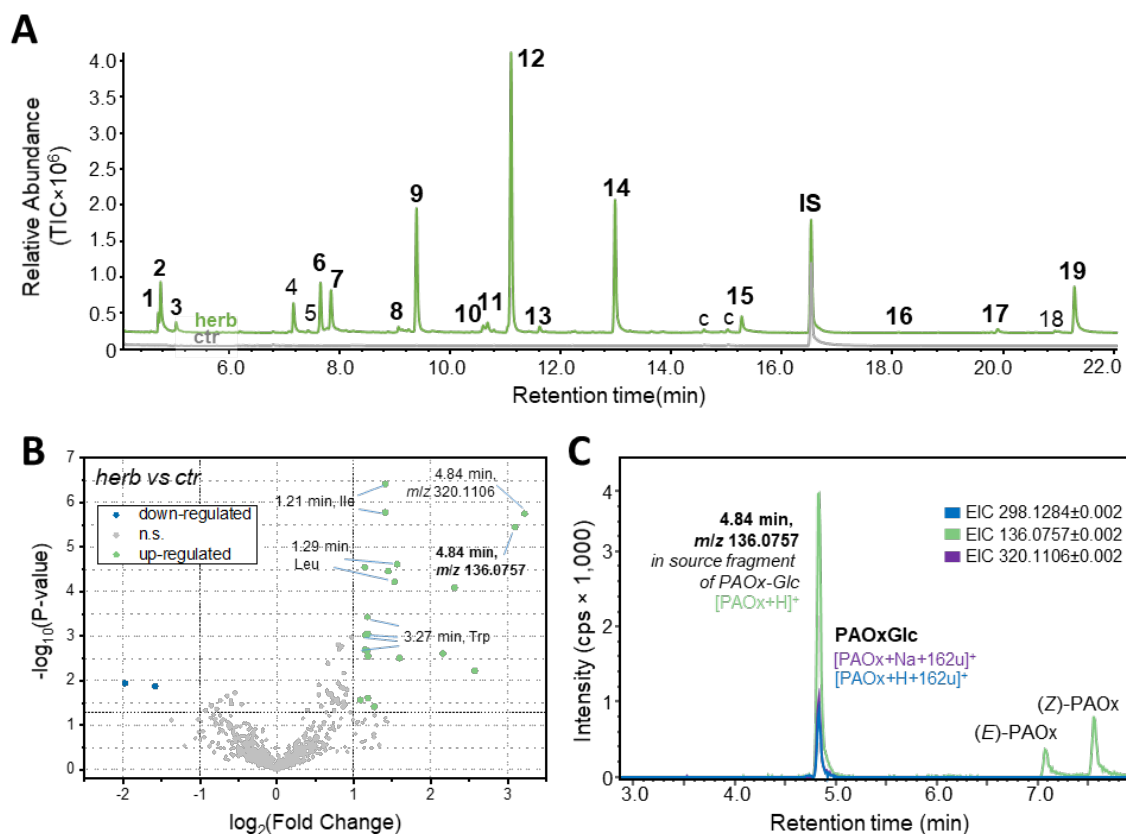


Figure 1: Herbivore-induced volatile and non-volatile compounds in *Tococa quadrialata*. (A) Comparison of the volatile bouquets of herbivore-damaged leaves (herb) and undamaged leaves (ctr). *Spodoptera littoralis* larvae were feeding on the leaves for 24 h and volatiles were collected simultaneously. Compounds were analyzed using gas chromatography-mass spectrometry and the total ion chromatograms (TIC) are shown. IS, internal standard; c, contamination; 1, 2-hexenal*; 2, 3-hexenol*, 3, 1-hexanol*; 4, 4-oxo-hex-2-enal and benzaldehyde; 5, unidentified; 6, 1-octen-3-ol*; 7, octan-3-one*; 8, benzyl alcohol*; 9, β -ocimene*; 10, linalool*; 11, nonanal*; 12, (*E*)-4,8-dimethyl-nonatriene (DMNT)*; 13, benzyl cyanide*; 14, methyl salicylate*; 15, indole*; 16, (*E*)- β -caryophyllene*; 17, α -farnesene*; 18, nerolidol; 19, (*E,E*)-4,8,12-trimethyl-1,3,7,11-tridecatetraene (TMTT)*. All compounds marked with an asterisk were identified using authentic standards, while the remaining compounds were tentatively identified using the NIST17 mass spectra library. (B) Methanolic extracts of herbivore-treated (herb) and undamaged control (ctr) leaves were analyzed with high-resolution liquid chromatography-quadrupole time-of-flight mass spectrometry (LC-qTOF-MS) operating in positive ionization mode and the relative abundances of the features compared. The volcano plot visualizes the metabolic differences, where the bright green color marks features that accumulate upon herbivory (fold change >2, $p < 0.05$, $n=12$). Important features are annotated as retention time and mass-to-charge ratio (m/z) or compound name. (C) Extracted ion chromatograms (EIC) of a methanolic tocooca leaf extract from *Spodoptera littoralis*-damaged leaves analyzed by LC-qTOF-MS. Identified compounds and detected ions are annotated. cps, counts per second (electron multiplier).

highly expressed in herbivore-damaged leaves, but only marginally in undamaged leaves (Figure 2B, Fig. S13). An amino acid alignment of CYP79A206 and CYP79A207 with characterized CYP79 proteins from other plant species confirmed that the tocooca CYP79 enzymes contained all conserved regions important for the catalytic activity (Fig. S14). The complete open reading frames (ORF) of CYP79A206 and CYP79A207 were amplified, cloned and expressed in yeast (*Saccharomyces cerevisiae*). Incubation of microsomes containing CYP79A206 or CYP79A207 with L-phenylalanine, L-tyrosine, or L-tryptophan in the presence of the cosubstrate NADPH resulted in the formation of

(*E/Z*)-PAOx, (*E/Z*)-*p*-hydroxyphenylacetaldoxime, and (*E/Z*)-indole-3-acetaldoxime, respectively, with L-phenylalanine being the preferred substrate (Figure 2C, Fig. S15). In contrast, the aliphatic amino acids L-leucine or L-isoleucine were not converted to their respective aldoximes (Fig. S15). In the absence of NADPH, only marginal activity towards L-phenylalanine was detectable, and when using microsomes prepared from a yeast strain expressing the empty vector, no enzyme activity was observed (Fig. S15).

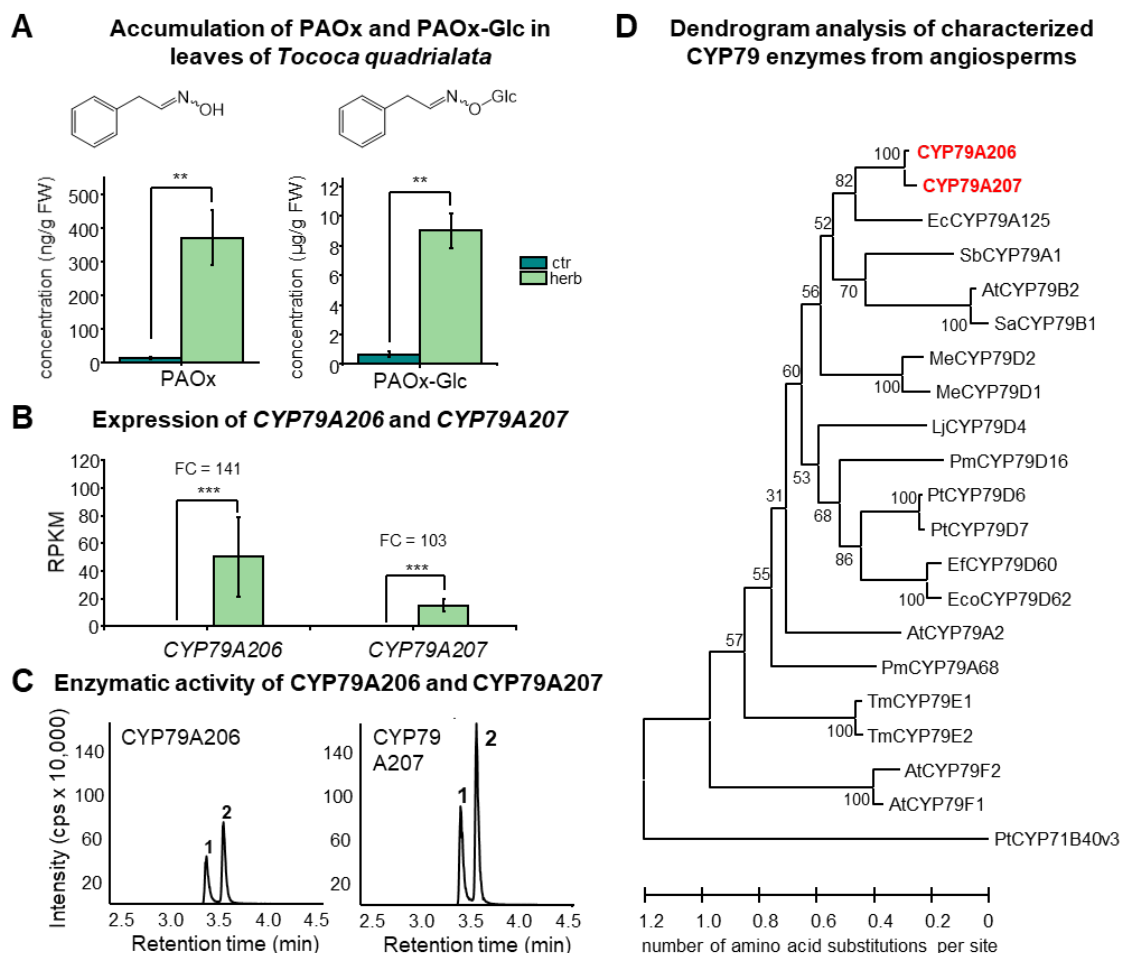


Figure 2: Two CYP79 enzymes are involved in the herbivore-induced formation of phenylacetaldoxime (PAOx) and its glucoside (PAOx-Glc) in leaves of *Tococa quadrialata*. (A) Accumulation of PAOx and PAOx-Glc in *Spodoptera littoralis*-damaged leaves (herb, 24 h treatment) and undamaged control leaves (ctr). Compounds were extracted with methanol and analyzed using targeted liquid chromatography-tandem mass spectrometry (LC-MS/MS). Wilcoxon rank sum test: $n = 6$; $** = p < 0.01$; FW: fresh weight. (B) Expression of *CYP79A206* and *CYP79A207* in herbivore-damaged and undamaged leaves. The leaf transcriptome was sequenced, *de novo* assembled, and reads mapped to the assembly. Fold change (FC) and p-value were calculated via empirical analysis of digital gene expression (edge). RPKM, reads per kilo base per million mapped reads. (C) Enzymatic activity of *CYP79A206* and *CYP79A207* with L-phenylalanine. The two genes were heterologously expressed in *Saccharomyces cerevisiae* and microsomes containing the recombinant enzymes were incubated with NADPH and L-phenylalanine. Products were extracted with methanol and detected using targeted LC-MS/MS. cps: counts per second (electron multiplier). 1, (*E*)-phenylacetaldoxime; 2, (*Z*)-phenylacetaldoxime. (D) Dendrogram analysis of *CYP79A206* and *CYP79A207* with characterized CYP79 enzymes from other angiosperms. The tree was inferred with the Maximum Likelihood method and $n = 1000$ replicates for bootstrapping. Bootstrap values are shown next to each node. PtCYP71B40v3 was used as an outgroup. *Tococa* CYP79s are shown in red and bold. At, *Arabidopsis thaliana*; Ec, *Eucalyptus cladocalyx*; Eco, *Erythroxylum coca*; Ef, *Erythroxylum fischeri*; Ja, *Prunus mume*; Lj, *Lotus japonicus*; Me, *Manihot esculenta*; Pt, *Populus trichocarpa*; Sa, *Sinapis alba*; Sb, *Sorghum bicolor*; Tm, *Triglochin maritima*.

CYP71E76 converts PAOx to benzyl cyanide *in vitro*

Since we detected benzyl cyanide in tococha emission, we sought candidate enzymes for the conversion of PAOx to this nitrile. CYP71 and CYP736 enzymes have been implicated in this conversion before, so we conducted a TBLASTN search against the tococha transcriptome using CYP71E1 from sorghum as a query. Among the resulting 12 full-length candidate genes, seven were expressed upon herbivory, but only one gene was upregulated upon wounding (Figure 3A,D, Fig. S13). This gene was designated *CYP71E76* and its complete ORF (Fig. S16) was cloned and heterologously expressed in yeast. Microsomes containing the recombinant protein were incubated with different aldoximes and the cosubstrate NADPH. From the four compounds tested, CYP71E76 accepted only (*E/Z*)-PAOx as substrate and catalyzed the formation of benzyl cyanide in the presence of NADPH (Figure 3C; Fig. S17, S18). Besides benzyl cyanide, no other products were detected in the assays, neither mandelonitrile as described for hydroxynitrile-forming CYP71s nor its degradation product benzaldehyde (Yamaguchi *et al.*, 2014). Although low levels of benzyl cyanide were also detected in various negative control assays without NADPH, with microsomes from yeast cells expressing the empty vector, or with CYP79E206, these are likely due to thermal dehydration of the aldoxime substrate during high-temperature GC injection (Ouedraogo *et al.*, 2009).

UGT85A122, UGT85A123, and UGT75AB1 can produce PAOx-Glc *in vitro*

As the generation of PAOx-Glc from PAOx requires a UDP-glycosyltransferase (UGT), the tococha transcriptome was searched for UGT genes significantly upregulated ($p < 0.05$, fold change ≥ 2) in herbivore-damaged leaves. Five putative UGT85-like genes were induced upon herbivory (Table S10). As UGTs of this subfamily are involved in the biosynthesis of cyanogenic glycosides, the two most highly expressed UGT85 genes were designated *UGT85A122* (contig_533) and *UGT85A123* (contig_7014) and selected for subsequent studies. However, because UGTs have a broad substrate range and their substrate affinity is difficult to predict from sequence similarity, two putative UGT genes from other subfamilies were also included. We chose the candidate gene with the highest fold change, a putative UGT of the subfamily 76 designated *UGT76AH1* (contig_23826) and the candidate gene with the highest expression level in wounded samples, encoding a UGT75, designated *UGT75AB1* (contig_20911). An amino acid alignment of UGT85A122, UGT85A123, UGT75AB1, and UGT76AH1 with already characterized UGTs from other plants showed that all selected candidates contained

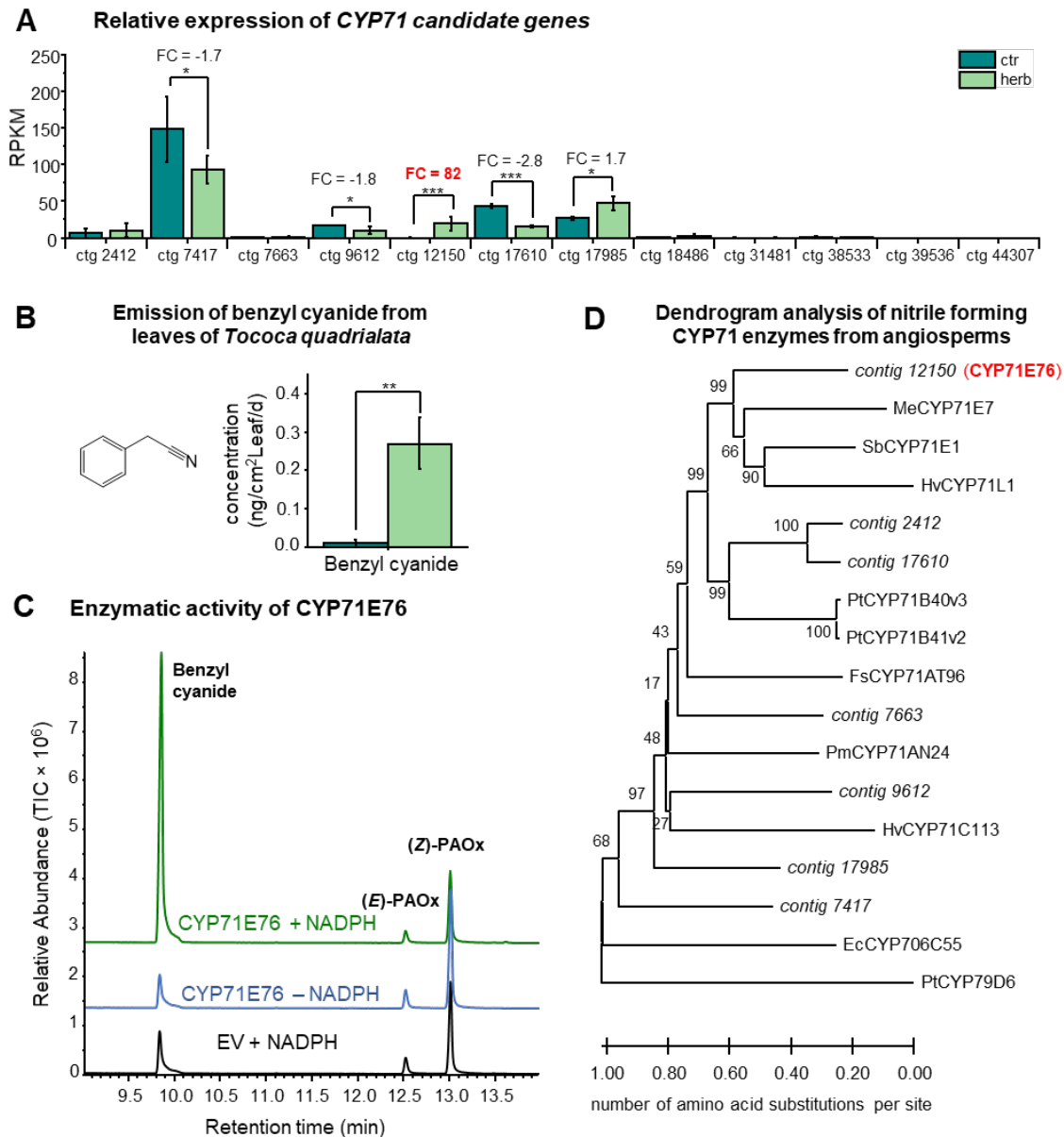


Figure 3: Identification and characterization of CYP71E76. (A) Expression of CYP71 candidate genes in herbivore-damaged and undamaged leaves. The leaf transcriptome was sequenced, *de novo* assembled, and reads mapped to the assembly. Fold change (FC) and p-value were calculated via empirical analysis of digital gene expression. RPKM, reads per kilo base per million mapped reads. (B) Emission of benzyl cyanide from *Spodoptera littoralis*-damaged leaves (herb) and undamaged control leaves (ctr). Samples were analyzed by gas chromatography-mass spectrometry (GC-MS) and quantified by gas chromatography-flame ionization detection. Wilcoxon rank sum test: $n = 11-12$, ** = $p < 0.01$. (C) Formation of benzyl cyanide by CYP71E76. The gene was expressed in *Saccharomyces cerevisiae* and microsomes containing the enzyme were used for activity assays with (*E,Z*)-phenylacetaldoxime (PAOx) as substrate. The reaction product benzyl cyanide was analyzed using gas chromatography-mass spectrometry. TIC, total ion chromatogram. EV, empty vector. (D) Dendrogram analysis of CYP71E76 and other expressed CYP71 candidate genes with characterized nitrile forming CYP71 enzymes from other angiosperms. The tree was inferred with the Neighbor-joining method and $n = 1000$ replicates for bootstrapping. Bootstrap values are shown next to each node. PtCYP79D6 was used as an outgroup. *Tococa* CYP71 candidates are shown in italics, the characterized one in red and bold. Ec, *Eucalyptus cladocalyx*; Fs, *Fallopia sachalinensis*; Hv, *Hordeum vulgare* L.; Pm, *Prunus mume*; Me, *Manihot esculenta*; Pt, *Populus trichocarpa*; Sb, *Sorghum bicolor*.

the conserved regions necessary for enzymatic activity (Fig. S19). Heterologous expression in *Escherichia coli* and subsequent enzyme assays with various potential substrates revealed that UGT85A122, UGT85A123, and UGT75AB1 were able to glycosylate PAOx (Figure 4), but with different efficiencies. Unlike UGT75AB1, which accepted a wider range of phenolic substrates, UGT85A122 and UGT85A123 only glycosylated the tested aromatic aldoximes (Fig. S20). However, UGT85A122, UGT85A123, and UGT76AH1 also accepted the monoterpene geraniol and the structurally similar fatty acid-derived octen-3-ol as substrates. A comparison of the UGT activities towards (*E/Z*)-PAOx revealed that UGT85A123 had the highest conversion rate, 25 times higher than UGT85A122, whereas UGT75AB1 was only able to produce trace amounts of PAOx-Glc (Fig. S21).

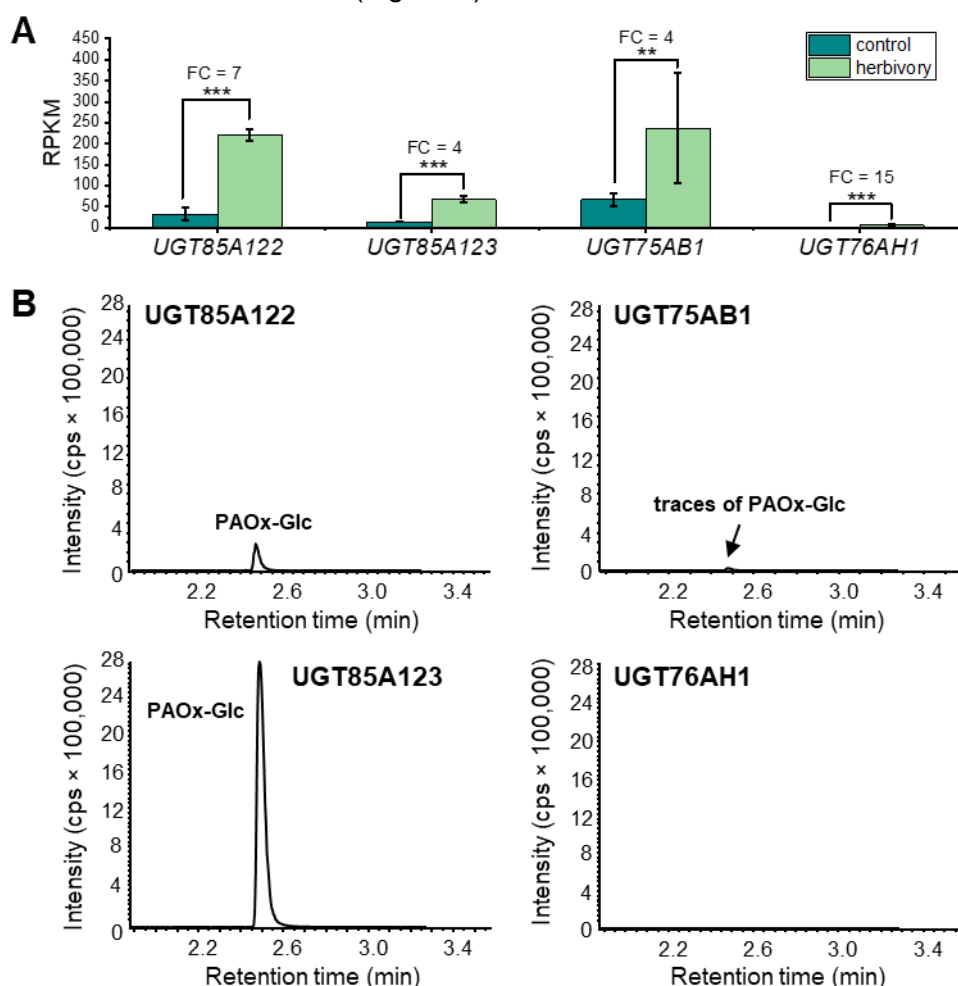


Figure 4: Formation of phenylacetaldoxime glucoside (PAOx-Glc) by UGTs from tococa. (A) Expression of *UGT85A122*, *UGT85A123*, *UGT75AB1*, and *UGT76AH1* in herbivore-damaged (herbivory) and undamaged (control) leaves. The leaf transcriptomes were sequenced, *de novo* assembled, and reads mapped to the assembly. Fold change (FC) and p-values were calculated via empirical analysis of digital gene expression (EDGE). RPKM, reads per kilo base per million mapped reads. **(B)** *UGT85A122*, *UGT85A123*, *UGT75AB1*, and *UGT76AH1* were heterologously expressed in *Escherichia coli* as His-tag fusions and purified enzymes were incubated with (*E,Z*)-phenylacetaldoxime as substrate. Reaction products were extracted with methanol from the assays and analyzed using targeted liquid chromatography-tandem mass spectrometry (LC-MS/MS). cps, counts per second.

Overexpression of CYP79A206/207, CYP71E76, and UGT85A123 in *N. benthamiana* enabled reconstitution of the pathways

To verify the activities of the candidate enzymes *in planta*, we transiently expressed them either alone or in different combinations in *N. benthamiana*. Plants expressing only *CYP79A206* or *CYP79A207* accumulated substantial amounts of PAOx, whereas this compound could not be detected in eGFP-expressing control plants (Fig. S22). Co-expression of *CYP79A206* or *CYP79A207* with *CYP71E76*, however, resulted in a significant production of benzyl cyanide and a reduction of PAOx compared to plants expressing only the *CYP79* genes. PAOx-Glc could already be detected in plants expressing only *CYP79A206* or *CYP79A207*, indicating that *N. benthamiana* possesses an intrinsic UGT activity for PAOx. However, co-expression of *CYP79A206* or *CYP79A207* with *UGT85A123* resulted in a significantly increased accumulation of the glucoside and decreased PAOx levels.

Turnover and spatial distribution of PAOx and PAOx-Glc in tocooca leaves after herbivory

Glucosides often represent storage forms of unstable or toxic natural products (Gachon et al., 2005). To test whether herbivory-induced PAOx-Glc levels in tocooca leaves remain stable after herbivory, we measured PAOx-Glc and PAOx in tocooca leaves before caterpillar feeding, immediately after 24 h of caterpillar feeding, as well as one, three, six, and nine days after removal of *S. littoralis* caterpillars that had fed on them. Liquid chromatography-tandem mass spectrometry (LC-MS/MS) analysis showed that the accumulation of PAOx-Glc continued after herbivore removal, while free PAOx had already returned to almost baseline levels one day after herbivory (Figure 5A; Fig. S23). Undamaged control plants showed only trace amounts of PAOx and low levels of PAOx-Glc.

Apart from this temporal dimension, we were also interested in where PAOx and PAOx-Glc accumulate after herbivore feeding. Therefore, we conducted an experiment where the caterpillars had a predefined leaf area to feed on, and measured the accumulation of PAOx and PAOx-Glc after 24 h herbivory at the site of damage as well as in more distal parts of the leaves. Interestingly, the accumulation of both compounds was restricted to the site of herbivory (Figure 5B).

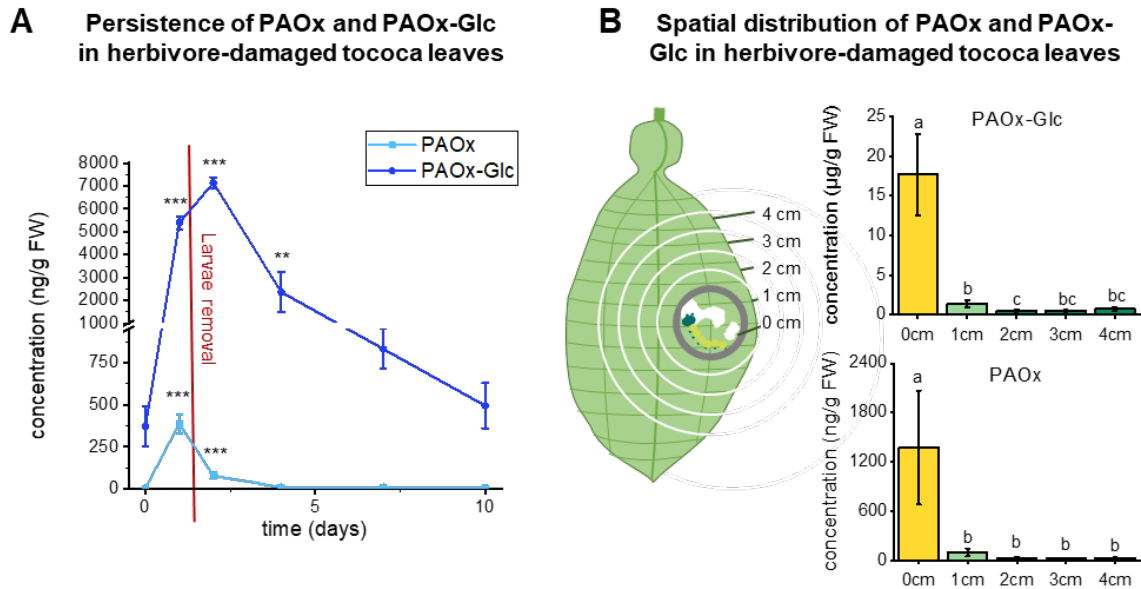


Figure 5: Temporal and spatial distribution of PAOx and PAOx-Glc in herbivore-damaged *Tococa quadrialata* leaves. (A) Leaves were exposed to herbivory by *Spodoptera littoralis* caterpillars for 24 hours and the accumulation of PAOx and PAOx-Glc was monitored for ten days. Compounds were extracted with methanol from leaf powder and analyzed using targeted liquid chromatography-tandem mass spectrometry (LC-MS/MS). FW, fresh weight. Asterisks indicate significant differences (***: $p < 0.001$, **: $p < 0.01$) to respective control (0d) based on a One-Way ANOVA with log-transformed data ($F_{5,18, \text{PAOx-Glc}} = 12.92$, $F_{5,18, \text{PAOx}} = 41.03$, $p \leq 0.001$) and Dunnett's *post hoc* test. Means \pm SEM are shown; $n = 3-5$. **(B)** A clip cage was installed on tococa leaves and *S. littoralis* larvae were allowed to feed within the cage for 24 h. Thereafter, leaf discs with the diameter of the cage were excised ("0 cm") as well as rings of 1 cm width around the wounding site whose outer edge was 1, 2, 3, or 4 cm from the cage ("1 cm"- "4 cm"). Leaf pieces were extracted with methanol and analyzed using LC-MS/MS. FW, fresh weight. Different letters indicate significant differences ($p < 0.05$) between the samples based on linear mixed-effect models with log-transformed data ($L\text{-ratio}_{\text{PAOx}} = 12.821$, $p_{\text{PAOx}} = 0.012$; $L\text{-ratio}_{\text{PAOx-Glc}} = 12.529$, $p_{\text{PAOx-Glc}} = 0.014$) and Tukey Contrasts *post hoc* tests. Means \pm SEM are shown; $n = 6$.

Mechanical wounding leads to the induction of PAOx-Glc in tococa leaves

Since PAOx and PAOx-Glc are formed in tococa leaves after herbivory (Müller et al., 2022; Figure 2A), we investigated the internal signals inducing their production. In our previous paper (Müller et al., 2022), we showed that JA and its bioactive isoleucine conjugate JA-Ile (the typical phytohormones involved in plant responses to herbivory) accumulate in tococa leaves upon herbivory and that spraying of JA resulted in high levels of free amino acids such as phenylalanine, the precursor of PAOx. Here, we compared the effects on PAOx and PAOx-Glc accumulation of other treatments that induce plant defenses, including mechanical wounding and herbivore oral secretions (Malik et al., 2020) to learn more about what triggers accumulation of these compounds. As expected, the bioactive JA-Ile accumulated in plants sprayed with JA, and to even higher levels when plants were also mechanically wounded (Figure 6). Mechanical wounding alone also induced JA-Ile, but at lower levels than any of the other treatments. Interestingly, the pattern of JA-Ile induction was very different from those of PAOx and

PAOx-Glc. None of the treatments resulted in the formation of PAOx-Glc in concentrations as high as those seen after herbivory; however, mechanical wounding resulted in PAOx-Glc levels significantly higher than in control leaves, whereas the application of JA or oral secretion (OS) did not alter this response. Interestingly, elevated amounts of PAOx and benzyl cyanide (Fig. S24) were only detectable in herbivore-treated samples, not in JA treated samples, matching the respective gene expression pattern (Fig. S24).

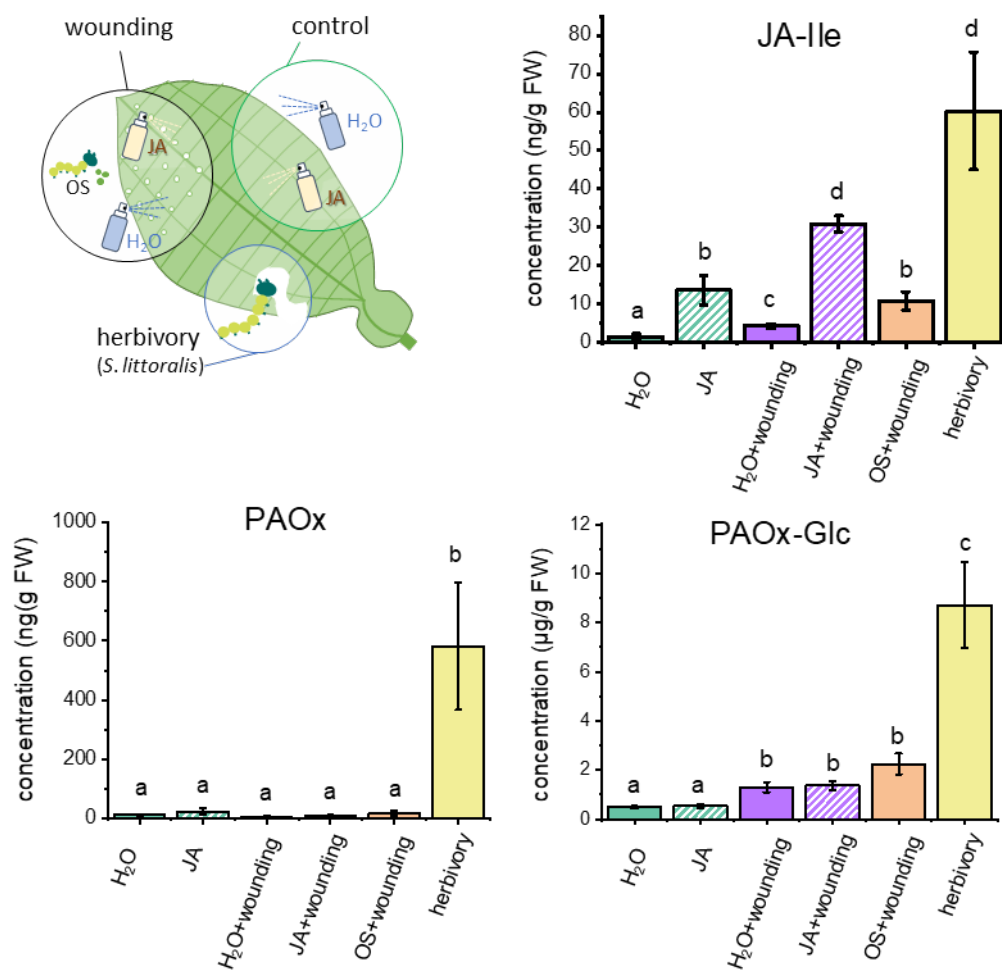


Figure 6: Formation of PAOx and PAOx-Glc in tocooca leaves in response to different treatments.

Leaves were sprayed with jasmonic acid (JA), oral secretion collected from *Spodoptera littoralis* (OS), or water (H₂O) after mechanical wounding or without further treatment. *S. littoralis* feeding served as a positive control. All leaves were harvested 24 h after the (beginning of the) respective treatment, and the phytohormone JA-Ile as well as PAOx and PAOx-Glc contents were quantified via targeted liquid chromatography-tandem mass spectrometry (LC-MS/MS). Different letters indicate significant differences ($p < 0.05$) between treatments, based on linear (gls) models ($L\text{-ratio}_{\text{PAOx}} = 27.797$, $p_{\text{PAOx}} < 0.001$, $L\text{-ratio}_{\text{JA-Ile}} = 73.824$, $p_{\text{JA-Ile}} < 0.001$) or One-Way ANOVA ($F\text{-value}_{\text{PAOx-Glc}} = 37.02$, $p_{\text{PAOx-Glc}} < 0.001$) with log-transformed data and subsequent Tukey Contrasts/HSD *post hoc* tests. Means \pm SEM are shown; $n = 6-11$.

Insect gut protein extracts but not plant protein extracts can hydrolyze PAOx-Glc in vitro

Aldoximes have been reported to be toxic to mammals, insects, fungi, and microorganisms (Drumm et al., 1995; Bartosova et al., 2006; Irmisch et al., 2013). Therefore, PAOx-Glc stored in tobacco leaves upon herbivory may represent a barrier against subsequent herbivore attack. Since the release of toxic aglucones from their glucosides is often catalyzed by enzymes in the insect gut, we examined the capacity of three lepidopteran insect species to hydrolyze PAOx-Glc in their guts. Non-boiled (native) and boiled (control) protein extracts prepared from dissected guts of the generalist caterpillars *S. littoralis*, *Lymantria dispar*, and *Heliothis virescens* were incubated with PAOx-Glc and the release of PAOx was measured using LC-MS/MS. While native (non-boiled) gut protein extracts of *L. dispar* and *H. virescens* were able to hydrolyze the glucoside, the native gut protein extract of *S. littoralis* showed only trace activity towards PAOx-Glc (Figure 7). Boiling completely inactivated any hydrolytic activity, suggesting that the release of PAOx from its glucoside in gut protein extracts from *L. dispar* and *H. virescens* is enzymatically catalyzed. The protein extracts were also tested for activity towards the cyanogenic glucoside amygdalin, which was efficiently hydrolyzed by all extracts (Fig. S25). Interestingly, plant protein extracts made from three different PAOx-Glc-producing species (see next paragraph) showed no hydrolysis activity towards PAOx-Glc, but efficiently hydrolyzed amygdalin (Fig. S26).

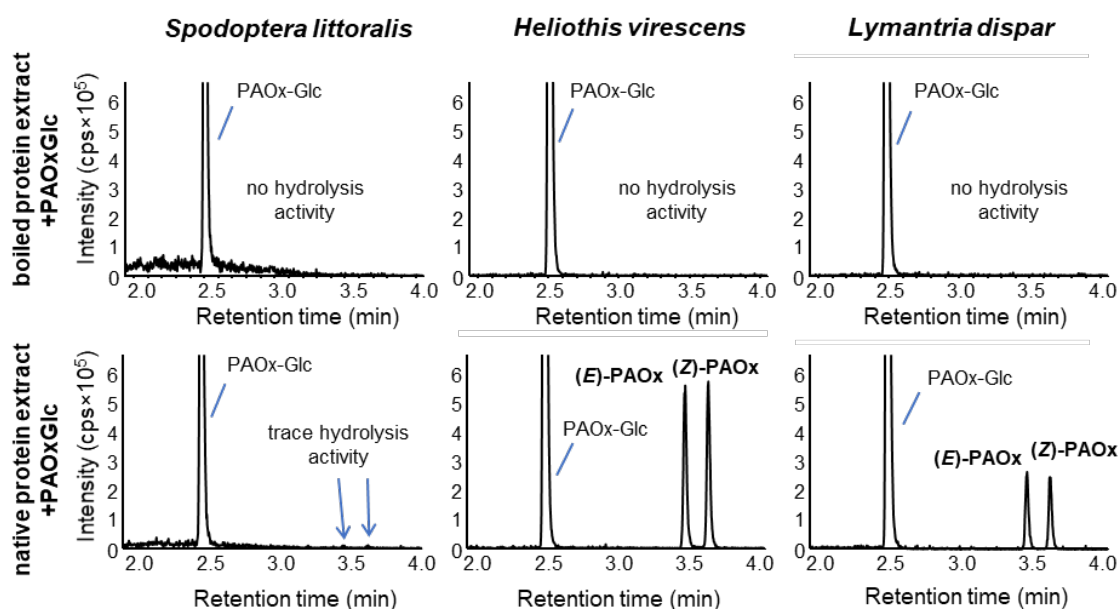


Figure 7: Deglycosylation of PAOx-Glc by gut protein extracts of different insect caterpillars. Gut extracts of *Heliothis virescens*, *Spodoptera littoralis*, and *Lymantria dispar* were incubated with PAOx-Glc. Hydrolysis products were extracted with methanol from the assays and analyzed using targeted liquid chromatography-tandem mass spectrometry (LC-MS/MS). cps, counts per second.

Biotic stresses induce the accumulation of PAOx-Glc in poplar, crape jasmine, and soybean

Various poplar species including *Populus trichocarpa*, *P. nigra*, *P. x canescens*, and *P. simonii x pyramidalis* have been described to produce volatile and semi-volatile aldoximes in response to herbivory (Zeng-hui et al., 2004; Irmisch et al., 2013; Clavijo McCormick et al., 2014). However, whether aldoximes can also be glycosylated in these species was unclear. In the present study, LC-MS/MS analysis of *L. dispar* and *Chrysomela populi*-damaged *P. trichocarpa* leaf samples showed that herbivory indeed resulted in PAOx-Glc accumulation (Fig. S27).

Crape jasmine (*Tabernaemontana divaricata*) is a medicinal plant known for its indole alkaloids. While the biosynthesis of these compounds has been studied in detail, studies on other metabolites in the plant are scarce. When we analyzed leaves of crape jasmine after *S. littoralis* feeding, we found a very high accumulation of PAOx in herbivore-treated leaves along with increased levels of PAOx-Glc (Fig. S27).

Since the phytoalexin camalexin, which is derived from indole-3-acetaldoxime, accumulates upon pathogen infection in *Arabidopsis* (Glawischnig, 2007) and the aldoxime-producing CYP79B1 is induced in *Arabidopsis* in response to this treatment (Lemarie et al., 2015), we hypothesized that aldoximes may also be produced as pathogen defenses in other species. Therefore, a soybean (*Glycine max*) cell culture was treated with a crude elicitor fraction, a branched β -glucan cell wall component, from the oomycete *Phytophthora sojae* and aldoxime formation was analyzed. Interestingly, elicitor-treated soybean cells also produced both PAOx-Glc and free PAOx, while untreated controls showed no accumulation of these compounds (Fig. S27).

PAOx negatively affects the growth of plant pathogenic bacteria

Since aldoxime metabolites accumulated in soybean in response to pathogens and the literature has previously suggested a role for aldoximes in defense against pathogens, we challenged bacterial plant pathogens with PAOx in growth inhibition assays. We found that the growth of the gram-positive bacteria *Curtobacterium flaccumfaciens* and *Clavibacter michiganensis* (kindly provided by Dr. Matthew Agler, FSU, Jena) and the gram-negative bacteria *Agrobacterium tumefaciens* and *Pseudomonas syringae* (kindly provided by Dr. Katrin Krause, FSU, Jena) were significantly reduced by PAOx in a concentration-dependent manner (Fig. S28). Moreover, all bacteria tested were able to hydrolyze PAOx-Glc into free PAOx (Fig. S29).

Discussion

Aldoximes are known to be precursors of important defense compounds such as cyanogenic glycosides, glucosinolates, and volatile nitriles (Tapper et al., 1967; Underhill, 1967; Andersen et al., 2000; Wittstock and Halkier, 2000; Irmisch et al., 2014). Recent work has shown that they can also act as defense compounds themselves (Irmisch et al., 2013). Here, we found that in addition to free phenylacetaldoxime (PAOx), the glucoside phenylacetaldoxime glucoside (PAOx-Glc) accumulates as the dominant form of aldoxime in herbivore-damaged tocooca leaves. To the best of our knowledge, this compound has not yet been described in plants, nor have aldoxime glucosides been found in nature to date. The aim of our study was to investigate how PAOx-Glc and related compounds are produced in tocooca and what functions they perform in plant defense.

Enzymes for the biosynthesis of free PAOx and volatile benzyl cyanide have so far only been discovered in a few plants, including poplar (Irmisch et al., 2013; Irmisch et al., 2014), coca (*Erythroxylum coca*) (Luck et al., 2016), maize (Irmisch et al., 2015), and giant knotweed (*Fallopia sachalinensis*) (Yamaguchi et al., 2016). Homology-based searches allowed us to identify candidate enzymes in tocooca, and *in vitro* activity assays and overexpression of *CYP79A206*, *CYP79A207*, and *CYP71E76* in *N. benthamiana* confirmed their role in the formation of PAOx and benzyl cyanide (Figure 8). Analogous to other studies on herbivore-induced aldoxime formation, the accumulation of PAOx in tocooca was strongly associated with the expression of the *CYP79* gene(s) (Irmisch et al., 2013; Irmisch et al., 2015; Luck et al., 2016; Liao et al., 2020). Similarly, most of the benzyl cyanide-producing *CYP71*s characterized to date showed an expression pattern that strongly correlated with the emission of this volatile nitrile (Irmisch et al., 2014; Yamaguchi et al., 2016; Liao et al., 2020).

Like other glycosyltransferases accepting aldoxime-related compounds as substrates (Jones et al., 1999; Takos et al., 2011; Knoch et al., 2016), UGT85A122 and UGT85A123 identified in this study also belong to the UGT subfamily 85 (Fig. S30). Although UGT85A122 and UGT85A123 were able to glycosylate PAOx *in vitro*, we conclude from their expression patterns, *in vitro* characterization, and reconstitution of PAOx-Glc formation in *N. benthamiana* that UGT85A123 is mainly responsible for the accumulation of PAOx-Glc in wounded tocooca leaves, whereas UGT85A122 may play only a minor role (Figure 8).

Interestingly, a deeper phylogenetic analysis suggests that UGT85A122 and UGT85A123 are not directly related to other UGTs involved in PAOx and nitrile glucosylation (Fig. S31), indicating the possibility of an independent evolution of this activity. However, since the bootstrap values are at times very low, this interpretation should be treated with caution. Convergent evolution of

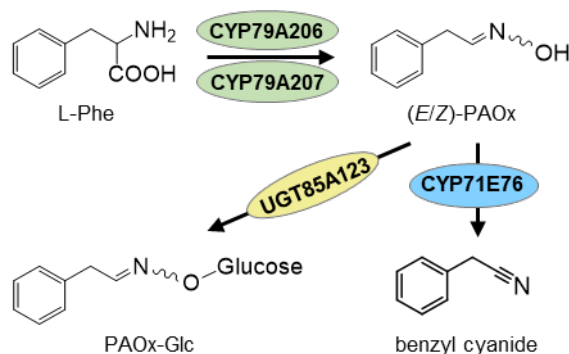


Figure 8: The formation and metabolism of phenylacetaldoxime (PAOx) in *Tococa quadrialata*.

aldoxime-metabolizing enzymes in different lineages has already been shown for nitrile- and hydroxynitrile-forming enzymes. Poplar, for example, uses a CYP71 for nitrile formation (Irmisch et al., 2014), while in *Lotus japonicus* and in *Eucalyptus cladocalyx* a CYP736 and a CYP706, respectively, are involved in nitrile production (Tako et al., 2011; Hansen et al., 2018). In contrast, CYP79 genes have been found in the genomes and transcriptomes of nearly all sequenced angiosperms and gymnosperms (Irmisch et al., 2013; Luck et al., 2017), and all CYP79 enzymes characterized to date produce aldoximes, suggesting a monophyletic origin of aldoxime formation in seed plants. Notably, ferns also produce aldoximes as intermediates for cyanogenic glycosides (Thodberg et al., 2020), but instead of a CYP79, they use a flavin-dependent monooxygenase for the biosynthesis of PAOx. Thus, aldoxime formation has evolved at least twice independently, but is conserved in angiosperms and gymnosperms, and thus seems to have a general role in spermatophytes.

PAOx has already been shown to act as a toxin against generalist caterpillars (Irmisch et al., 2013) and benzyl cyanide is repellent to herbivorous insects (Irmisch et al., 2014). Given these properties as well as the fact that PAOx(-Glc) and benzyl cyanide are formed specifically after insect herbivory, it is reasonable to assume that they function as defense compounds in *tococa*. However, since aldoximes are also highly reactive (Grootwassink et al., 1990; Bak et al., 1999; Morant et al., 2007), the question arises as to how plants can protect themselves from potential autotoxic effects. Glycosylation is a typical response for coping with toxic compounds in all organisms (Jones and Vogt, 2001). Many plants use glycosylation to inactivate toxic compounds and store them in the vacuole (Gachon et al., 2005). The bioactive aglycones are only released upon tissue or cell damage, as has been described in detail for e.g. glucosinolates and cyanogenic glycosides (Dewick, 1984). Thus, the glycosylation of PAOx may represent a self-protection mechanism of the plant against high levels of free aldoxime. We have

shown that generalist caterpillars possess glucosidase enzyme activity that can release the toxic PAOx from the glucoside (Fig. 7), while plant protein extracts showed no PAOx-Glc hydrolysis activity (Fig. S26). It is therefore likely that PAOx is first formed from its glucoside in the caterpillar gut, where it then acts as a toxin. Since PAOx is relatively unstable (Jones and Vogt, 2001) and semi-volatile, conversion to the stable and non-volatile glucoside may also provide an elegant way to prevent loss of this nitrogenous and thus metabolically valuable defense compound by decay or emission. Indeed, our studies on the turnover of PAOx and PAOx-Glc showed that PAOx is produced only during injury and is undetectable shortly after herbivory (Fig. 5). However, PAOx-Glc continues to accumulate in the plant for several days after herbivory. This suggests that the production of PAOx is a direct response to herbivore attack, while the storage of PAOx-Glc may help the plant to protect itself from subsequent insect feeding.

Many plant pathogens require a wound site to invade the plant (Savatin et al., 2014). Because herbivory by feeding insects can lead to extensive wounding and concomitant secondary infections, we performed antimicrobial assays with several plant pathogenic bacteria to determine a possible role for PAOx in pathogen defense. Indeed, we found that PAOx reduced the growth of these bacteria. Notably, the concentrations of PAOx active in the *in vitro* assays were very high compared to those measured in tocooca leaves. However, considering the facts that PAOx-Glc and PAOx accumulate exclusively in an area of a few millimeters around the wound site (Fig. 5), and that PAOx-Glc is also deglycosylated by the bacteria (Fig. S29), adding to the PAOx levels, the tested PAOx concentrations could be reached, if not in tocooca, then at least in other plants (poplar, crape jasmine) with higher PAOx levels. We therefore hypothesize that PAOx and its glucoside play a role not only in defense against caterpillars, but also in the prevention of secondary infections by phytopathogenic bacteria and fungi.

Experiments on the inducibility of PAOx and PAOx-Glc formation have shown that mechanical wounding is necessary for PAOx-Glc accumulation and that continuous feeding of caterpillars is required to obtain higher levels of these compounds (Fig. 6), indicating that the production of PAOx and PAOx-Glc correlates with the extent of wounding. This is very similar to the results of a recent study by Liao et al. (2020), which showed that continuous wounding is necessary for the production of PAOx and benzyl cyanide in tea (*Camellia sinensis*) leaves. Interestingly, jasmonic acid and its bioactive derivatives appear to play little or no role in regulating the formation of PAOx and PAOx-Glc in tocooca (Fig. 6). This is in contrast to previous experiments with coca (Luck et al., 2016), tea (Liao et al., 2020), or giant knotweed (Yamaguchi et al., 2016), in which the

formation of aldoximes and nitriles could be induced by an artificial jasmonic acid treatment.

Our study showed that the production of PAOx-Glc in response to biotic stress is not restricted to tocooca (order: Myrtales, family: Melastomataceae), but could also be detected in poplar (order: Malpighiales, family: Salicaceae), soybean (order: Fabales, family: Fabaceae), and crape jasmine (order: Gentianales, family: Apocynaceae) (Fig. S27). Similar to cyanogenic glycosides, glycosylated aldoximes appear to be widespread in the eudicotyledons and not restricted to a particular family or order like other natural products such as salicinoids or glucosinolates. Given our knowledge of the biosynthetic pathway, induction pattern, and mode of action of PAOx and its glucoside, we conclude that their formation represents a widespread and common plant defense response to tissue damage, helping to protect the injured site from further damage. Future studies on the occurrence of these compounds in the plant kingdom and their distribution relative to cyanogenic glycosides may provide interesting insights into the evolutionary relationship of these compounds as well as the ancestral function of aldoximes in higher plants.

Material and methods

Plants and Insects

Tococa (*Tococa quadrialata*) plants were grown from seeds in a glasshouse (see Table S1). Experiments were performed with mature plants (ca. 30 cm tall). *Spodoptera littoralis* larvae were hatched from eggs obtained from Syngenta Crop Protection AG (Switzerland) and reared on an agar-based optimal diet at 23°C–25°C with 16 h light/8 h dark cycles (Bergomaz and Boppre, 1986). Second and third instar larvae were chosen for the herbivory experiments and starved 24 h prior to plant feeding. *Nicotiana benthamiana* plants were grown as described in Irmisch et al., 2013. Western balsam poplar (*Populus trichocarpa*) trees, gypsy moth (*Lymantria dispar*) larvae, and poplar leaf beetles (*Chrysomela populi*) were reared as described in Lackus et al. (2020); Lackus et al. (2021), and the insects were starved for 13 h prior to the herbivory experiment. Crape jasmine (*Tabernaemontana divaricata*) trees were kindly provided by Sarah E. O'Connor (Max Planck Institute for Chemical Ecology, Germany) and grown under the same climatic conditions as the tocooca plants.

Tococa herbivore experiment and volatile collection

Tococa plants were randomly divided into treatment and control groups. One leaf of each plant was enclosed in a PET bag (Toppits® Bratschlauch, Minden, Germany). Three *S. littoralis* larvae were placed on all leaves of the “treatment” group and allowed to feed for 24 h. Volatiles were collected simultaneously over 24 h using a push-pull system, where charcoal-purified air was pumped into the bag at a flow rate of 0.6 L min⁻¹, while 0.4 L min⁻¹ was pumped out of the system, passing through a 20 mg PoraPak-Q™ filter (Alltech, IL, USA), which absorbed the volatiles. At the end of the experiment, all leaves were excised and photographed to determine the leaf area, the domatium was removed, and the leaf blade was flash-frozen in liquid nitrogen. All leaf samples were ground in liquid nitrogen before being split in half, and one-half of each sample was lyophilized and the other stored at -80 °C until further processing. To test whether benzyl cyanide is produced by the plant or the caterpillars, a similar experiment was conducted with *S. littoralis* feeding on tococa leaves for 24 h and simultaneous volatile collection, as described above. The caterpillars were then removed from the leaves, the larvae were placed in PET bags, and the volatiles from the wounded leaves and the caterpillars were collected separately for another 24 h using the same parameters as described before.

Analysis of herbivory-induced volatiles

As described in Müller et al. (2022), volatiles were analyzed via GC-MS and GC-FID after elution from PoraPak-Q™ filters using 200 µL dichloromethane containing 10 ng/µL *n*-bromodecane (Sigma-Aldrich, Taufkirchen, Germany) as an internal standard.

Processing and extraction of leaf samples

For the quantification of benzyl cyanide, 100 mg of ground leaf powder from transiently transformed *Nicotiana benthamiana* plants were extracted with 400 µL *n*-hexane containing 10 ng/µL bromodecane as an internal standard. To analyze phytohormones, aldoximes, and unknown semipolar compounds, frozen and ground fresh leaf material (usually 100 mg) was extracted with methanol (100 µL per 10 mg sample) containing internal isotopically-labeled phytohormone standards (40 ng/mL D₆-JA (HPC Standards GmbH, Germany) and 8 ng/mL D₆-JA-Ile (HPC Standards GmbH). After mixing for 30 min, the homogenates were centrifuged at 16,000 g for 10 min. Freeze-dried plant

material was processed similarly, but the extraction of 20 and 40 mg powder was achieved with 0.5 mL and 1.0 mL MeOH, respectively.

HPLC-MS/MS analysis

The analysis of JA and JA-Ile, as well as untargeted metabolomics of the methanolic extracts of tocooca leaves and initial UGT activity assays with various substrates were performed as described in Müller et al. (2022) and Rizwan et al. (2021), respectively (see also Tables S2, S3, S11). Aldoximes and PAOx-Glc concentrations were measured from methanolic extracts as described in Luck et al. (2017) with minor modifications. The exact LC separation and MS analysis parameters are listed in Tables S2 and S3. The concentrations of PAOx and PAOx-Glc were determined using external standard curves of authentic standards synthesized as described below. Whenever the concentration of the compounds in the samples was outside the linear range, the extracts were diluted accordingly with MeOH and re-measured. Glucosidase activity was confirmed by analyzing the accumulation of prunasin with the corresponding HPLC-MS/MS method described in Table S2 and S3.

GC-MS and GC-FID analyses of CYP79 and CYP71 products

The n-hexane phase of CYP71E76 activity assays and leaf extracts of transformed *N. benthamiana* were analyzed by GC-MS and GC-FID as described in Müller et al. (2022), with changes only in the temperature ramp (Table S4). Compounds were identified by comparison to the authentic standards benzyl cyanide (Merck, Darmstadt, Germany) and PAOx (synthesized as described below). Quantification was achieved by comparing their FID peak area with that of the internal standard, applying equal response factors on a weight basis.

RNA extraction and cDNA synthesis

Leaf RNA was isolated as described by Müller et al. (2022). For transcriptome sequencing, RNA was extracted from flash-frozen and ground powder of the stem, the roots, and an ant domatium of a control plant as described. cDNA synthesis from 800 ng RNA was performed with the RevertAid First Strand cDNA Synthesis Kit (Thermo Scientific, Schwerte, Germany) using oligo (dT)₁₈ primers according to the manufacturer's instructions.

Transcriptome sequencing and analysis

Total RNA extracted from the leaves of three herbivore-treated and three undamaged control tocooca plants as well as from the stem, the roots, and a domatium of a single undamaged plant was sent to the Max Planck Genome Center, Cologne, Germany for sequencing (25 M paired-end reads, 150 bp, Illumina HiSeq3000 (San Diego, CA, USA)). Trimming of the obtained reads, *de novo* assembly, and read mapping were performed using CLC Genomics Workbench (Qiagen Bioinformatics). Specifically, the trimmed reads of a herbivore-treated and an undamaged control leaf transcriptome and of a stem, root, and domatium transcriptome were pooled, randomly reduced by half, and then used to generate a *de novo* assembly (for details see Table S5). Empirical analysis of digital gene expression (EDGE) implemented in CLC Genomics Workbench was performed for gene expression analysis.

Identification and cloning of putative tocooca CYP79 and CYP71 genes

Putative tocooca *CYP79* genes were identified by TBLASTN analysis using the amino acid sequence of CYP79A1 (GenBank, AAA85440.1) from sorghum (*Sorghum bicolor*) as query and the *de novo* assembled tocooca transcriptome as reference. The complete open reading frames (ORF) of the two candidate genes *CYP79A206* and *CYP79A207* were amplified from leaf cDNA, PCR products were cloned into the sequencing vector pJET1.2/blunt (Thermo Scientific), and both strands were fully sequenced using the Sanger method. Putative tocooca *CYP71* genes were identified by BLAST analysis using the amino acid sequence of CYP71E1 (Genbank: AAC39318) from sorghum against the *de novo* assembled tocooca transcriptome. Considering only full-length sequences expressed in wounded leaves (RPKM ≥ 0.5) and upregulated upon herbivory (FC ≥ 2 , $p < 0.05$) reduced the number of candidates to one. Hence, the ORF of *CYP71E76* was amplified and cloned as described for the *CYP79* candidate genes (primers: Table S9).

Identification and cloning of putative tocooca UGT genes

Putative tocooca *UGT* genes were identified by searching the *de novo* assembly for *UGTs* with a high fold change and/or expression level upon herbivory. Since only *UGT76AH1* could be inserted into the *Escherichia coli* expression vector pET100/D-TOPO (Thermo Scientific), *UGT85A122*, *UGT85A123*, and *UGT75AB1* were synthesized as codon-optimized sequences (see Table S12) and subsequently cloned into the same vector.

Heterologous expression of CYP79A206, CYP79A207, and CYP71E76 in *Saccharomyces cerevisiae*

The complete open reading frames of CYP79A206, CYP79A207, and CYP71E76 were cloned into the pESC-Leu2d vector (Ro et al., 2008) as *NotI-PacI* (CYP79A206) or *SpeI-SacI* (CYP79A207, CYP71E76) fragments. The *S. cerevisiae* strain WAT11 (Pompon et al., 1996), carrying the Arabidopsis *cytochrome P450 reductase 1*, was used for the heterologous expression of the enzymes following the protocol described in Irmisch et al. (2013).

Heterologous expression of UGT candidate genes in *Escherichia coli*

Chemically competent *E. coli* OneShot® BL21Star™ (DE3) cells (Thermo Fisher Scientific) were used for heterologous expression of the target genes. Cells were grown at 25 °C and 220 rpm until an OD₆₀₀ value of 0.6 was reached, induced by the addition of IPTG at a final concentration of 1 mM and subsequently maintained at 18 °C and 220 rpm for an additional 20 h. Bacteria were separated from the culture medium by centrifugation (7 min; 5000 × g; 4 °C) and resuspended in 4 mL of resuspension buffer (Table S6). After 30 min incubation on ice, cells were disrupted by four freeze-thaw cycles using liquid nitrogen and a 25 °C water bath, respectively. After centrifugation (4 °C, 16000 × g, 45 min), the supernatant was further purified by affinity chromatography with the Ni-NTA Spin Kit (Qiagen), following the manufacturer's instructions. Buffer exchange with Illustra™ NAP™-5 columns (GE Healthcare, Buckinghamshire, UK), yielded 1 mL of the purified proteins in assay buffer (Table S6). Protein concentration was determined using the QuickStart™ Bradford Protein Assay (Bio-Rad, München, Germany).

***In vitro* assays of recombinant CYP79A206 and CYP79A207**

20 µL of microsomal extracts were incubated with 1 mM substrate (L-Phe, L-Leu, L-Ile, L-Tyr, or L-Trp) and 1 mM NADPH in 75 mM sodium phosphate buffer (pH 7.0) in a total reaction volume of 300 µL at 25 °C and 300 rpm for 2 h before stopping the reaction by adding 300 µL MeOH. After another 60 min incubation on ice and removal of the denatured enzymes by centrifugation (11,000 g for 10 min), the supernatant was transferred to a glass vial and the reaction products were analyzed by targeted LC-MS/MS.

***In vitro* assays of recombinant CYP71E76**

20 μ L of microsomal extracts were incubated with 1 mM substrate (PAOx, acetaldoxime, salicylaldoxime or benzaldoxime) and 1 mM NADPH in 75 mM sodium phosphate buffer (pH 7.0) in a total reaction volume of 300 μ L at 25 °C and 300 rpm. The assay mixture was overlaid with 150 μ L *n*-hexane. The reaction was stopped after 2 h by mixing and freezing the samples in liquid nitrogen. The hexane phase was then transferred to a glass vial and the reaction products were analyzed by GC-MS.

***In vitro* assays of recombinant UDP-glucosyltransferases**

10 μ g of the purified protein in assay buffer (Table S6) was incubated with 5 mM of UDP-glucose (Sigma, dissolved in ddH₂O), 1 mM of varying substrates (Figure S20, dissolved in DMSO) or varying amounts of PAOx (substrate affinity assay) and 5 mM β -mercaptoethanol (in assay buffer) in a total volume of 200 μ L for 90 min (30 min for substrate affinity assay) at 30 °C under shaking conditions (300 rpm). The reaction was stopped by adding 200 μ L MeOH, vigorous mixing and, after 30 min incubation on ice, the removal of the denatured enzymes by centrifugation (11,000 g for 10 min). The supernatant was transferred into a glass vial and the reaction products were analyzed by targeted LC-MS/MS and untargeted LC-qTOF-MS).

Transient expression of candidate enzymes in *N. benthamiana*

Expression was performed as described in Irmisch et al. (2013) with a few modifications. Briefly, the coding regions of *CYP79A206*, *CYP79A207*, *CYP71E76*, and *UGT85A123* were cloned into the pCAMBiA2300U vector (primers: Table S9). *Agrobacterium tumefaciens* strain GV3101 was transformed with either one of these vectors, an *eGFP* construct, or the pBIN:p19 construct. For the *N. benthamiana* transformation, 50 mL of LB selection media (Table S6) were inoculated with 5 mL of an overnight culture (220 rpm, 28°C) and, after overnight growth under the same conditions, the cells were harvested by centrifugation (6000 \times g, 15 min, 14 °C), and resuspended in infiltration buffer (Table S6) to reach a final OD of 0.6. After shaking for 1-3 h at 25 °C, 25 mL of pBIN:p19-containing cultures were mixed with 25 mL cultures carrying *CYP79* or *eGFP*, or with a combination of 12.5 mL *CYP79* and 12.5 mL *CYP71E76* or *UGT85A123*. 3-week-old *N. benthamiana* plants were transformed by syringe infiltration, i.e., the opening of a soaked 1 mL syringe was held against the abaxial side of the leaf and the

suspension pressed into the leaves. Four leaves per plant were transformed. Plants were kept in a shaded place for 1 d before being transferred to a location with high light intensity. Leaves were harvested five days after transformation, pooled for each plant and stored at -80 °C.

NMR spectroscopy

NMR measurements were carried out on a 400 MHz Bruker Avance III HD spectrometer (Bruker Biospin GmbH, Rheinstetten, Germany) for phenylacetaldoxime. Data for phenylacetaldoxime glucoside were measured on a 500 MHz Bruker Avance III HD spectrometer, equipped with a TCI cryoprobe, using standard pulse sequences as implemented in Bruker Topspin ver. 3.6.1. Chemical shifts were referenced to the residual solvent signals of CDCl₃ (δ_{H} 7.26/ δ_{C} 77.16) and MeOH-*d*₃ (δ_{H} 3.31/ δ_{C} 49.0), respectively.

Synthesis of PAOx

The synthesis of PAOx from phenylacetaldehyde followed the protocol of Castellano et al. (2011). ¹H-NMR (400 MHz, CDCl₃) δ ppm: 8.32 (*brs*, 1H, OH), 7.41-7.23 (*m*, 5H, Ar-H), 6.94 (*t*, *J* = 5.3 Hz, 1H, NCH), 3.78 (*d*, *J* = 5.3 Hz, 2H, CH₂). The chemical shifts were in agreement with published data (Castellano et al., 2011). *E/Z*-configurations were assigned based on chemical shifts of the oxime protons (Karabatsos and Hsi, 1967). HRMS (ESI-TOF, positive) *m/z*: calculated for C₈H₁₀NO [M+H]⁺ 136.0757, found 136.0757.

Synthesis of phenylacetaldoxime glucoside (PAOx-Glc)

Phenylacetaldoxime glucoside was synthesized from *O*- β -D-glucopyranosyl-oxyamine (Lagnoux et al., 2005; Amano et al., 2018) following a published method (Tejler et al., 2005). To *O*- β -D-glucopyranosyl-oxyamine (3.8 mg, 0.019 mmol) in THF (160 μ L) was added benzoacetaldehyde (2.7 mg, 0.22 mmol), H₂O (160 μ L), and aqueous 0.1 M HCl solution (19 μ L). The reaction mixture was stirred overnight. The mixture was neutralized with aqueous 0.1 M NaHCO₃ solution and concentrated *in vacuo*. The residue was purified by short-path chromatography using a SPE cartridge (CHROMABOND HR-X, 3 mL, 200 mg, MACHEREY-NAGEL, MeOH:H₂O = 50:50 to 100:0) to give

phenylacetaldoxime glucoside (3.29 mg, 0.011 mmol, 58%, *E: Z* = 3:1). NMR data are shown in Figure S3-12. HRMS (ESI-TOF, positive) *m/z*: calculated for C₁₄H₂₀NO₆ [M+H]⁺ 298.1285, found 298.1285.

qRT-PCR analysis

qRT-PCR was performed to confirm results of the RNASeq experiment and to analyze gene expression upon different treatments. Experimental details are given in Table S7, S8, and the respective Figures S13 and S24.

Long-term response to herbivory

After a leaf of tocooca was wrapped in a perforated plastic bag, three *S.littoralis* larvae were placed on the leaf, allowed to feed for 24 h and removed. Leaf samples were harvested right before the treatment (0 d), upon removal of the caterpillars (1 d), or one to nine days after larval removal (2-10 d). All leaves were flash-frozen in liquid nitrogen and stored at -80 °C.

Spatial distribution of PAOx and PAOx-Glc

S. littoralis larvae were placed in clip cages (3.8 cm diameter) installed on single tocooca leaves and were allowed to feed on the leaves for 24 h. Afterwards, leaf samples were harvested using a stencil that enabled cutting out the clip cage area as well as leaf pieces with a distance of 1 cm to the previous piece (see Figure 5B). All samples were flash-frozen in liquid nitrogen and stored at -80 °C.

Induction of PAOx and PAOx-Glc by different simulations of herbivory

To investigate a potential effect of jasmonic acid (JA) on aldoxime production, tocooca leaves were sprayed with 1 mL 1 mM JA (1:90 in EtOH/dH₂O) or with a control solution (1:90 EtOH/ dH₂O). The same experiment was also conducted including a wounding step: utilizing a pattern wheel, tiny holes were punched into the leaves before spraying the JA or control solution. We also included an oral secretion (OS) treatment. The OS was collected beforehand from *S. littoralis* larvae (5th instar) feeding on tocooca leaves, centrifuged and the supernatant diluted 1:1 with dH₂O. Leaves were wounded with the pattern wheel before 200 µL diluted OS were applied to the adaxial and abaxial side of the leaf, respectively.

After application of the respective solution, leaves were dried for 1 h, before being wrapped in PET bags, to collect volatiles via the before mentioned push-pull system using the same parameters as described above for another 23 h. As a positive control, a 24 h *S. littoralis* feeding treatment with simultaneous volatile collection was performed as described before. All leaf samples were harvested 24 h after the respective treatment, flash-frozen in liquid nitrogen and stored at -80 °C.

Treatments of crape jasmine, poplar, and soybean

Clip cages with (treatment) or without (control) three *S. littoralis* larvae were placed on randomly selected middle-aged leaves of *T. divaricata* (crape jasmine) trees. The caterpillars fed slowly at first, and so they were allowed to feed for 48 h. Then, the leaves were excised, and green and brown parts of the leaves collected separately in liquid nitrogen. For *P. trichocarpa*, leaves were numbered according to the leaf plastochron index (LPI; Irmisch et al. (2013)). Then 10 *L. dispar* caterpillars or 12 *C. populi* beetles were released on *P. trichocarpa* leaves LPI3–7, allowed to feed for 24 h and removed. Leaf material was harvested 8 h after removal, flash-frozen in liquid nitrogen, ground, and one part stored at -80°C, while the other part was lyophilized and stored at 4°C. Soybean (*Glycine max* L. cv. Harosoy 63) cell suspension cultures were cultivated and the assay conducted according to Nißler et al. (2022). Briefly, cells were kept in the dark under shaking conditions (110 rpm, 26 °C) and were sub-cultured in fresh medium every 7 days. For the actual experiment, soybean cell suspension cultures were sub-cultured after 5 days in fresh medium (6 g cells in 40 mL medium) and grown for 2 days before, the suspension culture was carefully transferred to a 24 well plate (1 mL/well) (CELLSTAR® 662102, Greiner Bio-One, Kremsmünster, Austria). Ten µL raw elicitor (50 mg/mL ddH₂O) isolated from the cell walls of the oomycete *Phytophthora sojae* were added to the treatment group, whereas pure ddH₂O served as control. The plate was kept in the dark under shaking conditions (100 rpm, RT) for 4 days. Then, the suspensions were transferred to suitable tubes for centrifugation, cells were removed (5000 rpm, 4 °C, 20 min), and the supernatant transferred to a new vial for subsequent chemical analysis.

Raw protein extracts and β-glucosidase activity assays

After the larvae were immobilized by placing them on ice, the entire gut was extracted from the larvae and rinsed with 0.9% aqueous sodium chloride solution. For protein

extraction, 1 mL of prechilled gut extraction buffer (Table S6) and three metal beads were added to the isolated gut. The tissue was disrupted using 2010 Geno/Grinder® (SPEX®SamplePrep, Metuchen, NJ, USA) (4 °C, 1250 rpm, 2 ×1 min) and cell debris was removed by centrifugation (30 min, 13000 × g, 4 °C). The supernatant contained soluble proteins and enzymes. Similarly, proteins were extracted from 100 mg of *S. littoralis* damaged leaves (frozen, ground) by adding 3-4 metal beads and 1 mL gut extraction buffer (soybean, crape jasmine) or tococa protein extraction buffer (tococa, Table S6), tissue disruption using 2010 Geno/Grinder®, and removal of cell debris (same parameters). β -Glucosidase activity was tested by incubating 30 μ L crude protein extract with 30 μ L PAOx-Glc (20 μ g/mL) in 140 μ L assay buffer (Table S6) for 2.5 h at 30 °C under shaking conditions (300 rpm). The reaction was stopped by adding 200 μ L MeOH. As a positive control, the assay was carried out with 2.5 mM amygdalin (Roth, Karlsruhe, Germany) as substrate. As negative control, the assays were repeated with 30 μ L of boiled crude extracts (95 °C, 10 min). β -Glucosidase activity was analyzed by targeted LC-MS/MS. To test for glucosidase activity of the pathogenic bacteria, bacteria were grown under the same conditions as described in the subsequent paragraph for antimicrobial assays in the presence or absence of PAOx-Glc. After 24 h, samples were centrifuged to pellet the cells (4 °C, 10 min, 12 000 ×g), and the supernatant 1:100 diluted in methanol before analysis via LC-MS/MS.

Antimicrobial assays

PAOx was tested for antimicrobial effects on *Agrobacterium tumefaciens*, *P. syringae* pv. *syringae*, *Curtobacterium flaccumfaciens*, and *Clavibacter michiganensis*. Varying concentrations of PAOx (5 mM, 2.5 mM, 1.25 mM, 0.6 mM, 0.125 mM and 0 mM in a 20 μ L volume of DMSO/ddH₂O (1:10, v/v)) were added to 20 μ L of freshly grown bacterial cultures (OD_{600} = 0.025 (*C. flaccumfaciens*, *P. syringae*) - 0.1 (*C. michiganensis*, *A. tumefaciens*)) and 160 μ L LB-medium in a sterile 96-well microtiter plate. As a blank, 20 μ L DMSO:ddH₂O (1:10, v/v) were added to 180 μ L of LB-medium. Bacterial growth was monitored with a SPECTRAMax 250-Photometer (Molecular Devices, San Jose, CA, USA) by measuring the OD_{600} every 30 min for 22 h.

Phylogenetic analysis

For the construction of phylogenetic trees, amino acid alignments of the putative tococa enzymes and characterized enzymes from other plant species were created using the

MUSCLE algorithm (gap open, -2.9; gap extend, 0; hydrophobicity multiplier, 1.5; clustering method, UPGMA) implemented in MEGA6 (Tamura et al., 2013) and tree reconstructions were achieved with MEGA6 using the maximum-likelihood algorithm (Jones-Taylor-Thompson (JTT) model) for UGTs and CYP79 or the neighbor-joining algorithm (JTT model) for CYP71 sequences. Bootstrap resampling analyses with 1000 replicates were performed to evaluate the tree topologies. Amino acid alignments were also generated using the ClustalW algorithm and visualized with BioEdit (<http://www.mbio.ncsu.edu/bioedit/bioedit.html>). Accession numbers are listed in Supplemental Table S13.

Statistical analyses

Statistical analyses were performed with R (Posit_team, 2022). All data were tested for statistical assumptions (normal distribution and homogeneity of variances) using diagnostic plots and were log-transformed when necessary. Depending on whether or not the criteria were met, statistical tests were selected accordingly. Statistical details are provided in the figures (mean \pm SEM; significance) and figure legends (n, test, significance). Data for the volcano plot (Fig. 1B) were calculated using the MetaboAnalyst package (Pang et al., 2021) after data preprocessing with MetaboScape (Bruker Daltonics). Data were filtered by interquartile range and normalized using the Pareto algorithm. All results were visualized with OriginPro, version 2019 (OriginLab Corporation, Northampton, MA, USA).

Data availability

The RNA-Seq data generated in this study are deposited at NCBI SRA under the accession number PRJNA974355. Sequence data for characterized enzymes can be found under the following Genbank identifiers: CYP79A206 (OQ921381), CYP79A207 (OQ921382), CYP71E76 (OQ921383), UGT85A122 (OQ921379), UGT85A123 (OQ921380), UGT75AB1 (OQ921384), and UGT76AH1 (OQ921385). The paper does not report original code. The data that support the findings of this study are available in the supplementary material of this article. Any additional information will be provided by the corresponding author upon reasonable request.

Acknowledgements

We thank Michael H. Court (UGT nomenclature committee) and David R. Nelson (University of Tennessee) for UGT and P450 nomenclature, respectively, Grit Kunert for statistical advice, Birgit Arnold and all gardeners of the MPI-CE for helping us growing the plants, Sarah E. O'Connor and Francesco Trenti for providing crape jasmine trees, and Kilian Ossetek for help in the lab. The research was funded by the Max Planck Society, fellowships of the Friedrich Schiller University Jena as part of the IMPRS, and the German Academic Exchange Service (DAAD) to ATM.

Conflict of interest

All authors declare that they have no competing interests.

Author's contributions

TGK, AM, ATM, and JG designed the research. ATM, MR, NDL, and KL performed the research. YN synthesized the compounds of interest and performed NMR analysis. ATM, MR, and EC analyzed the data. ATM and TGK wrote the article with input from all other authors.

References

- Alvarez G, Armbrrecht I, Jimenez E, Armbrrecht H, Ulloa-Chaco P** (2001) Ant-plant association in two *Tococa* species from a primary rain forest of Colombian Choco (Hymenoptera: Formicidae). *Sociobiology* **38**: 585-602
- Amano Y, Nakamura M, Shiraishi S, Chigira N, Shiozawa N, Hagio M, Yano T, Hasegawa T** (2018) Preparation and functional analysis of gossypols having two carbohydrate appendages with enaminoxy linkages. *Carbohydr. Res.* **458-459**: 67-76
- Andersen MD, Busk PK, Svendsen I, Møller BL** (2000) Cytochromes P-450 from cassava (*Manihot esculenta* Crantz) catalyzing the first steps in the biosynthesis of the cyanogenic glucosides linamarin and lotaustralin. Cloning, functional expression in *Pichia pastoris*, and substrate specificity of the isolated recombinant enzymes. *J. Biol. Chem.* **275**: 1966-1975
- Bak S, Kahn RA, Nielsen HL, Møller BL, Halkier BA** (1998) Cloning of three A-type cytochromes P450, CYP71E1, CYP98, and CYP99 from *Sorghum bicolor* (L.) Moench by a PCR approach and identification by expression in *Escherichia coli* of CYP71E1 as a multifunctional cytochrome P450 in the biosynthesis of the cyanogenic glucoside dhurrin. *Plant Mol. Biol.* **36**: 393-405

- Bak S, Olsen CE, Petersen BL, Møller BL, Halkier BA** (1999) Metabolic engineering of p-hydroxybenzylglucosinolate in *Arabidopsis* by expression of the cyanogenic CYP79A1 from *Sorghum bicolor*. *Plant J.* **20**: 663-671
- Bartosova L, Kuca K, Kunesova G, Jun D** (2006) The acute toxicity of acetylcholinesterase reactivators in mice in relation to their structure. *Neurotox. Res.* **9**: 291-296
- Bergomaz R, Boppre M** (1986) A simple instant diet for rearing arctiidae and other moths. *J. Lepid. Soc.* **40**: 131-137
- Cabrera GM** (2006) Mass spectrometry in the structural elucidation of natural products: glycosides. *Phytochemistry*: 1-22
- Castellano S, Kuck D, Viviano M, Yoo J, López-Vallejo F, Conti P, Tamborini L, Pinto A, Medina-Franco JL, Sbardella G** (2011) Synthesis and biochemical evaluation of Δ^2 -Isoxazoline derivatives as DNA methyltransferase 1 inhibitors. *J. Med. Chem.* **54**: 7663-7677
- Clavijo McCormick A, Irmisch S, Reinecke A, Boeckler GA, Veit D, Reichelt M, Hansson BS, Gershenzon J, Köllner TG, Unsicker SB** (2014) Herbivore-induced volatile emission in black poplar: regulation and role in attracting herbivore enemies. *Plant Cell Environ.* **37**: 1909-1923
- Dejean A, Delabie JHC, Cerdan P, Gibernau M, Corbara B** (2006) Are myrmecophytes always better protected against herbivores than other plants? *Biol. J. Linn. Soc. Lond.* **89**: 91-97
- Dewick P** (1984) The biosynthesis of cyanogenic glycosides and glucosinolates. *Nat. Prod. Rep.* **1**: 545-549
- Drumm JE, Adams JB, Brown RJ, Campbell CL, Erbes DL, Hall WT, Hartzell SL, Holliday MJ, Kleier DA, Martin MJ, Pember SO, Ramsey GR** (1995) Oxime fungicides: Highly active broad-spectrum protectants. *In* Synthesis and Chemistry of Agrochemicals IV, Vol 584. American Chemical Society, pp 396-405
- Gachon CMM, Langlois-Meurinne M, Saindrenan P** (2005) Plant secondary metabolism glycosyltransferases: the emerging functional analysis. *Trends Plant Sci.* **10**: 542-549
- Glawischnig E** (2007) Camalexin. *Phytochemistry* **68**: 401-406
- Gonzalez-Teuber M, Kaltenpoth M, Boland W** (2014) Mutualistic ants as an indirect defence against leaf pathogens. *New Phytol* **202**: 640-650
- Grootwassink JWD, Balsevich JJ, Kolenovsky AD** (1990) Formation of sulfatoglucosides from exogenous aldoximes in plant cell cultures and organs. *Plant Sci.* **66**: 11-20
- Gunther J, Irmisch S, Lackus ND, Reichelt M, Gershenzon J, Köllner TG** (2018) The nitrilase PtNIT1 catabolizes herbivore-induced nitriles in *Populus trichocarpa*. *BMC Plant Biol.* **18**: 251
- Halkier BA, Nielsen HL, Koch B, Møller BL** (1995) Purification and characterization of recombinant cytochrome P450TYR expressed at high levels in *Escherichia coli*. *Arch. Biochem. Biophys.* **322**: 369-377
- Hansen CC, Sorensen M, Veiga TAM, Zibrandtsen JFS, Heskes AM, Olsen CE, Boughton BA, Møller BL, Neilson EHJ** (2018) Reconfigured cyanogenic glucoside biosynthesis in *Eucalyptus cladocalyx* involves a cytochrome P450

CYP706C55. *Plant Physiol.* **178**: 1081-1095

- Irmisch S, Clavijo McCormick A, Gunther J, Schmidt A, Boeckler GA, Gershenzon J, Unsicker SB, Köllner TG** (2014) Herbivore-induced poplar cytochrome P450 enzymes of the CYP71 family convert aldoximes to nitriles which repel a generalist caterpillar. *Plant J.* **80**: 1095-1107
- Irmisch S, McCormick AC, Boeckler GA, Schmidt A, Reichelt M, Schneider B, Block K, Schnitzler JP, Gershenzon J, Unsicker SB, Köllner TG** (2013) Two herbivore-induced cytochrome P450 enzymes CYP79D6 and CYP79D7 catalyze the formation of volatile aldoximes involved in poplar defense. *Plant Cell* **25**: 4737-4754
- Irmisch S, Zeltner P, Handrick V, Gershenzon J, Köllner TG** (2015) The maize cytochrome P450 CYP79A61 produces phenylacetaldoxime and indole-3-acetaldoxime in heterologous systems and might contribute to plant defense and auxin formation. *BMC Plant Biol.* **15**: 128
- Jones P, Vogt T** (2001) Glycosyltransferases in secondary plant metabolism: tranquilizers and stimulant controllers. *Planta* **213**: 164-174
- Jones PR, Møller BL, Hoj PB** (1999) The UDP-glucose:p-hydroxymandelonitrile-O-glucosyltransferase that catalyzes the last step in synthesis of the cyanogenic glucoside dhurrin in *Sorghum bicolor*. Isolation, cloning, heterologous expression, and substrate specificity. *J. Biol. Chem.* **274**: 35483-35491
- Jørgensen K, Morant AV, Morant M, Jensen NB, Olsen CE, Kannangara R, Motawia MS, Møller BL, Bak S** (2011) Biosynthesis of the cyanogenic glucosides linamarin and lotaustralin in cassava: isolation, biochemical characterization, and expression pattern of CYP71E7, the oxime-metabolizing cytochrome P450 enzyme. *Plant Physiol.* **155**: 282-292
- Karabatsos GJ, Hsi N** (1967) Structural studies by nuclear magnetic resonance—XI: Conformations and configurations of oxime o-methyl ethers. *Tetrahedron* **23**: 1079-1095
- Knoch E, Motawie MS, Olsen CE, Møller BL, Lyngkjaer MF** (2016) Biosynthesis of the leucine derived α -, β - and γ -hydroxynitrile glucosides in barley (*Hordeum vulgare L.*). *Plant J.* **88**: 247-256
- Lackus ND, Müller A, Krober TDU, Reichelt M, Schmidt A, Nakamura Y, Paetz C, Luck K, Lindroth RL, Constabel CP, Unsicker SB, Gershenzon J, Köllner TG** (2020) The occurrence of sulfated salicinoids in poplar and their formation by sulfotransferase1. *Plant Physiol.* **183**: 137-151
- Lackus ND, Schmidt A, Gershenzon J, Köllner TG** (2021) A peroxisomal β -oxidative pathway contributes to the formation of C6–C1 aromatic volatiles in poplar. *Plant Physiol.* **186**: 891-909
- Lagnoux D, Darbre T, Schmitz ML, Reymond J-L** (2005) Inhibition of mitosis by glycopeptide dendrimer conjugates of Colchicine. *Chem. Eur. J.* **11**: 3941-3950
- Lemarie S, Robert-Seilantantz A, Lariagon C, Lemoine J, Marnet N, Levrel A, Jubault M, Manzanares-Dauleux MJ, Gravot A** (2015) Camalexin contributes to the partial resistance of *Arabidopsis thaliana* to the biotrophic soilborne protist *Plasmodiophora brassicae*. *Front. Plant Sci.* **6**: 539
- Liao Y, Zeng L, Tan H, Cheng S, Dong F, Yang Z** (2020) Biochemical pathway of benzyl nitrile derived from L-phenylalanine in tea (*Camellia sinensis*) and its formation in response to postharvest stresses. *J. Agric. Food Chem.* **68**: 1397-

1404

- Luck K, Jia Q, Huber M, Handrick V, Wong GK, Nelson DR, Chen F, Gershenzon J, Köllner TG** (2017) CYP79 P450 monooxygenases in gymnosperms: CYP79A118 is associated with the formation of taxiphyllin in *Taxus baccata*. *Plant Mol. Biol.* **95**: 169-180
- Luck K, Jirschwitzka J, Irmisch S, Huber M, Gershenzon J, Köllner TG** (2016) CYP79D enzymes contribute to jasmonic acid-induced formation of aldoximes and other nitrogenous volatiles in two *Erythroxylum* species. *BMC Plant Biol.* **16**: 215
- Malik NAA, Kumar IS, Nadarajah K** (2020) Elicitor and receptor molecules: Orchestrators of plant defense and immunity. *Int. J. Mol. Sci.* **21**: 963
- Michelangeli FA** (2003) Ant protection against herbivory in three species of *Tococa* (Melastomataceae) occupying different environments. *Biotropica* **35**: 181-188
- Morant AV, Jørgensen K, Jørgensen B, Dam W, Olsen CE, Møller BL, Bak S** (2007) Lessons learned from metabolic engineering of cyanogenic glucosides. *Metabolomics* **3**: 383-398
- Morawetz W, Henzl M, Wallnöfer B** (1992) Tree killing by herbicide producing ants for the establishment of pure *Tococa occidentalis* populations in the Peruvian Amazon. *Biodivers. Conserv.* **1**: 19-33
- Müller AT, Reichelt M, Cosio EG, Salinas N, Nina A, Wang D, Moossen H, Geilmann H, Gershenzon J, Köllner TG, Mithöfer A** (2022) Combined –omics framework reveals how ant symbionts benefit the Neotropical ant-plant *Tococa quadrialata* at different levels. *iScience* **25**: 105261
- Naur P, Petersen BL, Mikkelsen MD, Bak S, Rasmussen H, Olsen CE, Halkier BA** (2003) CYP83A1 and CYP83B1, two nonredundant cytochrome P450 enzymes metabolizing oximes in the biosynthesis of glucosinolates in Arabidopsis. *Plant Physiol.* **133**: 63-72
- Nißler R, Müller AT, Dohrman F, Kurth L, Li H, Cosio EG, Flavel BS, Giraldo JP, Mithöfer A, Kruss S** (2022) Detection and imaging of the plant pathogen response by near-infrared fluorescent polyphenol sensors. *Angew. Chem. Int.* **61**: e202108373
- Pang Z, Chong J, Zhou G, de Lima Morais DA, Chang L, Barrette M, Gauthier C, Jacques P-É, Li S, Xia J** (2021) MetaboAnalyst 5.0: narrowing the gap between raw spectra and functional insights. *Nucleic Acids Res.* **49**: W388-W396
- Pfaffl MW** (2001) A new mathematical model for relative quantification in real-time RT-PCR. *Nucleic Acids Res.* **29**: e45
- Pompon D, Louerat B, Bronine A, Urban P** (1996) Yeast expression of animal and plant P450s in optimized redox environments. *Methods Enzymol* **272**: 51-64
- Posit_team** (2022) RStudio: Integrated Development Environment for R. *In* PBC, ed, <http://www.posit.co/>. Posit Software, PBC, Boston, MA
- Rizwan HM, Zhimin L, Harsonowati W, Waheed A, Qiang Y, Yousef AF, Munir N, Wei X, Scholz SS, Reichelt M, Oelmüller R, Chen F** (2021) Identification of fungal pathogens to control postharvest passion fruit (*Passiflora edulis*) decays and multi-omics comparative pathway analysis reveals purple is more resistant to pathogens than a yellow cultivar. *J.Fungi* **7**: 879
- Ro D-K, Ouellet M, Paradise EM, Burd H, Eng D, Paddon CJ, Newman JD, Keasling**

- JD** (2008) Induction of multiple pleiotropic drug resistance genes in yeast engineered to produce an increased level of anti-malarial drug precursor, artemisinic acid. *BMC Biotechnol.* **8**: 83
- Savatin DV, Gramegna G, Modesti V, Cervone F** (2014) Wounding in the plant tissue: the defense of a dangerous passage. *Front. Plant Sci.* **5**: 470
- Sibbesen O, Koch B, Halkier BA, Møller BL** (1995) Cytochrome P-450TYR is a multifunctional heme-thiolate enzyme catalyzing the conversion of L-tyrosine to p-hydroxyphenylacetaldehyde oxime in the biosynthesis of the cyanogenic glucoside dhurrin in *Sorghum bicolor* (L.) Moench. *J. Biol. Chem.* **270**: 3506-3511
- Sorensen M, Neilson EHJ, Møller BL** (2018) Oximes: Unrecognized chameleons in general and specialized plant metabolism. *Mol. Plant* **11**: 95-117
- Takos AM, Knudsen C, Lai D, Kannangara R, Mikkelsen L, Motawia MS, Olsen CE, Sato S, Tabata S, Jørgensen K, Møller BL, Rook F** (2011) Genomic clustering of cyanogenic glucoside biosynthetic genes aids their identification in *Lotus japonicus* and suggests the repeated evolution of this chemical defence pathway. *Plant J.* **68**: 273-286
- Tamura K, Stecher G, Peterson D, Filipowski A, Kumar S** (2013) MEGA6: Molecular Evolutionary Genetics Analysis version 6.0. *Mol Biol Evol* **30**: 2725-2729
- Tapper BA, Conn EE, Butler GW** (1967) Conversion of α -keto-isovaleric acid oxime and isobutyraldoxime to linamarin in flax seedlings. *Arch. Biochem. Biophys.* **119**: 593-595
- Tejler J, Leffler H, Nilsson UJ** (2005) Synthesis of O-galactosyl aldoximes as potent LacNAc-mimetic galectin-3 inhibitors. *Bioorg. Med. Chem. Lett.* **15**: 2343-2345
- Thodberg S, Sørensen M, Bellucci M, Crocoll C, Bendtsen AK, Nelson DR, Motawia MS, Møller BL, Neilson EHJ** (2020) A flavin-dependent monooxygenase catalyzes the initial step in cyanogenic glycoside synthesis in ferns. *Commun. Biol.* **3**: 507
- Underhill EW** (1967) Biosynthesis of Mustard Oil Glucosides. *Eur. J. Biochem.* **2**: 61-63
- Wittstock U, Halkier BA** (2000) Cytochrome P450 CYP79A2 from *Arabidopsis thaliana* L. catalyzes the conversion of L-phenylalanine to phenylacetaldoxime in the biosynthesis of benzylglucosinolate. *J. Biol. Chem.* **275**: 14659-14666
- Yamaguchi T, Noge K, Asano Y** (2016) Cytochrome P450 CYP71AT96 catalyses the final step of herbivore-induced phenylacetonitrile biosynthesis in the giant knotweed, *Fallopia sachalinensis*. *Plant Mol. Biol.* **91**: 229-239
- Yamaguchi T, Yamamoto K, Asano Y** (2014) Identification and characterization of CYP79D16 and CYP71AN24 catalyzing the first and second steps in L-phenylalanine-derived cyanogenic glycoside biosynthesis in the Japanese apricot, *Prunus mume* Sieb. et Zucc. *Plant Mol. Biol.* **86**: 215-223
- Zeng-hui H, Di Y, Ying-bai S** (2004) Difference in volatiles of poplar induced by various damages. *J. For. Res.* **15**: 280-282
- Zhu B, Wang Z, Yang J, Zhu Z, Wang H** (2012) Isolation and expression of glucosinolate synthesis genes CYP83A1 and CYP83B1 in Pak Choi (*Brassica rapa* L. ssp. *chinensis* var. *communis* (N. Tsen & S.H. Lee) Hanelt). *Int. J. Mol. Sci.* **13**: 5832-5843

2.4 Manuscript III

Manuscript title: Detection and Imaging of the Plant Pathogen Response by Near-Infrared Fluorescent Polyphenol Sensors

Authors: Robert Nißler, Andrea T. Müller, Frederike Dohrman, Larissa Kurth, Han Li, Eric G. Cosio, Benjamin S. Flavel, Juan P. Giraldo, Axel Mithöfer, Sebastian Kruss

Bibliographic information: Angewandte Chemie International Edition (2022), 61(2), e202108373. doi: 10.1002/anie.202108373

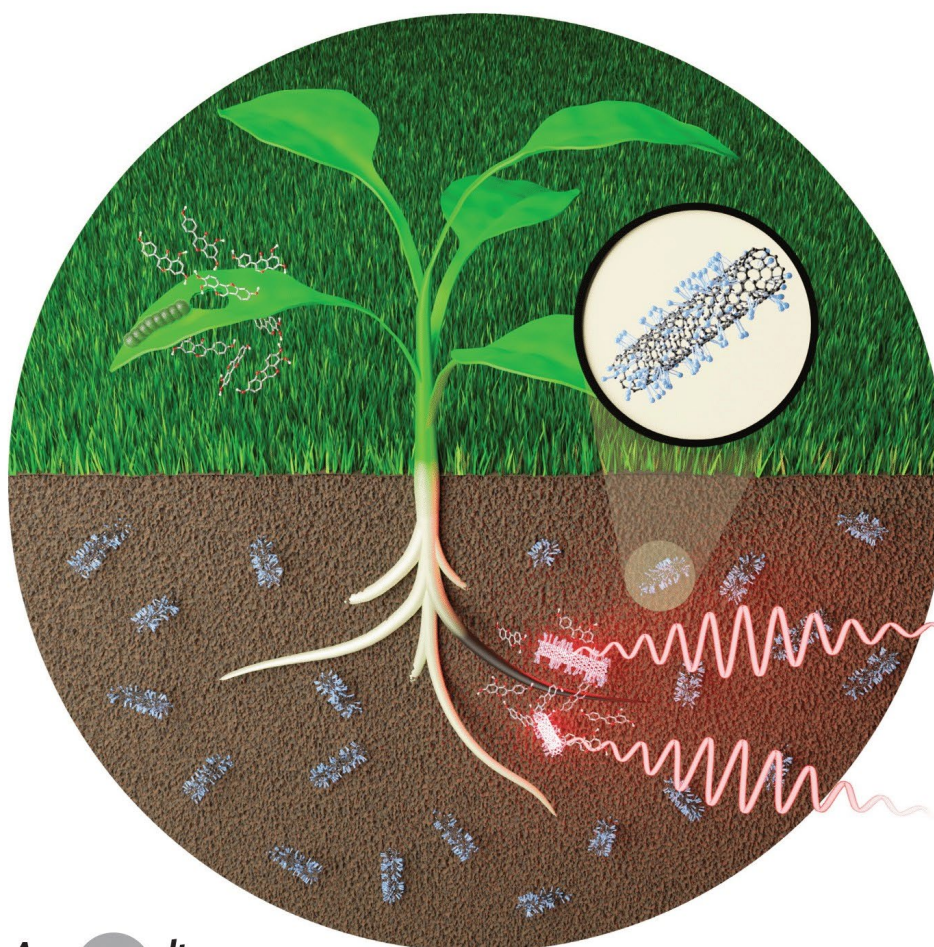
The candidate is

First author, Co-first author, Corresponding author, Co-author

Status: published

Authors' contributions (in %) to the given categories of the publication

| Author | Conceptual | Data analysis | Experimental | Writing the manuscript | Provision of material |
|------------------|------------|---------------|--------------|------------------------|-----------------------|
| Andrea T. Müller | 15% | 20% | 30% | 15% | - |
| Robert Nißler | 40% | 70% | 60% | 60% | - |
| Axel Mithöfer | 25% | - | - | 5% | 30% |
| Sebastian Kruss | 10% | - | - | 15% | 50% |
| Others: | 10% | 10% | 10% | 5% | 20% |
| Total: | 100% | 100% | 100% | 100% | 100% |

 **Biosensors** **Hot Paper**How to cite: *Angew. Chem. Int. Ed.* **2022**, *61*, e202108373
International Edition: doi.org/10.1002/anie.202108373
German Edition: doi.org/10.1002/ange.202108373 **Detection and Imaging of the Plant Pathogen Response by Near-Infrared Fluorescent Polyphenol Sensors***Robert Nißler, Andrea T. Müller, Frederike Dohrman, Larissa Kurth, Han Li, Eric G. Cosio, Benjamin S. Flavel, Juan Pablo Giraldo, Axel Mithöfer, and Sebastian Kruss**

Abstract: Plants use secondary metabolites such as polyphenols for chemical defense against pathogens and herbivores. Despite their importance in plant pathogen interactions and tolerance to diseases, it remains challenging to detect polyphenols in complex plant tissues. Here, we create molecular sensors for plant polyphenol imaging that are based on near-infrared (NIR) fluorescent single-wall carbon nanotubes (SWCNTs). We identified polyethylene glycol–phospholipids that render (6,5)-SWCNTs sensitive ($K_d=90$ nM) to plant polyphenols (tannins, flavonoids, ...), which red-shift (up to 20 nm) and quench their emission (ca. 1000 nm). These sensors report changes in total polyphenol level after herbivore or pathogen challenge in crop plant systems (Soybean *Glycine max*) and leaf tissue extracts (*Tococa spp.*). We furthermore demonstrate remote chemical imaging of pathogen-induced polyphenol release from roots of soybean seedlings over the time course of 24 h. This approach allows *in situ* visualization and understanding of the chemical plant defense in real time and paves the way for plant phenotyping for optimized polyphenol secretion.

Introduction

Smart agricultural solutions are required to optimize production practices and crop yields to enable a sustainable food supply for a rising global population. The rapid growth in human population will require a 60% increase or more in food production by 2050 relative to 2005–2007 levels.^[1] In contrast, pathogen-induced stresses significantly reduce crop health and yield.^[2,3] One solution is precision agriculture that aims for early detection of crop disease using vehicle remote imaging or sensing^[4] and crop phenotyping aims to breed plants with improved tolerance to pathogen stress. Tools for quantifying plants' internal chemical signals associated with stress in real-time are needed to boost these agriculture and phenotyping efforts.^[5,6]

Recent advances in chemistry and nanotechnology can contribute to improve crop production via novel sensor approaches allowing for remote analysis and optimization of

plant traits.^[7,8] Semiconducting single-wall carbon nanotubes (SWCNTs) are a powerful building block for these plant sensors because of their distinct photophysical properties.^[9–11] Particularly, they fluoresce in the near-infrared (NIR) region of the electromagnetic spectrum, which corresponds to the optical tissue transparency window due to decreased scattering and ultra-low background.^[12] The discrete emission wavelength ranges from around 850 to 2400 nm and depends on their carbon lattice (band gap) structure, determined by the chirality (n,m).^[13] SWCNTs are not prone to photobleaching and can be used as optical labels and sensors, which are sensitive to their chemical environment.^[14–16] SWCNT-based sensors have been used as powerful imaging tools to analyze biological processes with high spatiotemporal resolution.^[17–19] This technique was applied to detect genetic material,^[20] proteins^[21,22] lipids,^[23] bacterial motives^[24] or small signaling molecules such as neurotransmitters,^[19,25] reactive oxygen species (ROS)^[26–28] or nitric oxide (NO).^[29] More recently, their utilization as non-genetically encoded sensors enabled the visualization of ROS patterns,^[27,30,31] auxins^[32] or heavy metal uptake^[33] in plants.^[34] To tailor the SWCNT-sensor properties, different chemical design strategies for surface functionalization have been developed. Most commonly, biopolymers such as single-stranded (ss)DNA are adsorbed on the SWCNT surface, which mediates colloidal stability in aqueous solution and molecular recognition of the analyte.^[35–38] Other design and sensing concepts rely on non-covalent functionalization with aptamers,^[17,39] phospholipids,^[40] peptides,^[41,42] proteins,^[43] or peptide–DNA hybrids.^[44,45] Recently, also covalent modification of fluorescent SWCNTs with (bio)molecules has been reported.^[46,47]

Detecting dynamic physiological processes in plants, such as defense responses to pathogen attack, could improve our understanding of plant pathogen interactions and help breed plants with increased biotic stress tolerance. Polyphenols, ubiquitous in the plant kingdom, are a prominent class of plant secondary metabolites involved in the constitutive and also inducible defense against pathogens and herbivores.^[48,49] They can be generally found in all plant tissues and organs

[*] R. Nißler, Prof. Dr. S. Kruss
Physical Chemistry II, Bochum University
Universitätsstrasse 150, 44801 Bochum (Germany)
E-mail: sebastian.kruss@rub.de
R. Nißler, F. Dohrman, L. Kurth, Prof. Dr. S. Kruss
Institute of Physical Chemistry
Georg-August Universität Göttingen
Tammannstrasse 6, 37077 Göttingen (Germany)
A. T. Müller, Priv.-Doz. Dr. A. Mithöfer
Research Group Plant Defense Physiology
Max Planck Institute for Chemical Ecology
Hans-Knöll-Strasse 8, 07745 Jena (Germany)
Dr. H. Li, Dr. B. S. Flavel
Institute of Nanotechnology
Karlsruhe Institute of Technology (KIT)
76344 Eggenstein-Leopoldshafen (Germany)
Prof. Dr. E. G. Cosio
Institute for Nature Earth and Energy (INTE-PUCP)
Pontifical Catholic University of Peru
Av. Universitaria 1801, San Miguel 15088, Lima (Peru)

Prof. J. P. Giraldo
Department of Botany and Plant Sciences
University of California
Riverside, CA 92507 (USA)
Prof. Dr. S. Kruss
Fraunhofer Institute for Microelectronic Circuits and Systems
Finkenstrasse 61, 47057 Duisburg (Germany)

Supporting information and the ORCID identification number(s) for the author(s) of this article can be found under:
<https://doi.org/10.1002/anie.202108373>.

© 2021 The Authors. Angewandte Chemie International Edition published by Wiley-VCH GmbH. This is an open access article under the terms of the Creative Commons Attribution License, which permits use, distribution and reproduction in any medium, provided the original work is properly cited.

and comprise a great variety of chemical structures with diverse ecological roles.^[50] One distinct aspect of polyphenol-related plant defense is chemical secretion into the rhizosphere (root exudates), which modulates plant interactions within the soil ecosystem.^[51] These exudates/secretions are able to repel, inhibit, or even kill pathogenic microorganisms.^[51] Hence, increased production improves natural plant defense and is a goal of plant breeding.^[52]

However, in situ detection and visualization of these biological processes remain a challenge because most analytical approaches cannot non-invasively access in vivo systems.^[53–55] Here, we created a NIR-fluorescent sensor/probe for plant polyphenol detection and imaging. It responds to polyphenols in vitro and enables in vivo/in situ chemical imaging of polyphenols released from plant roots challenged with pathogen-related stress.

Results and Discussion

Plant polyphenols are natural products with diverse chemical structures. Therefore, we tested how polyphenols (Figure 1b) from different subgroups (e.g. tannins, flavonoids, phenolic acids) modulate the NIR fluorescence of SWCNT-based molecular sensors. To assess the impact of surface chemistry (Figure 1) we used ssDNA with variable nucleotide composition (A,T,G,C) and polyethylene glycol (PEG)-phospholipid macromolecules for molecular assembly. Our rationale was that some of them have been known to interact with compounds that possess multiple hydroxy groups such as

tannins.^[56] In general, the modified SWCNTs either increased or decreased their fluorescence in response to the target molecules, as shown for C₃₀- and PEG(5 kDa)-PL-SWCNTs (Figure 1c–e). For different SWCNT conjugates we observed changes in fluorescence (Figure 1f) after addition of polyphenols in the physiologically relevant concentration range.^[50,57,58] To exclude pH- or ionic strength-related sensing effects,^[59] all experiments were performed in buffer. There is a general tendency of fluorescence increase for ssDNA-SWCNTs and a decrease for PEG-PL-SWCNTs (see also Supplementary Figure S1). All tested compounds with two or more hydroxy residues on the phenol structure led to a significant fluorescence change, while salicylic acid did not alter the emission features of the tested SWCNTs. This finding was further supported by the lacking response of a trimethylated version of gallic acid (GaA) (Supplementary Figure S1).

Next to the evaluated intensity changes, also shifts in the emission wavelengths occurred. This phenomenon is most prominently observed for tannic acid (TaA) (Figure 2a–c), resulting in ≈ 3 nm shifts for ssDNA- and ≈ 20 nm shifts for PEG-PL-SWCNTs. Only TaA caused a large emission wavelengths shift, whereas GaA changed ssDNA-SWCNTs intensity more strongly (up to > 100%). These results suggest that the three-dimensional structure of TaA affects sensing, an observation likely true also for other structurally large polyphenols. To better understand the interaction between tannins and the sensors, concentration-dependent measurements were performed for different ssDNA-SWCNTs. Interestingly, the fluorescence intensity increased in the nM

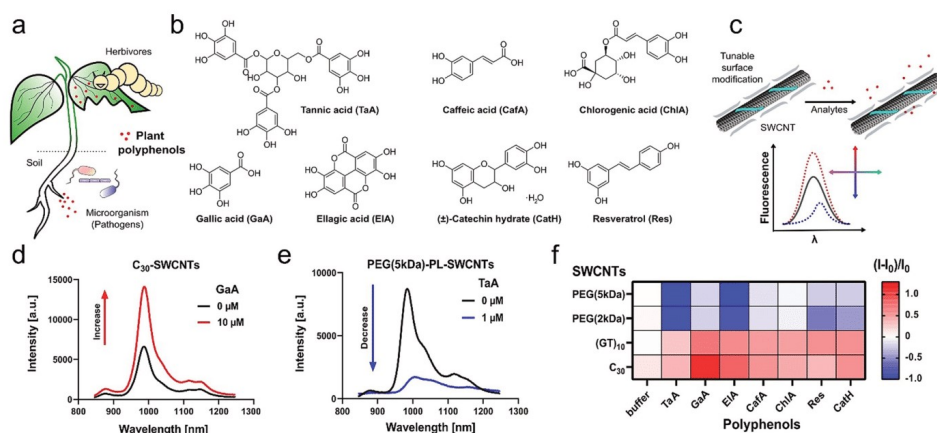


Figure 1. NIR fluorescent nanosensors for plant polyphenols. a) Plant polyphenols are released from leaves and roots in response to pathogens or herbivores and play an important role in chemical plant defense. b) Selected plant polyphenols investigated in this study. The compounds represent the subclasses of tannins, flavonoids and phenolic acids (see Supplementary Figure S1 for complete list). c) Non-covalently modified SWCNTs with different kinds of biopolymers can change their fluorescence in response to polyphenols and serve as sensors by modulating emission intensity and energy (wavelength). d) NIR fluorescence spectra of single-stranded (ss)DNA and e) PEG-phospholipid (PL)-modified SWCNTs as examples for SWCNTs that change their fluorescence in response to polyphenols. f) Fluorescence change $((I-I_0)/I_0)$ of selected sensors in response to plant polyphenols (mean, $n=3$). Shades of blue indicate fluorescence decrease and shades of red fluorescence increase (polyphenol concentration = 10 μ M; TaA = 1 μ M).

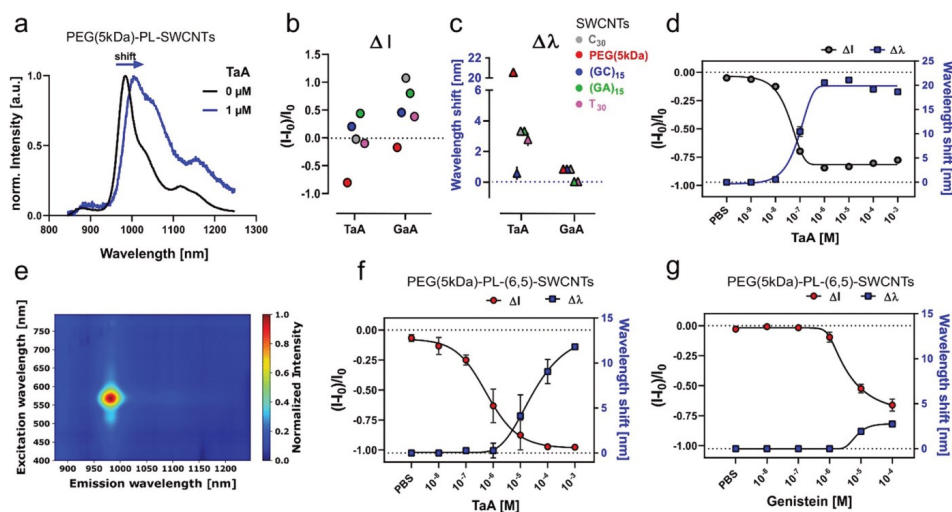


Figure 2. NIR detection of tannins in vitro. a) Normalized NIR fluorescence spectra of PEG-PL-SWCNTs without (black) and in presence (blue) of tannic acid (TaA). The emission wavelength shifts in addition to a change in fluorescence intensity. b) Comparison of intensity and in c) wavelength shifts of functionalized SWCNTs interacting with TaA and its subunits gallic acid (GaA) (10 μ M; mean \pm SD, $n=3$). Similar trends are visible for intensity changes, while emission wavelengths are not shifted in presence of GaA. It suggests that the 3D structure of TaA and less the gallic acid subunits are crucial. d) NIR fluorescence shifts of PEG-PL-SWCNTs in response to TaA. Intensity (black fit) decreases and wavelength shift (blue fit) increases in a concentration-dependent manner (mean \pm SD, $n=3$). e) 2D-excitation emission photoluminescence spectra of chirality-pure (6,5)-SWCNTs. f) Monochiral sensor response of PEG-PL-(6,5)-SWCNTs to TaA and g) to genistein addition. Intensity changes are indicated in red; wavelength shifts in blue (line = fit, mean \pm SD, $n=3$).

regime, whereas it decreased for most sequences in the μ M to mM range (Supplementary Figure S2). A uniform result was observed for PEG-PL-SWCNTs (Figure 2a,d). Unlike for most ssDNA-SWCNTs, the intensity decrease was clearly concentration dependent ($K_d=9.1 \times 10^{-8}$ M) and saturated in the lower μ M range ($\sim 80\%$ intensity change and ≈ 20 nm emission wavelength shift). GaA (1 mM) in contrast led to a much smaller sensor response of $\leq -36\%$ and ≤ 3 nm shift. In addition to the change in emission of PEG-PL-SWCNTs also E_{11} absorption maximum was redshifted by ≈ 10 nm (Supplementary Figure S2). Overall, such interplay indicates a sensing mechanism based on a change in fluorescence quantum yield, without dominant aggregation effects. It furthermore suggests a strong interaction between sensor and analyte that goes beyond polyphenols acting as antioxidants^[60,61] and might include changes in solvation that affects exciton diffusion. Hence, PEG-PL-SWCNTs showed the most promising response to plant polyphenols.

Next, we evaluated if sensing with monochiral SWCNTs of a well-defined emission wavelength (color) is possible. Non-overlapping emission spectra are required for multiplexed sensing and hyperspectral imaging approaches. To obtain monochiral (6,5)-SWCNTs, aqueous two-phase separation (ATPE) was performed, followed by surface exchange to PEG-PL (Figure 2e, Supplementary Figure S3). Monochiral sensors responded in a similar fashion ($K_d=4.3 \times$

10^{-6} M) (Figure 2f). Similar sensor responses were observed for the isoflavonoid called genistein (Figure 2g). It has been described that mainly surface modification imparts sensitivity and selectivity and not chirality.^[62] However, experiments with multi-chirality (HiPco) PEG-PL-SWCNTs showed distinct differences pointing to a polyphenol profile and chirality-dependent response (Supplementary Figure S4).

To test these sensors in more complex environments we used plant tissue extract and culture medium. For this purpose, methanol extracts from *Tococa* spp. leaf tissue (Figure 3a) and liquid media from soybean (*Glycine max*) suspension cell cultures (Figure 3b) were tested. Neotropical *Tococa* spp. is known for its high polyphenol content (e.g. ellagitannins, Supplementary Figure S5) and serves as a model system for polyphenol releasing plants. The sensors showed a strong fluorescence decrease (Figure 3c) along with a large emission shift in a low μ g mL $^{-1}$ range. This response correlates with the response of pure polyphenols (Figure 1 and Figure 2). The total phenol content was additionally quantified with an established colorimetric assay (Folin-Ciocalteu reagent^[63]). The sensor responses ($K_d=1.5$ μ M for purified polyphenols, Supplementary Figure S5) correlated with total phenol content (expressed as gallic acid equivalents). When correlating all tested *Tococa* leaf methanol extracts, an overall curve fitting with $K_d \approx 140$ μ M was obtained (Figure 3d). These results indicate that the sensors are able to probe the

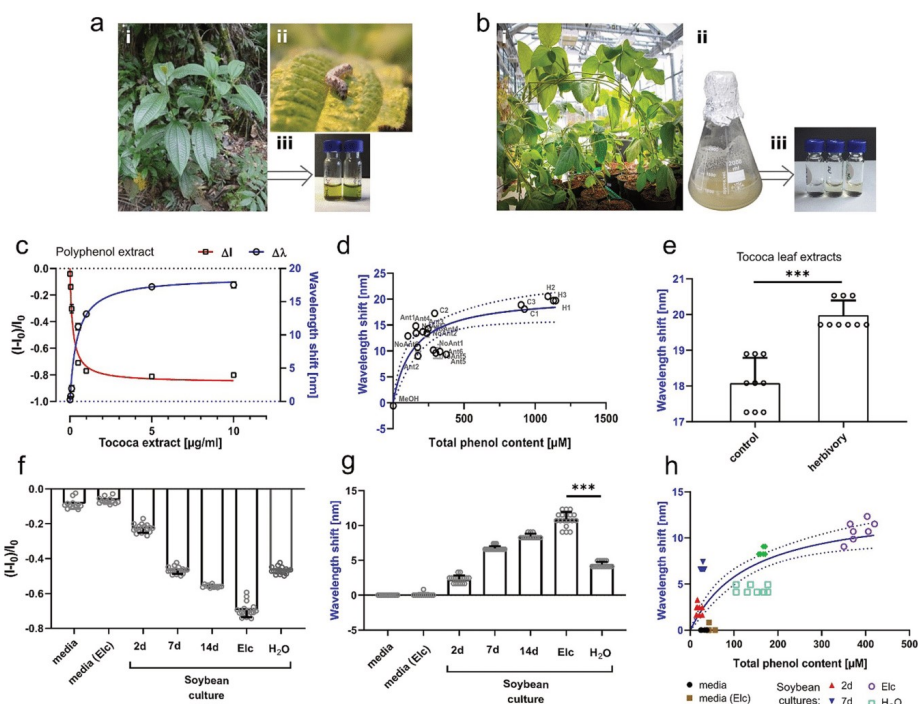


Figure 3. Polyphenol detection in plant extracts. a) *Tococa* spp. plants. i—wild plants found in the Peruvian rain forest. ii—the herbivore *Spodoptera littoralis* on a *Tococa* leaf. iii—crude MeOH leaf extracts used for sensor testing. b) Soybean (*Glycine max*) plants. i—an adult *G. max* plant grown in the greenhouse. ii—*G. max* suspension cell culture. iii—cell culture supernatant used for nanosensor testing. c) Nanosensor (PEG-PL-SWCNTs) response against purified polyphenol extract from *Tococa* spp., containing all extractable leaf polyphenols with a predominantly high ellagitannin content. The NIR fluorescence decreases and simultaneously the emission wavelength shifts (mean \pm SD, $n=3$, colored line = hyperbolic fit). d) Correlation of emission wavelength shift and the total phenol content from multiple *Tococa* leaf MeOH extracts (measured using the Folin–Ciocalteu reagent, which is an established colorimetric assay). The dynamic range of the sensor is in the μM range ($K_d=142 \mu\text{M}$, expressed as gallic acid equivalents) (mean \pm SD, $N=1$, $n=3$, tested as $2 \mu\text{L}$ non-diluted MeOH extracts, blue line = hyperbolic fit; C = control, H = herbivory, Ant = plants with ant symbionts). e) *Tococa* leaf extracts from plants challenged with herbivores (*S. littoralis*) give a significantly different nanosensor response compared to non-treated plants (mean \pm SD, $N=3$, $n=3$, unpaired t-test). f) Soybean (*Glycine max*) cell culture samples decrease fluorescence and shift emission wavelengths (g) of nanosensors, which allows detection of age- and pathogen-induced (Elic, elicitor) changes in polyphenol levels (mean \pm SD, $N=6$, $n=3$, $***P < 0.001$; one-way ANOVA). h) Correlation of emission wavelength shift with total phenol content (quantified by Folin–Ciocalteu reagent) shows a hyperbolic trend with a K_d of $140 \mu\text{M}$ ($N=6$, $n=2$, blue line = hyperbolic fit).

species-specific phenol content as relative increases even within a complex background (Supplementary Figure S6). Additionally, extracts of plants stressed by insect herbivory caused a significant difference in sensor response (Figure 3e), which correlated with an increased total phenolic content (Figure 3d). The results are in agreement with classical HPLC–MS polyphenol detection (Supplementary Figure S7) and demonstrate that these NIR fluorescent sensors identify polyphenols even with a chlorophyll or sugar background (methanol extraction). Plant extracts from the field (Peruvian rainforest in the Tambopata National Reserve) showed a similar response as HPLC–MS-based detection (Supplementary Figure S7). Therefore, these nanosensors are a val-

uable tool for rapid and high-throughput screening, requiring very small volume (few μL) of plant extracts. These hallmarks are desired for testing of plant analytes that are difficult to extract in large volumes, for example, phloem sap, or with low concentration of analytes, for example, xylem sap. The second plant system were soybean-based (*Glycine max*) suspension cells (Figure 3b, Supplementary Figure S8). They are known to release polyphenols, in particular pterocarpanes, into the medium during aging or due to pathogen stress.^[64,65] We directly added the cell-free supernatant of the culture to the nanosensors, without further purification. Mature cells showed a stronger sensor response, which means that they

produced more polyphenols (Figure 3 f,g, Supplementary Figure S9).

These soybean cultures were also stimulated with a pathogen-derived elicitor, a branched β -glucan cell wall component of the Oomycete fungus *Phytophthora sojae*, which induces a defense-related response that triggers secretion of polyphenols.^[66–68] This elicitor (Elc) caused a significant sensor response (intensity changes and emission wavelength shift, Figure 3 f,g). Both the control (H_2O) and the stimulated cultures were 7 days old, hence containing next to the elicitor-induced polyphenols, pterocarpan derivatives, also aging-related ones like genistein. HPLC–MS analysis further confirmed the increase in polyphenols after elicitor stimulus (see Supplementary Figure S8 and S10). Furthermore, soybean defensive polyphenols genistein and trihydroxypterocarpan (THP) modulate the NIR fluorescence in a concentration-dependent manner (Supplementary Figure S11). Together these results show that our sensor can report polyphenol release from plants or cells in vitro.

The sensor response to total phenol content of soybean cells (Figure 3 h) is hyperbolic ($K_d \approx 140 \mu M$) and is not biased by cell medium or elicitor (Figure 3 g,h). Even though there are differences in sensitivity toward different polyphenols, the presented PEG-PL-SWCNT is therefore a total polyphenol content sensor. A major advantage of a fluorescent sensor/probe is that it can be used for imaging and provide additional spatiotemporal information compared to standard analytical methods (e.g. HPLC/GC–MS, colorimetric assays, biosensors).^[53–55, 63]

To image plant polyphenol secretion over time (Figure 4 a) we embedded the sensors in agar and let soybean seedlings grow on top. First, we had to optimize the conditions for embedding PEG-PL-SWCNTs into agar, as agar and salt concentration seemed to play an important role for photoluminescence and sensing (Supplementary Figure S12). The representative polyphenols genistein and THP were used to evaluate the sensing performance (Figure 4 b) and showed up to 30% fluorescence decrease ($100 \mu M$) within 30 min. On the other hand, potential interfering substances from the root, such as sugars or H_2O_2 , did not alter the fluorescence emission (Supplementary Figure S13). The plant defense by polyphenols was then imaged remotely in real-time by a NIR stand-off imaging^[24] system (Supplementary Figure S13). For this purpose, soybean seedlings were plated onto the optimized sensor agar (Figure 4 c) and the embryonic root was imaged for 24 h with elicitor stimulus or its respective control (Supplementary Video S1 and S2). The NIR (Figure 4 d) signal decreased close to the wound, indicating polyphenol secretions close to the elicitor-induced root area, as hypothesized before.^[64] These results confirm studies with pathogen (*P. sojae*)-infected soybean seedlings,^[69, 70] performed by laborious and tissue-destructive methods involving antibodies in combination with cryotome-prepared root tissue sections. Polyphenol secretion and diffusion increase in the first 4–8 h and remain stable over the 24-hour experimental timeframe (see also Supplementary Figure S14). When wounding the embryonic root and applying H_2O instead of the elicitor, no enhanced nanosensor response was detected (Figure 4 e), which confirms that both mechanical wounding and a chem-

ical elicitor are necessary similar to a pathogen attack.^[69] The difference in polyphenol secretion between individual plants (Figure 4 f) could be used to identify plant cultivars with improved pathogen response. The largest sensor fluorescence modulation occurred in close proximity to the embryonic root (see Figure 4 g), indicating higher changes of polyphenol content in this region of the rhizosphere. To further improve imaging we also implemented ratiometric sensing in which one sensor reports the analyte of interest at one wavelength and another sensor serves as reference at a different wavelength that is not affected by the analyte.^[30] For such an approach, (n,m) chirality-pure or even enantiomer-pure SWCNTs are necessary.^[62] We prepared chirality-pure (6,5)-SWCNTs with PEG–PL to act as polyphenol-responsive sensor, while monochiral (7,6)-SWCNTs coated with (AT)₁₅-ssDNA served as reference that does not react to polyphenols (Figure 4 h, Supplementary Figure S1, S15). Inside agar, they allowed ratiometric imaging using appropriate emission filters (PEG-PL-(6,5)-SWCNTs: 900–1100 nm and (AT)₁₅-(7,6)-SWCNTs: > 1100 nm). This approach enabled ratiometric detection of the important soybean polyphenol genistein (Figure 4 i) and also ratiometric imaging of the elicitor-induced secretion of root polyphenols (Figure 4 j,k, Supplementary Video S3). The concept could be expanded to multiplexing to study the co-secretion of multiple plant-defense molecules (exudates) and improve our understanding of spatiotemporal chemical processes in the complex rhizosphere.^[71] Additionally, this ratiometric approach is less prone to variations in the position of the light source and camera and therefore guarantees a more robust imaging concept with better signal/noise ratio.

Conclusion

We have synthesized molecular sensors based on SWCNTs for NIR imaging of polyphenols. They allow to observe the response of plants to pathogens via release of polyphenols with high spatiotemporal resolution in the beneficial NIR tissue transparency window. The sensors probe the polyphenol content in complex biological systems such as the plant rhizosphere. This tool can be used to better understand plant chemical defense mechanisms as well as plant chemical communication and accelerate phenotyping and identification of crop plants that are more tolerant to pathogens.^[72–74] We showcased the potential for a main crop plant species (soybean) and in plant extracts or tissue culture media without further purification. Sensor responses showed a strong correlation with classical analytical methods like colorimetric assays or HPLC–MS quantification but had the major advantage of in situ detection without further sample taking or handling. Additionally, the spatiotemporal resolution provided novel insights into the time scale and spatial dimensions of polyphenol secretion. Such rapid optical detection could be used for high-throughput screening tools that require minimal plant sample volumes down to the μL scale or to remotely visualize pathogen-induced plant defense and stress. In summary, this technique paves the way for

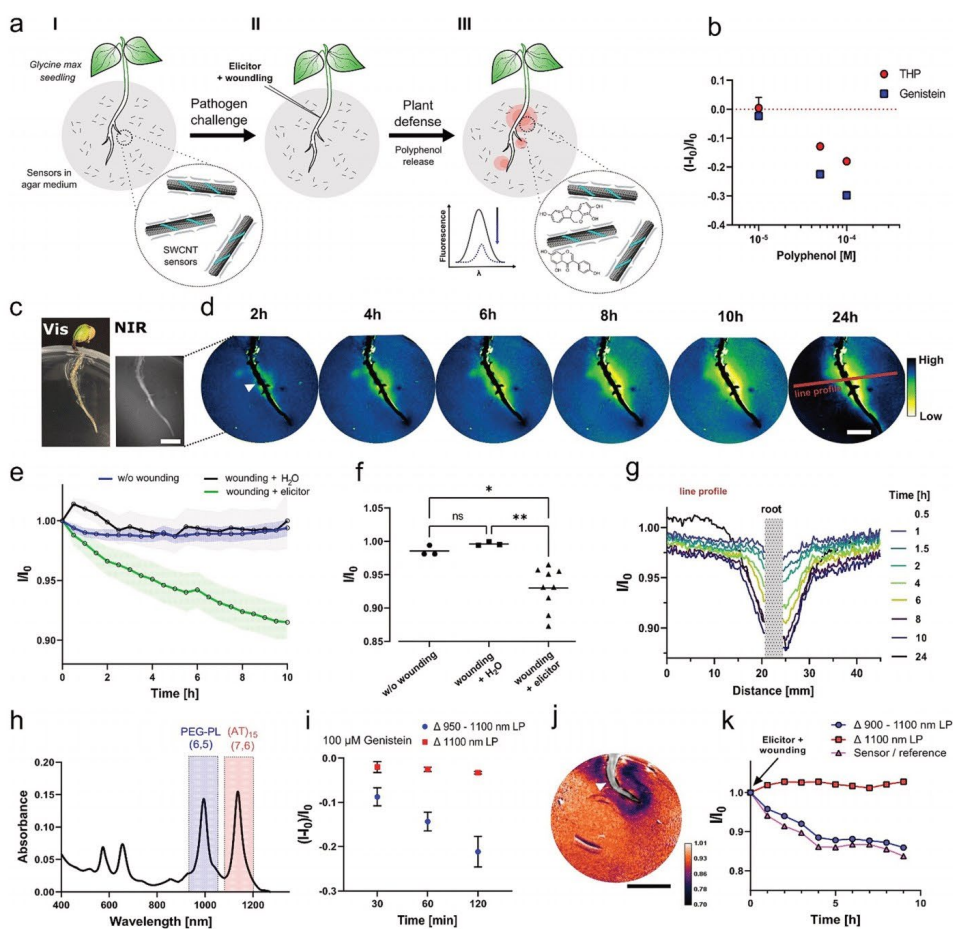


Figure 4. Real-time imaging of pathogen-induced polyphenol release from roots. a) Chemical imaging concept with SWCNT-based fluorescent sensors incorporated in culture medium agar. Soybean seedling (*G. max*) grow through the agar. The plant is challenged with a pathogen elicitor and the response (polyphenol secretion) is monitored by NIR fluorescent stand-off imaging (> 20 cm). b) Genistein and trihydroxyterocarpan (THP) as prominent components of the soybean (*G. max*) polyphenol profile quench the fluorescence of PEG-PL-SWCNTs in agar (mean \pm SD, $n=3$). c) Visible and NIR image of the soybean seedling (scale bar = 1 cm). d) The NIR fluorescence of the sensors (I/I_0) in the plant environment (rhizosphere) decreases over time close to the challenged root position (root tissue is overlaid with black; white triangle = position for elicitor induction; red line = line profile position, scale bar = 1 cm). e) Sensor image (500-pixel, $\approx 170 \text{ mm}^2$) reports polyphenol release to a fungal elicitor. In contrast, the sensor does not respond in the absence of stimulus (without wounding) or to wounding + H_2O (mean, error bars = SD, $n=1$). f) Sensor intensity changes 10 h after stimulus. Mean pixel intensities of 500-pixel areas close to the challenged root position (mean, control and H_2O $N=3$; elicitor $N=9$, $*P < 0.033$; $**P < 0.002$; ns = not significant; one-way ANOVA). g) Spatiotemporal profile of the plant defense via polyphenol release (line profile for 5-pixel width section shown in Figure 4d). h) Absorbance spectra of monochiral (6,5)-PEG-PL as polyphenol sensor and $(\text{AT})_{15}$ -(7,6)-SWCNTs (reference) in agar. i) NIR stand-off imaging of monochiral sensors and their response. The fluorescence of PEG-PL-(6,5)-SWCNTs (950 nm long pass (LP) filter image – 1100 nm LP filter image) decreases in response to genistein (100 μM). In contrast, $(\text{AT})_{15}$ -(7,6)-SWCNTs (1100 LP filter) are not strongly affected and serve as a reference. j) Ratiometric image of challenged soybean seedling ($t=9$ h post induction, ratio ΔH (900 LP – 1100 LP)/(1100 LP), white triangle = position for elicitor induction, scale bar = 1 cm). k) Ratiometric imaging of polyphenol release over time (sensor = PEG-PL-(6,5)-SWCNTs: 900–1100 nm; reference = $(\text{AT})_{15}$ -(7,6)-SWCNTs: > 1100 nm) (mean, $N=1$) measured as mean pixel intensity (500-pixel, $\approx 170 \text{ mm}^2$) over time.

precision agriculture and demonstrates the versatility of tailored nanoscale sensors for chemical imaging.

Acknowledgements

This project was supported by the VW foundation. Funded by the Deutsche Forschungsgemeinschaft (DFG, German Research Foundation) under Germany's Excellence Strategy—EXC 2033–390677874—RESOLV. We thank the DFG for funding within the Heisenberg program (S.K. & B.S.F.); the DAAD (German Academic Exchange Service) for scholarship funding (A.T.M.) and Dr. Michael Reichelt for support with the chemical analyses. Open Access funding enabled and organized by Projekt DEAL.

Conflict of Interest

The authors declare no conflict of interest.

Keywords: biosensors · carbon nanotubes · imaging · near-infrared fluorescence · plant polyphenols

- [1] N. Alexandratos, J. Bruinsma, "WORLD AGRICULTURE TOWARDS 2030/2050: The 2012 Revision. Food and Agriculture Organization of the United Nations: Rome, Italy," can be found under <http://www.fao.org/3/ap106e/ap106e.pdf>, 2012.
- [2] M. C. Fisher, D. A. Henk, C. J. Briggs, J. S. Brownstein, L. C. Madoff, S. L. McCraw, S. J. Gurr, *Nature* **2012**, *484*, 186–194.
- [3] S. Chakraborty, A. C. Newton, *Plant Pathol.* **2011**, *60*, 2–14.
- [4] P. J. Zarco-Tejada, C. Camino, P. S. A. Beck, R. Calderon, A. Hornero, R. Hernández-Clemente, T. Kattenborn, M. Montes-Borrego, L. Susca, M. Morelli, V. Gonzalez-Dugo, P. R. J. North, B. B. Landa, D. Boscia, M. Saponari, J. A. Navas-Cortes, *Nat. Plants* **2018**, *4*, 432–439.
- [5] S. Dhondt, N. Wuyts, D. Inzé, *Trends Plant Sci.* **2013**, *18*, 428–439.
- [6] Y. Fichman, G. Miller, R. Mittler, *Mol. Plant* **2019**, *12*, 1203–1210.
- [7] J. P. Giraldo, H. Wu, G. M. Newkirk, S. Kruss, *Nat. Nanotechnol.* **2019**, *14*, 541–553.
- [8] J. P. Giraldo, M. P. Landry, S. M. Faltermeier, T. P. McNicholas, N. M. Iverson, A. A. Boghossian, N. F. Reuel, A. J. Hilmer, F. Sen, J. A. Brew, M. S. Strano, *Nat. Mater.* **2014**, *13*, 400–408.
- [9] J. Li, G. P. Pandey, *Annu. Rev. Phys. Chem.* **2015**, *66*, 331–356.
- [10] V. Z. Zamolo, E. Vazquez, M. Prato, *Top. Curr. Chem.* **2013**, *350*, 65–109.
- [11] S. Nanot, E. H. Háröz, J. H. Kim, R. H. Hauge, J. Kono, *Adv. Mater.* **2012**, *24*, 4977–4994.
- [12] M. J. O'Connell, S. M. Bachilo, C. B. Huffman, V. C. Moore, M. S. Strano, E. H. Haroz, K. L. Rialon, P. J. Boul, W. H. Noon, C. Kittrell, J. Ma, R. H. Hauge, R. B. Weisman, R. E. Smalley, *Science* **2002**, *297*, 593–597.
- [13] S. M. Bachilo, M. S. Strano, C. Kittrell, R. H. Hauge, R. E. Smalley, R. B. Weisman, *Science* **2002**, *298*, 2361–2366.
- [14] S. Kruss, A. J. Hilmer, J. Zhang, N. F. Reuel, B. Mu, M. S. Strano, *Adv. Drug Delivery Rev.* **2013**, *65*, 1933–1950.
- [15] G. Hong, S. Diao, A. L. Antaris, H. Dai, *Chem. Rev.* **2015**, *115*, 10816–10906.
- [16] C. Farrera, F. Torres Andón, N. Feliu, *ACS Nano* **2017**, *11*, 10637–10643.
- [17] M. Dinarvand, E. Neubert, D. Meyer, G. Selvaggio, F. A. Mann, L. Erpenbeck, S. Kruss, *Nano Lett.* **2019**, *19*, 6604–6611.
- [18] M. Dinarvand, S. Elizarova, J. Daniel, S. Kruss, *ChemPlusChem* **2020**, *85*, 1465–1480.
- [19] S. Kruss, D. P. Salem, L. Vuković, B. Lima, E. Vander Ende, E. S. Boyden, M. S. Strano, *Proc. Natl. Acad. Sci. USA* **2017**, *114*, 1789–1794.
- [20] J. D. Harvey, P. V. Jena, H. A. Baker, G. H. Zerze, R. M. Williams, T. V. Galassi, D. Roxbury, J. Mittal, D. A. Heller, *Nat. Biomed. Eng.* **2017**, *1*, 0041.
- [21] G. Bisker, J. Dong, H. D. Park, N. M. Iverson, J. Ahn, J. T. Nelson, M. P. Landry, S. Kruss, M. S. Strano, *Nat. Commun.* **2016**, *7*, 10241.
- [22] A. Hendler-Neumark, G. Bisker, *Sensors* **2019**, *19*, 540.
- [23] T. V. Galassi, P. V. Jena, J. Shah, G. Ao, E. Molitor, Y. Bram, A. Frankel, J. Park, J. Jessurun, D. S. Ory, A. Haimovitz-Friedman, D. Roxbury, J. Mittal, M. Zheng, R. E. Schwartz, D. A. Heller, *Sci. Transl. Med.* **2018**, *10*, eaar2680.
- [24] R. Nißler, O. Bader, M. Dohmen, S. G. Walter, C. Noll, G. Selvaggio, U. Groß, S. Kruss, *Nat. Commun.* **2020**, *11*, 5995.
- [25] S. Kruss, M. P. Landry, E. Vander Ende, B. M. A. Lima, N. F. Reuel, J. Zhang, J. Nelson, B. Mu, A. Hilmer, M. Strano, *J. Am. Chem. Soc.* **2014**, *136*, 713–724.
- [26] D. A. Heller, H. Jin, B. M. Martinez, D. Patel, B. M. Miller, T. K. Yeung, P. V. Jena, C. Höbartner, T. Ha, S. K. Silverman, M. S. Strano, *Nat. Nanotechnol.* **2009**, *4*, 114–120.
- [27] H. Wu, R. Nißler, V. Morris, N. Herrmann, P. Hu, S. Jeon, S. Kruss, J. P. Giraldo, *Nano Lett.* **2020**, *20*, 2432–2442.
- [28] M. M. Safaei, M. Gravelly, D. Roxbury, *Adv. Funct. Mater.* **2021**, *33*, 2006254.
- [29] J. H. Kim, D. A. Heller, H. Jin, P. W. Barone, C. Song, J. Zhang, L. J. Trudel, G. N. Wogan, S. R. Tannenbaum, M. S. Strano, *Nat. Chem.* **2009**, *1*, 473–481.
- [30] J. P. Giraldo, M. P. Landry, S. Y. Kwak, R. M. Jain, M. H. Wong, N. M. Iverson, M. Ben-Naim, M. S. Strano, *Small* **2015**, *11*, 3973–3984.
- [31] T. T. S. Lew, V. B. Koman, K. S. Silmore, J. S. Seo, P. Gordiichuk, S.-Y. Y. Kwak, M. Park, M. C.-Y. Y. Ang, D. T. Khong, M. A. Lee, M. B. Chan-Park, N.-H. H. Chua, M. S. Strano, *Nat. Plants* **2020**, *6*, 404–415.
- [32] M. C.-Y. Ang, N. Dhar, D. T. Khong, T. T. S. Lew, M. Park, S. Sarangapani, J. Cui, A. Dehadrai, G. P. Singh, M. B. Chan-Park, R. Sarojam, M. Strano, *ACS Sens.* **2021**, *6*, 3032–3046.
- [33] T. T. S. Lew, M. Park, J. Cui, M. S. Strano, *Adv. Mater.* **2021**, *33*, 2005683.
- [34] E. Voke, R. L. Pinals, N. S. Goh, M. P. Landry, *ACS Sens.* **2021**, *6*, 2802–2814.
- [35] M. Zheng, A. Jagota, E. D. Semke, B. A. Diner, R. S. McLean, S. R. Lustig, R. E. Richardson, N. G. Tassi, *Nat. Mater.* **2003**, *2*, 338–342.
- [36] J. Zhang, M. P. Landry, P. W. Barone, J. H. Kim, S. Lin, Z. W. Ulissi, D. Lin, B. Mu, A. A. Boghossian, A. J. Hilmer, A. Rwei, A. C. Hincley, S. Kruss, M. A. Shandell, N. Nair, S. Blake, F. Şen, S. Şen, R. G. Croy, D. Li, K. Yum, J. H. Ahn, H. Jin, D. A. Heller, J. M. Essigmann, D. Blankschtein, M. S. Strano, *Nat. Nanotechnol.* **2013**, *8*, 959–968.
- [37] R. Nißler, F. A. Mann, P. Chaturvedi, J. Horlebein, D. Meyer, L. Vukovic, S. Kruss, *J. Phys. Chem. C* **2019**, *123*, 4837–4847.
- [38] A. Spreinat, M. M. Dohmen, N. Herrmann, L. F. Klepzig, R. Nißler, S. Weber, F. A. Mann, J. Lauth, S. Kruss, *J. Phys. Chem. C* **2021**, *125*, 18341–18351.
- [39] M. P. Landry, H. Ando, A. Y. Chen, J. Cao, V. I. Kottadiel, L. Chio, D. Yang, J. Dong, T. K. Lu, M. S. Strano, *Nat. Nanotechnol.* **2017**, *12*, 368–377.
- [40] K. Welsher, Z. Liu, S. P. Sherlock, J. T. Robinson, Z. Chen, D. Daranciang, H. Dai, *Nat. Nanotechnol.* **2009**, *4*, 773–780.

- [41] V. Shumeiko, Y. Paltiel, G. Bisker, Z. Hayouka, O. Shoseyov, *Biosens. Bioelectron.* **2021**, *172*, 112763.
- [42] A. F. Mann, J. Horlebein, N. F. Meyer, F. Thomas, S. Kruss, *Chem. Eur. J.* **2018**, *24*, 12241–12245.
- [43] A. Antonucci, J. Kupis-Rozmyslowicz, A. A. Boghossian, *ACS Appl. Mater. Interfaces* **2017**, *9*, 11321–11331.
- [44] E. Polo, T. Nitka, E. Neubert, L. Erpenbeck, L. Vuković, S. Kruss, *ACS Appl. Mater. Interfaces* **2018**, *10*, 17693–17703.
- [45] F. A. Mann, Z. Lv, J. Grosshans, F. Opazo, S. Kruss, *Angew. Chem. Int. Ed.* **2019**, *58*, 11469; *Angew. Chem.* **2019**, *131*, 11591.
- [46] A. Setaro, M. Adeli, M. Glaeske, D. Przyrembel, T. Bisswanger, G. Gordeev, F. Maschietto, A. Faghani, B. Paulus, M. Weinel, R. Arenal, R. Haag, S. Reich, *Nat. Commun.* **2017**, *8*, 14281.
- [47] F. A. Mann, N. Herrmann, F. Opazo, S. Kruss, *Angew. Chem. Int. Ed.* **2020**, *59*, 17732; *Angew. Chem.* **2020**, *132*, 17885.
- [48] S. Singh, I. Kaur, R. Kariyat, *Int. J. Mol. Sci.* **2021**, *22*, 14421.
- [49] R. V. Barbehenn, C. P. Constabel, *Phytochemistry* **2011**, *72*, 1551–1565.
- [50] J. Salminen, M. Karonen, *Funct. Ecol.* **2011**, *25*, 325–338.
- [51] U. Baetz, E. Martinoia, *Trends Plant Sci.* **2014**, *19*, 90–98.
- [52] A. Lanoue, V. Burlat, U. Schurr, U. S. R. Röse, *Plant Signaling Behav.* **2010**, *5*, 1037–1038.
- [53] A. Khoddami, M. A. Wilkes, T. H. Roberts, *Molecules* **2013**, *18*, 2328–2375.
- [54] F. Della Pelle, D. Compagnone, *Sensors* **2018**, *18*, 462.
- [55] M. David, M. Florescu, C. Bala, *Biosensors* **2020**, *10*, 112.
- [56] J. Zhou, Z. Lin, Y. Ju, M. A. Rahim, J. J. Richardson, F. Caruso, *Acc. Chem. Res.* **2020**, *53*, 1269–1278.
- [57] C. P. Constabel, K. Yoshida, V. Walker, in *Recent Advances in Polyphenol Research*, John Wiley & Sons, Ltd, **2014**, pp. 115–142.
- [58] S. Cesco, T. Mimmo, G. Tonon, N. Tomasi, R. Pinton, R. Terzano, G. Neumann, L. Weisskopf, G. Renella, L. Landi, P. Nannipieri, *Biol. Fertil. Soils* **2012**, *48*, 123–149.
- [59] D. P. Salem, X. Gong, A. T. Liu, V. B. Koman, J. Dong, M. S. Strano, *J. Am. Chem. Soc.* **2017**, *139*, 16791–16802.
- [60] K. Umemura, Y. Ishibashi, M. Ito, Y. Homma, *ACS Omega* **2019**, *4*, 7750–7758.
- [61] Y. Yamazaki, K. Umemura, *J. Near Infrared Spectrosc.* **2021**, *29*, 73–83.
- [62] R. Nibler, L. Kurth, H. Li, A. Spreinat, I. Kuhlemann, B. S. Flavel, S. Kruss, *Anal. Chem.* **2021**, *93*, 6446–6455.
- [63] E. A. Ainsworth, K. M. Gillespie, *Nat. Protoc.* **2007**, *2*, 875–877.
- [64] A. Mithöfer, A. A. Bhagwat, M. Feger, J. Ebel, *Planta* **1996**, *199*, 270–275.
- [65] J. Fliegmann, G. Schüler, W. Boland, J. Ebel, A. Mithöfer, *Biol. Chem.* **2003**, *384*, 437–446.
- [66] A. R. Ayers, J. Ebel, F. Finelli, N. Berger, P. Albersheim, *Plant Physiol.* **1976**, *57*, 751–759.
- [67] J. K. Sharp, P. Albersheim, P. Ossowski, A. Pilotti, P. Garegg, B. Lindberg, *J. Biol. Chem.* **1984**, *259*, 11341–11345.
- [68] J. Ebel, H. Grisebach, *Trends Biochem. Sci.* **1988**, *13*, 23–27.
- [69] M. G. Hahn, A. Bonhoff, H. Grisebach, *Plant Physiol.* **1985**, *77*, 591–601.
- [70] P. Moesta, H. Grisebach, *Nature* **1980**, *286*, 710–711.
- [71] L. J. Shaw, P. Morris, J. E. Hooker, *Environ. Microbiol.* **2006**, *8*, 1867–1880.
- [72] A. Sugiyama, *J. Adv. Res.* **2019**, *19*, 67–73.
- [73] S. Hassan, U. Mathesius, *J. Exp. Bot.* **2012**, *63*, 3429–3444.
- [74] A. Sugiyama, K. Yazaki, *Plant Biotechnol.* **2014**, *31*, 431–443.

Manuscript received: June 23, 2021
 Revised manuscript received: September 28, 2021
 Accepted manuscript online: October 5, 2021
 Version of record online: November 22, 2021

3 Discussion

Many studies on myrmecophytes have described the importance of ants as biotic defenders. However, there is a knowledge gap about the (defense) metabolism of myrmecophytes and how this is affected by the mutualistic ants. Therefore, I addressed the following questions: (i) do myrmecophytes still have chemical defenses or do they rely fully on ant protection? (ii) is any chemical defense inducible and regulated by jasmonate (JA) signaling? (iii) what is the nature of this chemical defense? To answer these questions, in this thesis, I aimed to unravel the chemistry of the Neotropical ant-plant *Tococa quadrialata*, to gain a deeper understanding of defense regulation and adaptation of ant-plants to their colonizers. To achieve that aim, I studied various aspects of the myrmecophyte's defense, and therein helped establish methods and made discoveries that go beyond the model *T. quadrialata* and even ant-plants. As the individual results are already discussed in the respective manuscripts, I will now focus on the highlights of this work and place them in a broader context.

3.1 No rose without thorns, no ant-plant without chemical defenses

Ever since Janzen (1966) discovered that acacia plants associated with ants (ant-acacias) taste different than non-myrmecophytic species, there has been an ongoing debate about whether or not ant-plants possess weaker 'abiotic' defenses. The original observation about cyanogenic glycosides in acacia is debatable but not yet contradicted: Rehr et al. (1973) compared three non-myrmecophytic *Acacia spp.* with five species of ant-acacias, and found that only the former were producing cyanogenic glycosides, whereas Seigler and Ebinger (1987) found that five out of twelve investigated myrmecophytic *Acacia spp.* were able to produce cyanogenic glycosides and had a β -glucosidase to allow release of toxic hydrogen cyanide. Another study in favor of the hypothesis showed a clear reduction of chitinases in ant-acacia as compared to non-mutualistic species (Heil et al., 2000), but that's where the evidence ends. While the genus *Macaranga* itself was found to be poor in chitinases as compared to plants from other genera and families, there was no difference between ant-plants and non-myrmecophytic species (Heil et al., 1999). And a broad survey of Heil et al. (2002) showed that while there is a high variation in the amounts of polyphenolics (flavonoids, hydrolyzable and condensed tannins) between species of *Acacia*, *Macaranga* and *Leonardoxa*, the variation cannot be explained by their association with ants. In some cases, as has been found for *Piper*, mutualistic species even produced six times more

amides and imides than a related non-myrmecophytic species (Fincher et al., 2008).

Altogether, the studies conducted to date were not able to demonstrate that myrmecophytic species have evolved to be chemically less defended than closely related non-myrmecophytic species. Nevertheless, many ant-exclusion studies have demonstrated that ant-protection is usually more effective than the other defenses of ant-plants (Vasconcelos, 1991; Alvarez et al., 2001; Michelangeli, 2003; Frederickson et al., 2012). Thus, the question is, whether the ants are the cherry on the top of an existing defense machinery or whether there are trade-offs in aspects of the defense that have not yet been considered. For one, so far, only constitutive defenses have been examined, and inducible defenses, which contribute much to plant defense in numerous species, have been largely ignored. Thus, there is a lack of knowledge as to whether ant-plants might not induce chemical defenses, relying solely on their ants as an effective induced defense (Christianini and Machado, 2004). Another option could be that myrmecophytes may still maintain their own defense machinery, but dynamically adapt their metabolism to biotic and abiotic conditions, depending on whether and by whom they are colonized and then selectively invest their resources in ants, growth, or chemical defenses as required by circumstances.

In order to tackle these questions, **manuscript I, II and III** aimed to identify the chemical defenses – constitutive and inducible, indirect and direct – or the absence of such in *T. quadrialata*. It was found that the myrmecophyte is rich in polyphenols, producing a number of ellagitannins and flavonoids including anthocyanins (**manuscript I, III**). Especially for ellagitannins, it is known that they act as feeding deterrents and are toxic to insect herbivores (Roslin and Salminen, 2008; Moctezuma et al., 2014; Anstett et al., 2019), and thus represent an important part of the direct defense of plants. As there was no upregulation of ellagitannins upon herbivory observed in *T. quadrialata*, neither in the field (**manuscript I**) nor in the greenhouse under controlled conditions (**manuscript II**), they were regarded as constitutive direct defenses.

Contrary to the initial hypothesis that inducible defenses other than the ants themselves might have been lost in ant-plants, *T. quadrialata* responded to insect herbivory by JA signaling, emission of herbivore-induced plant volatiles (HIPVs), accumulation of free amino acids, major transcriptional changes and the accumulation of phenylacetaldoxime (PAOx), its glucoside (PAOx-Glc) and the corresponding nitrile benzyl cyanide (**manuscript I,II**). This thesis (**manuscript II**) together with other studies (Irmisch et al., 2013; Irmisch et al., 2014) have demonstrated that PAOx and derivatives are deterrent or even toxic for caterpillars, and thus represent an important direct, inducible defense

and evidence that ant-plants can induce the production of their own defensive weapons whenever an attacker bypasses the bodyguards. Furthermore, it appeared that the presence or absence of ants on *T. quadrialata* did not alter the regulation of induced defenses, which makes sense in that herbivore damage is a signal that ants are failing to protect the plant. Similar findings and conclusions have been made by Frederickson et al. (2013) and Letourneau and Barbosa (1999), who observed that previous tissue damage lead to increased trichome density in subsequently produced leaves, independent of the ant-plant's colonization status. Nevertheless, this conclusion should be taken with caution as not all the genes and induced compounds and traits were studied in detail yet to draw a complete picture. The study of Hernandez-Zepeda et al. (2018) brings in another layer of complexity, as they found that while ant-acacia can still emit HIPVs, the number of HIPVs is lower as compared to other acacia species and the emitted compounds were not able to induce a systemic response. In the present studies (**manuscript I,II**), it was found that herbivore-damaged *T. quadrialata* produces a bouquet of typical HIPVs, including fatty-acid derivatives, terpenoids, phenolics and nitrogen-containing VOCs, and many of these compounds have been reported elsewhere to have a role in inter- and intra-plant signaling (e.g. indole, DMNT, octen-3-ol (Kishimoto et al., 2007; Erb et al., 2015; Meents et al., 2019)), as repellents (e.g. (*E*)- β -caryophyllene, benzyl cyanide, methyl anthranilate (North et al., 2000; Irmisch et al., 2014; Ahmad et al., 2018)) or signals to parasitoids/predators/ants (hexanal (Agrawal, 1998), possibly octen-3-ol (Takken and Kline, 1989)). Unfortunately, limited resources circumvented a comparison of the induction pattern of *T. quadrialata* to a non-myrmecophytic related species. Likewise, a lack of knowledge about natural herbivores of *Tococa* (see introduction) let alone parasitoids and predators of those herbivores hindered the study of the function of the HIPVs in *T. quadrialata*. Thus, it can neither be confirmed nor denied that something similar to what was found in acacia is true for *Tococa* yet, leaving these questions open to further investigation. One important aspect of herbivore-induced defenses however is indeed missing in *T. quadrialata*: there was no transcriptional upregulation of protease inhibitors (**manuscript I**), a typical JA induced defense found in many plant species like tea (*Camellia sinensis*, Theaceae), potato (*Solanum tuberosum*, Solanaceae), tomato (*Lycopersicon esculentum*, Solanaceae), and alfalfa (*Medicago sativa*, Fabaceae) (Farmer et al., 1992; Yamagishi et al., 1993; Zhu et al., 2019). Eberl et al. (2021) showed that Kunitz-type trypsin inhibitors are amongst the highest upregulated genes in *Populus nigra* (fold change of >1000) upon tissue damage by caterpillars and beetles. Together with the studies by

Hernandez-Zepeda et al. (2018) and Heil et al. (2004) – the latter showing that EFN production in colonized myrmecophytes is no longer JA-inducible – the findings of **manuscript I** suggest that while ant-plants have not lost their ability to induce defenses when needed altogether, they may indeed have reduced parts of their inducible defenses, or at least regulate them differently to optimize costs and benefits.

In summary, comparisons between related myrmecophytic and non-myrmecophytic species indicate that the evolution of ant-plant mutualism has not resulted in ant-plants having lost their possibilities to defend themselves directly via chemical or physical traits, but that there might be a reduction of inducible defenses other than symbiotic ants. When predicting the redundancy of defenses (ant protection vs chemical/physical defenses), it should be considered that the protective efficiency of ants varies quite strongly with species and habitat (McKey, 1984; Frederickson, 2005; Moraes and Vasconcelos, 2009; Bartimachi et al., 2015), as do the costs associated with ant-colonization (Izzo and Vasconcelos, 2002; Stanton and Palmer, 2011; Frederickson et al., 2012), and since ant-plants are usually long-lived, they are often inhabited by different ant species during their lifetime (Young et al., 1996; Palmer et al., 2010) – perhaps not at all for some time – with different advantages and disadvantages. Thus, it would be disadvantageous for myrmecophytic species to completely lose the ability to defend themselves.

3.2 Ant-colonization affects general and specialized metabolism of ant-plants

Following the line of thought that ant-plants cannot consistently rely on the defense provided by their mutualistic ants, it would be advantageous if myrmecophytes could regulate their own metabolism according to whether or not they are well protected by their ants and whether protection against herbivores, pathogens, or other plants that compete for light and nutrients is necessary. In that case, differences in plant defenses should become visible between different populations and individuals of the same species.

Studies on mechanical defenses such as leaf toughness and trichome density showed mixed results. For instance, Moraes and Vasconcelos (2009) found a trade-off between morphological traits and ant-colonization in *T. guianensis* but Bartimachi et al. (2015) could not confirm the results, and as mentioned before, in *Endospermum labios* and *Cordia nodosa* trichome density increased in response to herbivore damage, independent of ant-colonization (Letourneau and Barbosa, 1999; Frederickson et al., 2013). Chemical defenses, on the other hand, like amides in *Piper cenocladum* (Dodson

et al., 2000; Dyer et al., 2001; Dyer et al., 2004) and now hydrolyzable tannins of *T. quadrialata* (**manuscript I**) have indeed been found to accumulate at higher levels in the absence of ants – independent of whether the plants occur naturally without ants or the ants were excluded. Of course, the small number of studies conducted and compounds tested is not sufficient to conclude whether or not ant-plants in general adapt their defenses to different colonization status, but it does prove that this happens at least in some cases. Additional cues that ant-plants do adapt to the presence of their partners come from ant-nutritional studies. Heil et al. (1997) not only demonstrated that producing food bodies for mutualistic ants represents a big investment for myrmecophytes (9% of total energy costs of above-ground growth), but also that *Macaranga tribola* only produces large amounts of food bodies in the presence of ants. Similarly, *Cecropia peltata* populations on islands where no mutualistic ants occur do not produce trichilia with glycogen-rich food bodies ('Müllerian bodies') anymore (Janzen, 1973) and *Acacia cornigera* secreted three times more EFN on ant-inhabited branches (Hernandez-Zepeda et al., 2018).

The subsequent question is how ant-plants perceive whether they are colonized or not, and what mechanisms lead to the observed enrichment of chemical defenses (or ant diet). Most likely, myrmecophytes will not 'sense' the presence of ants directly, but they experience the effects of the ant-colonization and adjust to that. For one, unoccupied myrmecophytes usually suffer more from herbivore damage as compared to colonized plants, which then leads to increased levels of inducible defenses (e.g. trichomes) in non-colonized plants. Otherwise, ant feeding behavior has notable effects on the myrmecophytes: Folgarait et al. (1994) showed that the frequent removal of food by ants (or artificial means) is the cue that induces the food body production in *Cecropia spp.* and similar findings were made for *Macaranga spp.* (Heil et al., 1997). In other cases (see **manuscript I**, Solano and Dejean (2004); Dejean et al. (2017), and Sagers et al. (2000)), the associated ants obtained nutrients primarily from foraging on the plants and in the surroundings, and fertilized the plant – presumably by fecal droplets (Pinkalski et al., 2018) or deposition of feces and debris in domatia (Solano and Dejean, 2004) or rhizomes (Gay, 1993). This can result in increased levels of foliar nitrogen in ant-attended myrmecophytes, as shown in **manuscript I** for the first time for non-epiphytic plants. Increased nitrogen availability can then have a positive effect on the myrmecophyte's growth and defense strategy in multiple ways. For instance, Folgarait and Davidson (1995) found that *Cecropia* plants grew faster under high nitrogen conditions but reduced their polyphenol content as compared to low nitrogen, whereas

Dyer et al. (2004) found that fertilization of *Piper* plants increased the concentrations of toxic amides. These seemingly conflicting results can be explained by the so called carbon-nitrogen balance hypothesis (Bryant et al., 1983): how a plant allocates its resources depends on which factor – carbon or nitrogen – is more limited. As nitrogen is essential for general metabolism, for the biosynthesis of amino acids, proteins and nucleic acids, low nitrogen conditions restrict plant growth and result in the accumulation of photosynthetically fixed carbon in leaves, which is allocated to carbohydrates and carbon-based defenses (e.g. tannins, terpenes) (Bryant et al., 1983). Increasing defenses, especially those with a low turn-over such as polyphenolics, is an important strategy to cope with nutrient-deficient conditions as it prevents tissue loss and its costly replacement (Coley et al., 1985). On the other hand, whenever plants grow in a nutrient-rich environment, the photosynthetic efficiency and carbon fixation become the limiting factor, resulting in high nutrient concentrations in the tissue, increased levels of nitrogen-based defenses (e.g. alkaloids, cyanogenic glycosides) and/or growth, depending on the plant species, and reduced carbon-based defenses (Bryant et al., 1983; Coley et al., 1985). Especially for tannins, negative correlations with growth/nitrogen content have been described for many non-myrmecophytic plant species (Gershenson, 1984) as well as ant-plants like *Cecropia* (Coley, 1986; Folgarait and Davidson, 1995) and now *T. quadrialata* (**manuscript I**). The food preferences of mutualistic ants thus have serious consequences for the host plant (see Figure 4). They can either impose costs on the myrmecophyte, as the plant has to allocate nutrients to ant rewards (food bodies, EFN (Heil et al., 1997; Fischer et al., 2002; Gonzalez-Teuber and Heil, 2009)), which either leads to a trade-off with nitrogen-based defenses as seen for the amides of *Piper cenocladum* (Dodson et al., 2000; Dyer et al., 2001; Dyer et al., 2004) or a trade-off between maintenance of the ant colony and growth as found for *Acacia drepanolobium* and *Cordia nodosa* in an herbivore-free environment (Figure 4A) (Stanton and Palmer, 2011; Frederickson et al., 2012). Alternatively, the presence of ants may increase the plant's nutrient supply as shown here to be the case for *T. quadrialata* (**manuscript I**), which enables the colonized ant-plants to allocate more resources to general metabolism, especially amino acids, and growth, at the expense of phenolic defenses (Figure 4B).

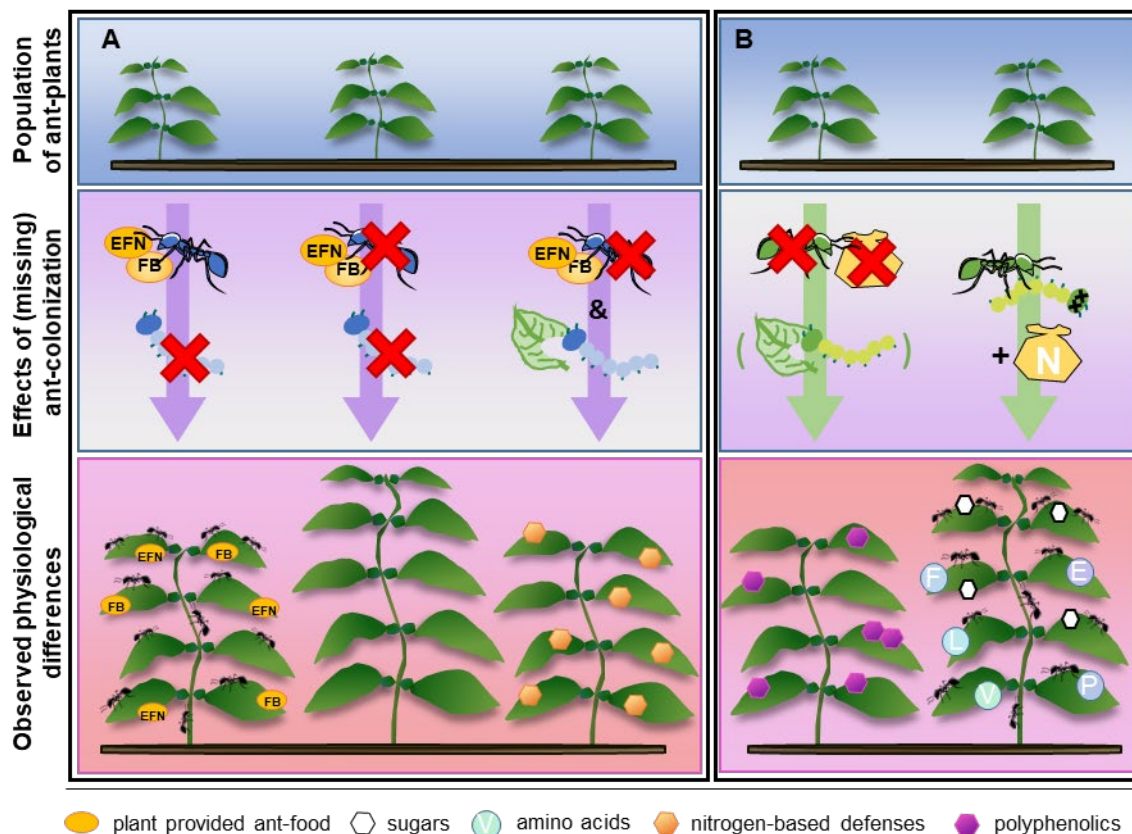


Figure 4: Effects of ant-colonization on the metabolism of myrmecophytes. The ants' nutritional choices and protective activity have consequences for the plants they colonize. **A:** Some ants (blue) solely live on plant-provided resources such as extrafloral nectar (EFN) or food bodies (FB) produced by the plants in exchange for protection against insect herbivores. The colonizing ants stimulate the plant to allocate their resources including nitrogen towards food rewards. In the absence of these ants, the counterparts of these plants do not allocate many resources to ant-rewards, but instead either to growth when there is no herbivore pressure or towards nitrogen-based defenses to protect themselves chemically. **B:** On the other hand, some ant-plants like *Tococa* live in symbiosis with ants that forage on the plant and in the surroundings and fertilize their hosts. Myrmecophytes colonized by these ants are protected against herbivory and can allocate the additional nitrogen into general metabolism and growth, while their counterparts with comparably low nitrogen levels invest in carbon-based defenses to protect their tissue.

In conclusion, ant-colonization changes the myrmecophyte's nutrient availability – due to the ants' feeding preferences and whenever mutualistic ants act as allelopathic agents – as well as the amount of damage caused by herbivores and pathogens, which in turn causes ant-plants to differentially regulate their general and specialized metabolism depending on their colonization status, ultimately resulting in the observed morphological and metabolic differences between colonized and uninhabited myrmecophytes. Notably, this thesis was the first to investigate all aspects of the mutualism, constitutive and induced defenses as well as the nutrient supply and general metabolism of the ant-plants at once, and not only demonstrated that ant-plants may adapt to their colonization status but also enabled a deeper understanding of the underlying physiological mechanisms.

3.3 Aldoximes go beyond the classical definition of specialized metabolites

Studying the defense of *T. quadrialata*, this thesis could identify PAOx and PAOx-Glc as major constituents of the inducible response to herbivory (**manuscript I,II**) and thus aimed to understand the biosynthesis and potential role(s) of these compounds in (ant-)plants. Typically, plant specialized metabolites have a particular role in a specific setting, like *Piper* amides being toxic for generalist caterpillars (Richards et al., 2010), oryzalexin A, B and C from rice inhibiting the growth of pathogens (Akatsuka et al., 1985), or the volatile chiloglottone emitted by orchid flowers attracting their pollinating wasps (Schiestl et al., 2003). However, in recent years, it has been shown that many times a specialist compound (class) fulfills various important functions in the interaction of plants with their surroundings. For instance, as reviewed by Mierziak et al. (2014), the isoflavonoids genistein and daidzein not only inhibited the growth of pathogenic fungi and bacteria (Gnanamanickam and Patil, 1977; Rivera-Vargas et al., 1993; Durango et al., 2013), but they also deter the nematode *Radopholus similis* (Wuyts et al., 2006), control the root nodule formation of nitrogen-fixing bacteria (Cooper, 2004) and show allelopathic effects when released into the soil (Chang et al., 1969). Similarly, aldoximes seem to fulfill multiple roles in plant defense, as summarized in Figure 5.

One of the best-studied aspects of plant aldoximes is them being intermediates in the biosynthesis of cyanogenic glycosides (Tapper et al., 1967; Andersen et al., 2000) and glucosinolates (Underhill, 1967; Wittstock and Halkier, 2000). As such, they help plants to protect themselves against all kinds of herbivores including insects, mollusks, mammals, nematodes (Newton et al., 1981; Compton and Jones, 1985; Sachdev-Gupta et al., 1993; Mawson et al., 1994; Lazzeri et al., 2004; Ballhorn et al., 2005) as well as pathogens (Smolinska et al., 2003; Plaszko et al., 2021). Interestingly, only plants of the order Brassicales, mainly within the Brassicaceae family, can form glucosinolates, with *Arabidopsis thaliana* and white mustard (*Sinapis alba*) being prominent representatives (Mithen et al., 2010). In contrast, cyanogenic glycosides are more widespread and have been found in various orders and families of angiosperms, including ant-plants such as *Acacia hindsii* and *A. globulifera*, as well as in gymnosperms and ferns (Seigler and Ebinger, 1987; Vetter, 2000; Luck et al., 2017; Thodberg et al., 2020). But also plants that are neither cyanogenic nor belong to the order Brassicales, such as poplar (*Populus spp.*), common evening primrose (*Oenothera biennis*), loquat (*Eriobotrya japonica*) and, as found in this thesis,

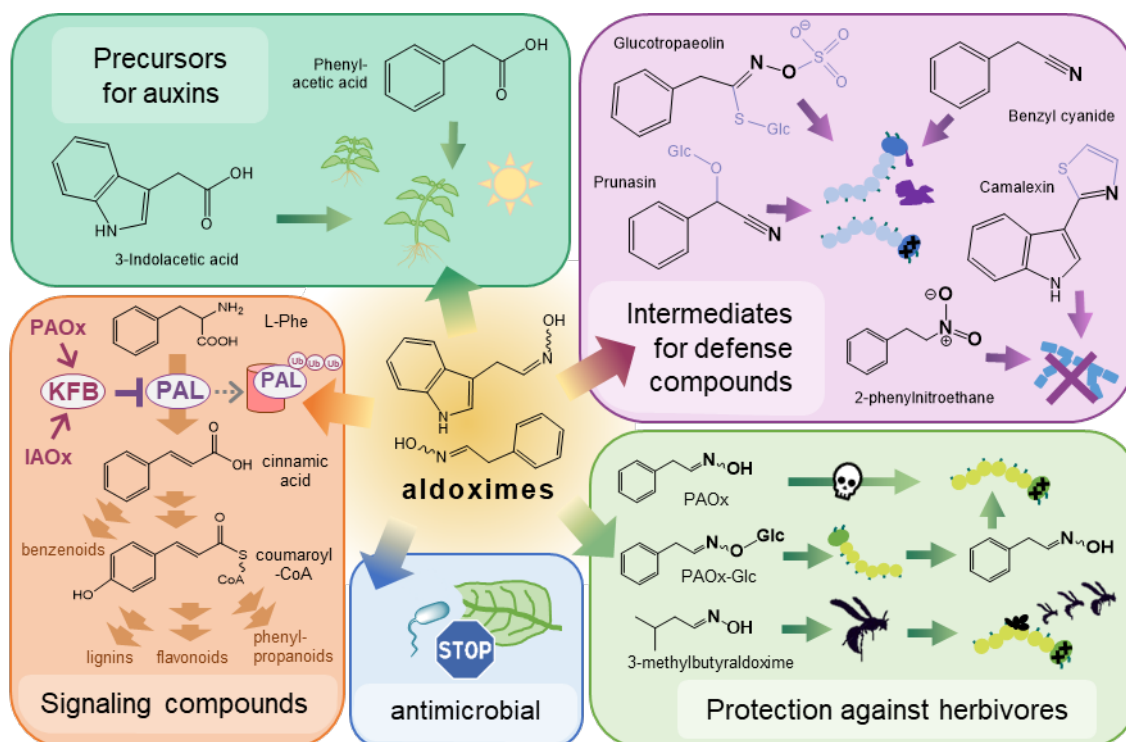


Figure 5: Role of amino acid-derived aldoximes in general and specialized plant metabolism. Aldoximes have several important functions in plant defense. They serve I. as precursors for specialized compound classes (modifications of the core structure shown in purple), II. as direct or indirect defense against insect herbivores, III. as antimicrobials, IV. as precursors for the phytohormones phenylacetic acid and 3-indolacetic acid (,auxins'), and V. as signaling compounds, modulating phenylpropanoid biosynthesis. The mode of action of each compound is shown as a pictogram, for further explanations see chapters 1.1.1.2 and 3.3. KFB: kelch-domain containing F-box protein; IAOx: indole-3-acetaldoxime; PAL: phenylalanine ammonia lyase; PAOx: phenylacetaldoxime; PAOx-Glc: phenylacetaldoxime glucoside; Ub: Ubiquitin.

T. quadrialata, use aldoximes as intermediates for volatile defensive compounds. As shown in **manuscript I** and **II**, and other works (Irmisch et al., 2014; Noge and Tamogami, 2018; Yamaguchi et al., 2021), such compounds include nitriles (benzyl cyanide and isovaleronitrile) and nitro-compounds (3-methyl-1-nitrobutane and 2-phenylnitroethane) where the former were shown to attract predators and repel generalist caterpillars (Clavijo McCormick et al., 2014; Irmisch et al., 2014; Noge and Tamogami, 2018) whilst the latter was shown to inhibit growth of pathogenic fungi (Oger et al., 1994). Also, talking about antifungal compounds, in arabidopsis, indole-3-acetaldoxime (IAOx) is not only the intermediate in indolic glucosinolate biosynthesis but also in the generation of the phytoalexin camalexin (Glawischmig, 2007). In sum, aldoximes are thus central intermediates in the biosynthesis of multiple classes of specialized metabolites involved in plant defense against herbivores and pathogens.

However, this is only one aspect of aldoximes. They are not just substrates, but they are bioactive themselves. In many plant species like maize (*Zea mays*) (Irmisch et al., 2015) poplar (Clavijo McCormick et al., 2014), lima bean (*Phaseolus lunatus*) (Dicke et al.,

1999), and, as presented in this work, crape jasmine (*Tabernaemontana divaricata*) and the ant-plant *T. quadrialata* (**manuscript II**), the free aldoximes accumulate upon herbivore damage as a direct (PAOx) or indirect (2- and 3-methylbutyraldoxime) defense against the attackers (Irmisch et al., 2013; Clavijo McCormick et al., 2014). Additionally, as many oximes serve as fungicides and antibiotics (Drumm et al., 1995; Parthiban et al., 2010; Skočibušić et al., 2018), a similar role was hypothesized for plant amino acid-derived aldoximes (Møller, 2010; Sorensen et al., 2018). In accordance with this, here it was found that PAOx accumulates in soybean (*Glycine max*) in response to a pathogenic oomycete elicitor and respective growth inhibition assays showed that PAOx reduced the growth of several plant pathogenic bacteria (**manuscript II**). Thus, the biotic stress-induced production of aldoximes seems to be a widespread strategy that protects plants against insect herbivores as well as possible secondary infections. In this context, it is particularly interesting that whenever I studied the biotic stress-induced accumulation of free aldoxime (PAOx), alongside with it, the respective glucoside (PAOx-Glc) accumulated in significant quantities – not only as initially studied in *T. quadrialata*, but also in poplar, crape jasmine and soybean (**manuscript I,II**). Given the experiments on the distribution and induction of PAOx-Glc in *T. quadrialata*, it seems to be a more stable, non-volatile version of PAOx with a lower turnover rate that is most likely not bioactive itself, but will be deglycosylated in the insect gut to release the toxic aldoxime (**manuscript II**). Strikingly, the biosynthesis (CYP79 and UGT85 enzymes), the widespread occurrence throughout the plant kingdom and the mode of action (activation by β -glucosidases) of PAOx-Glc are highly similar to cyanogenic glycosides, raising questions about their evolutionary relationship.

On that note, it is particularly interesting that aldoximes are not only important specialized metabolites, but they are also linked to the general metabolism of plants, as the enzymatic hydrolysis of aldoxime-derived benzyl cyanide and 3-indolacetonitrile leads to the production of the auxins phenylacetic acid and indole acetic acid (Bartel and Fink, 1994; Günther et al., 2018; Urbancsok et al., 2018). Auxins are phytohormones that are well known for regulating plant growth and development (Sauer et al., 2013; Perez et al., 2023), especially for organ formation (Benkova et al., 2003) and phototropism (Friml et al., 2002). Additionally, they also play a role in response to plant pathogens and herbivores, acting mostly antagonistic to salicylic acid and fine-tuning the JA response (Kazan and Manners, 2009; Machado et al., 2016; Pérez-Alonso and Pollmann, 2018). Notably, Qu et al. (2016) found that while there are several metabolic pathways leading to auxin, the aldoxime and nitrile dependent auxin formation is the

dominant biosynthetic pathway upon herbivore damage in maize roots, and that auxin only accumulates in the upper part of the root, inducing lateral root growth to compensate the loss. Unfortunately, they did not test whether this correlates with an induction of CYP79 and accumulation of IAOx in this area, as might be expected. Whether a similar herbivore-induced formation of auxins via aldoximes takes place in free aldoxime accumulating plants like *T. quadrialata* has not yet been investigated, but should be the subject of further studies, as this might be another cause for the observed distribution and temporal pattern of PAOx accumulation (**manuscript II**).

As IAOx and PAOx contribute both to glucosinolate and auxin biosynthesis in Brassicales, there have been several overproduction and knock-out mutant studies in arabidopsis, trying to decipher the regulation of these pathways. For instance, Zhao et al. (2002) overexpressed CYP79B2 and CYP79B3, leading to a high auxin phenotype, and increased amounts of indolic glucosinolates. Interestingly, however, when Kim et al. (2015) studied CYP83 (see Figure 2) knock-out lines, which were unable to use IAOx as substrate for glucosinolates, the mutant phenotype could not be explained by over-accumulation of auxins. They showed that the downregulation of phenolics, especially sinapoylmalate and flavonoids in leaves and coniferin and syringin in roots, was linked to the accumulation of IAOx, suggesting a crosstalk between aldoximes and phenylpropanoids in arabidopsis (Kim et al., 2015). In line with that, other studies of PAOx and aliphatic aldoxime-accumulating arabidopsis plants also found a suppressed phenylpropanoid biosynthesis (Hemm et al., 2003; Perez et al., 2021). The low phenylpropanoid levels in aldoxime-overaccumulating lines can be partially explained by reduced phenylalanine ammonia lyase (PAL) activity due to enhanced ubiquitination and proteasomal degradation of PAL. The latter was regulated by the kelch-domain containing F-box (KFB) proteins KFB39 and KFB50, which in turn are upregulated by aldoximes (PAOx and IAOx) (Kim et al., 2020; Perez et al., 2021). This regulatory pathway was not only found in arabidopsis, but also in *Camelina sativa*, a species that does not produce glucosinolates but camalexin: overexpression of an IAOx-producing CYP79 led to a decrease in phenolics due to increased PAL degradation mediated by F-box proteins and therefore reduced PAL activity (Zhang et al., 2020). Taken together, this suggests that at least in Brassicales, free aldoximes act as signaling molecules that transcriptionally regulate other biosynthetic pathways. The preliminary studies of this thesis showing that the addition of PAOx to soybean cell cultures and overexpression of CYP79A206 and CYP79A297 in *Nicotiana benthamiana* caused major metabolic changes (see Figure S1,2), are the first hints towards a role for PAOx in plant signaling

beyond Brassicales. Notably, in Brassicales and cyanogenic plants, free aldoximes do not accumulate naturally, but are channeled within their respective pathways (Møller, 2010). The formation of these metabolons might be, amongst others, a protection against leakage of free aldoximes and the related metabolic changes. Following this line of thought, one could speculate whether the glycosylation of PAOx observed in this thesis (**manuscript II**) is to control the levels of free PAOx in non-cyanogenic plants, thus avoiding any unwanted secondary signaling effects.

In sum, aldoximes are versatile metabolites involved in both general and specialized metabolism fulfilling multiple important functions. Their evolutionary relationship with cyanogenic glycosides remains unknown, but the finding of the respective aldoxime glucoside in all non-cyanogenic, non-glucosinolate forming plants investigated in this thesis, points towards a common origin and convergent evolution of these metabolites, at least in flowering plants.

3.4 The development of new analytical tools like carbon nanotubes for polyphenol detection can facilitate future work and research on non-model organisms

The identification, characterization and quantification of plant specialized compounds is a wide research field. It enables the investigation of metabolic pathways within plants and the chemical diversity of plants, revealing the constituents important for their pharmaceutical or dietary use, and thereafter enabling smart breeding to select for these traits. Additionally, in the field of chemical ecology, it helps to understand the evolved adaptation of plants to certain environmental conditions, as discussed in detail for ant-plants (chapter 3.1, 3.2) as well as to elucidate the biosynthesis and roles of certain compounds, like aldoximes (chapter 3.3). For that reason, a multitude of methods, techniques, and analysis systems of varying complexity have been developed to tackle the different research questions. For the structure elucidation of a novel compound, implementation of an isolation protocol yielding sufficient amounts of the pure compound and subsequent NMR (nucleic magnetic resonance) spectroscopy experiments are necessary (Kwan and Huang, 2008; Agerbirk and Olsen, 2012). For compound identification, the most common approach is a comparison of the chemical and physical properties, including retention times, fragmentation patterns and/or absorption spectra, of the compound of interest with an authentic standard (e.g. Agerbirk and Olsen (2012); Moilanen et al. (2013), see **manuscript I,II,III**). This requires an appropriate extraction method, the accessibility of the authentic standard, and analytical instrumentation such as HPLC-DAD, HPLC-MS/MS, at best with high-resolution, or GC-MS (e.g. de Rijke et

al. (2006); Salminen et al. (2011), see **manuscript I,II,III**). With the rise of untargeted metabolomics studies in recent years, another possibility for compound identification is the comparison of its obtained chromatographic and MS data to respective databases such as NIST/EPA/NIH mass spectral libraries (National Institute of Standards and Technology, see **manuscript I,II**), often utilizing software tools like CSI:FingerID or MS Finder (Blazenovic et al., 2018). These databases and tools are very valuable for a faster identification of compounds in new plant species, but again require analytical instrumentation with high-resolution MS/MS as a prerequisite. On the other hand, to get an idea of the compound classes present in a new plant species and their relative amount, methods are much simpler. Most chemical compound classes have certain characteristics, like the ability to precipitate proteins (tannins), their function as antioxidants (flavonoids), or their role as pigments (anthocyanins), which can be used for their detection. For tannin quantification, for instance, a bovine serum albumin (BSA) assay was developed, where tannins are precipitated with BSA to be dissolved again in the presence of ferric chloride with which they form violet complexes, detectable with a spectrophotometer (Hagerman and Butler, 1978). As previously described (see chapter 1.1.1.3), the Folin-Ciocalteu assay uses the antioxidant potential of a sample as an estimation of total phenol content, while for anthocyanins the characteristic changes in absorbance at 515 nm at different pH (pH 3.5 vs. pH <1) indicate the relative amount (Naczki and Shahidi, 2004). Spectrophotometric assays require less (expensive) equipment and complicated workflows than the aforementioned strategies, at the expense of a less detailed and accurate analysis. These assays are especially common in food science and industry, to compare the antioxidant or other properties of a certain variety of fruit to another (see e.g. Chen et al. (2015)). They are also widespread methods in basic research, whenever the plant's chemistry is not well known so that individual compounds of interest are not yet identified, when the focus is more on a comparison between different conditions than the specialized compounds themselves, and/or whenever the resources to harvest, process and analyze samples differently are not available. This has particularly often been the case for ant-plants. To compare chemical defenses within a genus or between colonized and ant-free plants, all analyses of phenolics – if any – aside from the research presented here (**manuscript I,II,III**) relied on colorimetric assays (e.g. Folgarait and Davidson (1994); Heil et al. (2002); Ward and Young (2002); Frederickson et al. (2013)).

In **manuscript III**, we present another option for a straightforward approach to estimate the relative amount of polyphenolics in plants. Single-wall carbon nanotubes (SWCNTs)

modified with polyethylene-glycol phospholipid (PEG-PL) macromolecules show strong fluorescence emission in the near-infrared (NIR) region. The interaction of PEG-PL polymers with polyphenols – likely via multiple hydroxyl groups – decreases this fluorescence intensity and shifts the emission wavelength to higher wavelengths in a concentration dependent manner (**manuscript III**). Compared to previous analytic methods, our approach is characterized by its simplified handling procedure. We showed that the SWCNT response can be read out even in complex matrices like crude plant extracts, the unprocessed supernatant of cell cultures or agar, thus reducing the number of processing steps, reagents, time, and amount of sample needed dramatically. This is crucial for high-throughput experiments, for instance screening polyphenol content in different fruit varieties, but is also important whenever resources are scarce and the timing is crucial. We successfully applied this method to detect the changes in polyphenol levels in response to biotic stress (fungal elicitor, herbivory), i.e. inducible plant defenses. Since the readout took only 3-5 s with 1 pixel $\approx 0.34 \text{ mm}^2$ (**manuscript III**), a high spatiotemporal resolution was possible. This allows the study of plant responses to biotic or abiotic stresses in real time and non-destructively. This is especially important for (ant-)plants such as *Tococa*, which grow in remote locations where the access to harvesting and processing facilities is very limited. For instance, the provision of liquid nitrogen to harvest the samples in the rainforest, transfer them safely to a laboratory with a lyophilizer, and then perform chemical analyses (**manuscript I**) turned out to be a major challenge in terms of logistics and handling. For this particular reason, the collected plant material is instead often dried in the field with silica or just air, at ambient temperatures or in an oven (Heil et al., 2002; Ward and Young, 2002; Frederickson et al., 2013). However, while these samples can be used to estimate their total polyphenol content, induced responses will be difficult to identify, as the long harvesting and sample processing procedure due to drying causes phytohormonal and other changes and leads to a modified polyphenol amount and composition by the time of analysis (e.g. Saifullah et al. (2019); Nguyen et al. (2022)). Since there are already portable devices available for NIR detection in the field, the SWCNT method could be further developed to enable a determination of the polyphenol content directly in the field. This could be realized by sampling the soil or leaves in a suitable solvent, or by adding SWCNTs directly to the organic material (Giraldo et al., 2014; Giraldo et al., 2015; Wong et al., 2017; Wu et al., 2020), followed by an immediate readout of the samples via NIR-spectroscopy. Furthermore, the strategy of using nanotubes for analyzing plant inducible defenses does not have to be limited to

polyphenol detection. Instead, the development of analogous methods based on nanoparticles that sense e.g. other specialized metabolites, certain phytohormones (Boonyaves et al., 2023), or the accumulation of reactive oxygen species (ROS) as an indicator of plant stress (Wu et al., 2020) is conceivable or is already being pursued. Thus, the use of fluorescent SWCNTs is a promising new strategy to study cellular processes in non-model plants in response to biotic stress *in vivo*, especially, as the alternative approach used in model species such as arabidopsis – i.e. the employment of genetically modified lines expressing reporter genes (see e.g. Meents et al. (2019); Malabarba et al. (2021)) – is difficult to implement in plants without mutant libraries or at least transformation protocols.

While the advantages of the SWCNT-based NIR-spectroscopy are evident, one should keep in mind that its applicability strongly depends on the research question as it does have its limitations just as any other technique. For one, the specificity of the sensors introduced here is similar to colorimetric assays, with analogous restrictions. For example, results of the Folin-Ciocalteu assay have to be taken with caution, as the varying reactivity of different phenolic compounds will influence the quantification, e.g. a given concentration of salicylic acid results in a weaker response than the same amount of gallic acid (Bravo, 1998; Everette et al., 2010). In addition, other compounds like ascorbic acid, thiols and metal complexes react with the reagents to form colored complexes and thus contribute to the ‘polyphenol’ amount detected (Bravo, 1998; Everette et al., 2010). Likewise, the SWCNT sensors showed differences in response intensity depending on the chemical compound, and at this stage it is not known whether other untested molecules exist that might influence the SWCNT emission in a similar way, thus influencing the results (**manuscript III**). Apart from that, it must be kept in mind that polyphenols are a large group of compounds with partly very different biological activities, and therefore, important effects can be missed when only studying the group as a whole. For instance, Moctezuma et al. (2014) found no correlation between total phenolics and levels of natural herbivory. However, when they looked at individual compounds and compound combinations, they found that the hydrolyzable tannins acutissimin B, mongolinin A, and vescalagin correlated with defense against herbivores and reduced the number of galls. Thus, it should be clear that precise analytic techniques such as MS cannot be easily replaced when trying to unravel the entirety of the complex chemical defense strategies of plants (Salminen and Karonen, 2011; Moctezuma et al., 2014). However, as long as the limitations of each technique are taken into account and appropriate controls are performed and included, each method can be

useful in their scope of application. Besides, further developments and research with the presented SWCNT-based detection technique are likely to improve some of the limiting aspects, particularly in terms of specificity.

3.5 Conclusion and future perspectives

Ant-plant mutualism is a fascinating example of how plants adapt to a complex environment and the importance of cooperation for survival. This thesis aimed to unravel the chemistry and molecular mechanisms behind this phenomenon. Metabolome and transcriptome analyses with various analytical techniques showed that *T. quadrialata* still maintains its own defense machinery, including the accumulation of constitutive defenses such as hydrolyzable tannins as well as biosynthesis of inducible defenses such as herbivore-induced plant volatiles and PAOx(-Glc). This thesis thus laid the foundation for future research on this mutualism. Now that the HIPVs are identified, studies of their role in *T. quadrialata* are necessary. This will answer questions such as whether any of these compounds is attractive to the mutualistic ants themselves or if they attract other natural enemies when the ant protection is failing. There is also the possibility that they could aim to attract an ant-queen to protect themselves from future damage, although other studies suggest that contact cues are more important for foundress queens than volatile cues (Inui et al., 2001; Jürgens et al., 2006; Dattilo et al., 2009; Blatrix and Mayer, 2010). Direct effects of some HIPVs – such as benzyl cyanide – on natural herbivores and intra- or inter-plant signaling of other HIPVs are further possible modes of action that need to be explored in the future in order to draw conclusions about the defensive reaction capacity of this ant-plant in comparison to other plants.

Along the same lines, this thesis demonstrated that herbivory induces JA signaling in ant-plants, which in turn activates indirect and direct defense mechanisms, implying that phytohormone signaling is very conserved in vascular plants and cannot easily be turned off in certain plant species. Nevertheless, there are hints for a differential regulation of inducible genes and compounds in *T. quadrialata* compared to non-myrmecophytes as seen for protease inhibitor genes, as well as for *CYP79s* and *CYP71* and the corresponding products PAOx and benzyl cyanide, with the latter not being inducible by JA treatment but only by herbivory itself - unlike in other plant species investigated this far (poplar (Irmisch et al., 2014), coca (Luck et al., 2016), tea (Liao et al., 2020), giant knotweed (Yamaguchi et al., 2016)). Future work should therefore include a more detailed investigation of the formation of JA(-Ile) and subsequent signaling in *T. quadrialata* and other ant-plants in comparison to non-myrmecophytes. A time course

analysis of JA formation and downstream gene regulation upon herbivory could also shed light on other factors that might prevent a more effective defense in ant-plants.

Not only did this thesis demonstrate that ant-plants still possess chemical defenses, but it also revealed that the general and defensive metabolism is altered by ant-colonization or the lack of such. Drawing conclusions from the current literature and the results of this work, ant nutrition seems to be a critical aspect for the outcome of this mutualism. Future studies in other ant-plants should therefore, similar to the research described here, not only look at one aspect of the mutualism (e.g. uptake of ^{15}N from ants in plant tissue) but also at the consequences of a certain treatment (e.g. higher/equal/lower levels of nitrogen in colonized versus ant-deprived plants, differing or similar phenotypes and/or metabolomes). This will facilitate the generation of a more holistic picture of this symbiosis. Of course, the story is expected to become more complicated as some ant-plant interactions including *Macaranga bancana*, *Acacia spp.*, *Cordia nodosa* and *Triplaris americana*, but not in *Piper*, *Tococa*, *Clidemia*, or *Duroia spp.*, involve a third player: ‘black yeasts’ of the ascomycete order Chaetothyriales have been found in the domatia of these ant-plants (Defosse et al., 2009; Mayer et al., 2014). And so far, at least for *Leonardoxa africana*, it has been shown that the associated *Petalomyrmex phylax* ants provide the fungus with nutrients and feed on the fungus, thus giving it a central role in the nutritional ecology of those plants (Defosse et al., 2009; Defosse et al., 2011; Blatrix et al., 2012). Therefore, it should be very interesting to see how this tripartite symbiosis affects overall plant metabolism and how it could be integrated into the scenarios discussed here.

The identification of herbivore-induced formation of PAOx-Glc alongside with PAOx in several non-cyanogenic plant species is another key finding of this thesis. While we studied the biosynthesis and possible biological roles of both compounds extensively *in vitro* and *in planta*, the final proof for both is still missing. The generation of *CYP79* and *UGT85* knock-out mutant lines would not only confirm their involvement in the biosynthesis, but also enable a validation of the proposed biological roles of PAOx(-Glc) *in vivo*. Unfortunately, no transformation protocols for *T. quadrialata* have been established yet. However, the corresponding *CYP79* in poplar were already identified and CRISPR/Cas9 protocols have been established for some *Populus spp.* (Fan et al., 2015; Zhou et al., 2015) opening up the possibility to investigate the functions of the metabolites – especially the potential role in signaling – beyond Brassicales and cyanogenic plant species *in vivo*.

As part of this thesis, a new detection method for polyphenols based on spectroscopy with near-infrared fluorescent single-wall carbon nanotubes (SWCNTs) was developed. The approach presented here is a very promising step towards facilitated research on ant-plants as well as other non-model organisms and/or plants in challenging locations such as remote places in the tropics, as it permits non-destructive analysis of plant material and a simplified workflow. However, until the SWCNTs can actually be used in the field, further studies and optimizations have to be conducted. In particular, it would be of utmost importance to establish and optimize protocols for simple extraction procedures or direct injection of SWCNTs into the organic material similar to the method of Wong et al. (2017) and for immediate and reliable read-outs in the field with portable and affordable NIR detection devices.

4 Summary

Plants have evolved a plethora of strategies to cope with herbivory. Among these is the production of diverse chemical defenses such as polyphenols, volatile organic compounds or aldoximes and derived compounds. In the tropics, where herbivore and pathogen pressure as well as competition with other plant species for nutrients and light are particularly high, some plants have secured additional help from the animal kingdom. The so-called ant-plants or myrmecophytes provide their associated plant-ants with preformed nesting sites – hollow structures at the base of the leaf blade, hollow stems, tubers or thorns called ‘domatia’. Additionally, many myrmecophytes offer food resources like extrafloral nectar to their inhabitants. In return, the ants protect their hosts against mammalian and insect herbivores, plant pathogens and/or competing plants. Whilst the ecological importance of these biotic defenders has been thoroughly studied, questions remain about the molecular mechanisms behind this mutualism and the chemical defense of myrmecophytes.

In this thesis, the Neotropical ant-plant *Tococa quadrialata* as a fast-growing shrub was chosen as a model species to study the chemical defenses of myrmecophytes and the influence of ant-colonization on plant metabolism in detail. Via a long-term ant- and herbivore-exclusion experiment in the Peruvian rainforest, this thesis demonstrated that *Azteca* cf. *tonduzi* ants not only defend their hosts efficiently against herbivores, but they also fertilize them and hence increase nitrogen content in colonized *T. quadrialata* plants. Therefore, ant-inhabited plants showed higher amino acid levels and growth rates as compared to ant-free *T. quadrialata* plants even in an herbivore-free environment, whereas ant-deprived plants accumulated more ellagitannins and related polyphenolics, presumably to better protect their not easily replaceable leaves. Controlled herbivory experiments with generalist caterpillars revealed that ant-plants still respond to leaf damage with the upregulation of jasmonic acid (JA) signaling and the production of inducible defenses such as herbivore-induced plant volatiles (HIPVs) of all the typical structural classes (terpenoids, nitrogenous amino acid derivatives, aromatic compounds, fatty acid derivatives). However, apart from the accumulation of free amino acids and the formation of phenylacetaldoxime (PAOx) and its glucoside (PAOx-Glc), neither metabolomics nor transcriptomics revealed many inducible defense compounds within the leaves. In particular, the lack of induction of protease inhibitor genes was noted, which together with results from other ant-plants hints towards a somehow reduced or differently regulated inducible defense in myrmecophytes as compared to other plant species. Taken together, the results of this thesis demonstrate that ant-plants

still possess their own defense machinery including constitutive (ellagitannins) and inducible (HIPVs, PAOx(-Glc)) chemical defenses. The thesis furthermore highlights how the presence or absence of mutualistic ants affects both the defense and general metabolism of myrmecophytes: the ants' nutritional choices (feeding on herbivorous insects/plant provided resources) and the protection provided against biotic stresses result in a differential availability and allocation of resources within the plants.

PAOx is a well-known intermediate in the biosynthesis of various defense compounds such as cyanogenic glycosides, glucosinolates and the volatile benzyl cyanide, as well as for the biosynthesis of the auxin phenylacetic acid. In addition, PAOx was previously shown to have toxic effects on caterpillars and signaling effects in genetically modified Brassicales. Therefore, it was very interesting to find PAOx and its glucoside PAOx-Glc, a previously undescribed natural product, amongst the strongest herbivore-induced compounds of *T. quadrialata* in both field and greenhouse experiments. Transcriptome analysis allowed the identification of candidate genes for the biosynthesis of PAOx, PAOx-Glc and the corresponding volatile benzyl cyanide. Biochemical characterization of the respective enzymes both *in vitro* and *in planta* revealed that most likely, CYP79A206 and CYP79A207 are responsible for the formation of PAOx and UGT85A123 is the primary glycosyltransferase involved in the formation of PAOx-Glc. On the other hand, another cytochrome P450, CYP71E76, catalyzes the biosynthesis of benzyl cyanide. Studies on the induction and distribution pattern of PAOx and PAOx-Glc further demonstrated that their accumulation upon herbivore damage is a strictly local and JA-independent phenomenon to protect the wounding site, with PAOx-Glc most likely representing a storage form of PAOx. *In vitro* activity assays revealed that PAOx-Glc can be hydrolyzed in insect guts and pathogenic bacteria, but not by plant glucosidases, providing an elegant mechanism to prevent potential self-intoxification or unwanted signaling effects caused by PAOx. Excitingly, the biotic stress-induced accumulation of PAOx-Glc alongside with PAOx is not specific for *T. quadrialata* or ant-plants, but was found to occur in several non-related, non-cyanogenic, non-Brassicales plant species. This indicates a widespread distribution of this biosynthesis pathway among flowering plants and raises questions about its evolutionary relationship with cyanogenic glycosides.

A major obstacle of this thesis, as well as research on ant-plants in general, is that myrmecophytes are non-model organisms, and not much is known about their specialized compounds. In addition, harvesting in the field and conserving the metabolic state of the plant tissue for subsequent chemical and molecular analysis is complicated.

Thus, it is often difficult to quantify compounds or compound classes using conventional methods. Therefore, in a collaboration, a new detection method was developed for a straightforward, fast and simple detection and relative quantification of plant polyphenols. Near-infrared (NIR) fluorescent single-wall carbon nanotubes (SWCNTs) were surface-modified with polyethylene glycol (PEG)–phospholipid (PL) macromolecules. The interaction of these PEG-PL polymers with polyphenols – likely via multiple hydroxyl groups – decreases the fluorescence intensity of the SWCNTs and shifts the emission wavelength to higher wavelengths in a concentration dependent manner. This enabled the detection of relative changes of total phenol content due to biotic stresses *in vitro* and *in vivo* in a physiologically relevant range (nM – μ M). The major advantages of this new strategy as compared to traditional techniques such as HPLC-DAD/MS and colorimetric assays, are firstly that it is a non-destructive way to obtain spatiotemporal information about polyphenol production or release from plant tissue in real time. Secondly, it reduces the sample processing steps and time and, with further developments, might be applied directly in the field, thus facilitating future investigations of (ant-)plants' defense metabolism. However, this ease of use comes at the expense of loss of information compared to more accurate methods such as HPLC-DAD-MS.

Overall, this thesis provides new insights into ant-plant mutualism and the defense strategies of myrmecophytes, a new method for the detection of stress responses in non-model (ant-)plants, and highlights the central role of aldoximes and their metabolism in vascular plants.

5 Zusammenfassung

Pflanzen haben eine Vielzahl von Verteidigungsstrategien entwickelt, um sich vor Fraßschaden zu schützen. Dazu zählt auch die Bildung verschiedener chemischer Verteidigungsstoffe, wie zum Beispiel Polyphenole, flüchtige organische Verbindungen oder Aldoxime und davon abgeleitete Verbindungen. In den Tropen, wo es besonders viele Fraßfeinde und Pathogene gibt, sowie viele Pflanzenspezies, die um Nährstoffe und Licht konkurrieren, haben sich einige Pflanzen zusätzliche Hilfe aus dem Tierreich gesucht. Die sogenannten Ameisenpflanzen oder Myrmekophyten bieten den mit ihnen assoziierten Pflanzenameisen vorgeformte geschützte Nistplätze – hohle Strukturen an der Blattbasis, hohle Stämme, Knollen oder Dornen die als „Domatien“ bezeichnet werden. Zusätzlich stellen viele Myrmekophyten ihren Bewohnern Nahrung zur Verfügung wie etwa extrafloralen Nektar. Im Gegenzug beschützen die Ameisen ihre Gastgeber vor Fraßfeinden, sowohl vor Säugetieren als auch Insekten, gegen Pflanzenpathogene und/oder gegen konkurrierende Pflanzen. Während die ökologische Bedeutung dieser biotischen Verteidiger bereits ausführlich untersucht wurde, sind viele Fragen bezüglich der molekularen Mechanismen, welche hinter diesem Mutualismus stecken und über die chemische Verteidigung der Myrmekophyten selbst noch offen.

In dieser Doktorarbeit wurde die neotropische Ameisenpflanze *Tococa quadrialata*, ein schnell wachsender Strauch, ausgewählt, um die chemische Verteidigung der Myrmekophyten und die Auswirkungen der Ameisenbesiedlung auf den pflanzlichen Metabolismus zu studieren. Mittels eines Langzeitexperiments im peruanischen Regenwald, in welchem die Pflanzen teilweise von Ameisen befreit und/oder vor Herbivoren geschützt waren, konnte diese Arbeit zeigen, dass *Azteca cf. tonduzi* Ameisen die von ihnen bewohnten Pflanzen nicht nur wirksam gegen Fraßfeinde verteidigen, sondern diese auch düngen und somit den Stickstoffgehalt in besiedelten Tococapflanzen erhöhen. Dies führte dazu, dass besiedelte Pflanzen im Vergleich zu unbesiedelten höhere Aminosäurekonzentrationen besaßen und schneller wuchsen, selbst wenn eine Bedrohung durch Pflanzenfresser für beide Gruppen ausgeschlossen war. Dagegen reicherten von Ameisen befreite Pflanzen mehr Ellagitannine und andere Polyphenole an, vermutlich um ihre nicht leicht zu ersetzenden Blätter besser zu beschützen. Kontrollierte Fraßexperimente mit generalistischen Raupen zeigten, dass Ameisenpflanzen auf Blattschaden mit der Hochregulierung des Jasmonsäure (JA) - signalwegs und der Biosynthese induzierbarer Verteidigungsstoffe wie etwa Herbivor-induzierter pflanzlicher Duftstoffe (HIPVs) aller typischen Strukturklassen (Terpenoide; stickstoffhaltige, von Aminosäuren abgeleitete Verbindungen; aromatische

Verbindungen; aus Fettsäuren gebildete Verbindungen) reagieren. Jedoch konnten mittels Metabolom- und Transkriptomanalysen, abgesehen von der Anhäufung freier Aminosäuren und Bildung des Phenylacetaldoxims (PAOx) und dessen Glukosid (PAOx-Glc), nicht viele induzierbare Verteidigungsstoffe in den Blättern gefunden werden. Besonders auffällig war die fehlende Induktion der Genexpression von Proteaseinhibitoren. Zusammen mit den Ergebnissen aus Studien anderer Ameisenpflanzen deutet dies auf eine in Teilen verringerte oder anders regulierte induzierbare Verteidigung in Myrmekophyten hin, verglichen mit anderen Pflanzenarten. Zusammengenommen zeigen die Ergebnisse dieser Arbeit, dass Ameisenpflanzen noch immer ihre eigenen Verteidigungsmechanismen besitzen, inklusive konstitutiver (Ellagitannine) und induzierbarer (HIPVs, PAOx(-Glc)) chemischer Verteidigungsstoffe. Diese Arbeit verdeutlicht außerdem, wie die An- bzw. Abwesenheit mutualistischer Ameisen sowohl den Verteidigungs- wie auch den generellen Metabolismus der Myrmekophyten beeinflusst: Die Ernährungsweise der Ameisen (herbivore Insekten/ von der Pflanze bereitgestellte Nahrung) und der Schutz vor biotischem Stress führen zu einer veränderten Verfügbarkeit und Verteilung von Ressourcen innerhalb der Pflanze.

PAOx ist ein bekanntes Zwischenprodukt in der Biosynthese von verschiedenen Verteidigungsstoffen wie etwa cyanogenen Glykosiden, Glukosinolaten, und des flüchtigen Benzylcyanids, wie auch für die Biosynthese des Auxins Phenylelessigsäure. Zudem ist PAOx selbst toxisch für Raupen und zeigte Signalwirkung in genetisch veränderten Pflanzen (Brassicales). Daher war die Identifizierung von PAOx und dessen Glykosid PAOx-Glc, eines bisher nicht beschriebenen Naturstoffs, als die am stärksten durch Fraßschaden induzierten Verbindungen in *T. quadrialata* – im Feld sowie unter kontrollierten Bedingungen im Gewächshaus – sehr interessant. Mittels Transkriptomanalyse konnten Kandidatengene für die Biosynthese von PAOx, PAOx-Glc und dem entsprechenden Duftstoff Benzylcyanid identifiziert werden. Eine biochemische Charakterisierung der entsprechenden Enzyme *in vitro* und *in planta* legte nahe, dass CYP79A206 und CYP79A207 für die Produktion von PAOx verantwortlich sind und dass UGT85A123 die Glykosyltransferase ist, welche hauptsächlich für die PAOx-Glc Bildung zuständig ist. Währenddessen katalysiert ein anderes Cytochrom P450 Enzym, CYP71E76, die Biosynthese von Benzylcyanid. Weitere Experimente zum PAOx bzw. PAOx-Glc Induktions- und Verteilungsmuster zeigten zudem, dass deren Anreicherung nach Fraßschaden ein sehr lokales, JA-unabhängiges Phänomen ist, um die Verwundungsstelle zu schützen. Dabei stellt PAOx-Glc vermutlich die Speicherform von PAOx dar. *In vitro* Aktivitätsstudien zeigten, dass PAOx-Glc im Insekten Darm und

von pathogenen Bakterien, nicht aber von pflanzlichen Glukosidasen hydrolysiert werden kann, was eine elegante Lösung darstellt, um potentielle Selbstvergiftung oder ungewollte Signalwirkungen von PAOx vorzubeugen. Interessanterweise ist die durch biotischen Stress ausgelöste Anreicherung von PAOx-Glc zusammen mit PAOx nicht spezifisch für *T. quadrialata*, sondern konnte in mehreren nichtverwandten, nicht-cyanogenen, nicht-kreuzblütlerartigen Pflanzenarten nachgewiesen werden. Dies deutet an, dass der Biosyntheseweg in Blütenpflanzen weitverbreitet ist und wirft die Frage nach der evolutionären Verwandtschaft mit den cyanogenen Glykosiden auf.

Zu den größten Hindernissen dieser Arbeit, wie auch der Forschung an Ameisenpflanzen im Allgemeinen gehört, dass diese Pflanzen keine sogenannten Modellorganismen sind, und daher wenig über ihre Naturstoffe bekannt ist. Zudem ist die Probenahme im Feld unter Erhalt des jeweiligen metabolischen Zustands des Pflanzenmaterials für die darauffolgenden chemischen und molekularbiologischen Analysen mitunter schwierig. Deshalb ist es oft nicht einfach, bestimmte Substanzen bzw. Stoffklassen der Pflanzen mit konventionellen Methoden zu quantifizieren. Um diesem Problem entgegenzuwirken, wurde im Rahmen einer Kollaboration eine neue Detektionsmethode entwickelt, welche einen unkomplizierten, schnellen und einfachen Nachweis sowie die relative Quantifizierung von pflanzlichen Polyphenolen ermöglicht. Dafür wurden die Oberflächen von im Nahinfrarot (NIR) fluoreszierenden einwandigen Kohlenstoffnanoröhren (SWCNTs) mit Polyethylenglykol (PEG) – Phospholipid (PL)-Makromolekülen modifiziert. Die Wechselwirkung dieser PEG-PL Polymere mit Polyphenolen – vermutlich über mehrere Hydroxygruppen – verringert konzentrationsabhängig die Intensität der SWCNT-Fluoreszenz und verschiebt - ebenfalls konzentrationsabhängig - die Emissionswellenlänge in den langwelligen Bereich. Dies ermöglichte den Nachweis relativer Veränderungen des Gesamtphenolgehalts durch biotischen Stress *in vitro* und *in vivo*, in einem physiologisch relevanten Bereich (nM - μ M). Die Vorteile dieses neuen Ansatzes gegenüber herkömmlichen Techniken wie HPLC-DAD/MS und kolorimetrischen Bestimmungen sind zum einen, dass es sich hierbei um eine nicht-destruktive Methode handelt, welche es erlaubt, die Produktion bzw. Freisetzung von Polyphenolen aus Pflanzengewebe räumlich und zeitlich aufgelöst in Echtzeit zu untersuchen. Zum anderen verringert sich der Zeit- und Arbeitsaufwand für die Probenvorbereitung, und die Technik könnte so weiterentwickelt werden, dass die SWCNTs direkt im Feld einsetzbar wären, was künftige Untersuchungen der Verteidigungsstrategien von (Ameisen-)Pflanzen erleichtern würde. Die vereinfachte Anwendung geht jedoch mit Informationsverlusten im Vergleich zu genaueren Methoden wie HPLC-DAD-MS einher.

Insgesamt liefert diese Arbeit neue Erkenntnisse über den Mutualismus zwischen Ameisen und Pflanzen und die Verteidigungsstrategien von Myrmekophyten, eine neue Methode zum Nachweis von Stressreaktionen in Nicht-Modell-(Ameisen-)pflanzen und zeigt die zentrale Rolle von Aldoximen und deren Metabolismus in Gefäßpflanzen auf.

6 References

- Adams LS, Seeram NP, Aggarwal BB, Takada Y, Sand D, Heber D** (2006) Pomegranate juice, total pomegranate ellagitannins, and punicalagin suppress inflammatory cell signaling in colon cancer cells. *Journal of Agricultural and Food Chemistry* **54**: 980-985
- Agerbirk N, Olsen CE** (2012) Glucosinolate structures in evolution. *Phytochemistry* **77**: 16-45
- Agrawal AA** (1998) Leaf damage and associated cues induced aggressive and recruitment in a Neotropical ant-plant. *Ecology* **79**: 2100-2112
- Agrawal AA, Dubin-Thaler BJ** (1999) Induced responses to herbivory in the Neotropical ant-plant association between *Azteca* ants and *Cecropia* trees: response of ants to potential inducing cues. *Behavioral Ecology and Sociobiology* **45**: 47-54
- Ahmad S, Saleem Z, Jabeen F, Hussain B, Sultana T, Sultana S, Al-Ghanim KA, Al-Mulhim NMA, Mahboob S** (2018) Potential of natural repellents methylantranilate and anthraquinone applied on maize seeds and seedlings against house sparrow (*Passer domesticus*) in captivity. *Brazilian Journal of Biology* **78**: 667-672
- Akatsuka T, Kodama O, Sekido H, Kono Y, Takeuchi S** (1985) Novel phytoalexins (Oryzalexins A, B and C) isolated from rice blast leaves infected with *Pyricularia oryzae*.: Part I: Isolation, characterization and biological activities of Oryzalexins Part II: Structural studies of Oryzalexins. *Agricultural and Biological Chemistry* **49**: 1689-1701
- Alvarez G, Armbrrecht I, Jimenez E, Armbrrecht H, Ulloa-Chaco P** (2001) Ant-plant association in two *Tococa* species from a primary rain forest of Colombian Choco (Hymenoptera: Formicidae). *Sociobiology* **38**: 585-602
- Andersen MD, Busk PK, Svendsen I, Møller BL** (2000) Cytochromes P-450 from cassava (*Manihot esculenta* Crantz) catalyzing the first steps in the biosynthesis of the cyanogenic glucosides linamarin and lotaustralin. Cloning, functional expression in *Pichia pastoris*, and substrate specificity of the isolated recombinant enzymes. *Journal of Biological Chemistry* **275**: 1966-1975
- Anstett DN, Cheval I, D'Souza C, Salminen JP, Johnson MTJ** (2019) Ellagitannins from the Onagraceae decrease the performance of generalist and specialist herbivores. *Journal of Chemical Ecology* **45**: 86-94
- Austin MB, Noel JP** (2003) The chalcone synthase superfamily of type III polyketide synthases. *Natural product reports* **20**: 79-110
- Baetz U, Martinoia E** (2014) Root exudates: the hidden part of plant defense. *Trends in Plant Science* **19**: 90-98
- Bak S, Kahn RA, Nielsen HL, Møller BL, Halkier BA** (1998) Cloning of three A-type cytochromes P450, CYP71E1, CYP98, and CYP99 from *Sorghum bicolor* (L.) Moench by a PCR approach and identification by expression in *Escherichia coli* of CYP71E1 as a multifunctional cytochrome P450 in the biosynthesis of the cyanogenic glucoside dhurrin. *Plant Molecular Biology* **36**: 393-405
- Ballare CL** (2014) Light regulation of plant defense. *In* SS Merchant, ed, *Annual Review of Plant Biology*, Vol 65, pp 335-363
- Ballhorn DJ, Lieberei R, Ganzhorn JU** (2005) Plant cyanogenesis of *Phaseolus lunatus* and its relevance for herbivore–plant interaction: The importance of quantitative data. *Journal of Chemical Ecology* **31**: 1445-1473
- Barbehenn RV, Constabel P** (2011) Tannins in plant-herbivore interactions. *Phytochemistry* **72**: 1551-1565
- Barbehenn RV, Jaros A, Lee G, Mozola C, Weir Q, Salminen J-P** (2009) Hydrolyzable tannins as “quantitative defenses”: Limited impact against *Lymantria dispar*

- caterpillars on hybrid poplar. *Journal of Insect Physiology* **55**: 297-304
- Barbehenn RV, Jones CP, Hagerman AE, Karonen M, Salminen J-P** (2006) Ellagitannins have greater oxidative activities than condensed tannins and galloyl glucoses at high pH: Potential impact on caterpillars. *Journal of Chemical Ecology* **32**: 2253-2267
- Bari R, Jones JD** (2009) Role of plant hormones in plant defence responses. *Plant Molecular Biology* **69**: 473-488
- Bartel B, Fink GR** (1994) Differential regulation of an auxin-producing nitrilase gene family in *Arabidopsis thaliana*. *Proceedings of the National Academy of Sciences of the United States of America* **91**: 6649-6653
- Bartimachi A, Neves J, Vasconcelos HL** (2015) Geographic variation in the protective effects of ants and trichomes in a Neotropical ant-plant. *Plant Ecology* **216**: 1083-1090
- Barton Kasey E, Koricheva J** (2010) The ontogeny of plant defense and herbivory: characterizing general patterns using meta-analysis. *The American Naturalist* **175**: 481-493
- Benkova E, Michniewicz M, Sauer M, Teichmann T, Seifertova D, Jurgens G, Friml J** (2003) Local, efflux-dependent auxin gradients as a common module for plant organ formation. *Cell* **115**: 591-602
- Bennett RN, Wallsgrove RM** (1994) Secondary metabolites in plant defence mechanisms. *New Phytologist* **127**: 617-633
- Blatrix R, Djiéto-Lordon C, Mondolot L, La Fisca P, Voglmayr H, McKey D** (2012) Plant-ants use symbiotic fungi as a food source: new insight into the nutritional ecology of ant-plant interactions. *Proceedings of the Royal Society B: Biological Sciences* **279**: 3940-3947
- Blatrix R, Mayer VE** (2010) Communication in ant-plant symbioses. *In* F Baluska, V Ninkovic, eds, *Plant communication from an ecological perspective*. Springer-Verlag, Berlin Heidelberg, pp 127-158
- Blazenovic I, Kind T, Ji J, Fiehn O** (2018) Software tools and approaches for compound identification of LC-MS/MS data in metabolomics. *Metabolites* **8**: 31
- Bleeker PM, Mirabella R, Diergaarde PJ, VanDoorn A, Tissier A, Kant MR, Prins M, de Vos M, Haring MA, Schuurink RC** (2012) Improved herbivore resistance in cultivated tomato with the sesquiterpene biosynthetic pathway from a wild relative. *Proceedings of the National Academy of Sciences of the United States of America* **109**: 20124-20129
- Bohlmann J, Meyer-Gauen G, Croteau R** (1998) Plant terpenoid synthases: Molecular biology and phylogenetic analysis. *Proceedings of the National Academy of Sciences of the United States of America* **95**: 4126-4133
- Boonyaves K, Ang MC-Y, Park M, Cui J, Khong DT, Singh GP, Koman VB, Gong X, Porter TK, Choi SW, Chung K, Chua N-H, Urano D, Strano MS** (2023) Near-infrared fluorescent carbon nanotube sensors for the plant hormone family gibberellins. *Nano Letters* **23**: 916-924
- Bravo L** (1998) Polyphenols: Chemistry, dietary sources, metabolism, and nutritional significance. *Nutrition Reviews* **56**: 317-333
- Broadway RM, Duffey SS** (1986) Plant proteinase inhibitors: Mechanism of action and effect on the growth and digestive physiology of larval *Heliothis zea* and *Spodoptera exiqua*. *Journal of Insect Physiology* **32**: 827-833
- Brouat C, McKey D, Bessière J-M, Pascal L, Hossaert-McKey M** (2000) Leaf volatile compounds and the distribution of ant patrolling in an ant-plant protection mutualism: Preliminary results on *Leonardoxa* (Fabaceae: Caesalpinioideae) and *Petalomyrmex* (Formicidae: Formicinae). *Acta Oecologica* **21**: 349-357
- Bruce TJA, Pickett JA** (2011) Perception of plant volatile blends by herbivorous insects – Finding the right mix. *Phytochemistry* **72**: 1605-1611

- Bruna EM, Lapola DM, Vasconcelos HL** (2004) Interspecific variation in the defensive responses of obligate plant-ants: experimental tests and consequences for herbivory. *Oecologia* **138**: 558-565
- Bryant JP, Chapin FS, Klein DR** (1983) Carbon/nutrient balance of boreal plants in relation to vertebrate herbivory. *Oikos* **40**: 357-368
- Buzzini P, Arapitsas P, Goretti M, Branda E, Turchetti B, Pinelli P, Ieri F, Romani A** (2008) Antimicrobial and antiviral activity of hydrolysable tannins. *Mini-Reviews in Medicinal Chemistry* **8**: 1179-1187
- Cabrera M, Jaffe K** (1994) A trophic mutualism between the myrmecophytic Melastomataceae *Tococa guianensis* and an *Azteca* ant species. *Ecotropicos* **7**: 1-10
- Chang C-F, Suzuki A, Kumai S, Tamura S** (1969) Chemical studies on "clover sickness". *Agricultural and Biological Chemistry* **33**: 398-408
- Chen H, Wilkerson CG, Kuchar JA, Phinney BS, Howe GA** (2005) Jasmonate-inducible plant enzymes degrade essential amino acids in the herbivore midgut. *Proceedings of the National Academy of Sciences of the United States of America* **102**: 19237-19242
- Chen PX, Tang Y, Marccone MF, Pauls PK, Zhang B, Liu R, Tsao R** (2015) Characterization of free, conjugated and bound phenolics and lipophilic antioxidants in regular- and non-darkening cranberry beans (*Phaseolus vulgaris* L.). *Food Chemistry* **185**: 298-308
- Cheynier V, Comte G, Davies KM, Lattanzio V, Martens S** (2013) Plant phenolics: Recent advances on their biosynthesis, genetics, and ecophysiology. *Plant Physiology and Biochemistry* **72**: 1-20
- Choh Y, Takabayashi J** (2006) Herbivore-induced extrafloral nectar production in lima bean plants enhanced by previous exposure to volatiles from infested conspecifics. *Journal of Chemical Ecology* **32**: 2073-2077
- Chomicki G, Renner SS** (2015) Phylogenetics and molecular clocks reveal the repeated evolution of ant-plants after the late Miocene in Africa and the early Miocene in Australasia and the Neotropics. *New Phytologist* **207**: 411-424
- Christianini AV, Machado G** (2004) Induced biotic responses to herbivory and associated cues in the Amazonian ant-plant *Maieta poeppigii*. *Entomologia Experimentalis et Applicata* **112**: 81-88
- Clavijo McCormick A, Irmisch S, Reinecke A, Boeckler GA, Veit D, Reichelt M, Hansson BS, Gershenzon J, Köllner TG, Unsicker SB** (2014) Herbivore-induced volatile emission in black poplar: regulation and role in attracting herbivore enemies. *Plant Cell & Environment* **37**: 1909-1923
- Coley PD** (1986) Costs and benefits of defense by tannins in a neotropical tree. *Oecologia* **70**: 238-241
- Coley PD, Bryant JP, Chapin FS** (1985) Resource availability and plant antiherbivore defense. *Science* **230**: 895-899
- Compton S, Jones D** (1985) An investigation of the responses of herbivores to cyanogenesis in *Lotus corniculatus* L. *Biological Journal of the Linnean Society* **26**: 21-38
- Cooper JE** (2004) Multiple responses of rhizobia to flavonoids during legume root infection. *In* *Advances in Botanical Research*, Vol 41. Academic Press, pp 1-62
- Cunningham JP, Moore CJ, Zalucki MP, West SA** (2004) Learning, odour preference and flower foraging in moths. *Journal of Experimental Biology* **207**: 87-94
- Dattilo WFC, Izzo TJ, Inouye BD, Vasconcelos HL, Bruna EM** (2009) Recognition of host plant volatiles by *Pheidole minutula* Mayr (Myrmicinae), an Amazonian ant-plant specialist. *Biotropica* **41**: 642-646
- Davidson D, Fisher B** (1991) Symbiosis of ants with *Cecropia* as a function of light regime. *In* C Huxley, DK Cutler, eds, *Ant-Plant Interactions*. Oxford University

- Press, New York, pp 289-309
- Davidson DW, Longino JT, Snelling RR** (1988) Pruning of host plant neighbors by ants: an experimental approach. *Ecology* **69**: 801-808
- Davidson DW, McKey D** (1993) The evolutionary ecology of symbiotic ant-plant relationships. *Journal of Hymenoptera research* **2**: 13-83
- Davies PJ** (1995) The plant hormones: their nature, occurrence, and functions. In PJ Davies, ed, *Plant Hormones: Physiology, Biochemistry and Molecular Biology*. Springer Netherlands, Dordrecht, pp 1-12
- De Gazelle J** (2014) Q'eqchi' Maya reproductive ethnomedicine, Vol 1. Springer International Publishing, Switzerland
- de Rijke E, Out P, Niessen WMA, Ariese F, Gooijer C, Brinkman UAT** (2006) Analytical separation and detection methods for flavonoids. *Journal of Chromatography A* **1112**: 31-63
- Defosse E, Djieto-Lordon C, McKey D, Selosse MA, Blatrix R** (2011) Plant-ants feed their host plant, but above all a fungal symbiont to recycle nitrogen. *Proceedings of the Royal Society B: Biological Sciences* **278**: 1419-1426
- Defosse E, Selosse M-A, Dubois M-P, Mondolot L, Faccio A, Djieto-Lordon C, McKey D, Blatrix R** (2009) Ant-plants and fungi: a new threeway symbiosis. *New Phytologist* **182**: 942-949
- Dejean A, Delabie JHC, Cerdan P, Gibernau M, Corbara B** (2006) Are myrmecophytes always better protected against herbivores than other plants? *Biological Journal of the Linnean Society* **89**: 91-97
- Dejean A, Djieto-Lordon C, Orivel J** (2008) The plant ant *Tetraponera aethiops* (Pseudomyrmecinae) protects its host myrmecophyte *Barteria fistulosa* (Passifloraceae) through aggressiveness and predation. *Biological Journal of the Linnean Society* **93**: 63-69
- Dejean A, Grangier J, Leroy C, Orivel J** (2008) Host plant protection by arboreal ants: looking for a pattern in locally induced responses. *Evolutionary Ecology Research* **10**: 1217–1223
- Dejean A, Grangier J, Leroy C, Orivel J** (2009) Predation and aggressiveness in host plant protection: a generalization using ants from the genus *Azteca*. *Naturwissenschaften* **96**: 57–63
- Dejean A, Petitclerc F, Azémar F, Corbara B, Delabie JHC, Compin A** (2017) Hollow internodes permit a Neotropical understory plant to shelter multiple mutualistic ant species, obtaining protection and nutrient provisioning (myrmecotrophy). *The American Naturalist* **190**: E124-131
- Delphia CM, Mescher MC, De Moraes CM** (2007) Induction of plant volatiles by herbivores with different feeding habits and the effects of induced defenses on host-plant selection by thrips. *Journal of Chemical Ecology* **33**: 997-1012
- Dicke M, Baldwin IT** (2010) The evolutionary context for herbivore-induced plant volatiles: beyond the 'cry for help'. *Trends in Plant Science* **15**: 167-175
- Dicke M, Gols R, Ludeking D, Posthumus MA** (1999) Jasmonic acid and herbivory differentially induce carnivore-attracting plant volatiles in lima bean plants. *Journal of Chemical Ecology* **25**: 1907-1922
- Dobson HEM, Danielson EM, Wesep IDV** (1999) Pollen odor chemicals as modulators of bumble bee foraging on *Rosa rugosa* Thunb. (Rosaceae). *Plant Species Biology* **14**: 153-166
- Dodson CD, Dyer LA, Searcy J, Wright Z, Letourneau DK** (2000) Cenocladamide, a dihydropyridone alkaloid from *Piper cenocladum*. *Phytochemistry* **53**: 51-54
- Drumm JE, Adams JB, Jr., Brown RJ, Campbell CL, Erbes DL, Hall WT, Hartzell SL, Holliday MJ, Kleier DA, Martin MJ, Pember SO, Ramsey GR** (1995) Oxime Fungicides. In *Synthesis and Chemistry of Agrochemicals IV*, Vol 584. American Chemical Society, pp 396-405

- Dudareva N, Negre F, Nagegowda DA, Orlova I** (2006) Plant volatiles: recent advances and future perspectives. *Critical Reviews in Plant Sciences* **25**: 417-440
- Durango D, Pulgarin N, Echeverri F, Escobar G, Quiñones W** (2013) Effect of salicylic acid and structurally related compounds in the accumulation of phytoalexins in cotyledons of common bean (*Phaseolus vulgaris* L.) cultivars. *In Molecules*, Vol 18, pp 10609-10628
- Dyer LA, Dodson CD, Beihoffer J, Letourneau DK** (2001) Trade-offs in antiherbivore defenses in *Piper cenocladum*: ant mutualists versus plant secondary metabolites. *Journal of Chemical Ecology* **27**: 581-592
- Dyer LA, Letourneau DK, Dodson CD, Tobler MA, Stireman III JO, Hsu A** (2004) Ecological causes and consequences of variation in defensive chemistry of a Neotropical shrub. *Ecology* **85**: 2795-2803
- Eberl F, Fabisch T, Luck K, Köllner TG, Vogel H, Gershenzon J, Unsicker SB** (2021) Poplar protease inhibitor expression differs in an herbivore specific manner. *BMC Plant Biology* **21**: 170
- Engelberth J, Alborn HT, Schmelz EA, Tumlinson JH** (2004) Airborne signals prime plants against insect herbivore attack. *Proceedings of the National Academy of Sciences of the United States of America* **101**: 1781-1785
- Erb M, Meldau S, Howe GA** (2012) Role of phytohormones in insect-specific plant reactions. *Trends in Plant Science* **17**: 250-259
- Erb M, Reymond P** (2019) Molecular interactions between plants and insect herbivores. *Annual Review of Plant Biology* **70**: 527-557
- Erb M, Veyrat N, Robert CA, Xu H, Frey M, Ton J, Turlings TC** (2015) Indole is an essential herbivore-induced volatile priming signal in maize. *Nature Communications* **6**: 6273
- Everette JD, Bryant QM, Green AM, Abbey YA, Wangila GW, Walker RB** (2010) Thorough study of reactivity of various compound classes toward the Folin-Ciocalteu reagent. *Journal of Agricultural and Food Chemistry* **58**: 8139-8144
- Fan D, Liu T, Li C, Jiao B, Li S, Hou Y, Luo K** (2015) Efficient CRISPR/Cas9-mediated targeted mutagenesis in *Populus* in the first generation. *Scientific Reports* **5**: 12217
- Farmer EE, Johnson RR, Ryan CA** (1992) Regulation of expression of proteinase inhibitor genes by methyl jasmonate and jasmonic acid. *Plant Physiology* **98**: 995-1002
- Federle W, Maschwitz U, Hölldobler B** (2002) Pruning of host plant neighbours as defence against enemy ant invasions: *Crematogaster* ant partners of *Macaranga* protected by "wax barriers" prune less than their congeners. *Oecologia* **132**: 264-270
- Fiala B, Maschwitz U, Pong TY, Helbig AJ** (1989) Studies of a South East Asian ant-plant association: protection of *Macaranga* trees by *Crematogaster borneensis*. *Oecologia* **79**: 463-470
- Fincher RM, Dyer LA, Dodson CD, Richards JL, Tobler MA, Searcy J, Mather JE, Reid AJ, Rolig JS, Pidcock W** (2008) Inter- and intraspecific comparisons of antiherbivore defenses in three species of rainforest understory shrubs. *Journal of Chemical Ecology* **34**: 558-574
- Fischer RC, Richter A, Wanek W, Mayer V** (2002) Plants feed ants: food bodies of myrmecophytic *Piper* and their significance for the interaction with *Pheidole bicornis* ants. *Oecologia* **133**: 186-192
- Folgarait PJ, Davidson DW** (1994) Antiherbivore defenses of myrmecophytic *Cecropia* under different light regimes. *Oikos* **71**: 305-320
- Folgarait PJ, Davidson DW** (1995) Myrmecophytic *Cecropia*: antiherbivore defenses under different nutrient treatments. *Oecologia* **104**: 189-206

- Folgarait PJ, Johnson HL, Davidson DW** (1994) Responses of *Cecropia* to experimental removal of Müllerian bodies. *Functional Ecology* **8**: 22-28
- Frederickson ME** (2005) Ant species confer different partner benefits on two neotropical myrmecophytes. *Oecologia* **143**: 387-395
- Frederickson ME, Greene MJ, Gordon DM** (2005) 'Devil's gardens' bedevilled by ants. *Nature* **437**: 495-496
- Frederickson ME, Ravenscraft A, Arcila Hernández LM, Booth G, Astudillo V, Miller GA, Kitzberger T** (2013) What happens when ants fail at plant defence? *Cordia nodosa* dynamically adjusts its investment in both direct and indirect resistance traits in response to herbivore damage. *Journal of Ecology* **101**: 400-409
- Frederickson ME, Ravenscraft A, Miller GA, Arcila Hernandez LM, Booth G, Pierce NE** (2012) The direct and ecological costs of an ant-plant symbiosis. *The American Naturalist* **179**: 768-778
- Friml J, Wiśniewska J, Benková E, Mendgen K, Palme K** (2002) Lateral relocation of auxin efflux regulator PIN3 mediates tropism in *Arabidopsis*. *Nature* **415**: 806-809
- Gatehouse JA** (2002) Plant resistance towards insect herbivores: a dynamic interaction. *New Phytologist* **156**: 145-169
- Gay H** (1993) Animal-fed plants: an investigation into the uptake of ant-derived nutrients by the far-eastern epiphytic fern *Lecanopteris* Reinw. (Polypodiaceae). *Biological Journal of the Linnean Society* **50**: 221-233
- Gershenzon J** (1984) Changes in the levels of plant secondary metabolites under water and nutrient stress. In BN Timmermann, C Steelink, FA Loewus, eds, *Phytochemical Adaptations to Stress*. Springer US, Boston, MA, pp 273-320
- Gimenez-Ibanez S, Solano R** (2013) Nuclear jasmonate and salicylate signaling and crosstalk in defense against pathogens. *Frontiers in Plant Science* **4**: 72
- Giraldo JP, Landry MP, Faltermeier SM, McNicholas TP, Iverson NM, Boghossian AA, Reuel NF, Hilmer AJ, Sen F, Brew JA, Strano MS** (2014) Plant nanobionics approach to augment photosynthesis and biochemical sensing. *Nature Materials* **13**: 400-408
- Giraldo JP, Landry MP, Kwak S-Y, Jain RM, Wong MH, Iverson NM, Ben-Naim M, Strano MS** (2015) A ratiometric sensor using single chirality near-infrared fluorescent carbon nanotubes: application to in vivo monitoring. *Small* **11**: 3973-3984
- Glawischnig E** (2007) Camalexin. *Phytochemistry* **68**: 401-406
- Glazebrook J** (2005) Contrasting mechanisms of defense against biotrophic and necrotrophic pathogens. *Annual Review of Phytopathology* **43**: 205-227
- Glinwood RT, Pettersson J** (2000) Change in response of *Rhopalosiphum padi* spring migrants to the repellent winter host component methyl salicylate. *Entomologia Experimentalis et Applicata* **94**: 325-330
- Gnanamanickam SS, Patil SS** (1977) Accumulation of antibacterial isoflavonoids in hypersensitively responding bean leaf tissues inoculated with *Pseudomonas phaseolicola*. *Physiological Plant Pathology* **10**: 159-168
- Gontijo DC, Gontijo PC, Brandao GC, Diaz MA, de Oliveira AB, Fietto LG, Leite JPV** (2019) Antioxidant study indicative of antibacterial and antimutagenic activities of an ellagitannin-rich aqueous extract from the leaves of *Miconia latecrenata*. *Journal of Ethnopharmacology* **236**: 114 - 123
- Gonzalez-Teuber M, Heil M** (2009) The role of extrafloral nectar amino acids for the preferences of facultative and obligate ant mutualists. *Journal of Chemical Ecology* **35**: 459-468
- Gonzalez-Teuber M, Kaltenpoth M, Boland W** (2014) Mutualistic ants as an indirect defence against leaf pathogens. *New Phytologist* **202**: 640-650

- Grubb DC, Zipp BJ, Ludwig-Müller J, Masuno MN, Molinski TF, Abel S** (2004) Arabidopsis glucosyltransferase UGT74B1 functions in glucosinolate biosynthesis and auxin homeostasis. *The Plant Journal* **40**: 893-908
- Gundlach H, Müller MJ, Kutchan TM, Zenk MH** (1992) Jasmonic acid is a signal transducer in elicitor-induced plant cell cultures. *Proceedings of the National Academy of Sciences* **89**: 2389-2393
- Günther J, Irmisch S, Lackus ND, Reichelt M, Gershenzon J, Köllner TG** (2018) The nitrilase PtNIT1 catabolizes herbivore-induced nitriles in *Populus trichocarpa*. *BMC Plant Biology* **18**: 251
- Hager FA, Krausa K** (2019) *Acacia* ants respond to plant-borne vibrations caused by mammalian browsers. *Current Biology* **29**: 717-725.e713
- Hagerman AE** (1989) Chemistry of tannin-protein complexation. In RW Hemingway, JJ Karchesy, SJ Branham, eds, *Chemistry and significance of condensed tannins*. Springer US, Boston, MA, pp 323-333
- Hagerman AE, Butler LG** (1978) Protein precipitation method for the quantitative determination of tannins. *Journal of Agricultural and Food Chemistry* **26**: 809-812
- Hahlbrock K, Grisebach H** (1975) Biosynthesis of flavonoids. In JB Harborne, TJ Mabry, H Mabry, eds, *The flavonoids*. Springer US, Boston, MA, pp 866-915
- Halkier BA, Gershenzon J** (2006) Biology and biochemistry of glucosinolates. *Annual Review of Plant Biology* **57**: 303-333
- Halkier BA, Nielsen HL, Koch B, Møller BL** (1995) Purification and characterization of recombinant cytochrome P450TYR expressed at high levels in *Escherichia coli*. *Archives of Biochemistry and Biophysics* **322**: 369-377
- Hammerbacher A, Coutinho TA, Gershenzon J** (2019) Roles of plant volatiles in defence against microbial pathogens and microbial exploitation of volatiles. *Plant Cell & Environment* **42**: 2827-2843
- Hanley ME, Lamont BB, Fairbanks MM, Rafferty CM** (2007) Plant structural traits and their role in anti-herbivore defence. *Perspectives in Plant Ecology, Evolution and Systematics* **8**: 157-178
- Hansen CC, Sorensen M, Veiga TAM, Zibrandtsen JFS, Heskes AM, Olsen CE, Boughton BA, Møller BL, Neilson EHJ** (2018) Reconfigured cyanogenic glucoside biosynthesis in *Eucalyptus cladocalyx* involves a cytochrome P450 CYP706C55. *Plant Physiology* **178**: 1081-1095
- Hansen CH, Du L, Naur P, Olsen CE, Axelsen KB, Hick AJ, Pickett JA, Halkier BA** (2001) CYP83b1 is the oxime-metabolizing enzyme in the glucosinolate pathway in *Arabidopsis*. *Journal of Biological Chemistry* **276**: 24790-24796
- Harborne JB** (1991) The chemical basis of plant defense. *Plant defenses against mammalian herbivory* **45**
- Hardie J, Isaacs R, Pickett JA, Wadhams LJ, Woodcock CM** (1994) Methyl salicylate and (-)-(1R,5S)-myrtenal are plant-derived repellents for black bean aphid, *Aphis fabae* Scop. (Homoptera: Aphididae). *Journal of Chemical Ecology* **20**: 2847-2855
- Hartmann A, Rothballer M, Schmid M** (2008) Lorenz Hiltner, a pioneer in rhizosphere microbial ecology and soil bacteriology research. *Plant and soil* **312**: 7-14
- Heil M** (2014) Herbivore-induced plant volatiles: targets, perception and unanswered questions. *New Phytologist* **204**: 297-306
- Heil M, Delsinne T, Hilpert A, Schürkens S, Linsenmair K, Andary C, Sousa SM, McKey D** (2002) Reduced chemical defence in ant-plants? A critical re-evaluation of a widely accepted hypothesis. *Oikos* **99**: 457-468
- Heil M, Fiala B, Kaiser W, Linsenmair KE** (1998) Chemical contents of *Macaranga* food bodies: adaptations to their role in ant attraction and nutrition. *Functional Ecology* **12**: 117-122

- Heil M, Fiala B, Linsenmair K** (1999) Reduced chitinase activities in ant plants of the genus *Macaranga*. *Naturwissenschaften* **86**: 146–149
- Heil M, Fiala B, Linsenmair KE, Zotz G, Menke P** (1997) Food body production in *Macaranga triloba* (Euphorbiaceae): a plant investment in anti-herbivore defence via symbiotic ant partners. *Journal of Ecology* **85**: 847-861
- Heil M, Fiala B, Maschwitz U, Linsenmair KE** (2001) On benefits of indirect defence: short- and long-term studies of antiherbivore protection via mutualistic ants. *Oecologia* **126**: 395-403
- Heil M, Greiner S, Meimberg H, Krüger R, Noyer J-L, Heubl G, Linsenmair E, Boland W** (2004) Evolutionary change from induced to constitutive expression of an indirect plant resistance. *Nature* **430**: 205-208
- Heil M, Koch T, Hilpert A, Fiala B, Boland W, Linsenmair K** (2001) Extrafloral nectar production of the ant-associated plant, *Macaranga tanarius*, is an induced, indirect, defensive response elicited by jasmonic acid. *Proceedings of the National Academy of Sciences of the United States of America* **98**: 1083-1088
- Heil M, Land WG** (2014) Danger signals - damaged-self recognition across the tree of life. *Frontiers in Plant Science* **5**: 578
- Heil M, Staehelin C, McKey D** (2000) Low chitinase activity in *Acacia* myrmecophytes: a potential trade-off between biotic and chemical defences? *Naturwissenschaften* **87**: 555–558
- Heil M, Ton J** (2008) Long-distance signalling in plant defence. *Trends in Plant Science* **13**: 264-272
- Hemm MR, Ruegger MO, Chapple C** (2003) The arabidopsis *ref2* mutant is defective in the gene encoding CYP83A1 and shows both phenylpropanoid and glucosinolate phenotypes. *The Plant Cell* **15**: 179-194
- Hernandez-Zepeda OF, Razo-Belman R, Heil M** (2018) Reduced responsiveness to volatile signals creates a modular reward provisioning in an obligate food-for-protection mutualism. *Frontiers in Plant Science* **9**: 1076
- Hildebrand DF, Brown GC, Jackson DM, Hamilton-Kemp TR** (1993) Effects of some leaf-emitted volatile compounds on aphid population increase. *Journal of Chemical Ecology* **19**: 1875-1887
- Howe GA, Jander G** (2008) Plant immunity to insect herbivores. *Annual Review of Plant Biology* **59**: 41-66
- Howe GA, Major IT, Koo AJ** (2018) Modularity in jasmonate signaling for multistress resilience. *Annual Review of Plant Biology* **69**: 387-415
- Hummelbrunner LA, Isman MB** (2001) Acute, sublethal, antifeedant, and synergistic effects of monoterpenoid essential oil compounds on the tobacco cutworm, *Spodoptera litura* (Lep., Noctuidae). *Journal of Agricultural and Food Chemistry* **49**: 715-720
- Inui Y, Itoika T, Murase K, Yamaoka R, Itino T** (2001) Chemical recognition of partner plant species by foundress ant queens in *Macaranga-Crematogaster* myrmecophytism. *Journal of Chemical Ecology* **27**: 2029-2040
- Irmisch S, Clavijo McCormick A, Günther J, Schmidt A, Boeckler GA, Gershenzon J, Unsicker SB, Köllner TG** (2014) Herbivore-induced poplar cytochrome P450 enzymes of the CYP71 family convert aldoximes to nitriles which repel a generalist caterpillar. *The Plant Journal* **80**: 1095-1107
- Irmisch S, McCormick AC, Boeckler GA, Schmidt A, Reichelt M, Schneider B, Block K, Schnitzler JP, Gershenzon J, Unsicker SB, Köllner TG** (2013) Two herbivore-induced cytochrome P450 enzymes CYP79D6 and CYP79D7 catalyze the formation of volatile aldoximes involved in poplar defense. *Plant Cell* **25**: 4737-4754
- Irmisch S, Zeltner P, Handrick V, Gershenzon J, Köllner TG** (2015) The maize cytochrome P450 CYP79A61 produces phenylacetaldoxime and indole-3-

- acetaldoxime in heterologous systems and might contribute to plant defense and auxin formation. *BMC Plant Biology* **15**: 128
- Isaza JH, Veloza LA, Ramirez LS, Guevara CA** (2007) Estimación espectrofotométrica de taninos hidrolizables y condensados en plantas Melastomatáceas. *Scientia et Technica Año XIII* **35**: 261-266
- Izzo TJ, Vasconcelos HL** (2002) Cheating the cheater: domatia loss minimizes the effects of ant castration in an Amazonian ant-plant. *Oecologia* **133**: 200-205
- Janzen DH** (1966) Coevolution of mutualism between ants and acacias in Central America. *International Journal of Organic Evolution* **20**: 249-275
- Janzen DH** (1967) Interaction of the bull's-horn acacia (*Acacia cornigera* L.) with an ant inhabitant (*Pseudomyrmex ferruginea* F. Smith) in Eastern Mexico. *University of Kansas Science Bulletin XLVII*: 315-558
- Janzen DH** (1969) Allelopathy by myrmecophytes: the ant *Azteca* as an allelopathic agent of *Cecropia*. *Ecology* **50**: 147-153
- Janzen DH** (1972) Protection of *Barteria* (Passifloraceae) by *Pachysima* ants (Pseudomyrmecinae) in a Nigerian rain forest. *Ecology* **53**: 885-892
- Janzen DH** (1973) Dissolution of mutualism between *Cecropia* and its *Azteca* ants. *Biotropica* **5**: 15-28
- Jez JM, Bowman ME, Dixon RA, Noel JP** (2000) Structure and mechanism of the evolutionarily unique plant enzyme chalcone isomerase. *Nature Structural Biology* **7**: 786-791
- Jung W, Yu O, Lau S-MC, O'Keefe DP, Odell J, Fader G, McGonigle B** (2000) Identification and expression of isoflavone synthase, the key enzyme for biosynthesis of isoflavones in legumes. *Nature Biotechnology* **18**: 208-212
- Jürgens A, Feldhaar H, Feldmeyer B, Fiala B** (2006) Chemical composition of leaf volatiles in *Macaranga* species (Euphorbiaceae) and their potential role as olfactory cues in host-localization of foundress queens of specific ant partners. *Biochemical Systematics and Ecology* **34**: 97-113
- Karban R, Shiojiri K, Huntzinger M, McCall AC** (2006) Damage-induced resistance in sagebrush: volatiles are key to intra- and interplant communication. *Ecology* **87**: 922-930
- Kazan K, Manners JM** (2009) Linking development to defense: auxin in plant-pathogen interactions. *Trends in Plant Science* **14**: 373-382
- Kessler A, Baldwin IT** (2001) Defensive function of herbivore-induced plant volatile emissions in nature. *Science* **291**: 2141-2144
- Kessler A, Baldwin IT** (2002) Plant responses to insect herbivory: the emerging molecular analysis. *Annual Review of Plant Biology* **53**: 299-328
- Kessler A, Heil M** (2011) The multiple faces of indirect defences and their agents of natural selection. *Functional Ecology* **25**: 348-357
- Kim JI, Dolan WL, Anderson NA, Chapple C** (2015) Indole glucosinolate biosynthesis limits phenylpropanoid accumulation in *Arabidopsis thaliana*. *Plant Cell* **27**: 1529-1546
- Kim JI, Zhang X, Pascuzzi PE, Liu CJ, Chapple C** (2020) Glucosinolate and phenylpropanoid biosynthesis are linked by proteasome-dependent degradation of PAL. *New Phytologist* **225**: 154-168
- Kishimoto K, Matsui K, Ozawa R, Takabayashi J** (2007) Volatile 1-octen-3-ol induces a defensive response in *Arabidopsis thaliana*. *Journal of General Plant Pathology* **73**: 35-37
- Knoch E, Motawie MS, Olsen CE, Møller BL, Lyngkjaer MF** (2016) Biosynthesis of the leucine derived α -, β - and γ -hydroxynitrile glucosides in barley (*Hordeum vulgare* L.). *The Plant Journal* **88**: 247-256
- Koo AJ** (2017) Metabolism of the plant hormone jasmonate: a sentinel for tissue damage and master regulator of stress response. *Phytochemistry Reviews* **17**:

51-80

- Koponen JM, Happonen AM, Mattila PH, Törrönen AR** (2007) Contents of anthocyanins and ellagitannins in selected foods consumed in Finland. *Journal of Agricultural and Food Chemistry* **55**: 1612-1619
- Kost C, Heil M** (2005) Increased availability of extrafloral nectar reduces herbivory in Lima bean plants (*Phaseolus lunatus*, Fabaceae). *Basic and Applied Ecology* **6**: 237-248
- Kroymann J** (2011) Natural diversity and adaptation in plant secondary metabolism. *Current Opinion in Plant Biology* **14**: 246-251
- Kumar P, Rathi P, Schöttner M, Baldwin IT, Pandit S** (2014) Differences in nicotine metabolism of two *Nicotiana attenuata* herbivores render them differentially susceptible to a common native predator. *PLoS One* **9**: e95982
- Kumar S, Pandey AK** (2013) Chemistry and biological activities of flavonoids: an overview. *The Scientific World Journal* **2013**: 162750
- Kwan EE, Huang SG** (2008) Structural elucidation with NMR spectroscopy: practical strategies for organic chemists. *European Journal of Organic Chemistry* **2008**: 2671-2688
- Larrea-Alcázar DM, Simonetti JA** (2007) Why are there few seedlings beneath the myrmecophyte *Triplaris americana*? *Acta Oecologica* **32**: 112-118
- Lazzeri L, Curto G, Leoni O, Dallavalle E** (2004) Effects of glucosinolates and their enzymatic hydrolysis products via myrosinase on the root-knot nematode *Meloidogyne incognita* (Kofoid et White) Chitw. *Journal of Agricultural and Food Chemistry* **52**: 6703-6707
- Lee JH, Johnson JV, Talcott ST** (2005) Identification of ellagic acid conjugates and other polyphenolics in muscadine grapes by HPLC-ESI-MS. *Journal of Agricultural and Food Chemistry* **53**: 6003-6010
- Letourneau DK** (1998) Ants, stem-borers, and fungal pathogens: experimental tests of a fitness advantage in *Piper* ant-plants. *Ecology* **79**: 593-603
- Letourneau DK, Barbosa P** (1999) Ants, stem borers, and pubescence in *Endospermum* in Papua New Guinea. *Biotropica* **31**: 295-302
- Liao Y, Zeng L, Tan H, Cheng S, Dong F, Yang Z** (2020) Biochemical pathway of benzyl nitrile derived from L-phenylalanine in tea (*Camellia sinensis*) and its formation in response to postharvest stresses. *Journal of Agricultural and Food Chemistry* **68**: 1397-1404
- Luck K, Jia Q, Huber M, Handrick V, Wong GK, Nelson DR, Chen F, Gershenzon J, Köllner TG** (2017) CYP79 P450 monooxygenases in gymnosperms: CYP79A118 is associated with the formation of taxiphyllin in *Taxus baccata*. *Plant Molecular Biology* **95**: 169-180
- Luck K, Jirschitzka J, Irmisch S, Huber M, Gershenzon J, Köllner TG** (2016) CYP79D enzymes contribute to jasmonic acid-induced formation of aldoximes and other nitrogenous volatiles in two *Erythroxylum* species. *BMC Plant Biology* **16**: 215
- Luft S, Curio E, Tacud B** (2003) The use of olfaction in the foraging behaviour of the golden-mantled flying fox, *Pteropus pumilus*, and the greater musky fruit bat, *Ptenochirus jagori* (Megachiroptera: Pteropodidae). *Naturwissenschaften* **90**: 84-87
- Machado RA, Robert CA, Arce CC, Ferrieri AP, Xu S, Jimenez-Aleman GH, Baldwin IT, Erb M** (2016) Auxin is rapidly induced by herbivore attack and regulates a subset of systemic, jasmonate-dependent defenses. *Plant Physiology* **172**: 521-532
- Madden D, Young TP** (1992) Symbiotic ants as an alternative defense against giraffe herbivory in spinescent *Acacia drepanolobium*. *Oecologia* **91**: 235-238
- Maffei M, Bossi S** (2006) Electrophysiology and plant responses to biotic stress. *In AG*

- Volkov, ed, Plant Electrophysiology: Theory and Methods. Springer Berlin Heidelberg, Berlin, Heidelberg, pp 461-481
- Maffei ME, Mithöfer A, Boland W** (2007) Before gene expression: early events in plant–insect interaction. *Trends in Plant Science* **12**: 310-316
- Maffei ME, Mithöfer A, Boland W** (2007) Insects feeding on plants: rapid signals and responses preceding the induction of phytochemical release. *Phytochemistry* **68**: 2946-2959
- Malabarba J, Meents AK, Reichelt M, Scholz SS, Peiter E, Rachowka J, Konopka-Postupolska D, Wilkins KA, Davies JM, Oelmüller R, Mithöfer A** (2021) ANNEXIN1 mediates calcium-dependent systemic defense in Arabidopsis plants upon herbivory and wounding. *New Phytologist* **231**: 243-254
- Mawson R, Heaney RK, Zdunczyk Z, Kozłowska H** (1994) Rapeseed meal-glucosinolates and their antinutritional effects. Part 3. Animal growth and performance. *Nahrung* **38**: 167-177
- Mayer V, Schaber D, Hadacek F** (2008) Volatiles of myrmecophytic *Piper* plants signal stem tissue damage to inhabiting *Pheidole* ant-partners. *Journal of Ecology* **96**: 962-970
- Mayer VE, Frederickson ME, McKey D, Blatrix R** (2014) Current issues in the evolutionary ecology of ant-plant symbioses. *New Phytologist* **202**: 749-764
- McKey D** (1984) Interaction of the ant-plant *Leonardoxa africana* (Caesalpiniaceae) with its obligate inhabitants in a rainforest in Cameroon. *Biotropica* **16**: 81-99
- McKey D** (1988) Promising new directions in the study of ant-plant mutualism. *In* W Greuter, B Zimmer, eds, Proceedings of the XIV International Botanical Congress. Koeltz, Königstein/Taunus, Königstein/Taunus, pp 335-355
- McKey D, Davidson DW** (1993) Ant-plant symbioses in Africa and the Neotropics - history, biogeography and diversity. *In* P Goldblatt, ed, Biological relationships between Africa and South America. Yale University Press, Yale, CT, USA, pp 568-606
- Meents AK, Chen SP, Reichelt M, Lu HH, Bartram S, Yeh KW, Mithöfer A** (2019) Volatile DMNT systemically induces jasmonate-independent direct anti-herbivore defense in leaves of sweet potato (*Ipomoea batatas*) plants. *Scientific Reports* **9**: 13
- Meents AK, Furch ACU, Almeida-Trapp M, Ozyurek S, Scholz SS, Kirbis A, Lenser T, Theissen G, Grabe V, Hansson B, Mithöfer A, Oelmüller R** (2019) Beneficial and pathogenic Arabidopsis root-interacting fungi differently affect auxin levels and responsive genes during early infection. *Frontiers in Microbiology* **10**: 380
- Meents AK, Mithöfer A** (2020) Plant-plant communication: is there a role for volatile damage-associated molecular patterns? *Frontiers in Plant Science* **11**: 583275
- Michelangeli FA** (2000) A cladistic analysis of the genus *Tococa* (Melastomataceae) based on morphological data. *Systemic Botany* **25**: 211-225
- Michelangeli FA** (2003) Ant protection against herbivory in three species of *Tococa* (Melastomataceae) occupying different environments. *Biotropica* **35**: 181-188
- Michelangeli FA** (2005) *Tococa* (Melastomataceae). *Flora Neotropica* **98**: 1-114
- Michelangeli FA** (2010) Neotropical Myrmecophilous Melastomataceae An annotated list and key. *Proceedings of the California Academy of Sciences* **61**: 409–449
- Michelangeli FA, Rodriguez E** (2005) Absence of cyanogenic glycosides in the tribe Miconieae (Melastomataceae). *Biochemical Systematics and Ecology* **33**: 335-339
- Mierziak J, Kostyn K, Kulma A** (2014) Flavonoids as important molecules of plant interactions with the environment. *Molecules (Basel, Switzerland)* **19**: 16240-16265
- Mithen R, Bennett R, Marquez J** (2010) Glucosinolate biochemical diversity and

- innovation in the Brassicales. *Phytochemistry* **71**: 2074-2086
- Mithöfer A, Boland W** (2008) Recognition of herbivory-associated molecular patterns. *Plant Physiology* **146**: 825-831
- Mithöfer A, Boland W** (2012) Plant defense against herbivores: chemical aspects. *The Annual Review of Plant Biology* **63**: 431-450
- Moctezuma C, Hammerbacher A, Heil M, Gershenzon J, Mendez-Alonzo R, Oyama K** (2014) Specific polyphenols and tannins are associated with defense against insect herbivores in the tropical oak *Quercus oleoides*. *Journal of Chemical Ecology* **40**: 458-467
- Moilanen J, Salminen J-P** (2007) Ecologically neglected tannins and their biologically relevant activity: chemical structures of plant ellagitannins reveal their in vitro oxidative activity at high pH. *Chemoecology* **18**: 73-83
- Moilanen J, Sinkkonen J, Salminen J-P** (2013) Characterization of bioactive plant ellagitannins by chromatographic, spectroscopic and mass spectrometric methods. *Chemoecology* **23**: 165-179
- Møller BL** (2010) Dynamic Metabolons. *Science* **330**: 1328-1329
- Moraes SC, Vasconcelos HL** (2009) Long-term persistence of a Neotropical ant-plant population in the absence of obligate plant-ants. *Ecology* **90**: 2375-2383
- Morawetz W, Henzl M, Wallnöfer B** (1992) Tree killing by herbicide producing ants for the establishment of pure *Tococa occidentalis* populations in the Peruvian Amazon. *Biodiversity and Conservation* **1**: 19-33
- Müller AT, Reichelt M, Cosio EG, Salinas N, Nina A, Wang D, Moossen H, Geilmann H, Gershenzon J, Köllner TG, Mithöfer A** (2022) Combined –omics framework reveals how ant symbionts benefit the Neotropical ant-plant *Tococa quadrialata* at different levels. *iScience* **25**: 105261
- Naczki M, Shahidi F** (2004) Extraction and analysis of phenolics in food. *Journal of Chromatography A* **1054**: 95-111
- Newton GW, Schmidt ES, Lewis JP, Conn E, Lawrence R** (1981) Amygdalin toxicity studies in rats predict chronic cyanide poisoning in humans. *Western Journal of Medicine* **134**: 97-103
- Nguyen Q-V, Doan M-D, Bui Thi B-H, Nguyen M-T, Tran Minh D, Nguyen A-D, Le T-M, Nguyen T-H, Nguyen T-D, Tran V-C, Hoang V-C** (2022) The effect of drying methods on chlorophyll, polyphenol, flavonoids, phenolic compounds contents, color and sensory properties, and in vitro antioxidant and anti-diabetic activities of dried wild guava leaves. *Drying Technology*: 1-12
- Nißler R, Müller AT, Dohrman F, Kurth L, Li H, Cosio EG, Flavel BS, Giraldo JP, Mithöfer A, Kruss S** (2022) Detection and imaging of the plant pathogen response by near-infrared fluorescent polyphenol sensors. *Angewandte Chemie International Edition* **61**: e202108373
- Noge K, Abe M, Tamogami S** (2011) Phenylacetonitrile from the giant knotweed, *Fallopia sachalinensis*, infested by the Japanese beetle, *Popillia japonica*, is induced by exogenous methyl jasmonate. *Molecules* **16**: 6481-6488
- Noge K, Tamogami S** (2018) Isovaleronitrile co-induced with its precursor, L-leucine, by herbivory in the common evening primrose stimulates foraging behavior of the predatory blue shield bug. *Bioscience, Biotechnology, and Biochemistry* **82**: 395-406
- North RD, Howse PE, Jackson CW** (2000) Agonistic behavior of the leaf-cutting ant *Atta sexdens rubropilosa* elicited by caryophyllene. *Journal of Insect Behavior* **13**: 1-13
- Oger JM, Richomme P, Guinaudeau H, Bouchara JP, Fournet A** (1994) *Aniba canelilla* (H.B.K.) Mez essential oil: analysis of chemical constituents, fungistatic properties. *Journal of Essential Oil Research* **6**: 493-497
- Okuda T, Yoshida T, Hatano T** (1995) Hydrolyzable tannins and related polyphenols.

- In* RGS Berlinck, T Hatano, T Okuda, T Yoshida, W Herz, GW Kirby, RE Moore, W Steglich, C Tamm, eds, Fortschritte der Chemie organischer Naturstoffe / Progress in the Chemistry of Organic Natural Products. Springer Vienna, Vienna, pp 1-117
- Ossipov V, Salminen J-P, Ossipova S, Haukioja E, Pihlaja K** (2003) Gallic acid and hydrolysable tannins are formed in birch leaves from an intermediate compound of the shikimate pathway. *Biochemical Systematics and Ecology* **31**: 3-16
- Palmer TM, Brody AK** (2013) Enough is enough: the effects of symbiotic ant abundance on herbivory, growth, and reproduction in an African acacia. *Ecology* **94**: 683-691
- Palmer TM, Doak DF, Stanton ML, Bronstein JL, Kiers ET, Young TP, Goheen JR, Pringle RM** (2010) Synergy of multiple partners, including freeloaders, increases host fitness in a multispecies mutualism. *Proceedings of the National Academy of Sciences USA* **107**: 17234-17239
- Pang Z, Chong J, Zhou G, de Lima Morais DA, Chang L, Barrette M, Gauthier C, Jacques P-É, Li S, Xia J** (2021) MetaboAnalyst 5.0: narrowing the gap between raw spectra and functional insights. *Nucleic Acids Research* **49**: W388-W396
- Parthiban P, Kabilan S, Ramkumar V, Jeong YT** (2010) Stereocontrolled facile synthesis and antimicrobial activity of oximes and oxime ethers of diversely substituted bispindines. *Bioorganic & Medicinal Chemistry Letters* **20**: 6452-6458
- Pérez-Alonso MM, Pollmann S** (2018) How auxin may contribute to the regulation of plant defense responses against herbivory. *Austin Journal of Plant Biology*
- Perez VC, Dai R, Bai B, Tomiczek B, Askey BC, Zhang Y, Rubin GM, Ding Y, Grenning A, Block AK, Kim J** (2021) Aldoximes are precursors of auxins in *Arabidopsis* and maize. *New Phytologist* **231**: 1449-1461
- Perez VC, Zhao H, Lin M, Kim J** (2023) Occurrence, function, and biosynthesis of the natural auxin phenylacetic acid (PAA) in plants. *Plants (Basel)* **12**: 266
- Piasecka A, Jedrzejczak-Rey N, Bednarek P** (2015) Secondary metabolites in plant innate immunity: conserved function of divergent chemicals. *New Phytologist* **206**: 948-964
- Pichersky E, Lewinsohn E** (2011) Convergent evolution in plant specialized metabolism. *Annual Review of Plant Biology* **62**: 549-566
- Pinkalski C, Jensen K-MV, Damgaard C, Offenberg J, McCulley R** (2018) Foliar uptake of nitrogen from ant faecal droplets: An overlooked service to ant-plants. *Journal of Ecology* **106**: 289-295
- Plaszko T, Szucs Z, Vasas G, Gonda S** (2021) Effects of glucosinolate-derived isothiocyanates on fungi: A comprehensive review on direct effects, mechanisms, structure-activity relationship data and possible agricultural applications. *Journal of Fungi* **7**: 539
- Qu W, Robert CAM, Erb M, Hibbard BE, Paven M, Gleede T, Riehl B, Kersting L, Cankaya AS, Kunert AT, Xu Y, Schueller MJ, Shea C, Alexoff D, Lee SJ, Fowler JS, Ferrieri RA** (2016) Dynamic precision phenotyping reveals mechanism of crop tolerance to root herbivory. *Plant Physiology* **172**: 776-788
- Quideau S, Deffieux D, Douat-Casassus C, Pouységu L** (2011) Plant polyphenols: chemical properties, biological activities, and synthesis. *Angewandte Chemie International Edition* **50**: 586-621
- Quideau S, Feldman KS** (1996) Ellagitannin chemistry. *Chemical Reviews* **96**: 475-504
- Raguso RA** (2008) Wake up and smell the roses: the ecology and evolution of floral scent. *Annual Review of Ecology, Evolution, and Systematics* **39**: 549-569
- Reddy MK, Gupta SK, Jacob MR, Khan SI, Ferreira D** (2007) Antioxidant, antimalarial and antimicrobial activities of tannin-rich fractions, ellagitannins and phenolic acids from *Punica granatum* L. *Planta Medica* **53**: 461-467
- Regueiro J, Sánchez-González C, Vallverdú-Queralt A, Simal-Gándara J, Lamuela-**

- Raventós R, Izquierdo-Pulido M** (2014) Comprehensive identification of walnut polyphenols by liquid chromatography coupled to linear ion trap-Orbitrap mass spectrometry. *Food Chemistry* **152**: 340-348
- Rehr SS, Feeny PP, Janzen DH** (1973) Chemical defence in central american non-ant-acacias. *Journal of Animal Ecology* **42**: 405-416
- Renner SS, Ricklefs RE** (1998) Herbicidal activity of domatia-inhabiting ants in patches of *Tococa guianensis* and *Clidemia heterophylla*. *Biotropica* **30**: 324-327
- Rhoades DF** (1979) Evolution of plant chemical defense against herbivores. In GA Rosenthal, DH Janzen, eds, *Herbivores: Their Interaction with Secondary Plant Metabolites*. Academic Press, pp 4–53
- Richards LA, Dyer LA, Smilanich AM, Dodson CD** (2010) Synergistic effects of amides from two *Piper* species on generalist and specialist herbivores. *Journal of Chemical Ecology* **36**: 1105-1113
- Rivera-Vargas LI, Schmitthenner AF, Graham TL** (1993) Soybean flavonoid effects on and metabolism by *Phytophthora sojae*. *Phytochemistry* **32**: 851-857
- Rizwan HM, Zhimin L, Harsonowati W, Waheed A, Qiang Y, Yousef AF, Munir N, Wei X, Scholz SS, Reichelt M, Oelmüller R, Chen F** (2021) Identification of fungal pathogens to control postharvest passion fruit (*Passiflora edulis*) decays and multi-omics comparative pathway analysis reveals purple is more resistant to pathogens than a yellow cultivar. *Journal of Fungi* **7**: 879
- Rodríguez-Concepción M, Boronat A** (2002) Elucidation of the methylerythritol phosphate pathway for isoprenoid biosynthesis in bacteria and plastids. a metabolic milestone achieved through genomics. *Plant Physiology* **130**: 1079-1089
- Rodríguez-Saona C, Crafts-Brandner SJ, Pare PW, Henneberry TJ** (2001) Exogenous methyl jasmonate induces volatile emissions in cotton plants. *Journal of Chemical Ecology* **27**: 679-695
- Rodríguez A, Alquézar B, Peña L** (2013) Fruit aromas in mature fleshy fruits as signals of readiness for predation and seed dispersal. *New Phytologist* **197**: 36-48
- Romero GQ, Izzo TJ** (2004) Leaf damage induces ant recruitment in the Amazonian ant-plant *Hirtella myrmecophila*. *Journal of Tropical Ecology* **20**: 675-682
- Roslin T, Salminen JP** (2008) Specialization pays off: contrasting effects of two types of tannins on oak specialist and generalist moth species. *Oikos* **117**: 1560-1568
- Rosumek FB, Silveira FA, de SNF, de UBNP, Diniz L, Oki Y, Pezzini F, Fernandes GW, Cornelissen T** (2009) Ants on plants: a meta-analysis of the role of ants as plant biotic defenses. *Oecologia* **160**: 537-549
- Rudgers JA, Strauss SY** (2004) A selection mosaic in the facultative mutualism between ants and wild cotton. *Proceedings of the Royal Society of London. Series B: Biological Sciences* **271**: 2481-2488
- Ruiz A, Hermosín-Gutiérrez I, Vergara C, von Baer D, Zapata M, Hitschfeld A, Obando L, Mardones C** (2013) Anthocyanin profiles in south Patagonian wild berries by HPLC-DAD-ESI-MS/MS. *Food Research International* **51**: 706-713
- Ryan CA** (1990) Protease inhibitors in plants: genes for improving defenses against insects and pathogens. *Annual Review of Phytopathology* **28**: 425-449
- Sachdev-Gupta K, Radke C, Renwick JAA, Dimock MB** (1993) Cardenolides from *Erysimum cheiranthoides*: Feeding deterrents to *Pieris rapae* larvae. *Journal of Chemical Ecology* **19**: 1355-1369
- Sagers CL, Ginger SM, Evans RD** (2000) Carbon and nitrogen isotopes trace nutrient exchange in an ant-plant mutualism. *Oecologia* **123**: 582–586
- Saifullah M, McCullum R, McCluskey A, Vuong Q** (2019) Effects of different drying methods on extractable phenolic compounds and antioxidant properties from lemon myrtle dried leaves. *Heliyon* **5**: e03044
- Salminen J-P, Karonen M** (2011) Chemical ecology of tannins and other phenolics: we

- need a change in approach. *Functional Ecology* **25**: 325-338
- Salminen JP** (2014) The chemistry and chemical ecology of ellagitannins in plant–insect interactions: from underestimated molecules to bioactive plant constituents. *In* A Romani, V Lattanzio, S Quideau, eds, *Recent Advances in Polyphenol Research*, Vol 4. Wiley-Blackwell, Chichester, UK, pp 83-113
- Salminen JP, Karonen M, Sinkkonen J** (2011) Chemical ecology of tannins: recent developments in tannin chemistry reveal new structures and structure-activity patterns. *Chemistry* **17**: 2806-2816
- Salminen JP, Ossipov V, Loponen J, Haukioja E, Pihlaja K** (1999) Characterisation of hydrolysable tannins from leaves of *Betula pubescens* by high-performance liquid chromatography–mass spectrometry. *Journal of Chromatography A* **864**: 283-291
- Sauer M, Robert S, Kleine-Vehn J** (2013) Auxin: simply complicated. *Journal of Experimental Botany* **64**: 2565-2577
- Schatz B, Djieto-Lordon C, Dormont L, Bessiere JM, McKey D, Blatrix R** (2009) A simple non-specific chemical signal mediates defence behaviour in a specialised ant-plant mutualism. *Current Biology* **19**: R361-362
- Schiestl FP, Peakall R, Mant JG, Ibarra F, Schulz C, Franke S, Francke W** (2003) The chemistry of sexual deception in an orchid-wasp pollination system. *Science* **302**: 437-438
- Schnee C, Köllner TG, Held M, Turlings TCJ, Gershenzon J, Degenhardt J** (2006) The products of a single maize sesquiterpene synthase form a volatile defense signal that attracts natural enemies of maize herbivores. *Proceedings of the National Academy of Sciences* **103**: 1129-1134
- Schupp EW** (1986) Azteca protection of *Cecropia*: ant occupation benefits juvenile trees. *Oecologia* **70**: 379-385
- Seigler DS, Ebinger JE** (1987) Cyanogenic glycosides in ant-acacias of Mexico and Central America. *the Southwestern Naturalist* **32**: 499-503
- Serna DM, Martinez JH** (2015) Phenolics and polyphenolics from Melastomataceae species. *Molecules* **20**: 17818-17847
- Sharma K, Kumar V, Kaur J, Tanwar B, Goyal A, Sharma R, Gat Y, Kumar A** (2021) Health effects, sources, utilization and safety of tannins: a critical review. *Toxin Reviews* **40**: 432-444
- Sibbesen O, Koch B, Halkier BA, Møller BL** (1995) Cytochrome P-450TYR is a multifunctional heme-thiolate enzyme catalyzing the conversion of L-tyrosine to *p*-hydroxyphenylacetaldehyde oxime in the biosynthesis of the cyanogenic glucoside dhurrin in *Sorghum bicolor* (L.) Moench. *Journal of Biological Chemistry* **270**: 3506-3511
- Singleton VL, Orthofer R, Lamuela-Raventós RM** (1999) Analysis of total phenols and other oxidation substrates and antioxidants by means of Folin-Ciocalteu reagent. *In* *Methods in Enzymology*, Vol 299. Academic Press, pp 152-178
- Skočibušić M, Odžak R, Ramić A, Smolić T, Hrenar T, Primožič I** (2018) Novel imidazole aldoximes with broad-spectrum antimicrobial potency against multidrug resistant gram-negative bacteria. *Molecules* **23**: 1212
- Smolinska U, Morra MJ, Knudsen GR, James RL** (2003) Isothiocyanates produced by Brassicaceae species as inhibitors of *Fusarium oxysporum*. *Plant Disease* **87**: 407-412
- Solano R, Dejean A** (2004) Ant-fed plants: comparison between three geophytic myrmecophytes. *Biological Journal of the Linnean Society* **83**: 433-439
- Sorensen M, Neilson EHJ, Møller BL** (2018) Oximes: unrecognized chameleons in general and specialized plant metabolism. *Molecular Plant* **11**: 95-117
- Stanton ML, Palmer TM** (2011) The high cost of mutualism: effects of four species of East African ant symbionts on their myrmecophyte host tree. *Ecology* **92**: 1073–

1082

- Staswick PE, Tiryaki I** (2004) The oxylipin signal jasmonic acid is activated by an enzyme that conjugates it to isoleucine in Arabidopsis. *The Plant Cell* **16**: 2117-2127
- Stipanovic RD, Lopez JD, Dowd MK, Puckhaber LS, Duke SE** (2006) Effect of racemic and (+)- and (-)-gossypol on the survival and development of *Helicoverpa zea* larvae. *Journal of Chemical Ecology* **32**: 959-968
- Svoma E, Morawetz W** (1992) Drüsenhaare, Emergenzen und Blattdomatien bei der Ameisenpflanze *Tococa occidentalis* (Melastomataceae). *Botanische Jahrbücher Systematik* **114**: 185-200
- Takken W, Kline DL** (1989) Carbon dioxide and 1-octen-3-ol as mosquito attractants. *Journal of the American Mosquito Control Association* **5**: 311-316
- Takos AM, Knudsen C, Lai D, Kannangara R, Mikkelsen L, Motawia MS, Olsen CE, Sato S, Tabata S, Jørgensen K, Møller BL, Rook F** (2011) Genomic clustering of cyanogenic glucoside biosynthetic genes aids their identification in *Lotus japonicus* and suggests the repeated evolution of this chemical defence pathway. *The Plant Journal* **68**: 273-286
- Tapper BA, Conn EE, Butler GW** (1967) Conversion of α -keto-isovaleric acid oxime and isobutyraldoxime to linamarin in flax seedlings. *Archives of Biochemistry and Biophysics* **119**: 593-595
- Thaler JS, Stout MJ, Karban R, Duffey SS** (1996) Exogenous jasmonates simulate insect wounding in tomato plants (*Lycopersicon esculentum*) in the laboratory and field. *Journal of Chemical Ecology* **22**: 15
- Thodberg S, Del Cueto J, Mazzeo R, Pavan S, Lotti C, Dicenta F, Jakobsen Neilson EH, Møller BL, Sánchez-Pérez R** (2018) Elucidation of the amygdalin pathway reveals the metabolic basis of bitter and sweet almonds (*Prunus dulcis*). *Plant Physiology* **178**: 1096-1111
- Thodberg S, Sorensen M, Bellucci M, Crocoll C, Bendtsen AK, Nelson DR, Motawia MS, Møller BL, Neilson EHJ** (2020) A flavin-dependent monooxygenase catalyzes the initial step in cyanogenic glycoside synthesis in ferns. *Communications Biology* **3**: 507
- Tholl D, Boland W, Hansel A, Loreto F, Rose US, Schnitzler JP** (2006) Practical approaches to plant volatile analysis. *The Plant Journal* **45**: 540-560
- Turlings TCJ, Erb M** (2018) Tritrophic interactions mediated by herbivore-induced plant volatiles: mechanisms, ecological relevance, and application potential. *Annual Review of Entomology* **63**: 433-452
- Turner IM** (1995) Foliar defences and habitat adversity of three woody plant communities in Singapore. *Functional Ecology* **9**: 279-284
- ul Hassan MN, Zainal Z, Ismail I** (2015) Green leaf volatiles: biosynthesis, biological functions and their applications in biotechnology. *Plant Biotechnology Journal* **13**: 727-739
- Ullah C, Unsicker SB, Fellenberg C, Constabel PC, Schmidt A, Gershenzon J, Hammerbacher A** (2017) Flavan-3-ols are an effective chemical defense against rust infection *Plant Physiology* **175**: 1560-1578
- Underhill EW** (1967) Biosynthesis of mustard oil glucosides. *European Journal of Biochemistry* **2**: 61-63
- Urbancsok J, Bones AM, Kissen R** (2018) Benzyl cyanide leads to auxin-like effects through the action of nitrilases in *Arabidopsis thaliana*. *Frontiers in Plant Science* **9**
- van der Fits L, Memelink J** (2000) ORCA3, a jasmonate-responsive transcriptional regulator of plant primary and secondary metabolism. *Science* **289**: 295-297
- Vancanneyt G, Sanz C, Farmaki T, Paneque M, Ortego F, Castañera P, Sánchez-Serrano JJ** (2001) Hydroperoxide lyase depletion in transgenic potato plants

- leads to an increase in aphid performance. Proceedings of the National Academy of Sciences **98**: 8139-8144
- Vasconcelos HL** (1991) Mutualism between *Maieta guianensis* Aubl., a myrmecophytic melastome, and one of its ant inhabitants: ant protection against insect herbivores. *Oecologia* **87**: 295-298
- Veitch NC, Grayer RJ** (2008) Flavonoids and their glycosides, including anthocyanins. *Natural product reports* **25**: 555-611
- Veitch NC, Grayer RJ** (2011) Flavonoids and their glycosides, including anthocyanins. *Natural Product Reports* **28**: 1626-1695
- Verma V, Ravindran P, Kumar PP** (2016) Plant hormone-mediated regulation of stress responses. *BMC Plant Biology* **16**: 86
- Vetter J** (2000) Plant cyanogenic glycosides. *Toxicon* **38**: 11-36
- Vogt T** (2010) Phenylpropanoid biosynthesis. *Molecular Plant* **3**: 2-20
- Wäckers FL, Wunderlin R** (1999) Induction of cotton extrafloral nectar production in response to herbivory does not require a herbivore-specific elicitor. *Entomologia Experimentalis et Applicata* **91**: 149-154
- Walling LL** (2000) The myriad plant responses to herbivores. *Journal of Plant Growth Regulation* **19**: 195-216
- War AR, Paulraj MG, Ahmad T, Buhroo AA, Hussain B, Ignacimuthu S, Sharma HC** (2012) Mechanisms of plant defense against insect herbivores. *Plant Signaling & Behavior* **7**: 1306-1320
- Ward D, Young TP** (2002) Effects of large mammalian herbivores and ant symbionts on condensed tannins of *Acacia drepanolobium* in Kenya. *Journal of Chemical Ecology* **28**: 921-937
- Wasternack C** (2007) Jasmonates: an update on biosynthesis, signal transduction and action in plant stress response, growth and development. *Annals of Botany* **100**: 681-697
- Wasternack C, Hause B** (2013) Jasmonates: biosynthesis, perception, signal transduction and action in plant stress response, growth and development. An update to the 2007 review in *Annals of Botany*. *Annals of Botany* **111**: 1021-1058
- Widhalm J, Dudareva N** (2015) A familiar ring to It: biosynthesis of plant benzoic acids. *Molecular Plant* **8**: 83-97
- Williams CA, Grayer RJ** (2004) Anthocyanins and other flavonoids. *Natural product reports* **21**: 539-573
- Wittstock U, Halkier BA** (2000) Cytochrome P450 CYP79A2 from *Arabidopsis thaliana* L. catalyzes the conversion of L-phenylalanine to phenylacetaldoxime in the biosynthesis of benzylglucosinolate. *Journal of Biological Chemistry* **275**: 14659-14666
- Wong DCJ, Pichersky E, Peakall R** (2017) The biosynthesis of unusual floral volatiles and blends involved in orchid pollination by deception: current progress and future prospects. *Frontiers in Plant Science* **8**: 1955
- Wong MH, Giraldo JP, Kwak S-Y, Koman VB, Sinclair R, Lew TTS, Bisker G, Liu P, Strano MS** (2017) Nitroaromatic detection and infrared communication from wild-type plants using plant nanobionics. *Nature Materials* **16**: 264-272
- Wu H, Nißler R, Morris V, Herrmann N, Hu P, Jeon S-J, Kruss S, Giraldo JP** (2020) Monitoring plant health with near-infrared fluorescent H₂O₂ nanosensors. *Nano Letters* **20**: 2432-2442
- Wu J, Hettenhausen C, Meldau S, Baldwin IT** (2007) Herbivory rapidly activates MAPK signaling in attacked and unattacked leaf regions but not between leaves of *Nicotiana attenuata*. *The Plant Cell* **19**: 1096-1122
- Wurzenberger M, Grosch W** (1984) The formation of 1-octen-3-ol from the 10-hydroperoxide isomer of linoleic acid by a hydroperoxide lyase in mushrooms (*Psalliota bispora*). *Biochimica et Biophysica Acta (BBA) - Lipids and Lipid*

- Metabolism **794**: 25-30
- Wuyts N, Swennen R, De Waele D** (2006) Effects of plant phenylpropanoid pathway products and selected terpenoids and alkaloids on the behaviour of the plant-parasitic nematodes *Radopholus similis*, *Pratylenchus penetrans* and *Meloidogyne incognita*. *Nematology* **8**: 89-101
- Xiao Y, Gao SH, Di P, Chen JF, Chen WS, Zhang L** (2009) Methyl jasmonate dramatically enhances the accumulation of phenolic acids in *Salvia miltiorrhiza* hairy root cultures. *Physiologia Plantarum* **137**: 1-9
- Yamagishi K, Mitsumori C, Takahashi K, Fujino K, Koda Y, Kikuta Y** (1993) Jasmonic acid-inducible gene-expression of a Kunitz-tyoe proteinase-inhibitor in potato-tuber disks. *Plant Molecular Biology* **21**: 539-541
- Yamaguchi T, Matsui Y, Kitaoka N, Kuwahara Y, Asano Y, Matsuura H, Sunohara Y, Matsumoto H** (2021) A promiscuous fatty acid ω -hydroxylase CYP94A90 is likely to be involved in biosynthesis of a floral nitro compound in loquat (*Eriobotrya japonica*). *New Phytologist* **231**: 1157-1170
- Yamaguchi T, Noge K, Asano Y** (2016) Cytochrome P450 CYP71AT96 catalyses the final step of herbivore-induced phenylacetone nitrile biosynthesis in the giant knotweed, *Fallopia sachalinensis*. *Plant Molecular Biology* **91**: 229-239
- Yang L, Wen KS, Ruan X, Zhao YX, Wei F, Wang Q** (2018) Response of plant secondary metabolites to environmental factors. *Molecules* **23**: 762
- Young TP, Stubblefield CH, Isbell LA** (1996) Ants on swollen-thorn acacias: species coexistence in a simple system. *Oecologia* **109**: 98-107
- Zhang D, Song YH, Dai R, Lee TG, Kim J** (2020) Aldoxime metabolism is linked to phenylpropanoid production in *Camelina sativa*. *Frontiers in Plant Science* **11**: 17
- Zhao Y, Hull AK, Gupta NR, Goss KA, Alonso J, Ecker JR, Normanly J, Chory J, Celenza JL** (2002) Trp-dependent auxin biosynthesis in Arabidopsis: involvement of cytochrome P450s CYP79B2 and CYP79B3. *Genes & Development* **16**: 3100-3112
- Zhou X, Jacobs TB, Xue LJ, Harding SA, Tsai CJ** (2015) Exploiting SNPs for biallelic CRISPR mutations in the outcrossing woody perennial *Populus* reveals 4-coumarate:CoA ligase specificity and redundancy. *New Phytologist* **208**: 298-301
- Zhu J, He Y, Yan X, Liu L, Guo R, Xia X, Cheng D, Mi X, Samarina L, Liu S, Xia E, Wei C** (2019) Duplication and transcriptional divergence of three Kunitz protease inhibitor genes that modulate insect and pathogen defenses in tea plant (*Camellia sinensis*). *Horticulture Research* **6**: 126

7 Acknowledgements

Finally, I want to thank all the people who enabled this project, supported me up to this point and without whom this thesis and the survival of the PhD would not have been possible. First of all, I want to thank the masterminds behind this thesis, my official and unofficial supervisors, the trinity, PD Axel Mithöfer, Professor Jonathan Gershenzon and Dr. Tobias Köllner.

Thank you Axel, for coming up with this great project idea about ant-plants and *Tococas* with which I fell in love right from the start, for giving me the opportunity to become a proud member of the MIT group, for giving me all the freedom to explore and develop my own ideas, experiments and thoughts while always being only two steps or one Whatsapp message away whenever I needed advice, support or just to vent about logistics at the other side of the world ;-). Thank you for your constant support, patience, understanding, motivation, and creating this great working environment in our group, which makes this work so much more fun! I will miss the lunch breaks with everyone, the group Christmas parties, the barbecues – though there haven't been enough of them lately! – and so on. Thank you for everything, including reviewing this thesis ☺

I also want to express my highest gratitude to my second official supervisor, Professor Jonathan Gershenzon, for giving this project idea a chance and agreeing to fund it, I am forever grateful for this opportunity. You were there to support my scientific career since my bachelors, and I am so grateful for everything that I learned as part of your lab. Thank you for giving me the freedom to develop this project, and work on it on the other side of the world, for being there and not giving up hope in the harsh beginning, for taking the time for all the scientific (and logistic) discussions, for revising all manuscripts and proposals, for always being supportive, bringing in great suggestions and advice, giving me the opportunity to present and discuss results in the GER lab meeting, to be member of the journal club, to walk around and use all of your machines ☺ and the list goes on and on.

Furthermore, I want to wholeheartedly thank Dr. Tobias Köllner, my mentor ever since my first steps into the world of academia (and Max Planck, to be specific). It has been my absolute pleasure to work with you for all these years and I couldn't have wished for a better supervisor and mentor. Thank you for everything you taught me throughout this journey, for raising me to become a “full-grown” PhD, thank you for your patience, your ongoing encouragement and support, for all the scientific discussions we had, for all the input, advice and help regarding the lab work as well as the experimental design and project ideas, for always having time for a coffee break, and generally, just always being there.

I also want to thank the persons and institutions that financed this crazy ride. Once more, many thanks to Professor Jonathan Gershenzon for funding my field trips, my first and last year as a PhD, and all the other fancy science that would not have been possible without your support. I also thank the DAAD for funding the more than one year research stays in Peru with a pandemic in the middle, and especially Frederik Stamm, who was my direct contact and helped me so that my ever-changing plans were still financed by the DAAD. I want to thank the IMPRS and Claudia Völkel who came up with some creative financing solutions and very importantly also the Friedrich Schiller University Jena and especially Professor Ralf Oelmüller, who did not only agree to be my third official supervisor and officially responsible for my financial well-being as a PhD student, but also to review this thesis. My sincere thanks for all of that!

I am also very grateful to my Peruvian hosts, to Professor Eric Cosio and Professor Norma Salinas, who gave me the opportunity to work in their labs and their field station

and basically were the backbone enabling the realization of this PhD project. You went with me through all the bad times of my PhD, but also some of the best, and I want to thank you for your support and patience with me. It was my pleasure to meet you, work with you and learn so much during this time in Peru.

Furthermore, I would like to express my gratitude to Professor Jörg-Peter Schnitzler for sacrificing his time to review and evaluate this thesis. Thank you so much for your effort.

Next, I want to say a big thanks to all of my co-authors, collaboration partners, my colleagues, and friends who helped me survive this time and made it so much more enjoyable, starting with the people who enabled my survival in Peru:

Many thanks to Rudi, Alex, Hammerly, Esteban, Hector, Richard, Eliana, Fabian, Cristian, Victor, Mariana, Erika and Mijail – for helping me with an enormous amount of paperwork, permits, field work, survival in Tambopata and Lima, for finding impossible solutions for any problem, for being with me in the lab or in the field on weekends and at night whenever needed, basically for rescuing my scientific career (jeje), for teaching me a lot about ecology, Spanish, how to prepare a Chilcano and play fantasma, and life in general. Si no fuera por ustedes, me habría rendido en algún momento. Fueron mis salvavidas y son la razón por la que volvería a hacerlo todo. Gracias por todo, el tiempo y la amistad con ustedes son lo mejor que me podía haber pasado.

I also want to thank Professor Alfredo Ibañez, Madina Mansurova and everyone else from ICOBA who welcomed me in their lab and allowed me to use their lab space and instruments. You were always so nice, helpful and friendly, I felt really welcomed.

Continuing with my list of life saving Peruvians, I want to thank AIDER, and especially Vanessa Hilaes and Norma Aguilar, who were so patient with me and my poor understanding of the formal regulations of research in an ANP, who helped me with all my permits, adendas, and logistics, shipping samples from Tambopata to Lima, buying material and food for me to survive and work in Tambopata, and even came to personally support me with maintenance of the nets – gracias por todo !

Next on my list are my PhD-life saving MPI people: a big thanks to the greenhouse team, and especially Birgit Arnold, who took care of the many plant species I happened to work on over the course of this PhD.

Another gigantic thanks goes to the workshop, Daniel Veit, who developed these great mobile volatile collection pumps that enabled my field work, along with a lot of other volatile systems I used throughout the years and all other gadgets, I sometimes didn't even know beforehand that I'd need them – but I sure did. Also, thank you for all the coffee breaks, endless sugar supply and open workshop doors whenever I needed a break and a friendly face 😊

And I'm also very thankful for having known and having had a lot of coffee breaks and fun with the other friendly workshop face that has left us far too soon.

From the GER department, I want to thank especially Dr. Michael Reichelt for teaching me everything I know about the MS machines in the department, for always taking the time to explain everything in detail and help me with doubts, settings, and scientific advice. It was a pleasure working with and learning from you. Talking about learning, I want to thank my master's supervisor Dr. Nathalie Lackus who taught me much back then and also was there to help me out during my PhD at the weirdest times whenever I encountered a problem or wasn't sure about something. Also, thanks to Dr. Felix Feistel, who happened to be in the same office and was equally helpful at all times. Big thanks also go to Katrin Luck, for teaching me CYP expression and Benta transformation, to Dr. Grit Kunert for statistical advice, to Bettina Raguschke for all my gene sequences and chemical requests, to Professor Sybille Unsicker and Dr. Christine

Walter for providing and explaining me PDMS tubes & the respective volatile collection, as well as diverse other lab stuff and advice. Thanks to all present and former members of the cake group, and of course to Mariaaaa for cake and/or crisis meetings and general support.

I also want to thank the NMR department, Dr. Yoko Nakamura and Dr. Christian Paetz for their help during my PhD, especially Christian, thank you for taking the time to help me separate all these crazy structures and teaching me so much about analytical chemistry. I will try my best that we still make something out of this. Also, thanks to Florian Schnurrer, who helped me around in the lab and taught me chemist things ☺

And last but not least of course I want to thank all current and former MIT-BOL PhDs and friends, especially Mama Moni, Frau Manja und Herr Vinciiii, Janinö, Robi (extra thanks for these fancy nanoparticles), Pierre-Jean (special thanks for all the discussions and ideas on ant-plant mutualism and help with statistics), Anne-Kathrin, Alberto, Liza and Shraddha, for great times in and outside the lab, especially with the badminton gang and tequila tuesdays <3. Thanks for being there for me, for having the best times with each other and moral support at worse times – and not to forget also great scientific input and discussions of course, as well as equally important discussions about life in general. Also all other (former) MIT members, Andrea, Asif, Laura, Marilia, Ding, Nataliaa, Mariia, Moniba, and Diana, thanks for the great working environment, and to my “6-weeks intern” Kilian for his trust, work and friendship ☺ and also thanks to all other people at the institute that made my PhD life more pleasant: Benjamin B and Benjamin H, Pauline, Riya, the lunch group - Andrea, Anja, Maritta, Mama Grit, Nataliaa and Kerstin - and my IT heroes, Martin and Walid.

Finally, I want to thank all my non-work friends, my flatmates, my family and especially Jonas for emotional support, motivation, love and always reminding me of the truly important things in life ☺ Thank you Jonas for being with me every step of the way, even when we were 1000 km apart, for endless support and patience when it comes to my PhD and my non-existing time management, for reading this thesis at the airport in your holidays and for so much more. ♥

8 Ehrenwörtliche Erklärung

Hiermit erkläre ich, dass mir die geltende Promotionsordnung (Fassung vom 23. September 2019) bekannt ist. Ich versichere, dass ich die vorliegende Dissertation selbstständig verfasst und keine Textabschnitte von Dritten oder eigenen Prüfungsarbeiten ohne Kennzeichnung verwendet habe. Es wurden ausschließlich die entsprechend angegebenen Hilfsmittel, Quellen und persönlichen Mitteilungen genutzt. Die Personen, welche mir bei der Planung, Ausführung und Auswertung von Experimenten, sowie beim Schreiben der Manuskripte geholfen haben, sind an den entsprechenden Stellen als Autor:innen vermerkt oder in der Danksagung zu finden. Ich bestätige, dass keine kommerzielle Promotionsvermittlung in Anspruch genommen wurde, und dass Dritte weder mittelbar noch unmittelbar geldwerte Leistung von mir erhalten haben, für Arbeiten, welche im Zusammenhang mit dem Inhalt der hier vorliegenden Dissertation stehen. Die vorliegende Dissertation wurde noch nicht als Prüfungsarbeit für eine staatliche oder andere wissenschaftliche Prüfung eingereicht, weder in dieser Form, noch als eine in wesentlichen Teilen ähnliche Arbeit.

Jena, den 15.06.2023

Andrea Müller

9 Curriculum Vitae

Personal information

Name : Andrea Teresa Müller
 Address : Teichgraben 3
 07743 Jena
 Date of birth : 02.10.1992
 Place of birth : Kulmbach

Education

since 02/2018 Friedrich Schiller University Jena /
 Max Planck Institute for Chemical Ecology

 Doctoral thesis: „Physiological and phytochemical aspects of
 ant plant mutualism“

10/2014 – 01/2017 Friedrich Schiller University Jena
 Degree: M.Sc. Chemical Biology (1,1)

 Master thesis: Distribution and biosynthesis of phenolic
 glycosides in Salicaceae (Max Planck Institute for Chemical
 Ecology)

10/2011 – 09/2014 Friedrich Schiller University Jena
 Degree: B.Sc. Biochemistry /Molecular Biology (1,2)

 Bachelor thesis: Characterization of diterpene synthases of the
 western balsam poplar (*Populus trichocarpa*)

09/2002 – 05/2011 Gymnasium Burgkunstadt
 Degree: Abitur (1,3)

Further practical experience

02/2017 – 12/2017 Work and Travel through South America and Europe

02/2016 – 03/2016 Internship at Helmholtz Center Munich,
 Topic: Molecular Pharming in Petunia and Tomato

11/2014 – 09/2015 Student assistant at the MPI-CE
 Topic: biosynthesis of volatile compounds in poplar

08/2014 – 09/2014 Ecological Internship at CEA Lisan Yacu (Ecuador)
 Topic: Reforestation and sustainable landuse

Awards and Scholarships

| | |
|-----------------|---|
| 04/2022 | Best poster award IMPRS Symposium, Dornburg, Germany |
| 10/2018-08/2021 | DAAD Scholarship for a one-year research stay in Peru Pontificia Universidad Católica del Perú, Lima, Perú |
| 09/2015-02/2016 | Erasmus Scholarship for a semester abroad in Scotland University of Strathclyde, Glasgow, Scotland |

Languages

| | |
|---------|----------------|
| German | native speaker |
| English | fluent (C1) |
| Spanish | fluent (B2) |
| French | basic (A2) |

Additional qualifications

| | |
|---------------|--|
| 2022 Courses: | Transcriptome and genome sequencing: theoretical and practical considerations and examples from the bench, Staatlich anerkannte, MPG-interne Online-Fortbildungsveranstaltung -Grundkurs- nach § 28 Abs. 2 Satz 1 Nr. 3 GenTSV |
| 2021 Courses: | Introduction to basic statistics and R, Scientific writing and publishing for natural scientists: the Basics, Plan B – Alternativen zur Wissenschaftskarriere |
| 2020 Courses: | Bioinformatic tools in mass spectrometry, Research data management, Overview Research funding, Grundlagen der Betriebswirtschaftslehre in Finanzen und Controlling, BWL kompakt, Project Management |
| 2019 Courses: | Scientific Image Processing and Analysis, Advanced Mass Spectrometry, Adobe Illustrator, Plant transformation workshop |
| 2018 Courses: | Good scientific practice, NMR spectroscopy |

Teaching and PR activities

| | |
|------------|---|
| 11/2022 | Presentation at Long Night of Science: "Ameisenpflanzen: Pflanzen mit Bodyguards" |
| 05-11/2022 | Supervised intern at Master's level |
| 05/2022 | Scientific image, article in magazine, post cards and podcast |

| | |
|---------|---|
| | for the campaign “Images of Science: 25 th Anniversary of Max Planck Institute for Chemical Ecology” |
| 05/2022 | Scientific image for the campaign “Micro Macro – Life Science in Jena”, by Friedrich Schiller University Jena, https://micro-macro.space/ |
| 03/2022 | Presentation: “Mutualismo entre plantas y hormigas: supervivencia mediante el trabajo en equipo” as part of the seminar “Experiencias de investigación científica en el Perú: Herramientas moleculares para descubrir la biodiversidad”, organized by SERNANP, Peru |
| 10/2021 | Article on Research in the Amazon, Wissenschaftsmagazin der Max-Planck-Gesellschaft |
| 07/2021 | Comment on Research in Covid times, in Max Mag |
| 12/2020 | "Ameisenpflanzen: Überleben durch Teamwork", Presentation on Youtube, as part of the series “Scientists explain” of the MPI-CE, https://www.youtube.com/watch?v=3KMSLVHVFH4 |
| 08/2020 | Social Media Portrait on Facebook, part of a MPI-CE campaign |
| 08/2020 | Supervised at IMPRS Recruitment 2020: Candidate parenting |
| 11/2019 | Long Night of science, Insects at the Max Planck Institute |
| 09/2019 | Supervised at IMPRS Recruitment 2019: Candidate parenting |
| 08/2018 | Supervised at IMPRS Recruitment 2018: Candidate parenting |

Publications

- 1 **Müller, A.T.**, Nakamura, Y., Reichelt, M., Luck, K., Lackus, N.D., Cosio, E.G., Gershenzon, J., Mithöfer, A., Köllner, T.G.: The biosynthesis, herbivore induction and defensive role of phenylacetaldoxime glucoside. *Submitted for publication to Plant Physiology*.
- 2 **Müller, A.T.**, Mithöfer, A. (*accepted*): „Ameisenpflanzen/Myrmekophyten – Pflanzen mit Bodyguards“. *Submitted for publication to Biologie in unserer Zeit*.
- 3 **Müller, A.T.**, Reichelt, M., Cosio, E.G., Salinas, N., Nina, A., Wang, D., Moossen, H., Geilmann, H., Gershenzon, J., Köllner, T.G., Mithöfer, A. (2022): Combined –omics framework reveals how ant symbionts benefit the Neotropical ant-plant *Tococa quadrialata* at different levels. *iScience* 25 (10), 105261.
- 4 Nißler, R., **Müller, A.T.**, Dohrman, F., Kurth, L., Li, H., Cosio, E.G., Flavel, B.S., Giraldo, J.P., Mithöfer, A., Kruss, S. (2022): Detection and imaging of the plant pathogen response by near infrared fluorescent polyphenol sensors. *Angewandte Chemie International Edition* 61(2), e202108373.
- 5 Lackus, N.D., **Müller, A.T.**, Kröber, T.D.U., Reichelt, M., Schmidt, A., Nakamura, Y., Paetz, C., Luck, K., Lindroth, R.L., Constabel, C.P., Unsicker, S., Gershenzon, J., Köllner, T.G. (2020). The occurrence of sulfated salicinoids in poplar and their formation by sulfotransferase 1. *Plant Physiology*, 183(1), 137-151.

-
- 6 Irmisch, S., **Müller, A.T.**, Schmidt, L., Günther, J., Gershenzon, J., Köllner, T.G. (2015). One amino acid makes the difference: the formation of *ent*-kaurene and 16a-hydroxy-*ent*-kaurane by diterpene synthases in poplar. *BMC Plant Biology*, 15 (262), 1-13.
-

Conference presentations

- 02-03/2023 "Working for bed and breakfast: Defense in the Neotropical ant-plant *Tococa quadrialata*", Poster presented at Gordon Research Seminar and Gordon Research Conference "Plant Herbivore Interactions in Action: Fundamentals to Applications", Ventura, California, USA
- 10/2022 "How *Tococa* plants benefit from *Azteca* ants", Talk given at the workshop "Métodos biofísicos y biométricos para la determinación de productividad primaria en ecosistemas", organized by the Pontificia Universidad Católica del Perú, Tambopata, Peru
- 04/2022 "Working for bed and breakfast: Defense in the Neotropical ant-plant *Tococa*", Poster presented at 21st IMPRS Symposium, Max Planck Institute for Chemical Ecology, IMPRS, Dornburg, DE
- 03/2022 "The formation of aldoximes and derivatives in a Neotropical ant-plant", Talk given at the PhD Workshop of the Natural Products Section of the German Society for Plant Science, Jena, DE
- 09/2021 "Formation of phenylacetaldoxime and derivatives in the Neotropical ant-plant *Tococa*" Talk given at the Institute Symposium, Max Planck Institute for Chemical Ecology, Jena, DE
- 06/2021 "Perception, signaling, and defense regulation in plant-insect interactions", Poster presented together with colleagues at: SAB Meeting 2021, Max Planck Institute for Chemical Ecology Jena, DE
- 04/2021 "Defense in the Neotropical myrmecophytic plant *Tococa*: the role of protective ants", Talk given at 20th IMPRS Symposium, Max Planck Institute for Chemical Ecology, IMPRS, Dornburg, DE

10 Supplemental information

10.1 Contribution to figures in manuscripts

10.1.1 Manuscript No. I

Short reference: Müller et al (2022), iScience

Contribution of the doctoral candidate

Contribution of the doctoral candidate to figures reflecting experimental data:

| | |
|---|--|
| <p>Figures # 2, S4, S6, Table S1-4</p> | <p><input checked="" type="checkbox"/> 100% (the data presented in this figure come entirely from experimental work carried out by the candidate)</p> <p><input type="checkbox"/> 0% (the data presented in this figure are based exclusively on the work of other co-authors)</p> <p><input type="checkbox"/> Approximate contribution of the doctoral candidate to the figure: _____</p> <p>Brief description of the contribution:</p> |
|---|--|

| | |
|--|--|
| <p>Figures # 3, S1, S2, S5,</p> | <p><input type="checkbox"/> 100% (the data presented in this figure come entirely from experimental work carried out by the candidate)</p> <p><input type="checkbox"/> 0% (the data presented in this figure are based exclusively on the work of other co-authors)</p> <p><input checked="" type="checkbox"/> Approximate contribution of the doctoral candidate to the figure: 90%</p> <p>Brief description of the contribution: Designing and conducting experiments and sampling in the field, sample preparation, measurements, statistical analysis, preparing the figures</p> |
|--|--|

| | |
|--------------------|--|
| Figure # S3 | <input type="checkbox"/> 100% (the data presented in this figure come entirely from experimental work carried out by the candidate) <input type="checkbox"/> 0% (the data presented in this figure are based exclusively on the work of other co-authors) <input checked="" type="checkbox"/> Approximate contribution of the doctoral candidate to the figure: 80% Brief description of the contribution: performed experiment, sampling, sample preparation, statistical analysis, figure preparation |
| Figure # 1 | <input type="checkbox"/> 100% (the data presented in this figure come entirely from experimental work carried out by the candidate) <input type="checkbox"/> 0% (the data presented in this figure are based exclusively on the work of other co-authors) <input checked="" type="checkbox"/> Approximate contribution of the doctoral candidate to the figure: 60% Brief description of the contribution: Designing and conducting experiments and sampling in the field, sample preparation (Fig. part B,C,D,E,H), measurements (B,E,H), statistical analysis (B,C,D,E,H), preparing the figures |
| Figure # 4 | <input type="checkbox"/> 100% (the data presented in this figure come entirely from experimental work carried out by the candidate) <input type="checkbox"/> 0% (the data presented in this figure are based exclusively on the work of other co-authors) <input checked="" type="checkbox"/> Approximate contribution of the doctoral candidate to the figure: 15% Brief description of the contribution: Designing and conducting experiments and sampling in the field, RNA extraction, preparing the figures |

10.1.2 Manuscript No. II**Short reference** Müller et al (2023), Plant Physiology**Contribution of the doctoral candidate**

Contribution of the doctoral candidate to figures reflecting experimental data

| | | |
|--|-------------------------------------|--|
| Figures # 4,5,6,7,8 S1,S13,S14,S16,S19, S21,S23,S25,S26, S28-31 | <input checked="" type="checkbox"/> | 100% (the data presented in this figure come entirely from experimental work carried out by the candidate) |
| | <input type="checkbox"/> | 0% (the data presented in this figure are based exclusively on the work of other co-authors) |
| | <input type="checkbox"/> | Approximate contribution of the doctoral candidate to the figure: _____% |
| Brief description of the contribution: | | |

| | | |
|--|-------------------------------------|--|
| Figures # 1,2,3,S2, S15,S17,S18,S20,S22, | <input type="checkbox"/> | 100% (the data presented in this figure come entirely from experimental work carried out by the candidate) |
| | <input type="checkbox"/> | 0% (the data presented in this figure are based exclusively on the work of other co-authors) |
| | <input checked="" type="checkbox"/> | Approximate contribution of the doctoral candidate to the figure: 90% |
| Brief description of the contribution: | | |
| Performed and interpreted the experiments with the help of co-authors, statistical analysis, preparing the figures | | |

| | | |
|-------------------|-------------------------------------|--|
| Figure S27 | <input type="checkbox"/> | 100% (the data presented in this figure come entirely from experimental work carried out by the candidate) |
| | <input type="checkbox"/> | 0% (the data presented in this figure are based exclusively on the work of other co-authors) |
| | <input checked="" type="checkbox"/> | Approximate contribution of the doctoral candidate to the figure: 70% |

Brief description of the contribution:

Conducting the experiments with soybean and crape jasmine, extraction and LC-MS/MS of PAOx/-Glc, statistical analysis, figure preparation.

| | | |
|-------------------|-------------------------------------|--|
| Figure S24 | <input type="checkbox"/> | 100% (the data presented in this figure come entirely from experimental work carried out by the candidate) |
| | <input type="checkbox"/> | 0% (the data presented in this figure are based exclusively on the work of other co-authors) |
| | <input checked="" type="checkbox"/> | Approximate contribution of the doctoral candidate to the figure: 20% |

Brief description of the contribution:

Conducting the experiment in the greenhouse, measurement of benzyl cyanide, RNA extraction, statistical analysis, figure preparation.

| | | |
|----------------------|-------------------------------------|--|
| Figures S3-12 | <input type="checkbox"/> | 100% (the data presented in this figure come entirely from experimental work carried out by the candidate) |
| | <input checked="" type="checkbox"/> | 0% (the data presented in this figure are based exclusively on the work of other co-authors) |
| | <input type="checkbox"/> | Approximate contribution of the doctoral candidate to the figure: _____% |

Brief description of the contribution:

10.1.3 Manuscript No. III

Short reference: Nißler et al (2022), Angewandte Chemie, Int. Ed.

Contribution of the doctoral candidate

Contribution of the doctoral candidate to figures reflecting experimental data:

| | | |
|--------------------------|-------------------------------------|--|
| Figures # S8, S10 | <input checked="" type="checkbox"/> | 100% (the data presented in this figure come entirely from experimental work carried out by the candidate) |
| | <input type="checkbox"/> | 0% (the data presented in this figure are based exclusively on the work of other co-authors) |
| | <input type="checkbox"/> | Approximate contribution of the doctoral candidate to the figure: _____ |

| | | |
|-------------------------|-------------------------------------|---|
| Figures # S5, S7 | <input type="checkbox"/> | 100% (the data presented in this figure come entirely from experimental work carried out by the candidate) |
| | <input type="checkbox"/> | 0% (the data presented in this figure are based exclusively on the work of other co-authors) |
| | <input checked="" type="checkbox"/> | Approximate contribution of the doctoral candidate to the figure: 70% Brief description of the contribution: Designing and conducting experiments and sampling in the field, sample preparation, measurements, statistical analysis, preparing the figures |

| | | |
|------------------------|-------------------------------------|---|
| Figures # 3, S9 | <input type="checkbox"/> | 100% (the data presented in this figure come entirely from experimental work carried out by the candidate) |
| | <input type="checkbox"/> | 0% (the data presented in this figure are based exclusively on the work of other co-authors) |
| | <input checked="" type="checkbox"/> | Approximate contribution of the doctoral candidate to the figure: 60% Brief description of the contribution: Designing and conducting experiments and sampling in the field, preparing the figures |

| | | |
|------------------------|-------------------------------------|--|
| Figures # S4,S6 | <input type="checkbox"/> | 100% (the data presented in this figure come entirely from experimental work carried out by the candidate) |
| | <input type="checkbox"/> | 0% (the data presented in this figure are based exclusively on the work of other co-authors) |
| | <input checked="" type="checkbox"/> | Approximate contribution of the doctoral candidate to the figure:25% Brief description of the contribution: Designing and conducting experiments and sampling in the field, preparing the figures |

| | | |
|---|-------------------------------------|---|
| Figure # 1, 2, 4, S1, S2, S3, S11- S15 | <input type="checkbox"/> | 100% (the data presented in this figure come entirely from experimental work carried out by the candidate) |
| | <input checked="" type="checkbox"/> | 0% (the data presented in this figure are based exclusively on the work of other co-authors) |
| | <input type="checkbox"/> | Approximate contribution of the doctoral candidate to the figure: Brief description of the contribution: |

10.2 Supplemental data of the manuscripts

10.2.1 Supplemental Data – Manuscript I

Supplemental Information

Combined –omics framework reveals how ant symbionts benefit the Neotropical ant-plant *Tococa quadrialata* at different levels.

Andrea T. Müller, Michael Reichelt, Eric G. Cosio, Norma Salinas, Alex Nina, Ding Wang, Heiko Moossen, Heike Geilmann, Jonathan Gershenzon, Tobias G. Köllner, Axel Mithöfer

iScience (2022), 25(10), 105261.

doi:10.1016/j.isci.2022.105261

List of Supplemental information files:

Document S1. Figures S1–S6 and Tables S1–S4.

Data S1. Video showing how *Azteca* ants attack an herbivore placed on a *Tococa* leaf until the herbivore falls off the leaf, related to Figure 3.

Data S2. Additional information about the transcriptome analyses is shown in the results section (Figures 1 and 4).

Note: Data S1 and Data S2 can be found on the enclosed CD with the electronic version of this thesis.

iScience, Volume 25

Supplemental information

**Combined –omics framework reveals how ant
symbionts benefit the Neotropical ant-plant**

***Tococa quadrialata* at different levels**

**Andrea T. Müller, Michael Reichelt, Eric G. Cosio, Norma Salinas, Alex Nina, Ding
Wang, Heiko Moossen, Heike Geilmann, Jonathan Gershenson, Tobias G.
Köllner, and Axel Mithöfer**

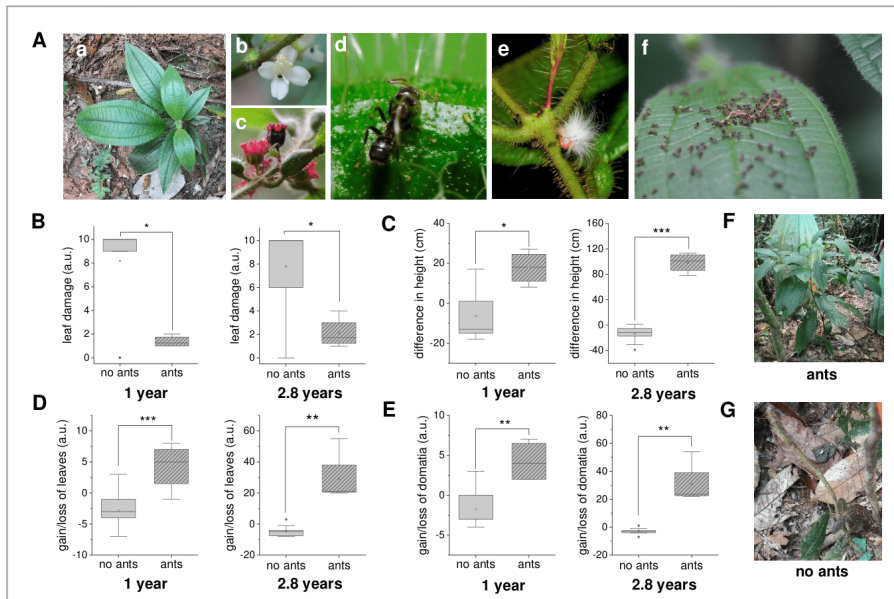


Figure S1: *Tococa* plants suffer from herbivory and reduced growth in the absence of their mutualistic ants. Related to Figure 1. Data were taken from a naturally occurring population of *Tococa quadrialata* plants in the Tambopata national reserve (Madre de Dios, Peru). Growth and performance were monitored for 2.8 years. Boxplots (25th percentile, median, mean (open circle) and 75th percentile) show plant growth parameters. **A:** The symbiosis between *Azteca cf. tonduzi* ants and *T. quadrialata*: a typical example of a young *T. quadrialata* plant (a) is shown and its flowers (b), and fruit development (c). *A. cf. tonduzi* workers shown patrolling the leaf (d); they attack anything placed on the plant, including invertebrates or inanimate objects, whether or not they feed on the plant (e, f; see SI File 1), and often eat the intruder (f). **B:** The level of naturally occurring herbivore damage was higher on uncolonized (no ants) compared to ant-inhabited (ants) plants (*: $p < 0.05$, Wilcoxon rank sum test, $n = 4-13$) at both examined timepoints. Ant-colonized plants grew taller (**C**) and had an increased number of leaves (**D**), and domatia (**E**) in comparison to uncolonized plants. Only ant-colonized plants exhibited net growth (*: $p < 0.05$; **: $p < 0.01$; ***: $p < 0.001$, Wilcoxon rank sum test or Student's t-test, $n = 4-13$). Example of ant-colonized (**F**) and uncolonized (**G**) plants after 2.6 yrs of monitoring. Both plants were of similar size when the monitoring started (1F: 10 cm tall, 4 leaves, 2 domatia; 1G: 8 cm tall, 8 leaves, 4 domatia), but while the ant-colonized plant gained 55 leaves over the 2.8 years, the uncolonized plant suffered through cycles of leaf gain, leaf loss, and regrowth (pers. observation). a.u.: arbitrary units.

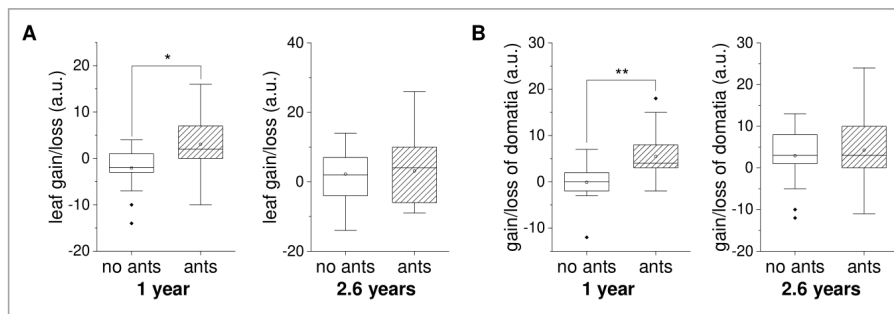


Figure S2: Growth of *T. quadrialata* plants protected from herbivory by nets. Related to Figure 1. Experimental design: A set of young *T. quadrialata* plants colonized by *Azteca cf. tonduzi* ants was split into two groups, and ants were removed from one group. Herbivore damage and ant recolonization were prevented by covering all plants with nets. The production and loss of leaves and formation of domatia by colonized (ant) and ant-deprived (no ants) plants were monitored for 2.6 years. It was accounted for leaves that were removed due to experiments. Leaf (A) and domatia (B) gain after 1 and 2.6 years of growth is presented as boxplots (25th percentile, median, mean (open circle) and 75th percentile) and was calculated by comparison to the respective numbers at the beginning of the monitoring period. Negative values indicate a net loss. a.u.: arbitrary units; Student's t-test, n=13-19, *p<0.05; **p<0.01.

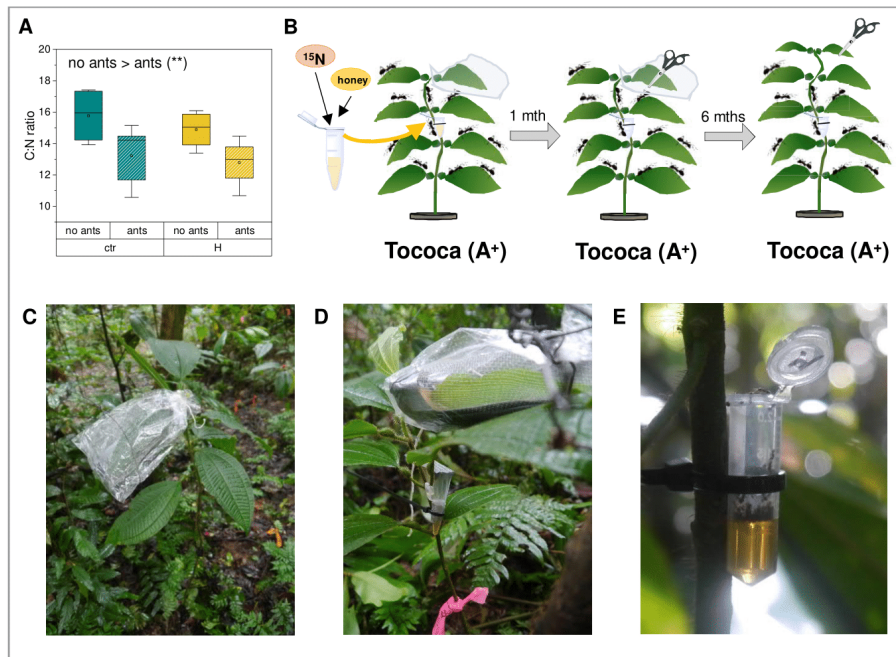


Figure S3: Effect of ant colonization on carbon:nitrogen ratio and setup for ¹⁵N labeling experiment. Related to Figure 1 and STAR Methods. **A:** The C:N ratio of ant-colonized (ants) and ant-deprived (no ants) *T. quadrialata* plants was determined for leaves from the herbivory experiment 1 yr after the start of ant exclusion and the results shown in boxplots (25th percentile, median, mean (open circle) and 75th percentile). Colonization by ants led to a lower C:N ratio (**: $p_{\text{colonization}} < 0.01$, $F_{1,16} = 9.789$, Two-way ANOVA, $n = 4-5$), herbivory treatment ($F_{13,14} = 0.73$, $p = 0.41$) or the interaction of herbivory and ant colonization ($F_{14,15} = 0.08$, $p = 0.78$) did not affect the ratio. **B:** Experimental setup: ¹⁵N-labeled glycine and honey were mixed in a tube that was attached to a colonized *T. quadrialata* plant (A⁺). One of the youngest leaves of the plant was enclosed with a perforated plastic bag beforehand to prevent ants from accessing the leaf. After a month, a sample of the protected leaf was taken for isotope analysis. After 6 months, a newly grown leaf was sampled for isotope analysis as well. **C-E:** pictures of the plants and setup in the field, showing the cover (**C**, **D**), the attached tube with honey (**D**, **E**) and *Azteca cf. tonduzi* ants consuming the ¹⁵N enriched honey (**E**).

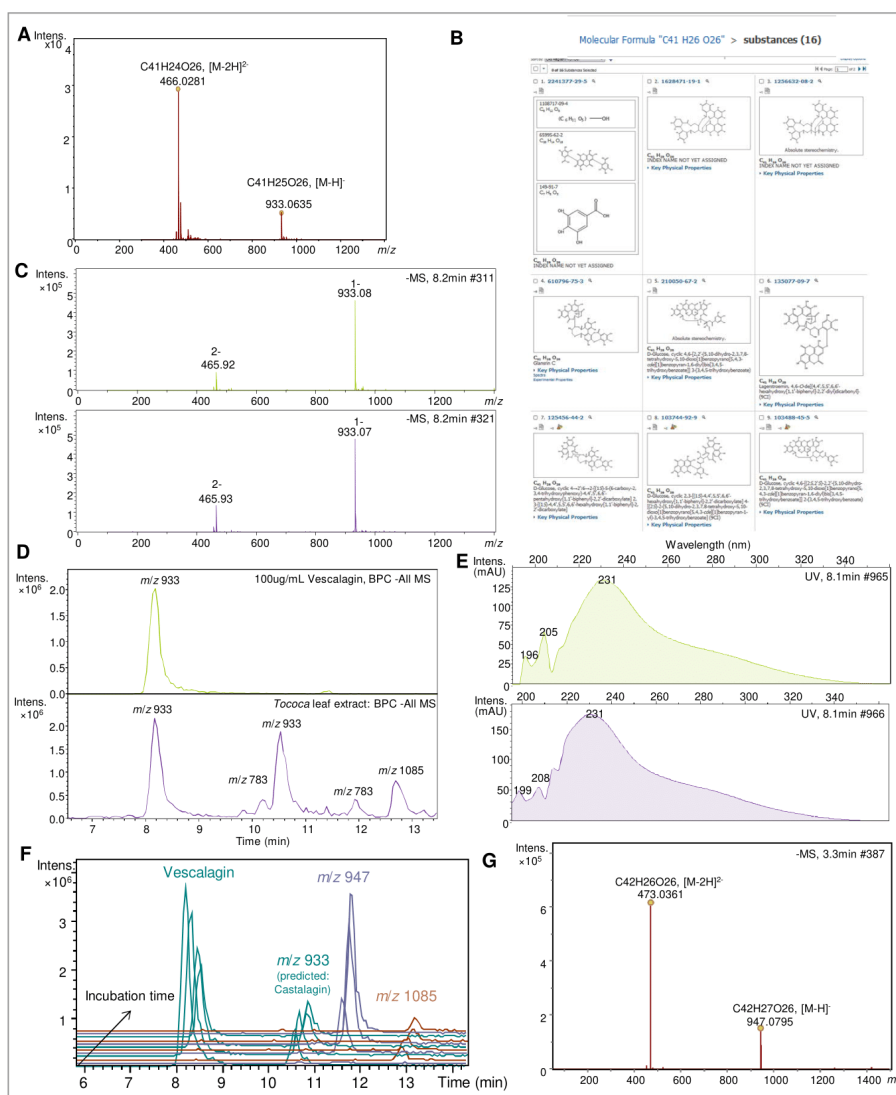


Figure S4: Identification of the ellagitannin vescalagin by high resolution MS and UV spectroscopy in comparison to literature data and an authentic standard. Related to Figure 2. High resolution MS allowed the calculation of the sum formula of this unknown feature (A), which enabled a search in the Scifinder data base for possible candidate structures (B). All 16 known possible structures with the sum formula $C_{41}H_{26}O_{26}$ belonged to the group of ellagitannins. Comparison of the mass spectra (C), chromatographic properties (D), and UV spectra (E) of the unknown feature (purple) with an authentic vescalagin standard (green) allowed the identification of vescalagin. F: Spiking with the standard revealed that vescalagin was not stable in the methanolic plant extract, but spontaneously converted to a compound with m/z 947 over time (z-axis). Extracted ion chromatograms of vescalagin (m/z 933) and m/z ratios of other predicted ellagitannins of a *Tococa* extract incubated for 0, 1.5, 3, 4.5 h at room temperature are shown. G: Based on the sum formula prediction gained by high resolution MS of the derivative, the spontaneous conversion product is an O-methylated vescalagin derivative, from now on referred to as 'MeVescalagin'.

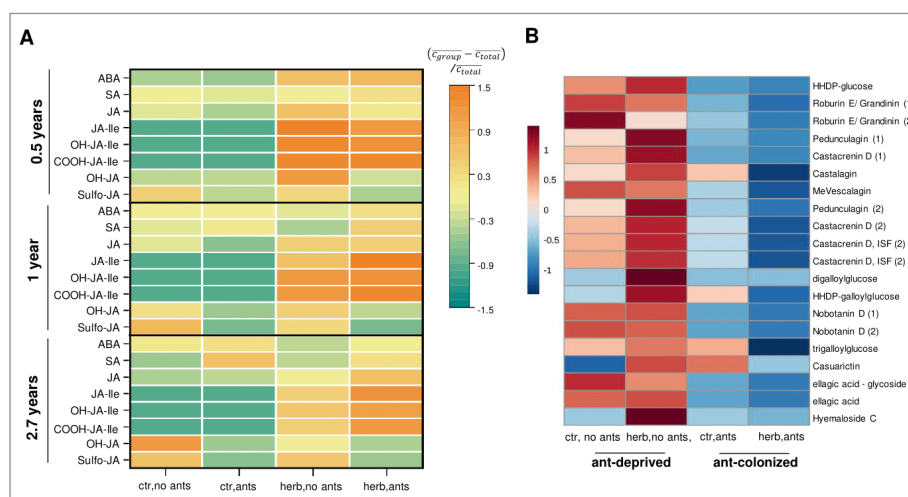


Figure S5: Effects of herbivory and ant colonization on phytohormones and ellagitannins in *Tococa quadrialata* plants. Related to Figure 3. Leaves of ant-colonized (ants) and ant-deprived (no ants) plants net-protected from herbivory otherwise were exposed to 24 h of feeding by *Spodoptera spp.* caterpillars (herb) 0.5 year ($n = 6-8$), 1 year ($n = 4-5$) and 2.7 years ($n = 5-6$) after installation of the nets. **A:** The phytohormones abscisic acid (ABA), salicylic acid (SA), jasmonic acid (JA) as well as prominent JA metabolites were quantified in all herbivore experiments, and their relative concentration visualized as a heatmap, showing that some phytohormones respond to herbivory whilst others were altered by ant-removal. **B:** Untargeted metabolomic analysis of the herbivore experiment 1 year after the plot was set up with mass spectrometer operating in negative mode indicated that many features predicted to be ellagitannin-related compounds (predicted compound name given, more information in Table S4) were enriched in ant-deprived compared to ant-colonized plants. The herbivory treatment, on the other hand, did not affect these features.

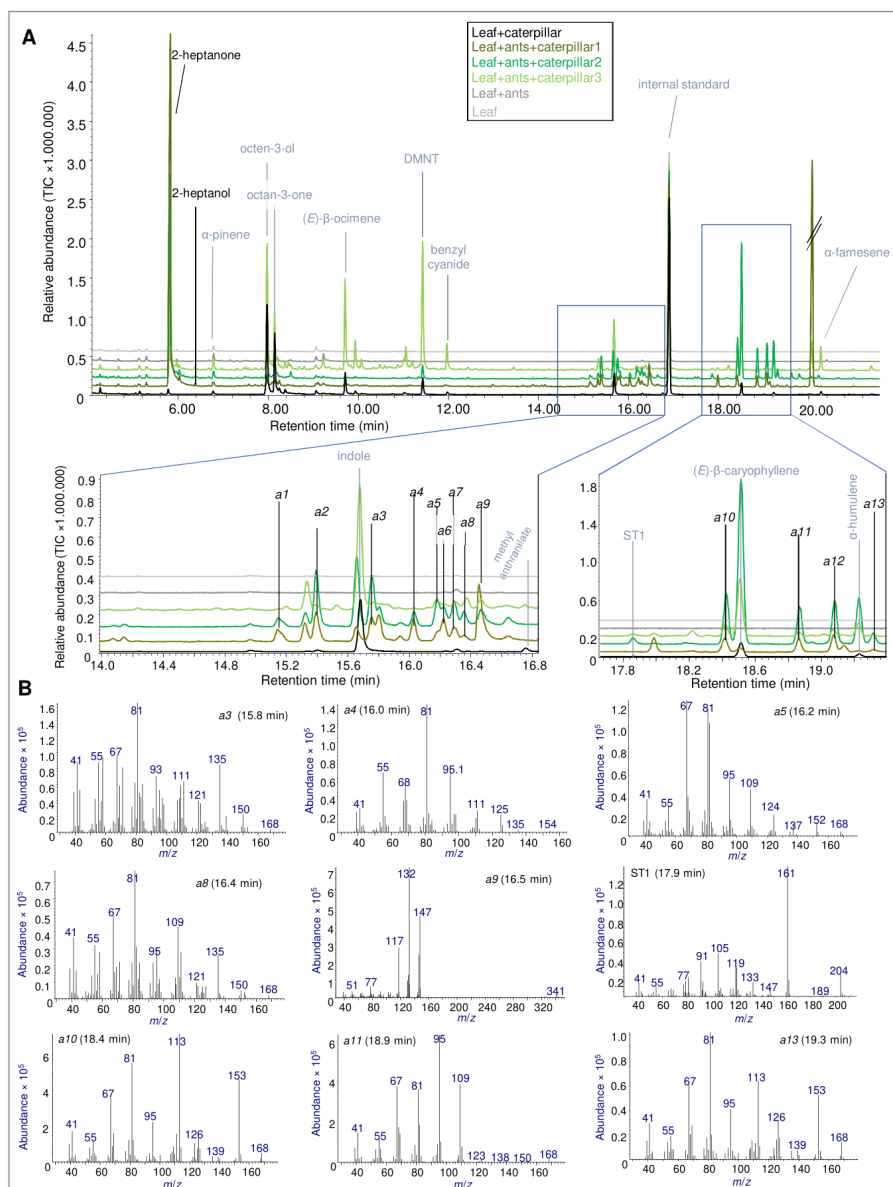


Figure S6: Identification of ant-specific and plant volatiles. Related to Figure 3. **A:** Comparison of the volatile blends of ant-colonized and ant-deprived *T. quadralata* leaves after insect damage revealed not only herbivore induced compounds (gray label, see Figure 3F), but also that some compounds were specific for herbivory-damaged plants colonized by ants (black label). Components identified with authentic standards are labeled with their respective name; unknown ant-specific volatiles are numbered according to their retention time *a1*-*a13*. **B:** The mass spectra of some of the unknown compounds are shown. In some cases, the spectra together with their retention time allowed compound prediction with the help of the NIST17 library and literature (Do Nascimento et al., 1998, Ohmura et al., 2009): *a2,3,7,8*: iridodial-isomers; *a10*: isodihydronepetalactone; *a11, a12*: Iridomyrmecin; *a13*: dihydronepetalactone; ST1: *unknown sesquiterpene* (see also Table S2).

Table S1: Statistical analysis of the accumulation of free amino acids upon herbivory or jasmonic acid (JA) treatment of ant-colonized and ant-deprived uncolonized *T. quadralata* plants.

| Compound | Explanatory variable | | | | | |
|---|-------------------------|------------|-------------------------|----------|--------------------------|---------|
| | Treatment | | Ant colonization | | Interaction (treat:ants) | |
| | F-value/ <i>L-ratio</i> | p-value | F-value/ <i>L-ratio</i> | p-value | F-value/ <i>L-ratio</i> | p-value |
| Herbivory experiment (0.5 yr) (n=6-8) | | | | | | |
| Phe [#] | 20.34 | <0.001 *** | 0.274 | 0.606 | 0.563 | 0.460 |
| Trp [#] | 20.81 | <0.001 *** | 0.001 | 0.971 | 1.412 | 0.246 |
| Tyr [#] | 2.302 | 0.142 | 1.451 | 0.240 | 1.658 | 0.210 |
| Val [#] | 8.754 | 0.007 ** | 1.104 | 0.304 | 0.439 | 0.514 |
| Ile [#] | 13.09 | 0.001 ** | 0.340 | 0.565 | 0.942 | 0.342 |
| Leu [#] | <i>11.89</i> | <0.001 *** | <i>0.255</i> | 0.613 | <i>0.453</i> | 0.501 |
| Pro [#] | 0.580 | 0.454 | 0.014 | 0.906 | 0.220 | 0.643 |
| Thr [#] | 1.260 | 0.273 | 0.295 | 0.592 | 0.174 | 0.680 |
| Glu [#] | 12.17 | 0.002 ** | 1.968 | 0.174 | 0.033 | 0.858 |
| Asp [#] | 0.008 | 0.928 | 1.020 | 0.323 | 0.008 | 0.929 |
| Met [#] | 1.638 | 0.213 | 0.687 | 0.415 | 0.099 | 0.756 |
| Ala [#] | 1.462 | 0.238 | 0.000 | 0.989 | 0.031 | 0.862 |
| Herbivory experiment (1 yr) (n=4-5) | | | | | | |
| Phe [#] | 45.22 | <0.001 *** | 1.040 | 0.325 | 0.111 | 0.744 |
| Trp [#] | 29.77 | <0.001 *** | 1.673 | 0.217 | 0.009 | 0.925 |
| Tyr [#] | 12.64 | 0.003 ** | 2.726 | 0.121 | 0.113 | 0.742 |
| Val [#] | 18.17 | <0.001 *** | 3.243 | 0.093 | 0.000 | 0.999 |
| Ile [#] | 24.41 | <0.001 *** | 2.633 | 0.127 | 0.029 | 0.868 |
| Leu [#] | 26.72 | <0.001 *** | 3.748 | 0.073 | 0.192 | 0.668 |
| Pro [#] | 6.361 | 0.023 * | 2.857 | 0.113 | 0.015 | 0.90 |
| Thr [#] | 5.412 | 0.034 * | 2.548 | 0.133 | 0.275 | 0.608 |
| Glu [#] | 0.732 | 0.407 | 8.053 | 0.012 * | 0.080 | 0.781 |
| Asp [#] | 0.631 | 0.440 | 9.290 | 0.008 ** | 0.525 | 0.481 |
| Met [#] | 0.961 | 0.343 | 0.765 | 0.396 | 0.628 | 0.441 |
| Ala [#] | 2.344 | 0.148 | 5.354 | 0.034 * | 0.184 | 0.675 |
| Herbivory experiment (2.6 yrs) (n=5-6) | | | | | | |
| Phe [#] | <i>27.64</i> | <0.001 *** | <i>7.264</i> | 0.007 ** | <i>0.645</i> | 0.422 |
| Trp [#] | <i>19.67</i> | <0.001 *** | <i>2.914</i> | 0.088 | <i>1.190</i> | 0.275 |
| Tyr [#] | 27.68 | <0.001 *** | 13.39 | 0.002 ** | 1.706 | 0.209 |
| Val [#] | 25.23 | <0.001 *** | 6.295 | 0.022 * | 1.496 | 0.238 |
| Ile [#] | 11.49 | 0.003 ** | 4.151 | 0.058 | 0.624 | 0.440 |
| Leu [#] | 22.04 | <0.001 *** | 8.447 | 0.009 ** | 2.035 | 0.172 |
| Pro [#] | 22.68 | <0.001 *** | 2.303 | 0.147 | 0.934 | 0.347 |
| Thr [#] | 4.787 | 0.041 * | 1.652 | 0.216 | 0.562 | 0.464 |
| Glu [#] | 2.862 | 0.109 | 3.605 | 0.075 | 0.002 | 0.969 |
| Asp [#] | 0.011 | 0.916 | 7.525 | 0.013 * | 0.356 | 0.559 |
| Met [#] | 0.194 | 0.665 | 2.717 | 0.118 | 0.112 | 0.741 |
| Ala [#] | 0.147 | 0.707 | 7.641 | 0.012 * | 0.446 | 0.513 |
| JA spraying experiment (2.7 yrs) (n=4-5) | | | | | | |
| Phe [#] | 89.85 | <0.001 *** | 8.912 | 0.001 ** | 1.658 | 0.220 |
| Trp [#] | 62.31 | <0.001 *** | 12.44 | 0.003 ** | 0.467 | 0.506 |
| Tyr [#] | 22.73 | <0.001 *** | 7.320 | 0.017 * | 0.007 | 0.933 |
| Val [#] | 44.51 | <0.001 *** | 12.29 | 0.004 ** | 1.200 | 0.293 |
| Ile [#] | 42.01 | <0.001 *** | 13.56 | 0.003 ** | 1.222 | 0.289 |
| Leu [#] | 30.62 | <0.001 *** | 14.57 | 0.002 ** | 1.418 | 0.255 |
| Pro [#] | 36.95 | <0.001 *** | 7.849 | 0.014 * | 1.647 | 0.222 |
| Thr [#] | 8.579 | 0.011 * | 10.99 | 0.004 ** | 0.112 | 0.743 |
| Glu [#] | 0.023 | 0.887 | 12.54 | 0.003 ** | 2.530 | 0.136 |
| Asp [#] | 0.876 | 0.367 | 3.592 | 0.0805 | 2.283 | 0.155 |
| Met [#] | 8.325 | 0.012 * | 4.953 | 0.043 * | 0.009 | 0.927 |
| Ala [#] | 0.501 | 0.491 | 9.067 | 0.009 ** | 3.176 | 0.098 |

Related to Figure 3. Depending on whether a Two-Way ANOVA or a gls model was used F-values or Likelihood (L)-ratios are given. L-ratios are in italics. Models were simplified to the minimal model. # indicates log-transformed data; *: p<0.05; **: p<0.01; ***: p<0.001.

Table S2: Details about the volatiles emitted in *Tococa* leaves of colonized and ant-deprived plants including names, Kovats indices for retention time, amounts and statistical analysis.

| Compound | KI | | rel. amount (pg/h/cm ² , mean ± SEM) | | | | statistics (Kruskal-Wallis rank sum test) | | |
|---|------|---------|---|-----------------------|-------------------------|--------------------------|---|----|---------|
| | Det. | Lit. | noants_C | ants_C | noants_H | ants_H | χ ² | df | p value |
| Terpenoids | | | | | | | | | |
| α-pinene | 933 | 933 | 26.7±6.9 | 26.6±4.2 | 29.1±4.4 | 31.3±5.2 | 1.5644 | 3 | 0.6675 |
| (E)-β-ocimene | 1049 | 1052 | 1.5±0.7 ^a | 1.2±0.3 ^a | 155.5±54.5 ^b | 306.9±150.1 ^b | 39.262 | 3 | <0.001 |
| DMNT | 1118 | 1114 | 2.7±1.7 ^a | 2.3±1 ^a | 119.5±35.1 ^b | 282±99.2 ^b | 40.898 | 3 | <0.001 |
| α-copaene | 1380 | 1380 | 0.2±0.2 ^a | 0.5±0.4 ^a | 4.6±1.5 ^b | 11.1±3.9 ^b | 17.722 | 3 | <0.001 |
| <i>unknown sesquiterpene 1</i> | 1393 | - | 0.3±0.2 ^a | 0.4±0.3 ^a | 4.3±1.1 ^b | 8.7±2.9 ^b | 18.975 | 3 | <0.001 |
| (E)-β-caryophyllene | 1425 | 1425 | 1.7±0.5 ^a | 1.2±0.6 ^a | 170.5±59.1 ^b | 268.4±102.5 ^b | 30.402 | 3 | <0.001 |
| α-humulene | 1459 | 1455 | 1.4±0.6 ^a | 0.8±0.5 ^a | 36.2±11.7 ^b | 62.9±23.9 ^b | 23.739 | 3 | <0.001 |
| germacrene D | 1487 | 1487 | 0±0 ^a | 0±0 ^a | 4.5±1.3 ^b | 8.3±2.7 ^b | 22.7 | 3 | <0.001 |
| α-farnesene | 1510 | 1507 | 0±0 ^a | 0.1±0.1 ^a | 20.7±6.2 ^b | 56.9±22.7 ^b | 34.265 | 3 | <0.001 |
| <i>nerolidol</i> | 1567 | 1565 | 0±0 ^a | 0±0 ^a | 10.8±4.2 ^b | 28.1±13.7 ^b | 32.394 | 3 | <0.001 |
| Nitrogenous compounds | | | | | | | | | |
| benzyl cyanide | 1141 | 1148 | 0.8±0.7 ^a | 0.5±0.3 ^a | 15.3±7.5 ^a | 26.4±9.9 ^b | 18.997 | 3 | <0.001 |
| indole | 1296 | 1290 | 0±0 ^a | 0±0 ^a | 61.9±24.6 ^b | 140±72.6 ^b | 34.297 | 3 | <0.001 |
| methyl anthranilate | 1347 | 1354 | 0±0 ^a | 0±0 ^a | 9.4±4.6 ^b | 35.8±17.3 ^b | 17.857 | 3 | <0.001 |
| Fatty acid derived compounds | | | | | | | | | |
| 2-heptanone [§] | 894 | 896 | 4.6±1.2 ^a | 6.4±1.9 ^a | 7±1.9 ^a | 772.9±243.9 ^b | 22.053 | 3 | <0.001 |
| 2-heptanol [§] | 903 | 900 | 1.3±0.5 ^a | 1.4±0.5 ^a | 5.2±1.9 ^a | 57.5±18.4 ^b | 22.564 | 3 | <0.001 |
| oct-1-en-3-ol | 981 | 983 | 1.8±0.8 ^a | 3.7±1.7 ^a | 302.7±83.3 ^b | 553.3±149.4 ^b | 46.484 | 3 | <0.001 |
| 3-octanone | 988 | 988 | 11.4±5.4 ^a | 6.2±2.4 ^a | 136±38 ^b | 215.1±64.4 ^b | 30.92 | 3 | <0.001 |
| octan-3-ol | 998 | 996 | 0±0 ^a | 0±0 ^a | 32.6±9.8 ^b | 75.5±25.8 ^b | 48.396 | 3 | <0.001 |
| Others | | | | | | | | | |
| a1 (<i>3-methyl-hexahydrophthalide</i>) [§] | 1273 | - | 0.8±0.4 | 0.7±0.2 ^a | 1.4±0.4 ^a | 13.4±5 ^b | 13.34 | 3 | 0.0040 |
| a2 (<i>iridodial</i>) [§] | 1281 | - | 2.9±0.5 ^{ab} | 1.4±0.4 ^a | 3.8±0.7 ^b | 19±7.6 ^b | 8.4578 | 3 | 0.0374 |
| a3 (<i>iridodial</i>) [§] | 1299 | - | 0.8±0.4 ^a | 1.1±0.3 ^a | 1.9±0.6 ^a | 28.2±11.4 ^b | 12.601 | 3 | 0.0056 |
| a4 [§] | 1301 | - | 0±0 ^a | 0±0 ^a | 0.2±0.2 ^a | 6.2±2.8 ^b | 20.013 | 3 | <0.001 |
| a5 [§] | 1307 | - | 0±0 ^a | 0±0 ^a | 0±0 ^a | 8.3±3.8 ^b | 22.723 | 3 | <0.001 |
| a6 [§] | 1311 | - | 1.1±0.3 ^a | 1±0.3 ^a | 1±0.3 ^a | 17.3±6.2 ^b | 10.431 | 3 | 0.0152 |
| a7 (<i>iridodial</i>) [§] | 1316 | - | 0.7±0.5 ^{ab} | 0.5±0.2 ^{ab} | 0.3±0.2 ^a | 5.1±2.9 ^b | 8.4023 | 3 | 0.0384 |
| a8 (<i>iridodial</i>) [§] | 1320 | - | 2.2±1 ^a | 2.5±1 ^a | 3.1±0.8 ^a | 15±4.4 ^b | 11.278 | 3 | 0.0103 |
| a9 (<i>2-(1-Methylcyclopropyl)aniline</i>) [§] | 1331 | 1331 | 0±0 ^a | 0.1±0.1 ^a | 0.4±0.3 ^a | 17.2±6.8 ^b | 15.133 | 3 | 0.0017 |
| a10 (<i>isodihydro-nepetalactone</i>) [§] | 1420 | 1414 | 2.4±1.9 ^a | 1.1±0.6 ^a | 0.5±0.2 ^a | 7.6±3.9 ^b | 11.128 | 3 | 0.0111 |
| a11 (<i>iridomyrcin</i>) [§] | 1442 | 1463 | 0±0 ^a | 0±0 ^a | 0.2±0.2 ^a | 22.1±8.6 ^b | 28.552 | 3 | <0.001 |
| a12 (<i>iridomyrcin</i>) [§] | 1452 | 1463 | 0±0 ^a | 0±0 ^a | 1.5±0.7 ^a | 34.6±14.2 ^b | 27.769 | 3 | <0.001 |
| a13 (<i>dihydro-nepetalactone</i>) [§] | 1463 | 1414-30 | 0±0 ^a | 0±0 ^a | 0.1±0.1 ^a | 7.7±3.1 ^b | 25.601 | 3 | <0.001 |

Related to Figure 3. Specific chemicals present at concentrations above 800 pg cm⁻² in at least two of the samples are depicted. Compounds only identified by library (NIST17) and literature (Do Nascimento et al., 1998; Ohmura et al., 2009) search without comparison to an authentic standard are in *italics*. To further confirm the identification or provide additional information on the compounds, the retention time indices were determined (Det.) with the temperature-programmed Kovats index (KI) and the values compared to NIST and literature (Lit). For mass spectra of these compounds, see Figure S6. [§] indicates that the compound is most likely produced by the ants. The Dunn-test was used as a *post hoc* test. Different letters indicate significant differences between groups (p<0.025); n=14-21.

Table S3: Statistical analysis of the changes in various defense hormones caused by herbivore damage and ant-colonization.

| Compound | Explanatory variable | | | | | |
|---|-----------------------------|------------|------------------|------------|--------------------------|---------|
| | Treatment (herbivory or JA) | | Ant-colonization | | Interaction (treat:ants) | |
| | F-value/ L-ratio | p-value | F-value/L-ratio | p-value | F-value/L-ratio | p-value |
| Herbivory experiment (0.5 yr) (n=6-8) | | | | | | |
| ABA [#] | 9.771 | 0.004 ** | 0.423 | 0.522 | 0.036 | 0.852 |
| SA [#] | 0.702 | 0.410 | 0.438 | 0.514 | 0.000 | 0.995 |
| JA | 12.05 | 0.002 ** | 2.727 | 0.112 | 0.264 | 0.612 |
| JA-Ile [#] | <i>68.73</i> | 0.003 ** | <i>0.000</i> | 0.989 | <i>0.036</i> | 0.851 |
| OH-JA-Ile [#] | <i>37.91</i> | <0.001 *** | <i>4.275</i> | 0.039 * | <i>1.028</i> | 0.311 |
| COOH-JA-Ile [#] | <i>48.90</i> | <0.001 *** | <i>2.247</i> | 0.134 | <i>0.369</i> | 0.543 |
| OH-JA [#] | 3.963 | 0.057 | 2.173 | 0.153 | 1.816 | 0.190 |
| Sulfo-JA | 1.224 | 0.280 | 37.16 | <0.001 *** | 0.194 | 0.664 |
| Herbivory experiment (1 yr) (n=4-5) | | | | | | |
| ABA [#] | 0.288 | 0.600 | 4.971 | 0.040 * | 0.030 | 0.866 |
| SA | 0.027 | 0.873 | 7.928 | 0.012 * | 2.046 | 0.175 |
| JA [#] | 6.207 | 0.024 * | 0.755 | 0.399 | 2.254 | 0.156 |
| JA-Ile [#] | <i>16.24</i> | <0.001 *** | <i>2.890</i> | 0.089 | <i>0.880</i> | 0.347 |
| OH-JA-Ile [#] | <i>20.73</i> | <0.001 *** | <i>1.672</i> | 0.196 | <i>1.713</i> | 0.191 |
| COOH-JA-Ile [#] | <i>24.14</i> | <0.001 *** | <i>1.186</i> | 0.276 | <i>0.391</i> | 0.532 |
| OH-JA | 0.146 | 0.708 | 9.129 | 0.008 ** | 0.071 | 0.793 |
| Sulfo-JA ^{\$} | 0.868 | 0.367 | 30.21 | <0.001 *** | 1.027 | 0.328 |
| Herbivory experiment (2.6 yrs) (n=5-6) | | | | | | |
| ABA [#] | 6.142 | 0.023 * | 5.745 | 0.027 * | 0.886 | 0.359 |
| SA | 0.285 | 0.600 | 15.11 | <0.001 *** | 2.668 | 0.120 |
| JA [#] | 5.403 | 0.031 * | 0.490 | 0.493 | 0.369 | 0.551 |
| JA-Ile [#] | <i>48.80</i> | <0.001 *** | <i>0.931</i> | 0.335 | <i>1.512</i> | 0.219 |
| OH-JA-Ile [#] | <i>21.19</i> | <0.001 *** | <i>0.120</i> | 0.729 | <i>3.450</i> | 0.063 |
| COOH-JA-Ile [#] | <i>17.69</i> | <0.001 *** | <i>0.499</i> | 0.480 | <i>4.357</i> | 0.037 * |
| OH-JA ^{\$} | 2.961 | 0.102 | 16.30 | <0.001 *** | 6.194 | 0.023 * |
| Sulfo-JA [#] | 0.022 | 0.885 | 14.00 | 0.001 ** | 0.240 | 0.630 |
| JA spraying experiment (2.7 yrs) (n=4-5) | | | | | | |
| ABA [#] | 1.097 | 0.314 | 7.493 | 0.015 * | 1.376 | 0.262 |
| SA | 0.847 | 0.374 | 3.873 | 0.068 | 2.091 | 0.172 |
| JA [#] | 386.4 | <0.001 *** | 0.069 | 0.797 | 4.470 | 0.054 |
| JA-Ile [#] | <i>24.18</i> | <0.001 *** | <i>0.099</i> | 0.753 | <i>2.449</i> | 0.118 |
| OH-JA-Ile | <i>28.13</i> | <0.001 *** | <i>0.771</i> | 0.380 | <i>1.090</i> | 0.297 |
| COOH-JA-Ile | <i>19.76</i> | <0.001 *** | <i>3.571</i> | 0.059 | <i>0.329</i> | 0.567 |
| OH-JA ^{\$} | 7.125 | 0.018 * | 1.503 | 0.242 | 0.062 | 0.807 |
| Sulfo-JA | 3.812 | 0.073 | 5.776 | 0.030 * | 0.021 | 0.886 |

Related to Figure 3. Depending on whether a Two-Way ANOVA or a gls model was used F-values or Likelihood (L)-ratios are given. L-ratios are in italics. Models were simplified to the minimal model. # indicates log-transformed data, \$ sqrt-transformed data; *: p<0.05; **: p<0.01; ***: p<0.001.

Table S4: Additional information about the features assigned as ellagitannins or related compounds that are shown in Figure 2 and Figure S5.

| RT | <i>m/z</i> (negative mode) | other <i>m/z</i> of the same compound (e.g. in source fragments) | Sum formula | possible compound |
|---|-------------------------------|---|---|----------------------------|
| <i>Measurements 1 year after ant exclusion</i> | | | | |
| 1.18 | 481.0625 | | C ₂₀ H ₁₈ O ₁₄ | HHDP-glucose |
| 2.20 | 532.0497 [M-2H] ²⁻ | | C ₄₆ H ₃₄ O ₃₀ | Roburin E/ Grandinin (1) |
| 2.55 | 532.0497 [M-2H] ²⁻ | | C ₄₆ H ₃₄ O ₃₀ | Roburin E/ Grandinin (2) |
| 2.81 | 783.0687 | | C ₃₄ H ₂₄ O ₂₂ | Pedunculagin (1) |
| 2.86 | 542.0340 [M-2H] ²⁻ | | C ₄₈ H ₃₀ O ₃₀ | Castacrenin D (1) |
| 3.03 | 466.0285 [M-2H] ²⁻ | | C ₄₁ H ₂₆ O ₂₆ | Castalagin |
| 3.25 | 473.0364 [M-2H] ²⁻ | | C ₄₂ H ₂₈ O ₂₆ | MeVescalagin |
| 3.37 | 783.0687 | | C ₃₄ H ₂₄ O ₂₂ | Pedunculagin (2) |
| 3.45 | 542.0341 [M-2H] ²⁻ | 457.0233 [M-GA-2H] ²⁻ 169.0143 [GA-H] ¹⁻ | C ₄₈ H ₃₀ O ₃₀ | Castacrenin D (2) |
| 3.58 | 483.0780 | | C ₂₀ H ₂₀ O ₁₈ | digalloylglucose |
| 3.75 | 633.0734 | | C ₂₇ H ₂₂ O ₁₈ | HHDP-galloylglucose |
| 4.18 | 392.0387 [M-2H] ²⁻ | | C ₃₄ H ₂₆ O ₂₂ | Tellimagrandin/Nobotanin D |
| 4.47 | 635.0891 | | C ₂₇ H ₂₄ O ₁₈ | trigalloylglucose |
| 4.50 | 392.0387 [M-2H] ²⁻ | | C ₃₄ H ₂₆ O ₂₂ | Nobotanin D/Tellimagrandin |
| 4.54 | 467.0362 [M-2H] ²⁻ | | C ₄₁ H ₂₆ O ₂₆ | Casuarictin |
| 4.89 | 447.0569 | | C ₂₀ H ₁₆ O ₁₂ | Ellagic acid glycoside |
| 5.28 | 300.9991 | | C ₁₄ H ₆ O ₈ | Ellagic acid |
| 5.51 | 875.0945 | | C ₄₀ H ₃₀ O ₂₃ | Hyemaloside C |
| <i>Measurements 2.6 years after ant exclusion</i> | | | | |
| 2.82 | 783.0690 | | C ₃₄ H ₂₄ O ₂₂ | Pedunculagin (1) |
| 3.05 | 466.0284 [M-2H] ²⁻ | | C ₄₁ H ₂₆ O ₂₆ | Castalagin |
| 3.26 | 473.0363 [M-2H] ²⁻ | | C ₄₂ H ₂₈ O ₂₆ | MeVescalagin |
| 3.40 | 783.0685 | | C ₃₄ H ₂₄ O ₂₂ | Pedunculagin (2) |
| 3.46 | 542.0339 [M-2H] ²⁻ | 457.0231 [M-GA-2H] ²⁻ 169.0143 [GA-H] ¹⁻ | C ₄₈ H ₃₀ O ₃₀ | Castacrenin D |
| 3.57 | 483.0781 | | C ₂₀ H ₂₀ O ₁₈ | digalloylglucose |
| 3.76 | 633.0736 | | C ₂₇ H ₂₂ O ₁₈ | HHDP-galloylglucose |
| 4.46 | 635.0893 | | C ₂₇ H ₂₄ O ₁₈ | trigalloylglucose |
| 4.50 | 392.0387 [M-2H] ²⁻ | | C ₃₄ H ₂₆ O ₂₂ | Nobotanin D |
| 4.57 | 467.0359 [M-2H] ²⁻ | | C ₄₁ H ₂₆ O ₂₆ | Casuarictin |
| 5.27 | 300.9991 | | C ₁₄ H ₆ O ₈ | Ellagic acid |
| 5.52 | 875.0950 | | C ₄₀ H ₃₀ O ₂₃ | Hyemaloside C |

Related to Figure 2. *m/z* corresponds to [M-H]⁻, if not noted otherwise. Compound names assigned based on SciFinder hits for the sum formula and comparison to literature (Fracassetti et al., 2013; Moilanen et al., 2013; Serna and Martinez, 2015; Yoshida et al., 1991). GA: gallic acid moiety, RT: retention time, HHDP: hexahydroxydiphenoyl.

10.2.2 Supplemental Data – Manuscript II

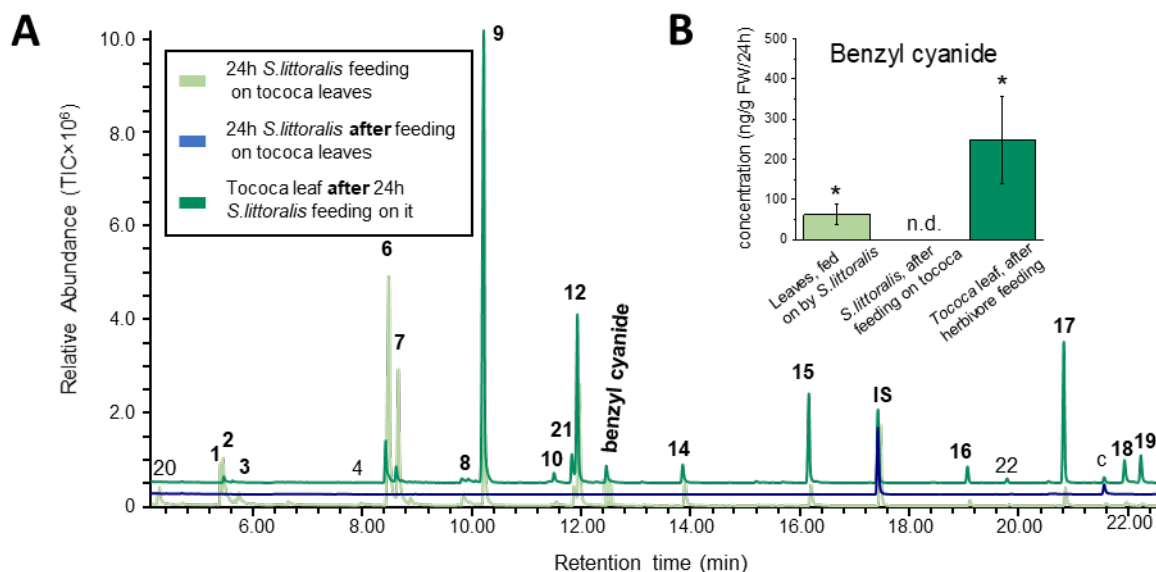


Figure S1: Formation of benzyl cyanide in tocooca leaves in response to herbivory (see Figure 1). 3-4 *S. littoralis* caterpillars were allowed to feed on leaves for 24 h and the volatiles were collected simultaneously (light green). Afterwards, the caterpillars were removed from the leaves, put into another bag and their volatiles collected for 24h (blue). Volatiles of the damaged leaves were collected for another 24 h as well (dark green). Samples were analyzed by GC-MS (A) and quantified by GC-FID (B). IS, internal standard; c, contamination; 1, 2-hexenal; 2, 3-hexenol; 3, 1-hexanol; 4, 4-oxo-hex-2-enal and benzaldehyde; 6, 1-octen-3-ol; 7, octan-3-one; 8, benzyl alcohol, 9, β -ocimene; 10, linalool; 12, (*E*)-4,8-dimethyl-nonatriene (DMNT); 14, methyl salicylate; 15, indole; 16, (*E*)- β -caryophyllene; 17, α -farnesene; 18, nerolidol; 19, (*E,E*)-4,8,12-trimethyl-1,3,7,11-tridecatetraene (TMTT); 20, 3-hexenal + hexanal; 21, phenylethyl alcohol; 22, α -humulene; TIC: total ion chromatogram. Means \pm SEM are shown; n = 5. Asterisk indicates significant accumulation of benzyl cyanide (> 0) based on one-tailed t-test, * = $p < 0.05$.

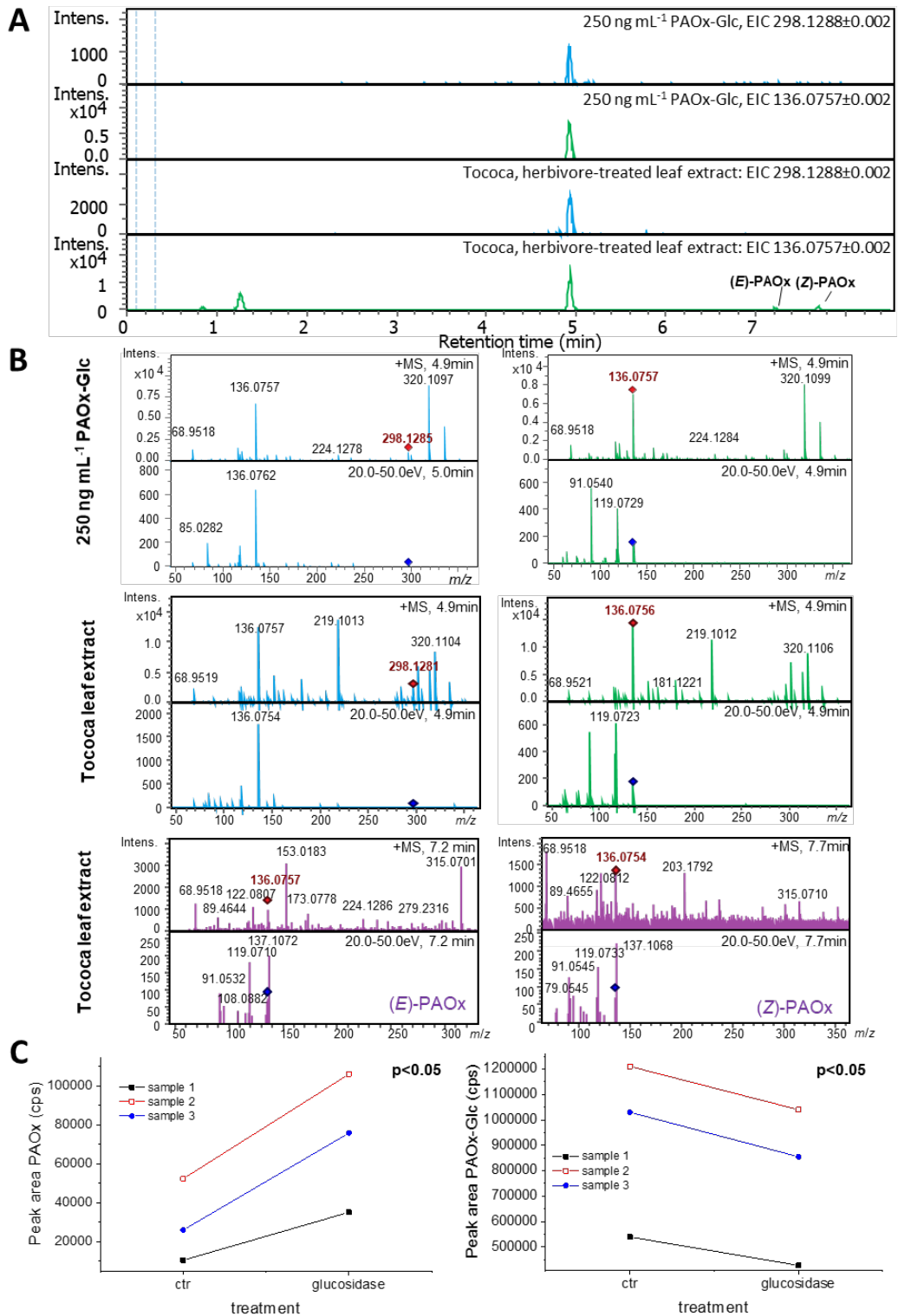


Figure S2: Identification of phenylacetaldoxime glucoside (PAOx-Glc) in herbivore-treated *tococa* leaves. (A) Comparison of retention time and (B) fragmentation pattern of synthetic PAOx-Glc and plant-derived PAOx-Glc and PAOx (methanolic extract of *Spodoptera littoralis*-damaged leaves) analyzed by LC-qTOF-MS/MS, the upper mass spectrum is the full scan spectrum, the lower spectra are MS2 spectra after CID of m/z 298.1285 and m/z 136.0757. (C) Compounds extracted with 100% methanol from herbivore-damaged leaves were treated with a commercial (Sigma-Aldrich) β -glucosidase from almonds (glucosidase), or only incubated in the reaction buffer (ctr). Paired t-test, $n=3$. cps: counts per second (electron multiplier).

Phenylacetaldoxime glucoside

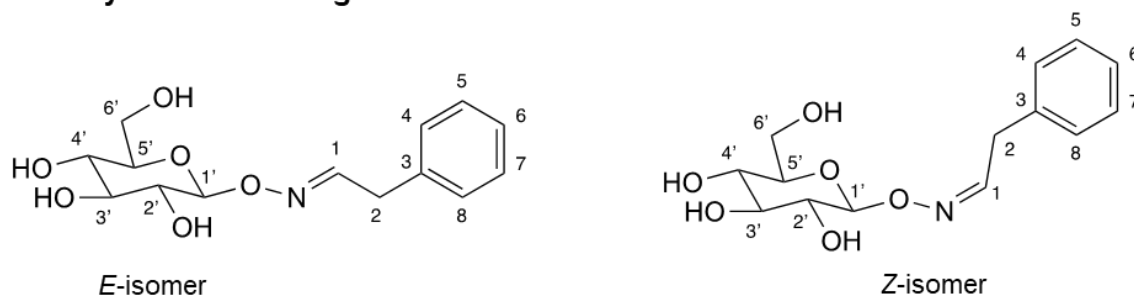


Figure S3: The structure of the synthesized phenylacetaldoxime glucoside. $^1\text{H-NMR}$ (500 MHz, $\text{MeOH-}d_3$) for the *E*-isomer: δ ppm: 7.63 (*dd*, $J = 6.7/6.7$ Hz 1H, H-1), 7.30 (*m*, 2H, H-5, H-7), 7.20-7.27 (*m*, 3H, H-4, H-6, H-8), 4.91 (*d*, $J = 8.2$ Hz, 1H, H-1'), 3.87 (*m*, 1H, H-6'), 3.70 (*m*, 1H, H-6'), 3.54 (*d*, $J = 6.7$ Hz, 2H, H-2), 3.30-3.44 (*m*, 4H, H-2', H-3', H-4', H-5'). For the *Z*-isomer (only non-overlapped signals are shown): 6.98 (*dd*, $J = 5.4/5.4$ Hz 1H, H-1), 4.96 (*d*, $J = 8.0$ Hz, 1H, H-1'), 3.77 (*d*, $J = 5.4$ Hz, 2H, H-2). $^{13}\text{C-NMR}$ (125 MHz, $\text{MeOH-}d_3$) *E*-isomer: δ ppm: 153.6 (C-1), 137.2 (C-3), 129.74 (C-4), 129.74 (C-8), 129.67 (C-5), 129.67 (C-7), 127.8 (C-6), 105.6 (C-1'), 78.3 (C-3'), 78.1 (C-5'), 73.56 (C-2'), 71.28 (C-4'), 62.56 (C-6'), 36.5 (C-2). *Z*-isomer: δ ppm: 153.9 (C-1), 137.8 (C-3), 129.8 (C-4), 129.8 (C-8), 129.67 (C-5), 129.67 (C-7), 127.6 (C-6), 105.7 (C-1'), 78.4 (C-3'), 78.1 (C-5'), 73.59 (C-2'), 71.3 (C-4'), 62.63 (C-6'), 33.4 (C-2). *E/Z*-configurations were assigned based on chemical shifts of the oxime protons (Karabatsos & Hsi, 1967).

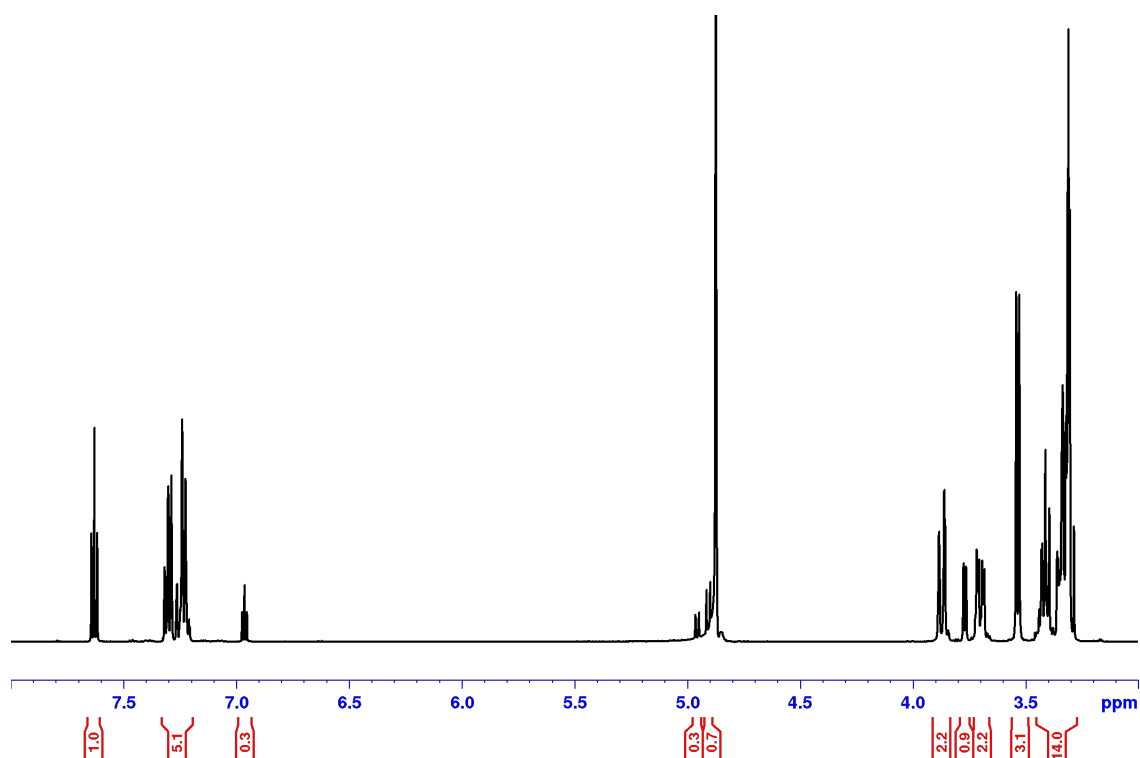


Figure S4: Phenylacetaldoxime glucoside, $^1\text{H NMR}$ with water suppression, full range in $\text{MeOH-}d_3$

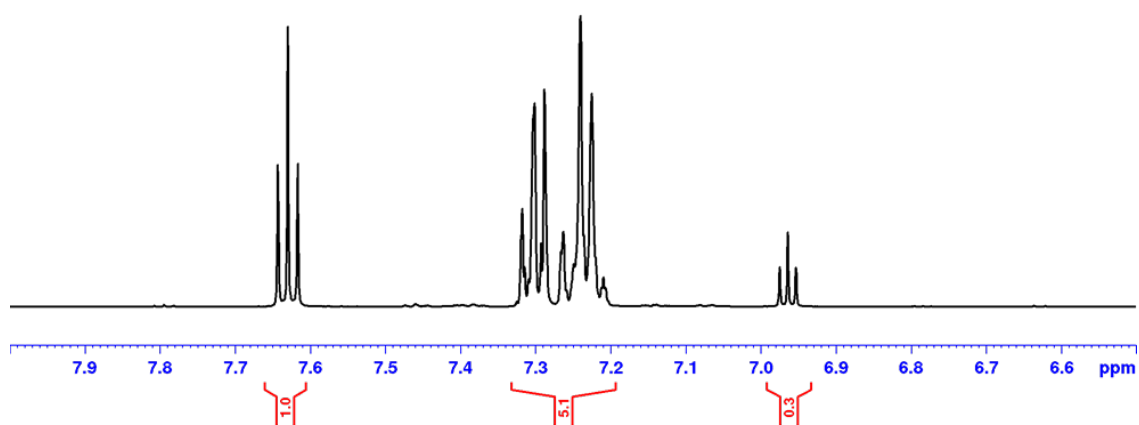


Figure S5: Phenylacetaldoxime glucoside, ^1H NMR with water suppression, aromatic range in $\text{MeOH-}d_3$

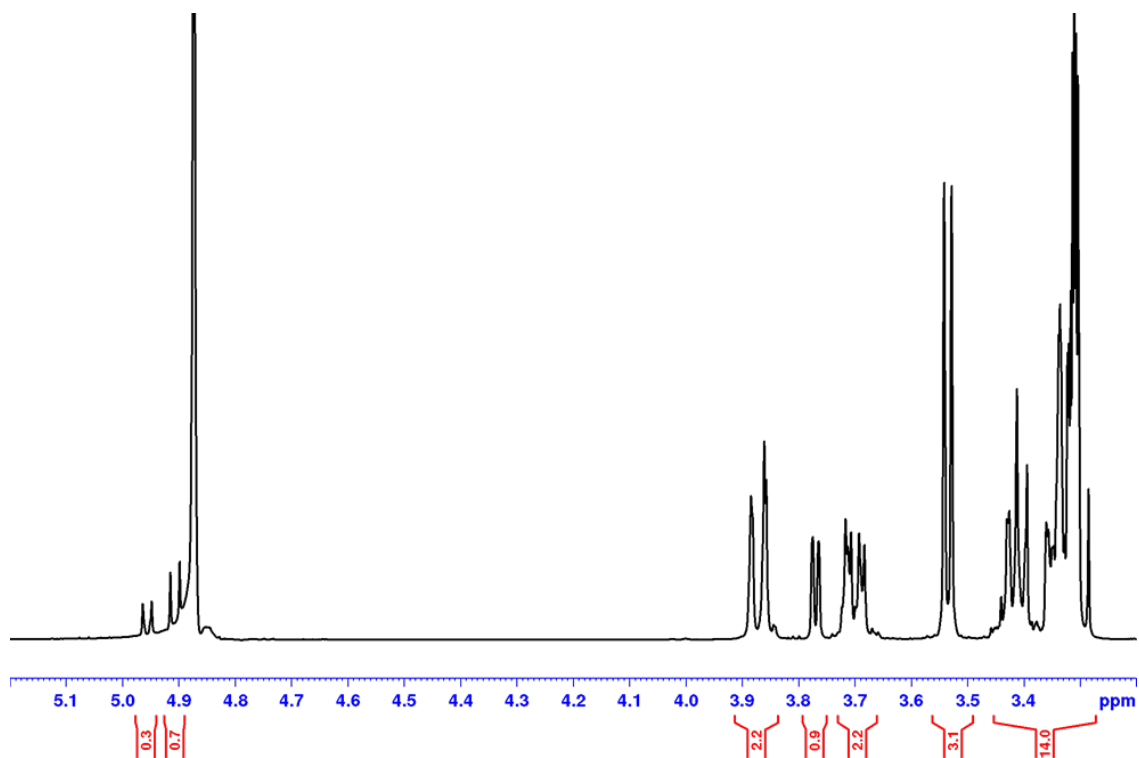


Figure S6: Phenylacetaldoxime glucoside, ^1H NMR with water suppression, aliphatic range in $\text{MeOH-}d_3$

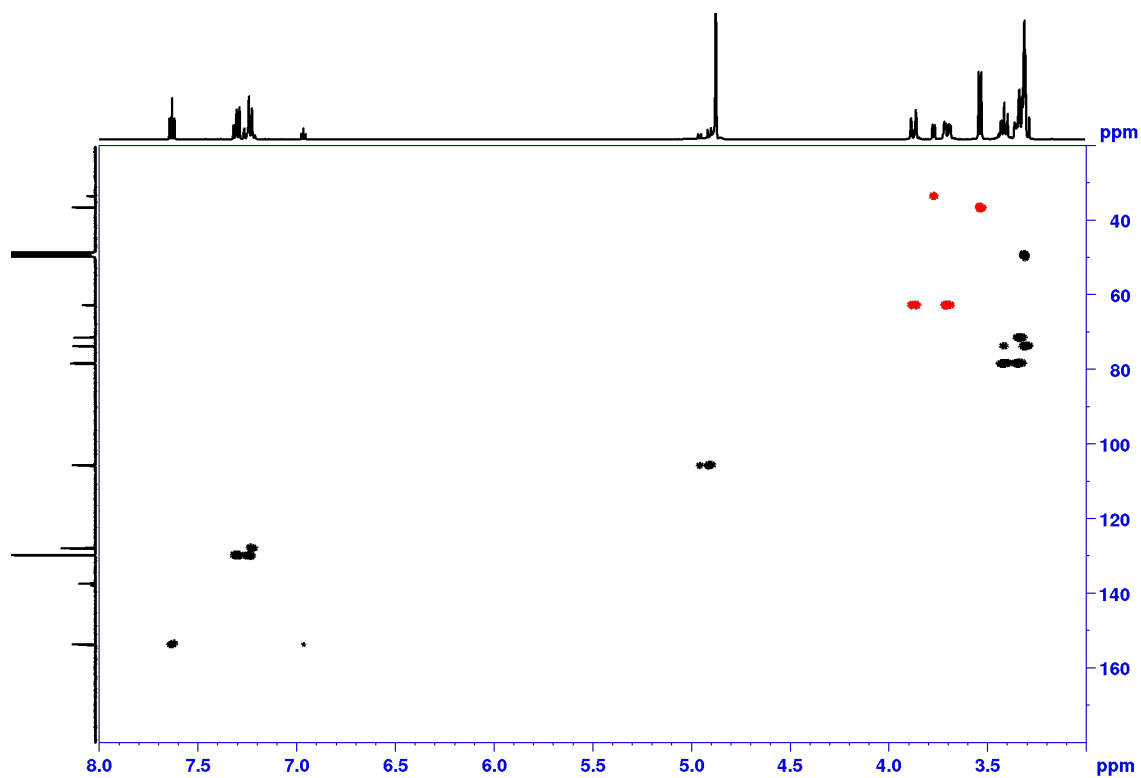


Figure S7: Phenylacetaldoxime glucoside, phase sensitive HSQC, full range in MeOH-*d*₃

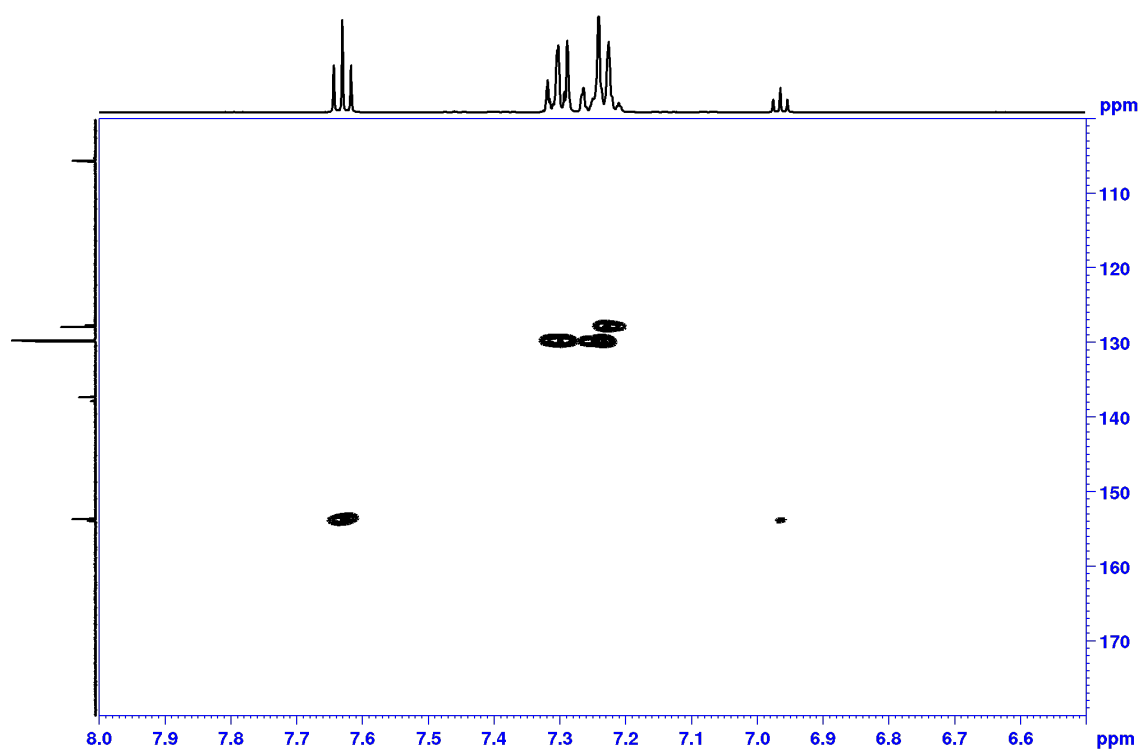


Figure S8: Phenylacetaldoxime glucoside, phase sensitive HSQC, aromatic range in MeOH-*d*₃

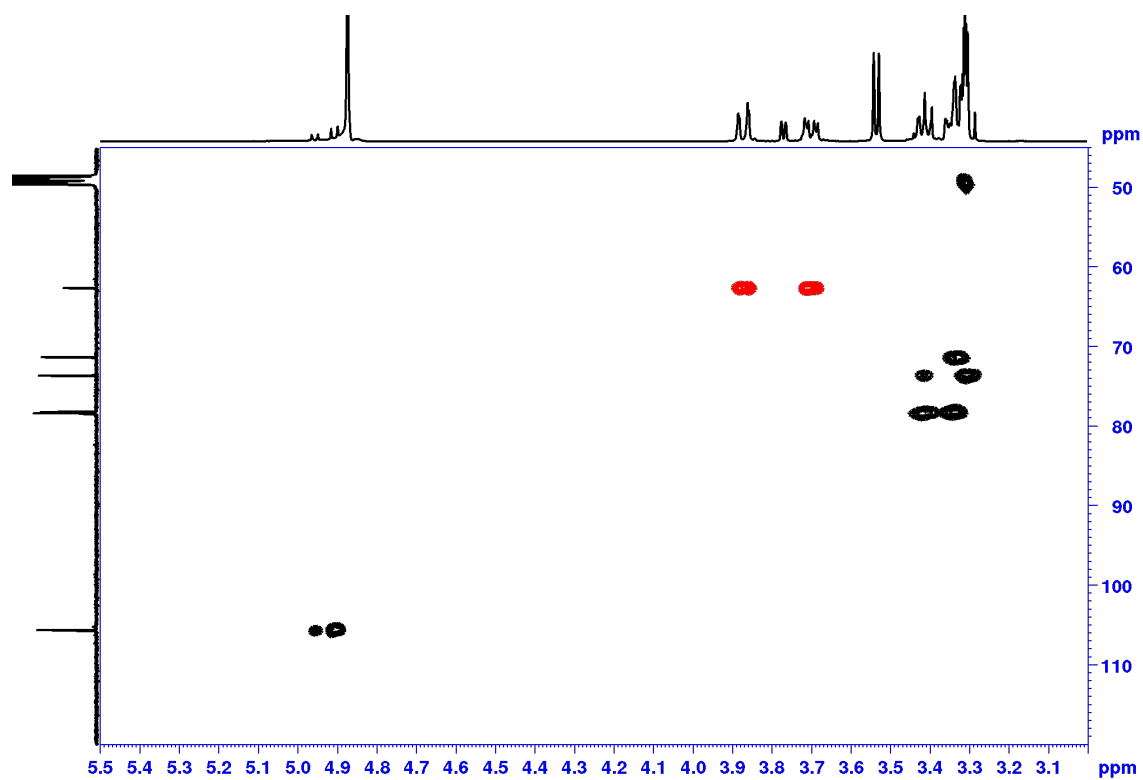


Figure S9: Phenylacetaldoxime glucoside, phase sensitive HSQC, aliphatic range in MeOH- d_3 . Shaded areas mark impurity and solvent, red: CH₂, black: CH, CH₃

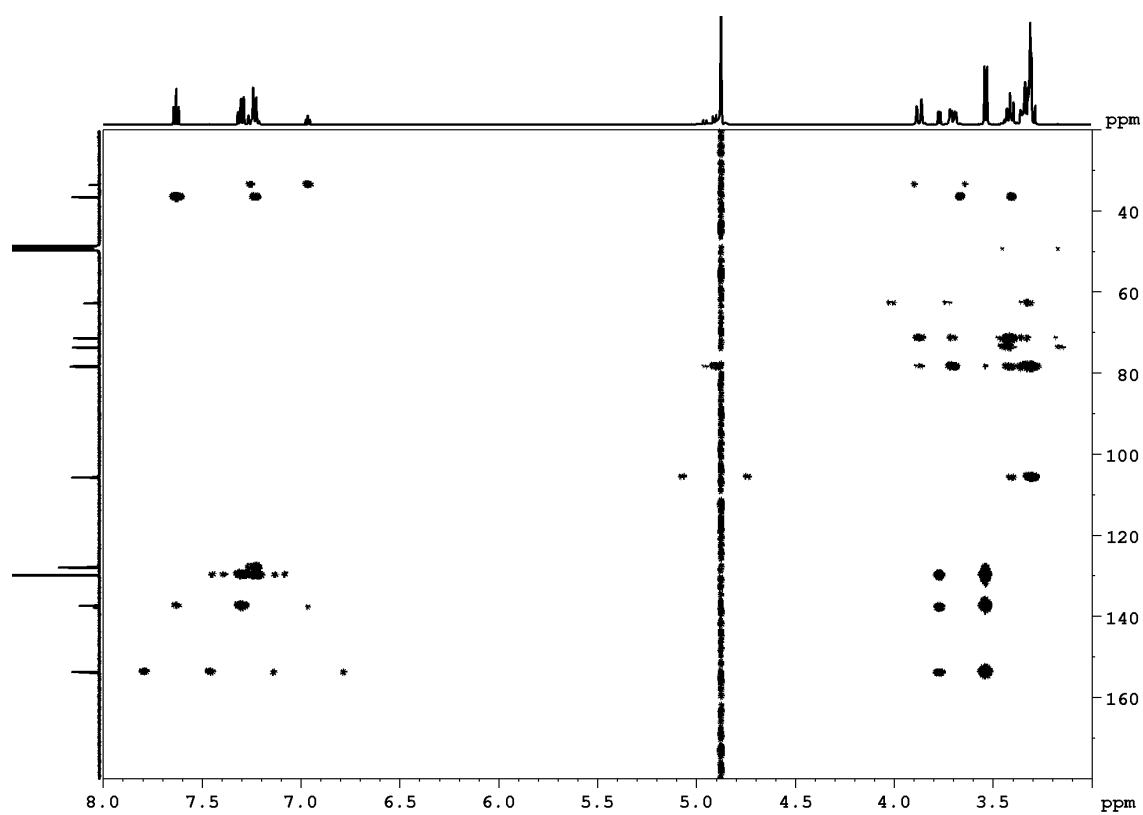


Figure S10: Phenylacetaldoxime glucoside, HMBC, full range in MeOH- d_3

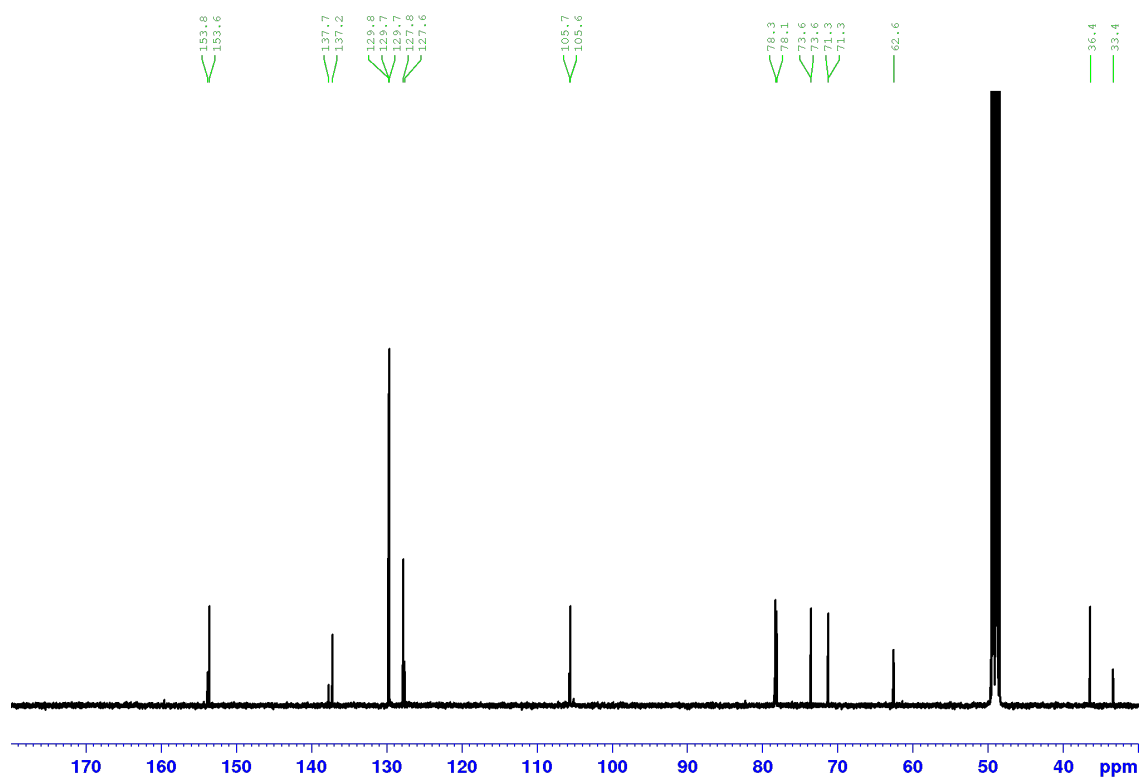


Figure S11: Phenylacetaldoxime glucoside, ^{13}C , full range in $\text{MeOH-}d_3$

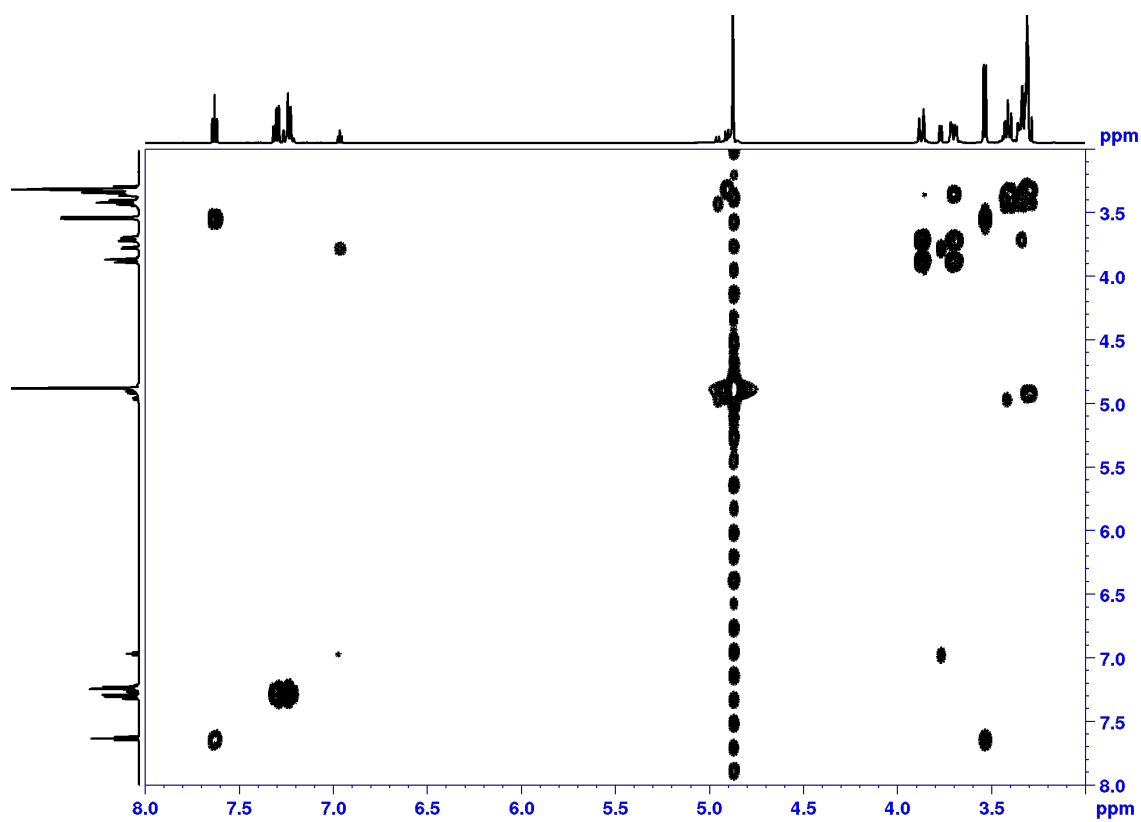


Figure S12: Phenylacetaldoxime glucoside, $^1\text{H-}^1\text{H}$ DQF COSY with water suppression. Magnitude mode processed, aliphatic range in $\text{MeOH-}d_3$

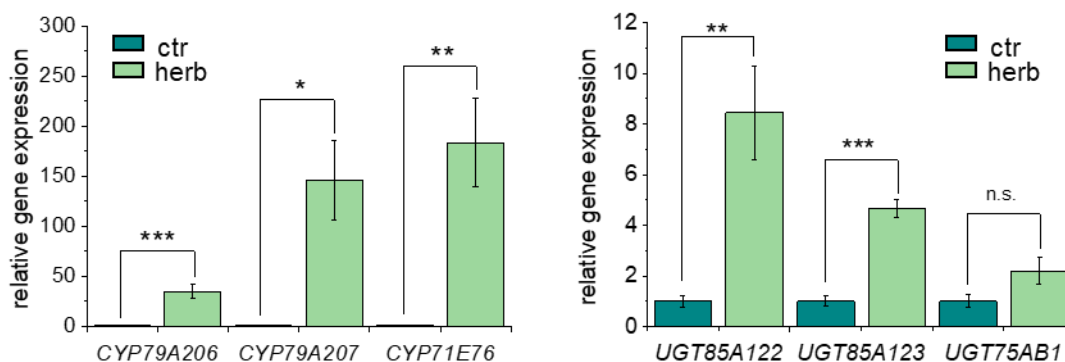


Figure S13: Quantitative reverse transcription (qRT) PCR of PAOx-Glc and benzyl cyanide biosynthesis genes. Expression was analyzed in *Spodoptera littoralis*-damaged and undamaged tocooca leaves. The RNA of the treated leaves was isolated, transcribed to cDNA, and qRT-PCRs performed using the primers mentioned in Table S8 and actin as housekeeping gene. Relative expression was calculated with the $\Delta\Delta$ Ct method (Pfaffl, 2001). Data are presented as mean \pm SEM; Student's t-test: n = 5 - 7, * = p<0.05, ** = p<0.01, *** = p<0.001.

Methodology: cDNA synthesis from 800 ng RNA was performed with the RevertAid First Strand cDNA Synthesis Kit (Thermo Scientific) using oligo (dT)₁₈ primers according to the manufacturer's instructions. The obtained cDNA was diluted 1:8 with ddH₂O. Primer pairs were designed to amplify the respective gene (Table S8), and their specificity confirmed by agarose gel electrophoresis, melting curve, and standard curve analysis. Samples were run in an optical 96-well plate on the CFX96 Touch™ Real-Time PCR System (Bio-Rad) with the Brilliant III Ultra-Fast SYBR Green QPCR Master Mix (Agilent). PCR conditions are given in Table S7. All samples were run in duplicates. Normalized fold expression was calculated with the $\Delta\Delta$ CP method (Pfaffl, 2001). As internal calibrator, cDNA from all samples was pooled and run on each plate.

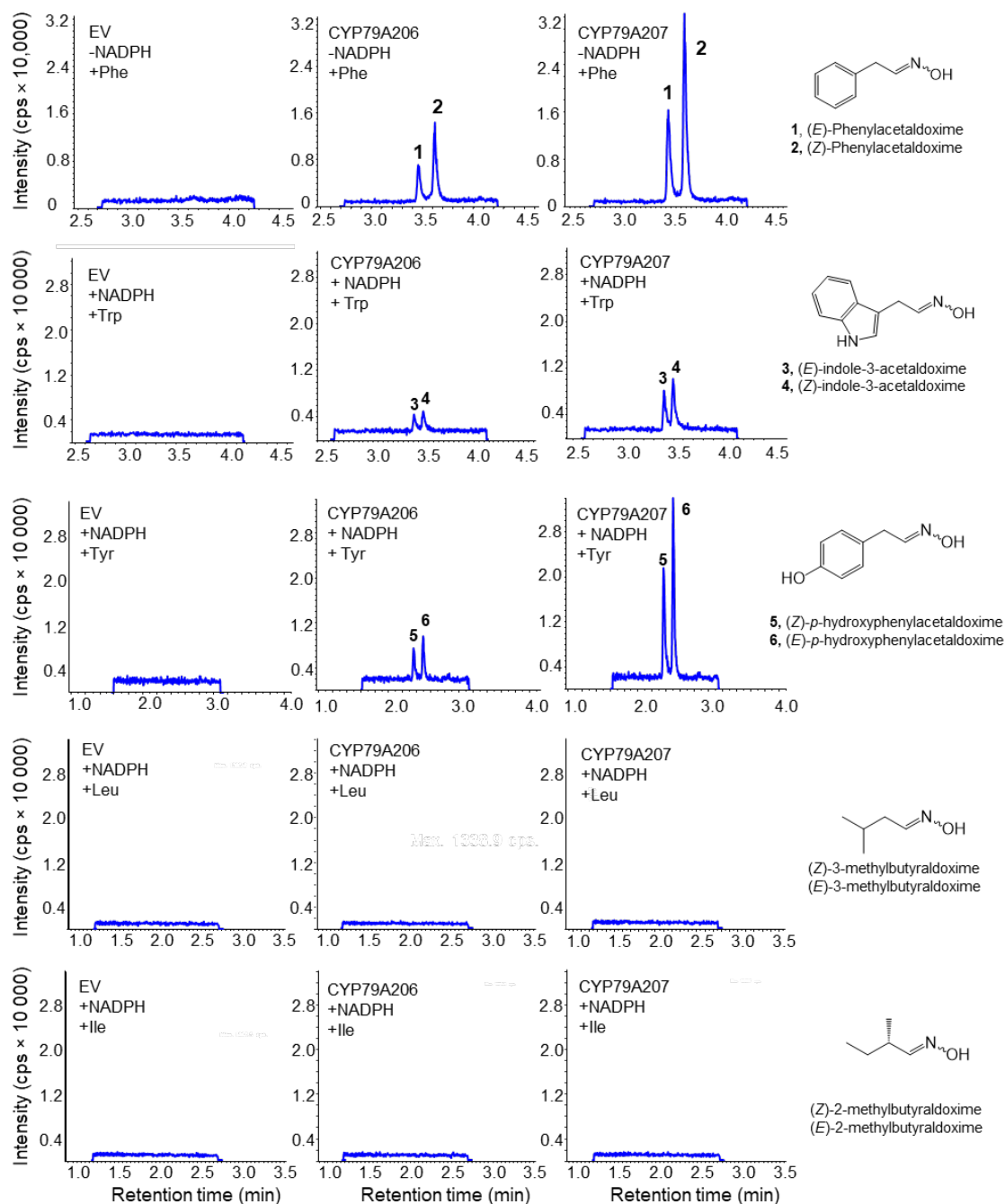


Figure S15: Enzymatic activity of CYP79A206 and CYP79A207 with different amino acid substrates. The two genes were heterologously expressed in *Saccharomyces cerevisiae* and microsomes containing the recombinant enzymes were incubated with NADPH and either L-tryptophan (Trp), L-tyrosine (Tyr), L-isoleucine (Ile), or L-leucine (Leu). As negative controls, *S. cerevisiae* was transformed with an empty vector (EV) and the respective microsomes were incubated with the substrates (Phe, Trp, Tyr, Ile, Leu) as well. As a second control, microsomes containing the recombinant enzymes were incubated with Phe in the absence of NADPH. Products were extracted with methanol and detected using LC-MS/MS. cps: counts per second (electron multiplier).

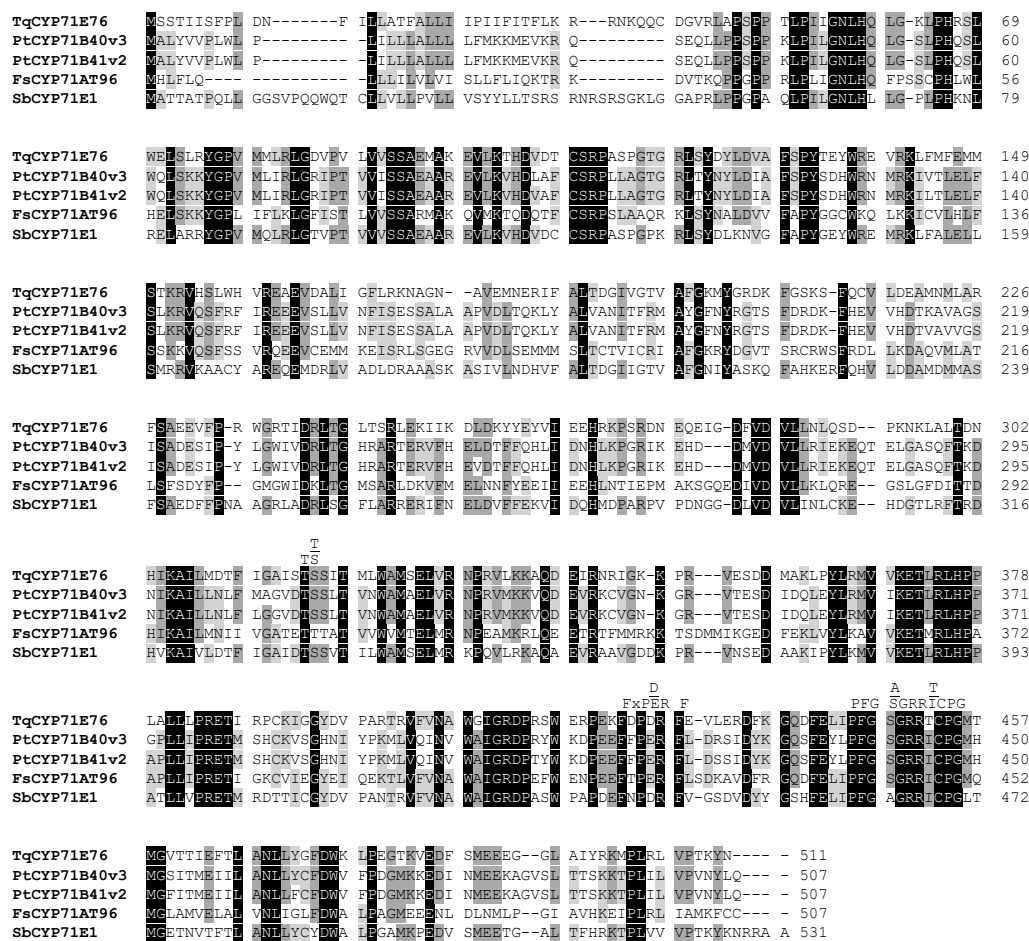


Figure S16: Amino acid sequence alignment of CYP71E76 with sequences of other nitrile-forming CYP71s and CYP71E1 from *Sorghum bicolor*. The alignment was achieved with the ClustalW algorithm using BioEdit. Black shading corresponds to conserved residues, dark grey shades mark residues identical in four of the sequences, and residues with light grey shading are identical in three of the sequences. Conserved motifs are indicated (Durst and Nelson 1995, Bak et al. 2011)

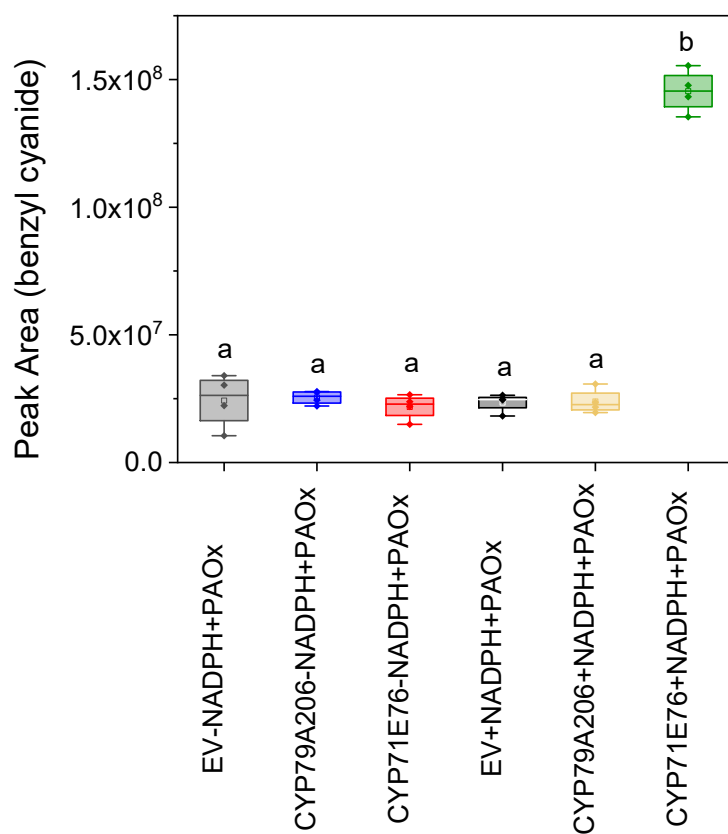


Figure S17: Formation of benzyl cyanide by CYP71E76 *in vitro*. Genes were expressed in *S. cerevisiae* and microsomes containing the respective enzymes were used for activity assays with phenylacet-aldoxime (PAOx) as substrate. The hexane phase was analyzed via GC-MS/FID. While benzyl cyanide is always formed from PAOx due to thermal degradation during GC injection, recombinant CYP71E76 in the presence of NADPH was able to generate amounts of benzyl cyanide significantly higher compared to the background. One-Way ANOVA ($F_{5,18} = 238.1$, $p < 0.001$) Tukey HSD *posthoc* test: $p < 0.05$; $n = 4$, EV = empty vector.

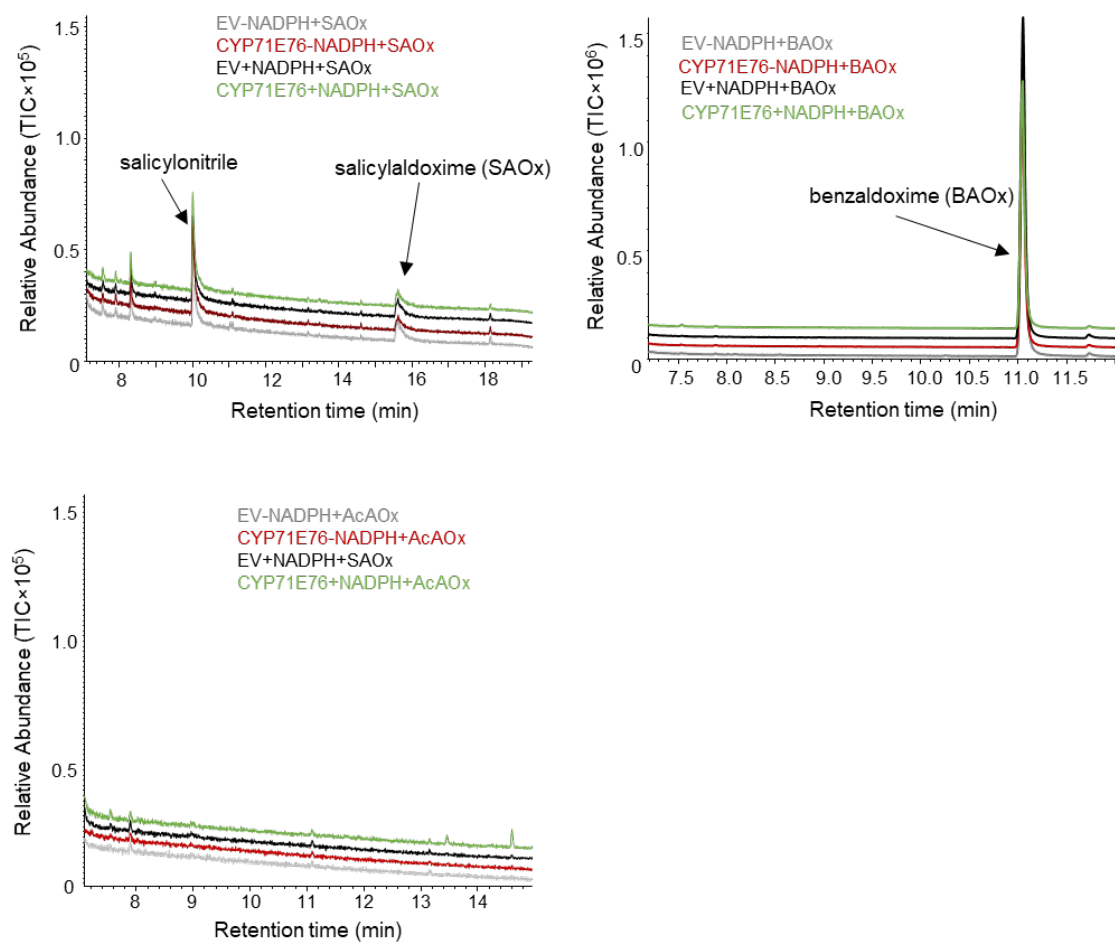


Figure S18: CYP71E76 has narrow substrate specificity. The gene was expressed in *S. cerevisiae* and microsomes containing the CYP71E76 were used for activity assays with benzaldehyde (BAOx), salicylaldehyde (SAOx), and acetaldehyde (AcAOx) as potential substrates. The hexane phase was analyzed via GC-MS/FID. Salicylonitrile was always formed from SAOx likely due to thermal degradation during GC injection. The amounts produced in the sample with recombinant CYP71E76 were not higher than the background, indicating no enzyme activity. In addition, no activity was detectable when the microsomes were incubated with BAOx or AcAOx. EV = empty vector.

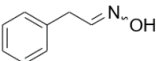
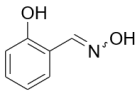
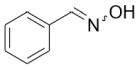
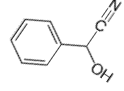
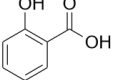
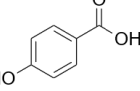
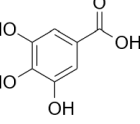
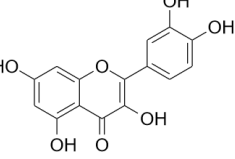
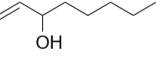
| Substrate | Structure | UGT85A122 | UGT85A123 | UGT75AB1 | UGT76AH1 |
|-------------------------|---|-----------|-----------|----------|----------|
| PAOx |  | yes | yes | yes | no |
| salicylaldoxime |  | yes | yes | yes | no |
| benzaldoxime |  | yes | yes | yes | no |
| β -mandelonitrile |  | yes | yes | no | no |
| salicylic acid |  | no | no | yes | no |
| 4-OH-benzoic acid |  | no | no | yes | no |
| gallic acid |  | no | no | yes | no |
| quercetin |  | no | no | yes | yes |
| epicatechin |  | no | no | no | no |
| geraniol |  | yes | yes | no | yes |
| oct-1-en-3-ol |  | yes | yes | no | yes |

Figure S20: Activity of UGT85A122, UGT85A123, UGT75AB1, and UGT76AH1 towards various substrates. Candidate UGT genes were heterologously expressed in *Escherichia coli* and the purified enzymes used for activity assays with various substrates. Compounds were detected with LC-qTOF-MS.

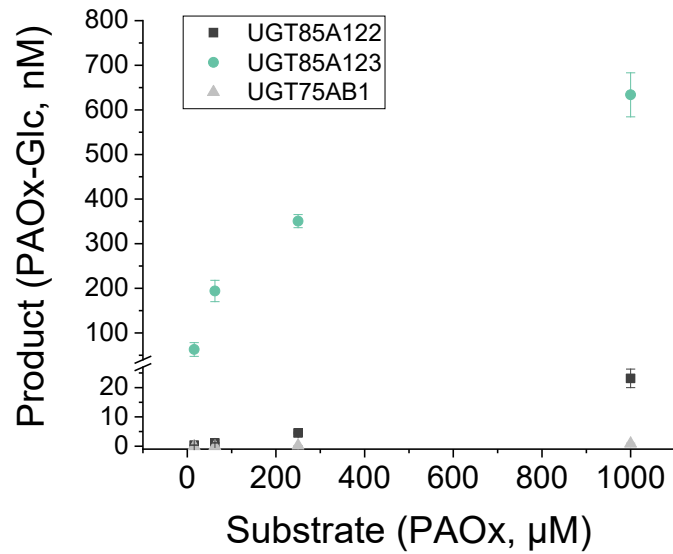


Figure S21: Substrate affinity of UGT85A122, UGT85A123, and UGT75AB1 towards PAOx. Heterologous expression in *E. coli* and activity assays showed that three candidate UGTs were able to use PAOx as substrate. To compare their substrate affinities, 10 μg of the purified enzymes were incubated with various concentrations of PAOx for 30 min. Product formation was detected with targeted LC-MS/MS.

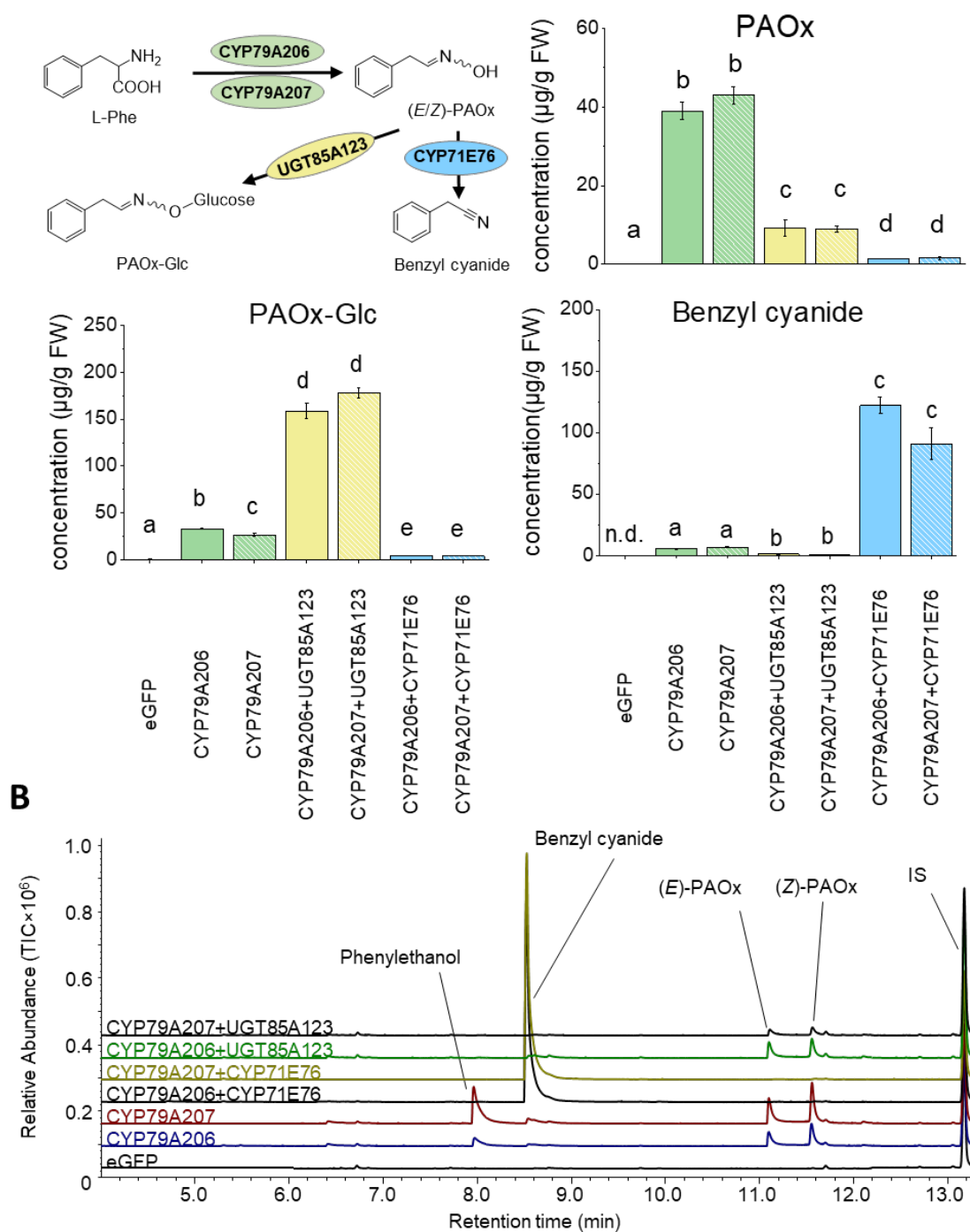


Figure S22: Reconstitution of the formation of benzyl cyanide and phenylacetaldoxime glucoside in *Nicotiana benthamiana* by overexpression of tobacco *CYP79*, *CYP71* and *UGT* genes. *N. benthamiana* was transformed with different combinations of recombinant *Agrobacterium tumefaciens* strains possessing CYP79A206, CYP79A207, CYP71E76, or UGT85A123, respectively. Accumulation of compounds was detected with targeted LC-MS/MS and GC-MS/FID. **(A)** Overview of the pathway and quantification of the compounds of interest in the different plants. **(B)** Chromatogram from GC-MS analysis of the samples. FW, fresh weight. TIC: total ion chromatogram. IS: internal standard. One-Way ANOVA ($F_{\text{PAOx}} = 372.2$, $p < 0.001$; $F_{\text{benzyl cyanide}} = 32.34$, $p < 0.001$) or linear (gls) model ($L\text{-ratio}_{\text{PAOx-Glc}} = 144.0$, $p < 0.001$) and Tukey *post hoc* test on log transformed data, different letters indicate $p < 0.05$; $n = 4-7$; n.d., not detectable.

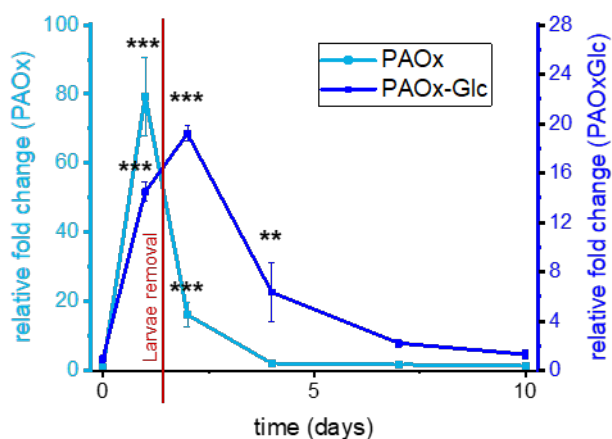


Figure S23: Relative temporal distribution of PAOx and PAOx-Glc in herbivore-damaged *Tococa quadrialata* leaves (see Figure 5). Leaves were exposed to herbivory by *Spodoptera littoralis* caterpillars for 24 hours and the accumulation of PAOx and PAOx-Glc was monitored for ten days. Compounds were extracted with methanol from leaf powder and analyzed using targeted LC-MS/MS. Here, we show the levels of PAOx and PAOxGlc relative to the respective concentration at the start of the experiment ($t = 0d$). Asterisks indicate significant differences to respective control ($0d$) based on One-Way ANOVA on log-transformed data ($F_{5,18,PAOx} = 41.03$, $F_{5,18,PAOxGlc} = 12.96$, $p_{PAOx,PAOxGlc} \leq 0.001$) and Dunnett's *post hoc* test. Means \pm SEM are shown; $n = 3-5$.

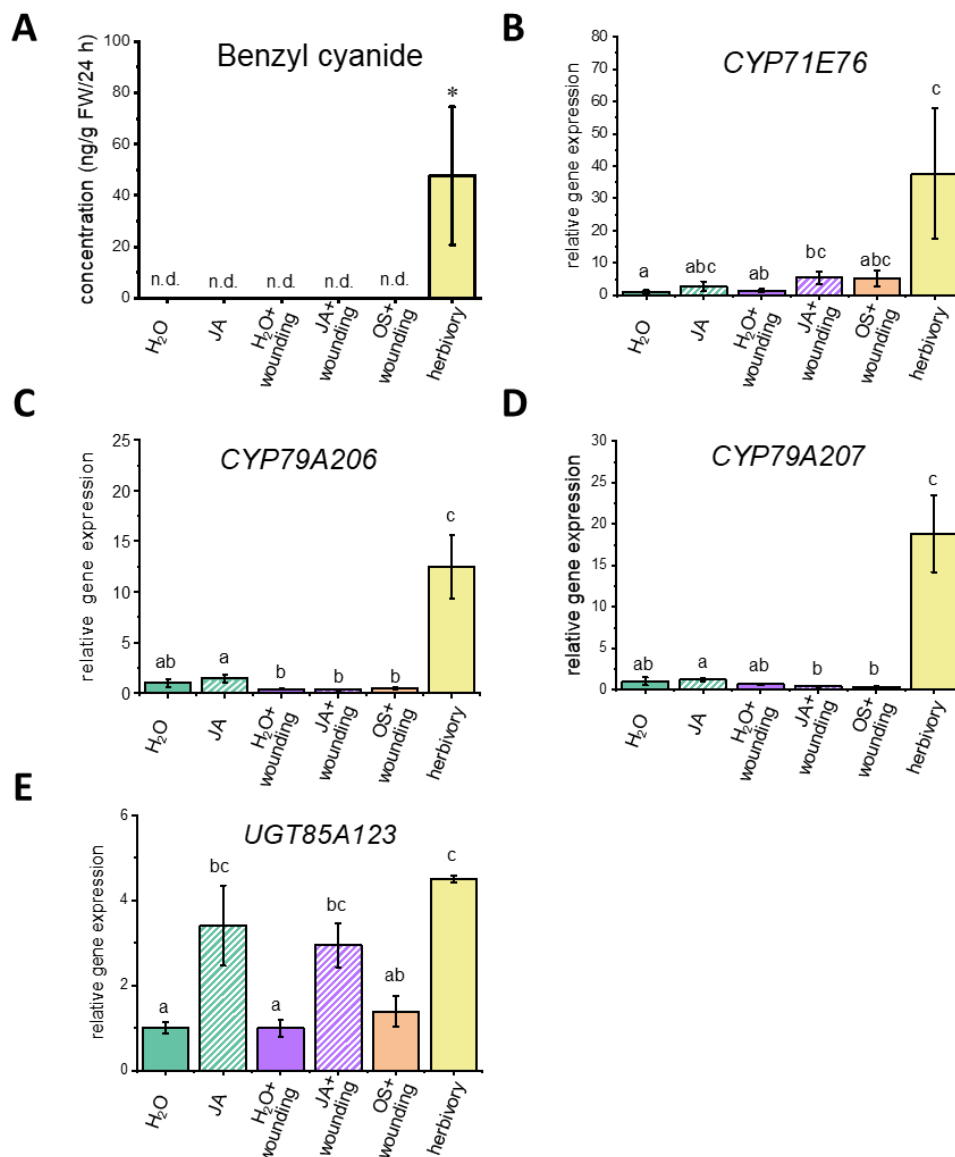


Figure S24: Gene expression of *CYP71E76*, *CYP79A206/207*, and *UGT85A123*, and formation of benzyl cyanide in toco leaves in response to different treatments (see Figure 6). Leaves were sprayed with jasmonic acid (JA), oral secretion (OS), or water (H₂O) after mechanical wounding or without further treatment. *S. littoralis* feeding served as a positive control. Volatiles were collected throughout the 24 h (after the) treatment, and quantified by GC-FID (**A**). Means \pm SEM are shown.; n = 6-11. Asterisk indicates significant accumulation of benzyl cyanide (> 0) based on Wilcoxon signed rank test, * = p < 0.05. All leaves were harvested 24 h after the (beginning of the) respective treatment, RNA extracted from leaf tissue, transcribed to cDNA, and qRT-PCRs performed (for primers see Table S8) with actin as housekeeping gene (**B,C,D,E**). Relative expression was calculated with the $\Delta\Delta$ Ct method (Pfaffl, 2001). Different letters indicate significant differences (p < 0.05) between treatments based on One Way ANOVAs ($F_{CYP71E76} = 5.842$, p = 0.001; $F_{UGT85A123} = 10.66$, p < 0.001) or GLS linear models (L-ratio_{CYP79A206} = 33.36, L-ratio_{CYP79A207} = 40.15, p < 0.001) analyses on log transformed data and subsequent Tukey *post hoc* tests.

Methodology: cDNA synthesis from 900 ng RNA was performed with the SuperScript™ III First-Strand Synthesis Kit (Thermo Scientific) using oligo (dT)₁₂₋₁₈ primers according to the manufacturer's instructions. The obtained cDNA was diluted 1:10 with ddH₂O. Primer pairs were designed to amplify the respective gene (Table S8), and their specificity confirmed by agarose gel electrophoresis, melting curve, and standard curve analysis. Samples were run in an optical 96-well plate on the CFX Connect Real-Time PCR System (Bio-Rad) with the Brilliant III Ultra-Fast SYBR Green QPCR Master Mix (Agilent). PCR conditions are given in Table S7. All samples were run in triplicates. Normalized fold expression was calculated with the $\Delta\Delta$ CP method (Pfaffl, 2001).

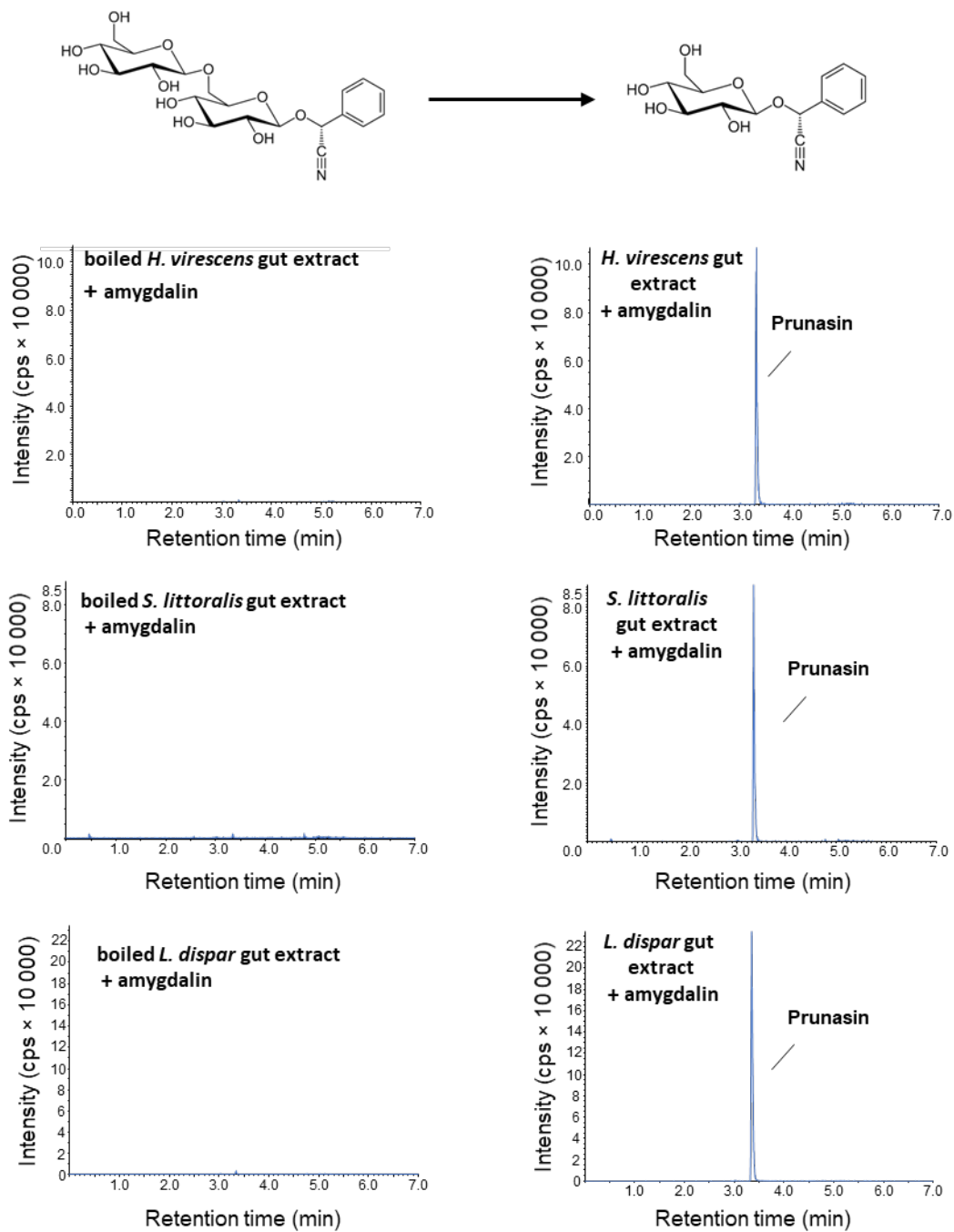


Figure S25: Deglycosylation of amygdalin by gut enzymes of different caterpillars. Gut extracts of *Heliiothis virescens*, *Spodoptera littoralis*, and *Lymantria dispar* were tested for their ability to form prunasin from amygdalin. Targeted LC-MS/MS analysis revealed glucosidase activities for all tested gut extracts. Boiled extracts were used as negative controls. Cps: counts per second.

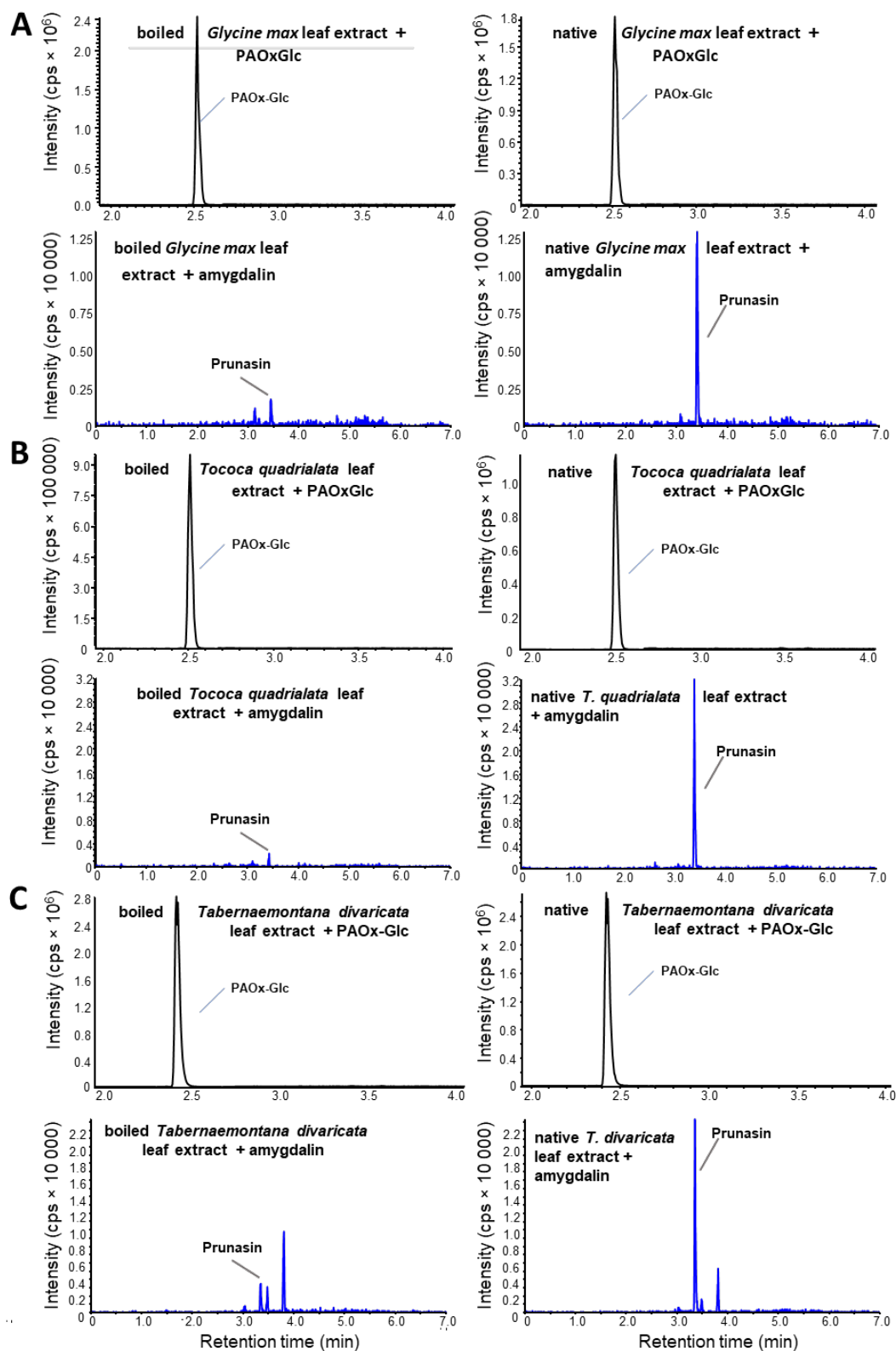
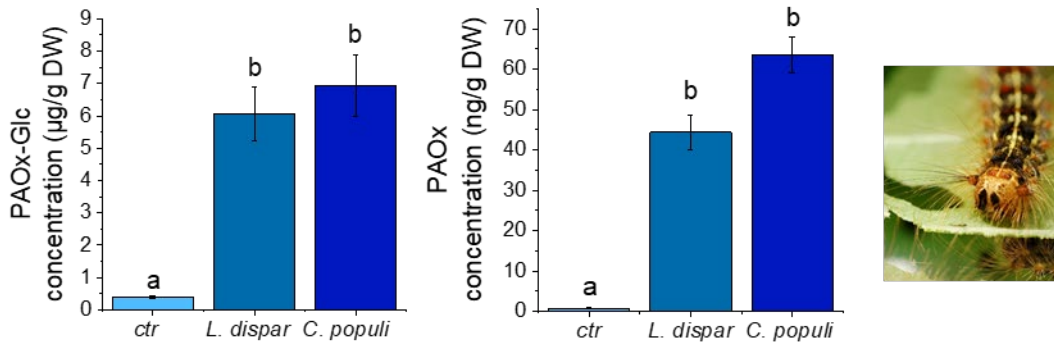
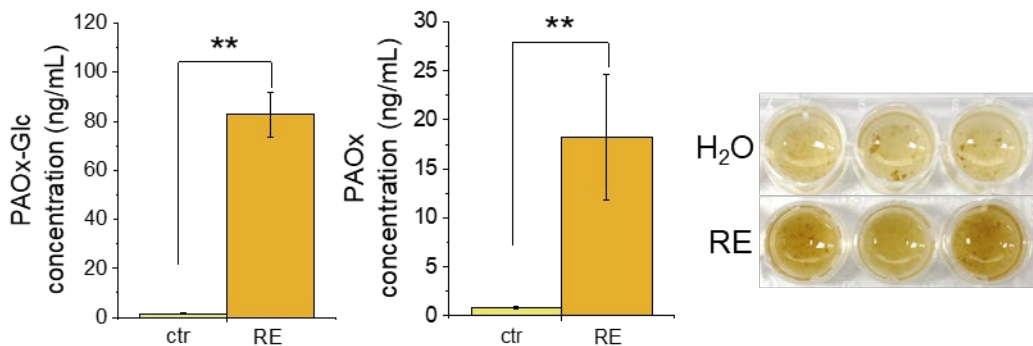


Figure S26: Deglycosylation of amygdalin but not PAOx-Glc by crude enzyme extracts of various plant species. Plant extracts of herbivore-damaged leaves of *Glycine max* (A), *Tococa quadrialata* (B), and *Tabernaemontana divaricata* (C) were tested for their ability to form prunasin from amygdalin and PAOx from PAOx-Glc. Targeted LC-MS/MS analysis revealed glucosidase activities towards amygdalin for these extracts. Boiled extracts served as negative controls. Cps: counts per second.

poplar leaves



soya cell culture



crape jasmine

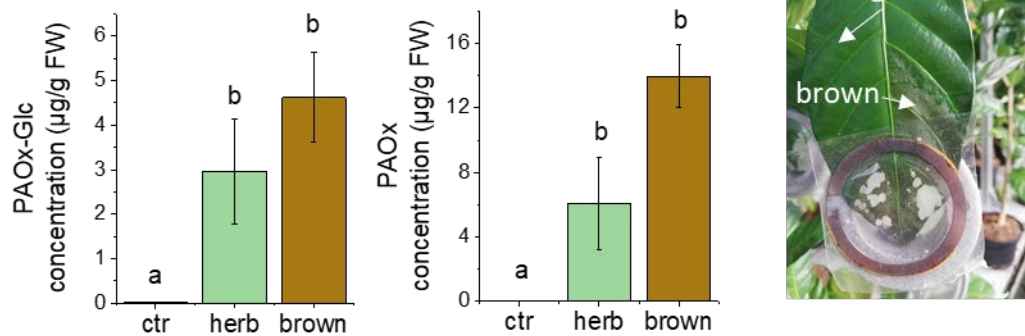


Figure S27: Identification of PAOx-Glc in different plant species upon biotic stress. Blue: accumulation in Western balsam poplar (*Populus trichocarpa*) leaves upon *Lymantria dispar* and *Chrysomela populi* feeding, One-Way ANOVA ($F_{\text{PAOx}} = 411.2$, $p < 0.001$; $F_{\text{PAOx-Glc}} = 125.1$, $p < 0.001$) with Tukey *post hoc* on log transformed data, different letters indicate significant differences ($p < 0.05$); $n = 8$; DW: dry weight. Yellow: soya bean cell cultures release PAOx and PAOx-Glc upon induction with raw elicitor (RE) from the oomycete *Phytophthora sojae*; Student's t-test; **: $p < 0.01$; $n = 6$. Green, brown: *Spodoptera littoralis*-wounded leaves of crape jasmine (*Tabernaemontana divaricata*) produce PAOx and PAOx-Glc; One-Way-ANOVA ($F_{\text{PAOx}} = 58.06$, $p < 0.001$; $F_{\text{PAOx-Glc}} = 34.38$, $p < 0.001$) with Tukey *post hoc* on log transformed data, different letters indicate significant differences ($p < 0.05$); $n = 3$; FW: fresh weight.

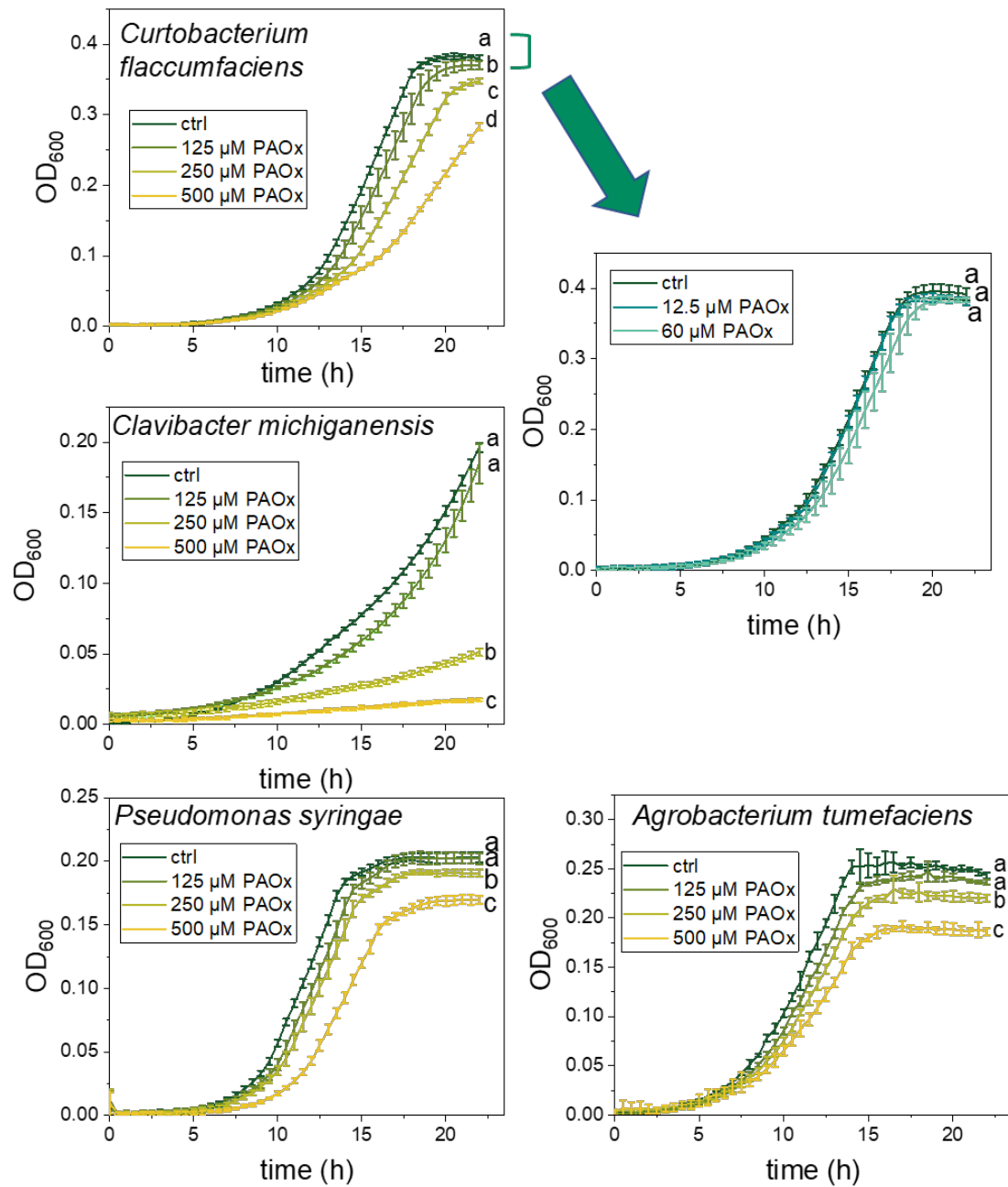


Figure S28: Negative effects of PAOx on the growth of several plant pathogenic bacteria. The effect of PAOx on gram-negative (*Agrobacterium tumefaciens*, *Pseudomonas syringae*) and gram-positive (*Curtobacterium flaccumfaciens*, *Clavibacter michiganensis*) bacteria strains was tested in a bacterial growth assay in microtiter plates. Growth of the cultures was monitored over 22 h by measuring the OD₆₀₀ every 30 min. Data are shown as means ± SD (n=3-6). Different letters indicate significant differences (p<0.05) between treatments after 22 h. *C. michiganensis*: log transformed; one-way ANOVA ($F_{C.michiganensis} = 1771$, p<0.001; $F_{A.tumefaciens} = 184.1$, p<0.001, $F_{P.syringae} = 108.8$, p<0.001) with Tukey HSD posthoc test or Kruskal-Wallis test ($\chi^2_{C.flaccumfaciens (highconc)} = 20.98$, p<0.001; $\chi^2_{C.flaccumfaciens (lowconc)} = 3.317$, p=0.19) followed by multiple pairwise comparisons using Wilcoxon rank sum tests with a Holm correction.

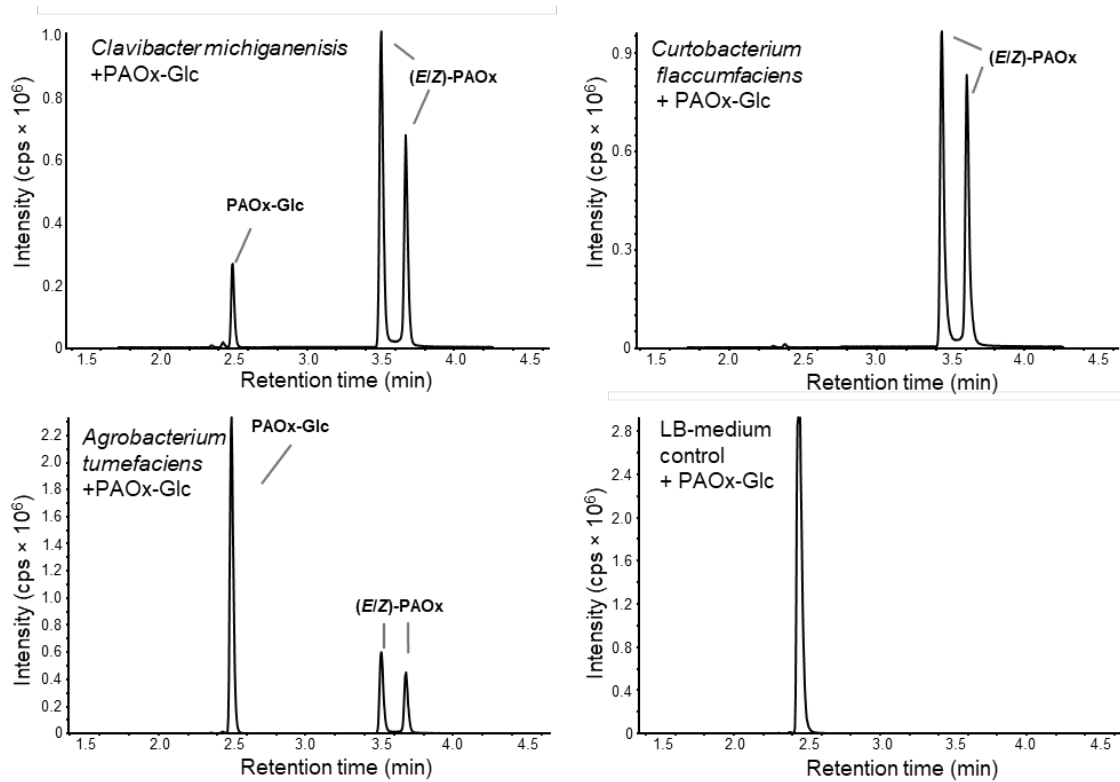


Figure S29: Several plant pathogenic bacteria are able to deglycosylate PAOx-Glc. Gram-negative (*Agrobacterium tumefaciens*) and gram-positive (*Curtobacterium flaccumfaciens*, *Clavibacter michiganensis*) bacteria strains were tested for their ability to deglycosylate PAOx-Glc. Bacteria were grown in the presence of PAOx-Glc for 24 h in a microtiter plate, and the LB-medium was analyzed afterwards using liquid chromatography-tandem mass spectrometry (LC-MS/MS).

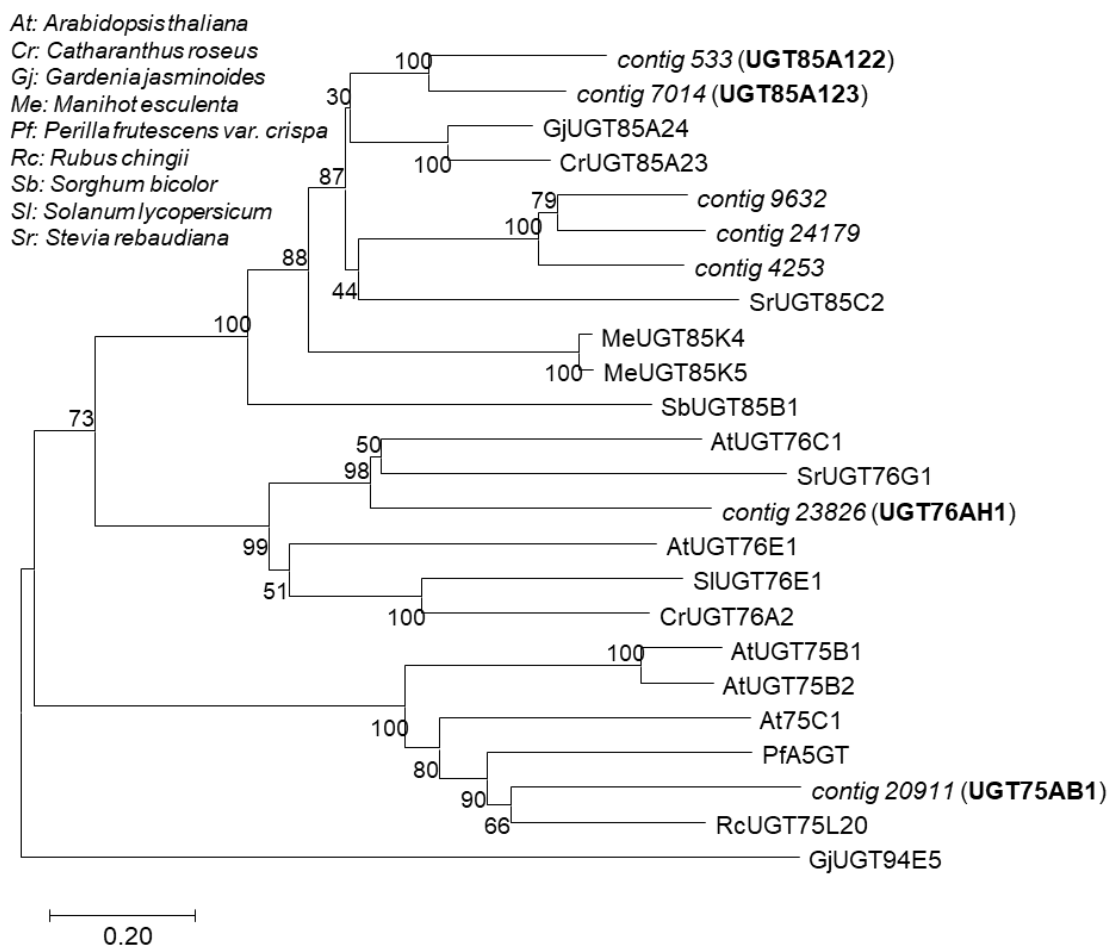


Figure S30: Phylogenetic tree of candidate UGTs from tocooca. The phylogenetic relationship of 7 putative *Tococa quadrialata* UGTs with already characterized UGTs of the respective subfamilies from other plants is shown. The tree was inferred with the Neighbor-joining method and $n = 1000$ replicates for bootstrapping. Bootstrap values are shown next to each node. The scale indicates in the number of substitutions per site. Putative UGTs from tocooca are shown in italics, the characterized ones in bold. GjUGT94E5 (BAK55744.1) was used as an outgroup. UGT: family 1 UDP-glycosyltransferase.

Table S1: Growth conditions for *Tococa quadrialata*

| Greenhouse conditions | |
|-------------------------|---|
| <i>Temperature</i> | |
| Day: | 23-25 °C |
| Night: | 16-18 °C |
| Humidity | 70% |
| Light/dark cycle | 16 h/8 h |
| composition of the soil | |
| <i>Percentage</i> | <i>Material</i> |
| 25% | Klasmann potting substrate (Klasmann-Deilmann, Geeste, Germany) |
| 25% | Latvian white peat |
| 25% | pine bark (7-15 mm) |
| 12.5% | Legaton (5-7 mm) |
| 12.5% | sand |
| Inoculated with | BioMyc™ Vital Mykorrhiza (BioMyc, Brandenburg, Germany). |

Table S2: Chromatographic gradients for the analysis of jasmonates, aldoximes, and prunasin using an LC-TripleQuad-MS system

| Gradient | HPLC | Solvents (A/B) | Flow (µl/min) | Time (min) | Temperature (°C) | Solvent A (%) | Solvent B (%) |
|----------|--------------|---|---------------|------------|------------------|---------------|---------------|
| A1 | Agilent 1200 | 0.2% FA in ddH ₂ O (A), Acetonitrile (B) | 1100 | 0 | 25 °C | 90 | 10 |
| | | | | 4 | | 30 | 70 |
| | | | | 4.1 | | 0 | 100 |
| | | | | 5 | | 0 | 100 |
| | | | | 5.1 | | 90 | 10 |
| | | | | 8 | | 90 | 10 |
| A2 | Agilent 1260 | 0.05% FA in ddH ₂ O, Acetonitrile (B) | 1100 | 0 | 20 °C | 90 | 10 |
| | | | | 4 | | 30 | 70 |
| | | | | 4.1 | | 0 | 100 |
| | | | | 5 | | 0 | 100 |
| | | | | 5.1 | | 90 | 10 |
| | | | | 8 | | 90 | 10 |
| B | Agilent 1260 | 0.05% FA in ddH ₂ O, Acetonitrile (B) | 1100 | 0 | 20 °C | 95 | 5 |
| | | | | 0.5 | | 95 | 5 |
| | | | | 4 | | 50 | 50 |
| | | | | 4.1 | | 0 | 100 |
| | | | | 4.5 | | 0 | 100 |
| | | | | 4.6 | | 95 | 5 |
| | | | | 7 | | 95 | 5 |
| C | Agilent 1260 | 0.05% FA in ddH ₂ O, Acetonitrile (B) | 1100 | 0 | 20 °C | 95 | 5 |
| | | | | 0.5 | | 95 | 5 |
| | | | | 6 | | 62.6 | 37.4 |
| | | | | 6.02 | | 80 | 80 |
| | | | | 7.5 | | 0 | 100 |
| | | | | 9.5 | | 0 | 100 |
| | | | | 9.52 | | 95 | 5 |
| | | | | 12 | | 95 | 5 |

All separations were achieved on a Zorbax Eclipse XDB C18 column (50 mm 4.6 mm, 1.8 µm, Agilent Technologies). For MS parameters, see Table S3.

Table S3: MRM parameters for the LC-MS/MS analysis of jasmonates, aldoximes, and prunasin using an LC-TripleQuad-MS system

| compound | Mass spectrometer | mode | HPLC gradient | Q1 | Q3 | DP (V) | CE (V) | Retention time (min) |
|------------------------------|-------------------|------|---------------|-------|-------|--------|--------|----------------------|
| (E/Z)-phenyl-acetaldoxime | API5000 | pos | A1 | 136.1 | 119.1 | 56 | 17 | 3.5; 3.7 |
| | API6500 | pos | A2 | 136.1 | 119.1 | 30 | 17 | 3.4; 3.6 |
| Phenylacetaldoxime glucoside | API5000 | pos | A1 | 298.0 | 136.0 | 70 | 13 | 2.5 |
| | API6500 | pos | A2 | 298.0 | 136.0 | 30 | 13 | 2.5 |
| Prunasin | API6500 | neg | B | 340.0 | 59.0 | -40 | -56 | 3.4 |
| JA | API6500 | neg | C | 209.1 | 59.0 | -30 | -24 | 7.2 |
| D ₆ -JA | API6500 | neg | C | 215.1 | 59.0 | -30 | -24 | 7.2 |
| D ₅ -JA | API6500 | neg | C | 214.1 | 59.0 | -30 | -24 | 7.2 |
| JA-Ile | API6500 | neg | C | 322.2 | 130.1 | -30 | -30 | 7.3 |
| D ₆ -JA-Ile | API6500 | neg | C | 328.2 | 130.1 | -30 | -30 | 7.3 |
| D ₅ -JA-Ile | API6500 | neg | C | 327.2 | 130.1 | -30 | -30 | 7.3 |

All separations were achieved according to Table S2.

Table S4: Temperature profile of benzyl cyanide measurements by GC-FID and GC-MS hexane extracts

| | | |
|----------------------------|--------|----------|
| Initial temperature | 60°C | 2 min |
| Ramp I | 60°C | |
| | ↓ | 6°C/min |
| | 160°C | |
| Ramp II | 160°C | |
| | ↓ | 60°C/min |
| | 300°C | |
| Final temperature | 300 °C | 2 min |

Table S5: Parameters used for the *de novo* assembly

| Assembly parameters | |
|---|------------------|
| Word size | 35 |
| Bubble size | 650 |
| Quality of the <i>de novo</i> assembly | |
| total contigs | 49,957 |
| N50 | 1,659 |
| Complete BUSCOs* | 78.5% |
| Missing BUSCOs* | 10.2% |
| Annotation | |
| BLAST2GO# | Swiss-Prot, NCBI |

*Benchmarking Universal Single-Copy Orthologs (BUSCO) analysis (<https://busco.ezlab.org/>, last accessed on 04.02.2022; (Simao et al., 2015))

#(Gotz et al., 2008)

Table S6: Buffers

| Name | Ingredients | pH |
|---|---|------|
| UGT resuspension buffer | 50 mM disodium hydrogen phosphate | 7.4 |
| | 500 mM sodium chloride | |
| | 10 mM imidazole | |
| | 10% glycerol | |
| | 10 ⁻² v/v protease inhibitor Mix HP (SERVA, Heidelberg, Germany) | |
| | 10 ⁻⁴ v/v Novagen® Benzonase® Nuclease (Merck) | |
| UGT assay buffer | 50 mM Tris-HCl | 7.5 |
| | 10% glycerol | |
| Gut protein extraction buffer | 50 mM citric acid | 6.5 |
| | 100 mM disodium hydrogen phosphate | |
| | 5×10 ⁻³ v/v protease inhibitor Mix HP (SERVA) | |
| Tococa protein extraction buffer | 25 mM HEPES | 7.2 |
| | 3% PVPP | |
| | 1% PVP | |
| | 4% Amberlite XAD4 | |
| | 1 mM EDTA | |
| | 5 mM Na ₂ HSO ₃ | |
| | 5 mM DTT | |
| 5×10 ⁻³ v/v protease inhibitor cocktail III (Calbiochem) | | |
| Glucosidase assay buffer | 50 mM citric acid | 6.5 |
| | 100 mM disodium hydrogen phosphate | |
| Infiltration buffer | 10mM MES | 5.7 |
| | 10mM MgCl ₂ | |
| | 100 µM acetosyringone | |
| LB selection media | LB media | n.a. |
| | 50 µg/ml kanamycin | |
| | 10 µg/ml rifampicin | |
| | 25 µg/ml gentamicin | |

Table S7: Thermocycler program for qPCR

| Phase | Time | | Temperature | |
|-------------------------|------------|-----------|--------------|-------|
| | Figure S24 | Figure 13 | | |
| Initial denaturation | 3 min | 3 min | 95 °C | |
| denaturation | 10 s | 20 s | 95 °C | } 40× |
| Annealing and extension | 10 s | 20 s | 60 °C | |
| Plate read | | | | |
| Final denaturation | 1 min | 1 min | 95 °C | |
| Melting curve | 5 s | 5 s | 55 °C→ 95 °C | |

Table S8: List of primers used for qPCR

| Name | Sequence | Amplicon length |
|--------------------|--------------------------|-----------------|
| CYP79A206_qPCR_fwd | CGACCTTCGTGTTACTTTACGC | 140 bp |
| CYP79A206_qPCR_rev | ACGGGCTTGTAGAGAGCATC | 140 bp |
| CYP79A207_qPCR_fwd | ACCTTCGTTCGTGCTTTACGC | 150 bp |
| CYP79A207_qPCR_rev | TCCAACGGAACACTGGCTTG | 150 bp |
| CYP71E76_qPCR_fwd | CGGAAACCTTCACCAACTCGG | 140 bp |
| CYP71E76_qPCR_rev | GCACCTCCTTAGCCATCTCG | 140 bp |
| UGT85A123_qPCR_fwd | CCCCCGTTAGTTGCGTAGTG | 200 bp |
| UGT85A123_qPCR_rev | CGACCGTGTCCAAGTATCCGT | 200 bp |
| UGT85A122_qPCR_fwd | ATCCCCACATTCATCCAGACGACC | 140 bp |
| UGT85A122_qPCR_rev | CGACTTCAAGGCACGCAGAAC | 140 bp |
| UGT75AB1_qPCR_fwd | TTCAACCCGCCACCGTCTTC | 300 bp |
| UGT75AB1_qPCR_rev | GCCTTCACCGCTTCTGCCT | 300 bp |
| Actin_fwd | CTCTGGTGATGGTGTCAGTCAC | 140 bp |
| Actin_rev | TGTAACCCCTTTCCGGTGAGG | 140 bp |

Table S9: Primers used for cloning.

| Name | Sequence | Usage |
|---------------------|---|---------------------------|
| CYP79A206_subc_fwd | ATGAATATTTCTGCTTCCGCC | cloning, in pJET1.2/blunt |
| CYP79A206_subc_rev | CTAGAATGACGGGTAAAGGTG | cloning, in pJET1.2/blunt |
| CYP79A207_subc_fwd | ATGAATATTTCCGCTTACGC | cloning, in pJET1.2/blunt |
| CYP79A207_subc_rev | CTAGAATGATGGGTAAAGGTG | cloning, in pJET1.2/blunt |
| CYP71E76_subc_fwd | ATGTCTTCTACAATTATTTCTTC | cloning, in pJET1.2/blunt |
| CYP71E76_subc_rev | TTAATTATATTTAGTTGGAACCAAACG | cloning, in pJET1.2/blunt |
| UGT85A123_subc_fwd | ATGAGTTCTGAACAAGAACAGAGC | cloning, in pJET1.2/blunt |
| UGT85A123_subc_rev | TCATTGCTCGGAAAGAAGCAGTG | cloning, in pJET1.2/blunt |
| CYP79A206_NotI_fwd | CAAGCGGCCGCA ATGAATATTTCTGCTTCCG | cloning, in pESC-Leu2d |
| CYP79A206_PacI_rev | GTC <u>TTAATTA</u> ACTAGAATGACGGGTAAAGGTG | cloning, in pESC-Leu2d |
| CYP79A207_SpeI_fwd | AAG <u>ACTAGTA</u> ATGAATATTTCCGCTTACGC | cloning, in pESC-Leu2d |
| CYP79A207_SacI_rev | ACA <u>GAGCTC</u> CTAGAATGATGGGTAAAGGTG | cloning, in pESC-Leu2d |
| CYP71E76_SpeI_fwd | TAA <u>ACTAGTA</u> ATGTCTTCTACAATTATTTCTTC | cloning, in pESC-Leu2d |
| CYP71E76_SacI_rev | ACG <u>GAGCTC</u> TTAATTATTTAGTTGGAACCAAAC | cloning, in pESC-Leu2d |
| CYP79A206_USER_fwd | GGCTTAAU ATGAATATTTCTGCTTCCGCCG | cloning, in pCAMBIA2300U |
| CYP79A206_USER_rev | GGTTAAU CTAGAATGACGGGTAAAGGTGC | cloning, in pCAMBIA2300U |
| CYP79A207_USER_fwd | GGCTTAAU ATGAATATTTCCGCTTACGCCG | cloning, in pCAMBIA2300U |
| CYP79A207_USER_rev | GGTTAAU CTAGAATGATGGGTAAAGGTGC | cloning, in pCAMBIA2300U |
| CYP71E76_USER_fwd | GGCTTAAU ATGTCTTCTACAATTATTTCTTCCC | cloning, in pCAMBIA2300U |
| CYP71E76_USER_rev | GGTTAAU TTAATTATATTTAGTTGGAACCAAACGC | cloning, in pCAMBIA2300U |
| UGT85A123_USER_fwd | GGCTTAAU ATGAGTTCTGAACAAGAACAGAGC | cloning, in pCAMBIA2300U |
| UGT85A123_USER_rev | GGTTAAU TCATTGCTCGGAAAGAAGCAGTG | cloning, in pCAMBIA2300U |
| UGT76AH1_pET100_fwd | <u>CACCATGGGCACA</u> CCTCAAGTCAAG | cloning, in pET100 |
| UGT76AH1_pET100_rev | TTATAATTTTCCGTTGGCATGAG | cloning, in pET100 |

Primer name indicates the gene to be amplified. The important sequence motif for cloning in the respective vector is underlined or in bold

Table S10: UGT candidate genes for the glycosylation of PAOx-Glc.

| Feature ID | P-value | Fold change | ctr - Mean RPKM | herb - Mean RPKM | UGT sub-family | Length | SWISSPROT: Description | NCBI: Description |
|---------------------|---------|-------------|-----------------|------------------|----------------|--------|--|--|
| contig_533 | 0.000 | 7 | 32 | 221 | UGT8_5 | 1928 | UGT2_GARJA ame: Full=7-deoxyloganetin glucosyltransferase ame: Full=Genipin glucosyltransferase ame: Full=UDP-glucose glucosyltransferase 2 Short= 2 ame: Full=UDP-glycosyltransferase 85A24 | 7-deoxyloganetin glucosyltransferase-like |
| contig_7014 | 0.000 | 4 | 15 | 67 | UGT8_5 | 2692 | UGT2_GARJA ame: Full=7-deoxyloganetin glucosyltransferase ame: Full=Genipin glucosyltransferase ame: Full=UDP-glucose glucosyltransferase 2 Short= 2 ame: Full=UDP-glycosyltransferase 85A24 | 7-deoxyloganetin glucosyltransferase-like isoform X1 |
| contig_4253 | 0.002 | 2 | 16 | 38 | UGT8_5 | 1657 | UGT2_GARJA ame: Full=7-deoxyloganetin glucosyltransferase ame: Full=Genipin glucosyltransferase ame: Full=UDP-glucose glucosyltransferase 2 Short= 2 ame: Full=UDP-glycosyltransferase 85A24 | 7-deoxyloganetin glucosyltransferase |
| contig_24179 | 0.001 | 6 | 3 | 16 | UGT8_5 | 1176 | U85A3_ARATH ame: Full=UDP-glycosyltransferase 85A3 | 7-deoxyloganetin glucosyltransferase |
| contig_9632 | 0.022 | 5 | 1 | 5 | UGT8_5 | 1630 | UGT2_GARJA ame: Full=7-deoxyloganetin glucosyltransferase ame: Full=Genipin glucosyltransferase ame: Full=UDP-glucose glucosyltransferase 2 Short= 2 ame: Full=UDP-glycosyltransferase 85A24 | 7-deoxyloganetin glucosyltransferase |
| contig_23826 | 0.001 | 15 | 0 | 6 | UGT7_6 | 1597 | U76B1_ARATH ame: Full=UDP-glycosyltransferase 76B1 | UDP-glycosyltransferase 76C2 |
| contig_329 | 0.012 | 2 | 7 | 15 | UGT7_6 | 2943 | UGT7_CATRO ame: Full=UDP-glucose iridoid glucosyltransferase ame: Full=UDP-glucose glucosyltransferase 7 Short= 7 ame: Full=UDP-glycosyltransferase 76A2 | UDP-glucose iridoid glucosyltransferase |
| contig_20911 | 0.007 | 4 | 67 | 237 | UGT7_5 | 1978 | UGT1_GARJA ame: Full=Crocin chloroplastic ame: Full=UDP-glucose glucosyltransferase 1 Short= 1 ame: Full=UDP-glycosyltransferase 75L6 Flags: Precursor | crocin chloroplastic |
| contig_11576 | 0.045 | 3 | 1 | 5 | UGT7_5 | 1121 | UGT1_GARJA ame: Full=Crocin chloroplastic ame: Full=UDP-glucose glucosyltransferase 1 Short= 1 ame: Full=UDP-glycosyltransferase 75L6 Flags: Precursor | crocin chloroplastic |
| contig_5159 | 0.000 | 3 | 17 | 54 | UGT7_3 | 1855 | SCGT_TOBAC ame: Full=Scopoletin glucosyltransferase ame: Full=Phenylpropanoid:glucosyltransferase 1 | scopoletin glucosyltransferase |
| contig_5158 | 0.000 | 5 | 8 | 44 | UGT7_3 | 1042 | SCGT_TOBAC ame: Full=Scopoletin glucosyltransferase ame: Full=Phenylpropanoid:glucosyltransferase 1 | scopoletin glucosyltransferase |
| contig_9912 | 0.045 | 2 | 3 | 8 | UGT7_3 | 1858 | SCGT_TOBAC ame: Full=Scopoletin glucosyltransferase ame: Full=Phenylpropanoid:glucosyltransferase 1 | scopoletin glucosyltransferase |
| contig_9005 | 0.021 | 3 | 3 | 7 | UGT8_3 | 1627 | U83A1_ARATH ame: Full=UDP-glycosyltransferase 83A1 | UDP-glycosyltransferase 83A1 |
| contig_8815 | 0.003 | 2 | 21 | 47 | UGT8_9 | 1638 | U89A2_ARATH ame: Full=UDP-glycosyltransferase 89A2 | UDP-glycosyltransferase 89A2-like |

All contigs of the *de novo* assembly encoding glycosyltransferase family 1 type glycosyltransferases with a minimum sequence length of 1000 bp that are significantly upregulated upon herbivore damage ($p < 0.05$, fold change ≥ 2) are listed. Sequences chosen for further characterization are in bold. Selection was based on UGT subfamily, RPKM values and fold change in herbivore-damaged samples.

Table S11: Non-target metabolite analysis by LC-ESI-Q-ToF-MS

| Chromatographic gradients for untargeted metabolite analysis using ultra-high-performance liquid chromatography–electrospray ionization– high resolution mass spectrometry (UHPLC–ESI–HRMS) | | | | | | | |
|--|--|---|---------------------------------|--------------------------|-------------------------|-------------------------|---|
| HPLC | column | Solvents (A/B) | Flow (µl/min) | Time (min) | Temperature (°C) | Solvent A (%) | Solvent B (%) |
| Dionex Ultimate 3000 series UHPLC (Thermo Scientific) | Zorbax Eclipse XDB-C18 column (100 mm × 2.1 mm, 1.8 µm, Agilent) | 0.1% FA in ddH ₂ O (A), Acetonitrile (B) | 300 | 0 | 25 °C | 95 | 5 |
| | | | | 0.5 | | 95 | 5 |
| | | | | 11 | | 40 | 60 |
| | | | | 11.1 | | 0 | 100 |
| | | | | 12 | | 0 | 100 |
| | | | | 12.1 | | 95 | 5 |
| 15 | 95 | 5 | | | | | |
| Parameters of the Bruker timsToF mass spectrometer (Bruker Daltonics, Bremen, Germany) | | | | | | | |
| Mode | Capillary voltage (kV) | End plate offset (V) | Nebulizer pressure (bar) | Drying gas | Acquisition (Hz) | Mass range (m/z) | Data processing software |
| positive | 4.5 | 500 | 2.8 | Nitrogen (8L/min, 280°C) | 12 | 50-1500 | MetaboScape (Bruker Daltonics) |
| negative | -3.5 | 500 | 2.8 | Nitrogen (8L/min, 280°C) | 12 | 50-1500 | MetaboScape software (Bruker Daltonics) |

At the beginning of each chromatographic analysis 10 µL of a sodium formate-isopropanol solution (10 mM solution of NaOH in 50/50 (v/v) isopropanol- water containing 0.2% formic acid) was injected into the dead volume of the sample injection for recalibration of the mass spectrometer using the expected cluster ion *m/z* values.

Table S12: Codon-optimized ORF of tococa UGTs for expression in *Escherichia coli*.dffg

| Encoded enzyme | Codon optimized nucleotide sequence |
|----------------|---|
| UGT85A122 | ATGGCACGTGATAGCGCAGTTGAAGCACTGCCTGGCACCAAAACCGCATGCAATTATTGTTCCGTA TCCGGCACAGGGTCATATTAATCCGCTGCTGAAACTGGCAAAAATTCTGCATGGTCTGGTGGTT TTCATGTGACCTTTGTTAATACCGAATAAACGCACGTCTGCTGCTGCGTAGCCGTGGTCCGACC AGCCTGGATGATATGCCAGGTTTTTCATTTTGAACCATTCGGATGGTCTGCCTCCGGTTGATGC AGATGTTATGCAGGATGTTCCGGCACTGAGCGATAGCCTGAGCCGTACCTGTTTTGAACCGTTG TTGAACTGGTTAGCAAAGTGAATCAGCATGGTGGTCCGCCTGCAACCTGCTTTGTTATGATGCA ATGATGCCGTTTGTGGCAGATGCAGCAGAAAAATTTGGTCTGCCAGCAGTTGCATTTTGGCCTCC GGCAGCATGTGCAATTTGGGGTGTGCACAGTATCCGAAACTGATTGAAAAAGGTCTGGTTCCGC TGAAGATAGCAGTTATCTGAGCAATGGTTTTCTGGATACCGTGATTGAATGGATCCGGGTATTG ATAATTTTCGCTGCGTGATATTCGACCTTTATTCAGACCACCGATCCGAATGATATATGGTG ATTACATGATTCGTAGCGTTGAAGTGAGCAGCAAAAAAGCATGTGCCGTTGTGTTAATACCTTTG ATGCACTGGAAGCAGATGTTCTGCGTGCCTGAAAAGCATTATCCGAGCATTATACCGTTGGT CCGCTGAATCTGGTTCTGGATCGTTATCCGGAAGAAGAACTGACCGCAGTTGGTAGCAATCTGTG GAAAGAAGATAATAGCTGTCTGAAATGGCTGGATAGCCAAGAACATGTAGCCTGTTTATGTA ATTTTGGTAGCATTACCGTTGCAACCGCAGAGCAGATGACCGAATTTGCATGGGGTTGCAAAAT AGCCGTATGCCGTTTCTGTGGGTTATTCGTCCGGATCTGGTTGTTGGTGAAGCGCAGTGTGC CACCGGTTTTACCGATGAAACCAGCGATCGTTGATGATTAGCGTTGGTGTCCGCAAGAAGAA GTTCTGAAACATCCGAGTATTGGTGGCTTTCTGACCCATAGTGGTTGGAATAGCACCTGGAAAG CATGAGTGCCGGTGTCCGATGTTTTGTTGGCCGTTTTTTGCCGATGACAGACCAATGTTGGT ATGGTAAAAATAGCTGGGGTATCGGCATGGAAATTGATCATGATGTGAAACCGCATAAAGTGGAA GGTATGTTAAAGAACTGATGGAAGGTGAAAGGGCAAAAGAAATGAAACGTCGTGCAGCAGGTT GGCGTAGCGCAGCCGAAAAAGCAGTTGCCCTGGTGGTAGCAGCTATAAAACCTGGAAAAACT GCTGAGCCTGCTGCTGCCAAAAATGA |
| UGT85A123 | ATGAGCAGCGAACAAGAACAGAGCATGAAAACCCATGTTTCATCCGAATCCGAAACCGCATGCAG TTTTTATTCCGTATCCGGCACAGGGTCATATTAATCCGATTCTGAAACTGGCAAAAATGCTGCATC GTTGTGCATGGCTTTCATGTTACCTTTGTGCATACCGAATAAACCATCGTCTGCTGCGTAGCC GTGGTCCGGATAGCCTGCTGGGTCTGCCTGGTTTTCGTTTTGAAACCATTCGGATGGTCTGCCT CCGACACCGGAAGATGCAAGTGATGATGTTACCCAGGATATTCGGACCTGTGTGATAGCACCA GCCGTACCTGTACCGCACCGTTTATTAGCCTGGTGCCTGCTGAATGCCGAAGAAGGTGGTCC GCCTGTTAGCTGTGTTGTTTTGATGGTGAATGAGCTTTGCACTGGATGCAACCGAAGAATTTG GTTTCCGGGTGTTGCATATTGGACCCGAGCGCATGTGGTGTCTGGCATAATAGCTATTATCAT AAGCTGGTCGAAAAAGGTCTGAGTCCGCTGAAAGATAGCAGTTATCTGACCAATGGTTATCTGGA TACCGTTGTTGATTGGATTCCGGGTATGAAAAAAACATTTGCTGCGTGATCTGCCGAGCTTTAT TCGTACCACCGATCCGAATGATGTGATGGTGAATTATGTGATTGGCGAAATTCAGCGTACCAGCC AGAAAAGCAGCGCACTGGTTCTGAATACCTTTGACAACTGGAAAAAGATGTTCTGGATGCACCTG AGCGCAATTTTCCGAGCGTTTATGCAATTGGTCCGATTAATCTGATGCTGGATCGTTAGTGAT GAAGATCTGGATAGCATTGGTAGCAATCTGTGGAAAGAAGAAAAATTTGGTGTCTGCATTGGCTGGA TAGCCAGGATCTGGGTAGCCTTATTTATGTTAATTTTGGCAGCATTACCGTGGCAACCAAGAGC AGATTACCGAATTTGCATGGGGTTTAGCAGATAGCAAAAAACCGTTTTCTGTGGGTTATTCTGCCG GATCTGGTTATTGGTGAAGCGCAGTTCTGCCTCCAGTTTTGGTGAACCAACCGTGTG GTATTCTGAGCGGTTGGTGTCCGCAAGAAGTGGTCTGAAACATCCGAGCATTGGTGGTTTTCTG ACCCATTGTGGTTGGAATAGCATGATGAAAGCGTTTGTAGCGGTGTGCCGTTATTTGTTGGCC GTTTTTTGCAGAACAGCAGACCAATTGTTGGTATGGTAAAAATGCCTGGGGTATTGGCATGGAAA TGGATAATGAAGTGAACCGCGACGAAGTTGAAGGTATGGTTCGTGAATGATGGATGGCGAAAAA GGCAAAAGAAATGAAACGTCGTGCAGCAGAATGGAAAGCAGCCGCAAGAAGAGCAGCAGCACT GGTGGTAGCAGCCATCAGAATCTGAAAAACTGGTTGCACTGCTGCTGAGCGAACAGTAA |
| UGT75AB1 | ATGGCACCGCCTAATTTCTGCTGTTACCTTTCCCTGGTCAGGGTCATATTAATCCGAGCCTGCG TTTTGCAGAACGTCGATTCGATTGGTTGTCATGTTACCTTTACCACCGCACTGAGCGCACGTC GTCGTATGAGCGATAGCAAAAGCCCTCCGCTGAAGGTCTGAGTTTTGCAACCTTTAGTGATGGT TATGATGAGGGCATTAAAGAAGCAGAATCGGATCTGGATGTGATATGAAAGAAATTACCCGTCG TGGTCCGGAACACTGCGTGAACGATTCTGGA AAAACGTCGATCGTGCCACCAATTTTACCACA TCTTTTTTACCATTCTGATGCCGTGGGCAGCAGATGTTGCACAGAGCCTGGGTCTGCGTAGCACC CTGGTTGGATTGAGCCTGCAACCGTTTTGATATCTACTACTACATTCACCTCAACGGCTATGACCAG CTGATTCGTTCAAGCGCAGATGCAGCAGCAGCCGATAATGGTATAGCCGTGAAATTCGCTGCTGC CTGGTATGCTGCCGATGACCAGCAGCTATTTCCGAGCTTTCTGGCAAGCGGTAATCAGTATCAT TTTTCACTGCCGGTATCAACGCCATTTTGAATTTCTGAATAGCGAAAAACCGGCACCATGAA CCGAAAGTTCTGGTTAATACCTTTGAAGAAGTGAAGCAGAAAGCGGTTAAAGCAATTGATGAAC GAATGTTATTCGGTGGTCCGTTTATTCCGCTGGCATTCTGGATGAACAGCATCCGACCGGATA CCAGCTTAGGTGGTACCTGTTTCAGAAAAAGCGGTGATCTGGATTATATTGACTGGCTGAATAAA CAGCAGGCAGCAAGCGTTATCTATATTAGCTTTGGTAGCCTGAGCCTGTTTAGCCGTCCGAGAA AGAAGAAATGGCAAAAGCACTGATTGCAATGGGTCTGCTGGTTTTCTGGGTTATTGTAACCGTA TGGGTGAAGAAGAGGAAGAGGACGATAAACTGAGCTATGAAGAAGAAGTGTGAGCAAACTGGTAT GATTGTTCCGTGGTGTAGCCAGGTTGAAGTTCTGAGCAATCCGAGCGTTGGTTGTTTTGTTACCC ATTGTGGTTGGAATAGCACCAGCGAAAGCCTGGTTTGTGGTGTCCGATGGTTGGTTTTCCGCGAG TGGTCAGATCAGCAGACCAATGCAAACTGGTTGAAGAGGTTGGCGTACCCTGGTTAGGTTG GTAAAGGCAATGGTGAAGGTGTTGTTGAAGCCGGTGAATGAACTGAGCTGTCTGGAAGTTGTTTTA GGTGATGGTGA AAAAGGTGCTGAACTGCGTGGTAAATGCAAAAAATGGGGTGAACCTGGCAAAA AAGCAGCAAAAGATGGTGGTAGCAGCGATAAATCTGCGTCTGTTTTGTTGATGGTCTGGTTAA GGCACCGCAAGCAGCGAATAA |

Table S13: Accession numbers of known enzymes that were used for the construction of the phylogenetic trees.

| Name | Accession number | Plant species | Name | Accession number | Plant species |
|----------------------|------------------|-------------------------------|--------------|-------------------|------------------------------|
| CYP79 enzymes | | | | | |
| AtCYP79A2 | ANM70027.1 | <i>Arabidopsis thaliana</i> | MeCYP79D1 | AAF27289 | <i>Manihot esculenta</i> |
| AtCYP79B2 | AEE87143.1 | <i>Arabidopsis thaliana</i> | PtCYP79D6 | AHF20912 | <i>Populus trichocarpa</i> |
| AtCYP79F1 | AEE29448 | <i>Arabidopsis thaliana</i> | PtCYP79D7 | AHF20913 | <i>Populus trichocarpa</i> |
| AtCYP79F2 | AAG24796 | <i>Arabidopsis thaliana</i> | JaCYP79A68 | BAP15883.1 | <i>Prunus mume</i> |
| EcoCYP79D62 | AOW44274 | <i>Erythroxylum coca</i> | JaCYP79D16 | BAP15884.1 | <i>Prunus mume</i> |
| EfCYP79D60 | KX344462 | <i>Erythroxylum fischeri</i> | SaCYP79B1 | AAD03415 | <i>Sinapis alba</i> |
| EcCYP79A125 | AYN73067 | <i>Eucalyptus cladocalyx</i> | SbCYP79A1 | AAA85440.1 | <i>Sorghum bicolor</i> |
| LjCYP79D4 | AAT11921.1 | <i>Lotus japonicus</i> | TmCYP79E1 | AAF66543 | <i>Triglochin maritima</i> |
| MeCYP79D2 | AAV97888.1 | <i>Manihot esculenta</i> | TmCYP79E2 | AAF66544 | <i>Triglochin maritima</i> |
| CYP71 enzymes | | | | | |
| EcCYP706C55 | AYN73068 | <i>Eucalyptus cladocalyx</i> | PtCYP71B40v3 | AIU56748 | <i>Populus trichocarpa</i> |
| FsCYP71AT96 | BAU59406 | <i>Fallopia sachalinensis</i> | PtCYP71B41v2 | AIU56747 | <i>Populus trichocarpa</i> |
| HvCYP71C113 | AK250744 | <i>Hordeum vulgare L.</i> | PmCYP71AN24 | BAP15888.1 | <i>Prunus mume</i> |
| HvCYP71L1 | AK248375 | <i>Hordeum vulgare L.</i> | SbCYP71E1 | AAC39318 | <i>Sorghum bicolor</i> |
| MeCYP71E7 | AAP57704.1 | <i>Manihot esculenta</i> | | | |
| UGT enzymes | | | | | |
| AtUGT76E1 | AED97208.1 | <i>Arabidopsis thaliana</i> | AtUGT75B1 | AEE27854.1 | <i>Arabidopsis thaliana</i> |
| AtUGT76C1 | AAP21281.1 | <i>Arabidopsis thaliana</i> | AtUGT75B2 | AEE27849.1 | <i>Arabidopsis thaliana</i> |
| CrUGT76A2 | BAO01108.1 | <i>Catharanthus roseus</i> | AtUGT75C1 | AAM47973.1 | <i>Arabidopsis thaliana</i> |
| SIUGT76E1 | NP001348276.1 | <i>Solanum lycopersicum</i> | PfA5GT | Q9ZR27 | <i>Perilla frutescens</i> |
| SrUGT76G1 | AAR06912.1 | <i>Stevia rebaudiana</i> | RcUGT75L20 | AWU66062.1 | <i>Rubus chingii</i> |
| AtUGT85A2 | BAA34687 | <i>Arabidopsis thaliana</i> | LuUGT85Q1 | ADV36300 | <i>Linum unisitatissimum</i> |
| AtUGT85A5 | AAF87255 | <i>Arabidopsis thaliana</i> | LjUGT85K3 | CM0241.610 (gene) | <i>Lotus japonicus</i> |
| AtUGT85A7 | AAF87257 | <i>Arabidopsis thaliana</i> | MeUGT85K4 | AEO45781.1 | <i>Manihot esculenta</i> |
| AtUGT85A1 | AAF18537 | <i>Arabidopsis thaliana</i> | MeUGT85K5 | AEO45782.1 | <i>Manihot esculenta</i> |
| CrUGT85A23 | BAK55749.1 | <i>Catharanthus roseus</i> | MtUGT85H2 | ABI94024.1 | <i>Medicago truncatula</i> |
| EcUGT85A59 | AYN73070.1 | <i>Eucalyptus cladocalyx</i> | PIUGT85K31 | VVC51334.1 | <i>Phaseolus lunatus</i> |
| GjUGT85A24 | BAK55737.1 | <i>Gardenia jasminoides</i> | PdUGT85A19 | ABV68925.1 | <i>Prunus dulcis</i> |
| GjUGT94E5 | BAK55744.1 | <i>Gardenia jasminoides</i> | PmUGT85A47 | BBE52863.1 | <i>Prunus mume</i> |
| HvUGT85F22 | AK252107 | <i>Hordeum vulgare L.</i> | SbUGT85B1 | AAF17077.1 | <i>Sorghum bicolor</i> |
| HvUGT85F23 | AK250769 | <i>Hordeum vulgare L.</i> | SrUGT85C2 | AAR06916.1 | <i>Stevia rebaudiana</i> |

Sequence data for all characterized enzymes can be found under the respective Genbank identifier.

Literature:

Bak S, Kahn RA, Nielsen HL, Moller BL, Halkier BA (1998) Cloning of three A-type cytochromes P450, CYP71E1, CYP98, and CYP99 from *Sorghum bicolor* (L.) Moench by a PCR approach and identification by expression in *Escherichia coli* of CYP71E1 as a multifunctional cytochrome P450 in the biosynthesis of the cyanogenic glucoside dhurrin. *Plant Mol Biol* **36**: 393-405

Durst F, Nelson DR (1995) Diversity and Evolution of Plant P450 and P450-Reductases. *Drug Metabolism and Drug Interactions* **12**: 189-206

Gachon CMM, Langlois-Meurinne M, Saindrenan P (2005) Plant secondary metabolism glycosyltransferases: the emerging functional analysis. *Trends in Plant Science* **10**: 542-549

Gotz S, Garcia-Gomez JM, Terol J, Williams TD, Nagaraj SH, Nueda MJ, Robles M, Talon M, Dopazo J, Conesa A (2008) High-throughput functional annotation and data mining with the Blast2GO suite. *Nucleic Acids Res* **36**: 3420-3435

Karabatsos GJ, Hsi N (1967) Structural studies by nuclear magnetic resonance—XI: Conformations and configurations of oxime o-methyl ethers. *Tetrahedron* **23**: 1079-1095

Luck K, Jirschitzka J, Irmisch S, Huber M, Gershenzon J, Kollner TG (2016) CYP79D enzymes contribute to jasmonic acid-induced formation of aldoximes and other nitrogenous volatiles in two *Erythroxylum* species. *BMC Plant Biol* **16**: 215

Pfaffl MW (2001) A new mathematical model for relative quantification in real-time RT-PCR. *Nucleic Acids Res* **29**: e45

Simao FA, Waterhouse RM, Ioannidis P, Kriventseva EV, Zdobnov EM (2015) BUSCO: assessing genome assembly and annotation completeness with single-copy orthologs. *Bioinformatics* **31**: 3210-3212

10.2.3 Supplemental Data – Manuscript III



Supporting Information

Detection and Imaging of the Plant Pathogen Response by Near-Infrared Fluorescent Polyphenol Sensors

*Robert Nißler, Andrea T. Müller, Frederike Dohrman, Larissa Kurth, Han Li, Eric G. Cosio, Benjamin S. Flavel, Juan Pablo Giraldo, Axel Mithöfer, and Sebastian Kruss**

anie_202108373_sm_miscellaneous_information.pdf
anie_202108373_sm_SV1.avi
anie_202108373_sm_SV2.avi
anie_202108373_sm_SV3.avi

Note: anie_202108373_sm_SV1.avi, anie_202108373_sm_SV2.avi and anie_202108373_sm_SV3.avi can be found on the enclosed CD with the electronic version of this thesis.

SUPPORTING INFORMATION

Table of Contents

| | |
|---|-----------|
| Experimental Procedures | 2 |
| SWCNT surface modification | 2 |
| NIR spectroscopy | 2 |
| SWCNT separation | 2 |
| NIR stand-off imaging | 2 |
| Plant material and classical polyphenol detection..... | 2 |
| Incorporation of <i>G. max</i> seedlings into NIR fluorescent agar..... | 4 |
| Polyphenol visualization | 4 |
| Image analysis | 4 |
| Results and Discussion | 5 |
| Figure S1: Sensor screening for plant polyphenol detection..... | 5 |
| Figure S2: Sensing of tannic acid (TaA)..... | 6 |
| Figure S3: SWCNT purification to obtain monochiral PEG-PL-(6,5)-SWCNT sensors | 7 |
| Figure S4: Polyphenol interaction with HiPco-SWCNTs..... | 8 |
| Figure S5: Total phenol content quantification and analysis of <i>Tococa spp.</i> polyphenol extract..... | 9 |
| Figure S6: Total phenol content quantification and analysis of <i>Tococa spp.</i> polyphenol extract..... | 9 |
| Figure S7: Analysis of crude <i>Tococa spp.</i> leaf extracts | 10 |
| Figure S8: Characterization of polyphenols from soybean cell cultures | 12 |
| Figure S9: Sensor response to soybean cell cultures..... | 13 |
| Figure S10: Untargeted metabolomics of treated and untreated soybean cell cultures..... | 14 |
| Figure S11: Sensor response to prominent soybean polyphenols..... | 15 |
| Figure S12: Tuning the nanosensor incorporation into functional agar medium..... | 16 |
| Figure S13: Imaging of sensor response during agar diffusion | 17 |
| Figure S14: Elicitor induced polyphenol release from soybean seedlings..... | 18 |
| Figure S15: Separated SWCNT fractions for hyperspectral sensing | 20 |
| References | 20 |
| Author Contributions | 20 |

SUPPORTING INFORMATION

Experimental Procedures

All materials, if not otherwise stated, were purchased from Sigma Aldrich.

SWCNT surface modification

(6,5)-chirality enriched CoMoCat SWCNTs (Sigma-Aldrich, product no. 773735) were modified with varying single-stranded (ss)DNA sequences such as (GT)₁₀, (CT)₁₅, (GA)₁₅, (GC)₁₅, (AT)₁₅, (A)₃₀, (T)₃₀ and (C)₃₀ (oligonucleotide sequences purchased by Sigma Aldrich) following a previously described protocol.^[1] In short, 100 μ L ssDNA (2 mg/mL in H₂O) were mixed with 100 μ L 2xPBS and 100 μ L SWCNTs (2 mg/mL in PBS), tip-sonicated for 15 min @ 30% amplitude (36 W output power, Fisher Scientific model 120 Sonic Dismembrator) and centrifuged 2x 30 min @ 16100x g.

Phospholipid-PEG-SWCNTs were assembled by performing dialysis of sodium cholate suspended SWCNTs.^[2] Here, 2 mg SWCNTs (CoMoCat (Sigma-Aldrich, product no. 773735) or HiPco (NanoIntegris HiPco Raw SWCNTs)) were tip-sonicated in 750 μ L sodium cholate (10 mg/mL in PBS). After centrifugation (2x 30 min @ 16100x g), 200 μ L supernatant was mixed with 800 μ L sodium cholate (12 mg/mL) containing 2 mg 18:0 PEG5000 PE (1,2-distearoyl-sn-glycero-3-phosphoethanolamine-N-[methoxy(polyethylene glycol)-5000]) or 2 mg DSPE-PEG(2000) Amine (1,2-distearoyl-sn-glycero-3-phosphoethanolamine-N-[amino(polyethylene glycol)-2000]), Avanti Lipids). The mixture was transferred to a 1 kDa dialysis bag (Spectra/Por®, Spectrum Laboratories Inc.) and dialyzed for several days (>5 d) against 1xPBS. The colloidal stable PEG-PL-SWCNTs sensors were obtained after centrifugation for 30 min @ 16100x g.

NIR spectroscopy

Absorption spectra were acquired with a JASCO V-670 device from 400 to 1350 nm in 0.2 nm steps in a 10 mm path glass-cuvette. 1D-NIR fluorescence spectra were measured with a Shamrock 193i spectrometer (Andor Technology Ltd., Belfast, Northern Ireland) connected to a IX73 Microscope (Olympus, Tokyo, Japan). Excitation was performed with a gem 561 laser (Laser Quantum, Stockport, UK) or a 785 nm laser (iBeam smart WS CW Laser). 2D excitation emission spectra were collected in the same setup as above with a Monochromator MSH150, equipped with a LSE341 light source (LOT-Quantum Design GmbH, Darmstadt, Germany) as excitation source.

NIR fluorescence analyte response measurements were performed, by using 180 μ L of a 0.2 nM ssDNA-SWCNT solution (calculation of molar nanotube concentration based on an approach by Schöppler et al.^[3]) or 180 μ L of a 0.1 absorbance (measured at E₁₁ transition, ~ 995 nm) PEG-PL-SWCNT solution. NIR fluorescence spectra were acquired at 150 mW excitation (561 nm) and 3 s integration time and 200 mW (785 nm) and 10 s integration time. Dose-response measurements were fitted with a one site – specific binding fit or with a hyperbolic fit (GraphPad Prism 9) using $Y = B_{max} * X / (K_d + X)$ with X = concentration of the analyte; Y = specific binding; B_{max} = Maximum binding and K_d = dissociation constant.

SWCNT separation

Separation of (6,5)-SWCNTs was performed according to a previously reported aqueous two-phase extraction (ATPE) protocol from Li et al.^[4] Briefly, in a three step approach SWCNT chiralities were separated between two aqueous phases, containing dextran (MW 70000 Da, 4% m/m) and PEG (MW 6000 Da, 8% m/m) through varying pH-values via HCl addition. The final B3 (bottom)-phase yielded monochiral (6,5)-SWCNTs, which were dialyzed against a 1% (w/v) DOC solution. After further surfactant exchange to sodium cholate, a similar dialysis approach for PEG-PL was performed as described before.^[2,5] Separation of (7,6)-SWCNTs and their surface modification to ssDNA was performed following a recently published protocol.^[5]

NIR stand-off imaging

NIR stand-off detection was performed with a custom made, portable set-up^[6], using a XEVA (Xenics, Leuven Belgium) NIR InGaAs camera (Kowa objective, f = 25 mm/F1.4) with a 900 nm long pass filter (FEL0900, ThorLabs) and a white light source (UHPLCC-01, UHP-LED-white, Prizmatix) equipped with a 700 nm short pass filter (FESH0700, ThorLabs) for excitation. Stand-off distance for NIR fluorescence detection for the seedling-agar experiments (3 s integration time, light intensity 48 mWcm⁻²) was 20 cm. Light intensity was measured at 570 nm with a power meter (PM16-121, ThorLabs). Hyperspectral imaging was performed with additional 950 nm (FEL0950, ThorLabs) and 1100 nm (FEL1100, ThorLabs) long pass filters and 5 s integration time.

Plant material and classical polyphenol detection

Plants and Insects

Tococa guianensis plants were raised from cuttings in a glasshouse (day, 23-25°C; night, 16-18°C; 60-70% rel. humidity; 16 h/8 h light/dark cycle). Once the plants were big enough, they were potted into a 400 mL pot filled with a mixture of 1/4 Klasmann potting substrate (Klasmann-Deilmann, Geeste, Germany), 1/4 Latvian white peat, 1/4 pine bark (7-15 mm), 1/8 sand and 1/8 Legan (5-7 mm) and inoculated with BioMyc™ Vital Mykorrhiza (BioMyc, Brandenburg/Havel, Germany). Experiments were performed with one-year-old *Tococa* plants.

SUPPORTING INFORMATION

Field studies on *Tococa quadrialata* were conducted in the Tambopata Reserve [12° 50' 10" S, 69° 17' 34" W] close to the Explorer's Inn lodge in the lowland Amazon basin in Peru at an elevation a.s.l. 210 m. The average annual rainfall is 2335 mm with a dry season from June until October. The maximum monthly temperature is around 30 °C whereas the monthly minimum is around 19 °C. The subpopulation of *Tococa quadrialata* used for this study was found alongside a small path. All these myrmecophytic plants were colonized by ants of the genus *Azteca spec.* (subfamily Dolichoderinae). The experiment was performed and leaves were sampled when the plants were on average 56 cm tall and had 14 leaves.

Spodoptera littoralis larvae used for the greenhouse herbivore experiment were hatched from eggs and reared on an agar-based optimal diet at 23 °C–25 °C with 8 h light/16 h dark cycles.^[7] Third instar *S. littoralis* larvae were chosen for the herbivory experiment and starved 24 h prior to plant feeding. For the field experiments, *Spodoptera* larvae of third to fifth instar were collected from a local area.

Herbivore treatment

One leaf of the second pair of fully expanded leaves was enclosed with a perforated PET bag. Two *Spodoptera* larvae were released on the bagged leaves and allowed to feed for 24 h, whereas the control leaves were enclosed with an empty bag for 24 h. At the end of the experiment, these leaves were excised and photographed to determine the leaf damage, domatia were removed and the leaves flash-frozen in liquid nitrogen. The field samples were lyophilized for the transport to Germany and subsequent chemical analyses.

Cell culture of *Glycine max*

Soybean (*Glycine max* L. cv. Harosoy 63) cell suspension cultures were cultivated according to Fliegmann et al.^[8] Briefly, cells were kept in the dark at 26 °C under shaking conditions (110 rpm) and were subcultured in fresh medium every 7 days. To document the accumulation of phenolic compounds with age, subcultures were harvested after 2, 7 and 14 days. More specifically, the cultures were filtrated utilizing Whatman® Grad 1 filter paper (GE Healthcare, Chicago, IL, USA) and the filtrates were used for further analyses.

For the induction of isoflavonoid production, soybean cell suspension cultures were sub-cultured after 5 days in fresh medium (6 g fresh mass per 40 mL medium) and after another 2 days of growth, 1 mL of suspension culture was carefully transferred to each well of a 24 well plate (CELLSTAR® 662102, Greiner Bio-One, Kremsmünster, Austria). 10 µL of 50 mg/mL raw elicitor isolated from the cell walls of the phytopathogenic oomycete *Phytophthora sojae* in ddH₂O was added to half of the wells. Wells to which 10 µL of pure ddH₂O were added served as control treatment. The plate was kept in the dark at room temperature under constant shaking conditions (100 rpm) for 4 days. The suspensions were then carefully transferred to 1.5 mL Eppendorf tubes (Eppendorf, Hamburg, Germany), cells spun down (5000 rpm, 4 °C, 20 min) and the supernatant transferred to a new vial for subsequent chemical analysis. As a negative control, six 1 mL samples of the starting culture were transferred to 1.5 mL Eppendorf tubes instead of the well plate and harvested immediately. 20 µL of the cell suspension supernatant was directly added to the nanosensors for polyphenol detection.

Extraction of ellagitannins and anthocyanins from *Tococa*

1 g freeze-dried, finely ground powder of *Tococa* leaves was extracted five times with 10 mL of acetone/water (7/3, v/v) containing 0.1 % (m/v) ascorbic acid to obtain the crude extract. Acetone was evaporated below 40 °C with a rotary evaporator and the remaining water phase was subjected to SPE using a CHROMABOND® HR-X column (6 mL, 500 mg; Macherey-Nagel, Düren, Germany). After the equilibration of the column with methanol and water, the extract was applied to the column and different fractions were subsequently eluted with water, increasing concentrations of acetone/water (1/1, 3/1, v/v) and acetone. Fraction volume was 6 mL per eluent, whereas three fractions per one eluent were collected. Whenever it was possible to obtain smaller fractions of similar chemical compounds based on visual hints, fractions smaller than 6 mL were collected. Fractions were analyzed by a diode array detector (DAD) system after separation by Agilent 1100 HPLC (Agilent Technologies, Santa Clara, CA, USA) using a Luna® Phenyl-Hexyl 100 Å (4.6 × 150 mm, 5 µm, Phenomenex, Aschaffenburg, Germany) column. The binary mobile phase consisted of acetonitrile (A) and 0.5 % trifluoroacetic acid in water (B) at the flow rate of 1 mL min⁻¹. The elution profile was: 0 – 18 min, 5 – 41 % A in B; 18 – 18.1 min, 41 – 100 % A in B; 18.1 – 21 min 100 % A in B; 21 – 21.1 min 100 – 5 % A in B; 22 – 26 min 5 % A. Absorbance was detected at 254 nm, 270 nm, 280 nm and 520 nm. 1 mL of the fraction of interest was dried under nitrogen stream to yield 38 mg of a red glittering solid residue enriched in ellagitannins and anthocyanins. This fraction was dissolved in MeOH and diluted to the desired concentration. 2 µL of this solution was added to the nanosensor solution for polyphenol sensing.

Further polyphenolic compounds

Anthocyanidins used for nanosensor screening were extracted from dried hibiscus (purchased in a local store), following a described protocol.^[9] Trihydroxypterocarpan (THP) were extracted from soybean according to previous literature.^[10,11]

Targeted analysis of herbivore treated leaves

40 mg of freeze-dried ground leaf powder or 100 mg of frozen fresh leaf powder ground in liquid nitrogen were extracted with 1 mL of methanol (MeOH) containing 10 ng/mL trifluoromethyl-cinnamic acid as an internal standard. The homogenate was mixed for 30 min and centrifuged at 16000 rcf for 10 min. The supernatant was used for subsequent analysis. Compound separation and targeted analysis was achieved by LC-MS/MS as described in Lackus et al.^[12], using multiple reaction monitoring to monitor analyte parent ion → product ion formation for detection of the phenolic compounds (Catechin: *m/z* 289 → 109; DP: -30 V CE: -32 V; Apigenin: *m/z* 269 → 117, DP: -30 V, CE: -44 V; TMCA (internal standard): *m/z* 215 → 171 DP: -30 V, CE: -18 V).

Chromatograms were analyzed using the software Analyst 1.6.3 (Applied Biosystems) with automated peak integration. The internal standard was used to normalize the peak areas. 2 µL of these MeOH extracts were added to the nanosensor solution for polyphenol sensing.

SUPPORTING INFORMATION

High-resolution mass spectrometry of *Tococa* and soybean samples

The methanolic extracts and interesting fractions of *Tococa* and the aqueous supernatants of the soybean cell cultures were furthermore subjected to high-resolution mass spectrometry in order to obtain the accurate masses of the compounds. Samples were analyzed with a Dionex Ultimate 3000 RS Pump system (Agilent) coupled to a timsTOF mass spectrometer with a turbospray ion source (Bruker Daltonics, Bremen, Germany). Separation was achieved as described by Lackus et al.^[12] The mass spectrometer was successively operated in negative and positive ionization mode scanning a mass range from m/z 50 to 1,500 with the capillary voltage set at 4,500 V (positive mode) or 3500 V (negative mode), respectively. Nitrogen served as drying gas (8 L/min, 280°C) and nebulizer gas (2.8 bar). As internal calibrators, sodium formate adducts were used. Compass Hystar 3.2 (Bruker) was used for data acquisition and MetaboScape (Bruker) for data processing, sum formula calculation, structure prediction and preliminary statistical analysis. Additionally, SciFinder (<https://scifinder.cas.org>) was used for structure prediction and compound identification. Peak integration of extracted ion chromatograms corresponding to known soybean compounds was achieved with Compass Quant Analysis (Bruker).

Total phenol content quantification

An established protocol^[13] enables the colorimetric quantification of the total phenol content. In short, 100 μ L sample were mixed with 200 μ L Folin-Ciocalteu reagent (10 %; *v/v*) and 800 μ L Na₂CO₃ (700 mM) and left for reaction (1.5 h at RT). Reaction tubes were shortly centrifuged (2 min @ 16,100x *g*) and subsequently the absorbance of the solution was measured at 765 nm with a JASCO V-670 device. Soybean cultures were directly used, while *Tococa* extracts were diluted accordingly, to not exceed the linear range of the calibration.

Incorporation of *G. max* seedlings into NIR fluorescent agar

PEG-PL-SWCNTs sensors were incorporated into 5 mL 0.4 % agarose culture medium (containing Murashige & Skoog (MS) media) and casted into a sterile petri dish (\varnothing 8.5 cm), yielding a final SWCNT absorbance of 0.3 at the E₁₁ transition at ~995 nm. Further UV sterilization was performed for 15 min (UV-Kontaktlampe Chroma41, 254 nm, Vetter GmbH) before placing 3-days old seedlings of *Glycine max* L. cv. Maraquise or cv. Edamame Green Shell onto the sensor-agar. The root of the seedling was covered with 10 mL 0.8 % agarose MS medium. Polyphenol sensing experiments were performed after >12 h post seedling incorporation.

Polyphenol visualization

Seedlings were challenged with 50 μ L (10 mg/mL) raw-elicitor of *Phytophthora sojae*, or as a control 50 μ L ddH₂O, after wounding the root tissue with a 0.4 mm cannula. Automated image recoding was performed for every 30 min over 10 h and subsequently after 24 h, using 3 s integration time. Excitation was synchronized in the same way, whereby only for NIR fluorescence acquisition the illumination system was turned on for 2 min.

Image analysis

NIR images were acquired with Xeneth Software 2.7 (Xenics, Leuven Belgium) and converted in ImageJ (1.51k) into 8-bit data format. Differential NIR fluorescent images (I/I_0) were obtained by dividing the time series of the recorded images (I) by the first image (I_0), while using a masked root tissue region. The intensity changes in the 32-bit images were then further analyzed with a 5-pixel with line profile or using a 500-pixel large area, close to the challenged root position. Hyperspectral images were analyzed by subtracting the corresponding 1100 nm long pass filter images from the ones acquired with a 900 or 950 nm long pass filter, to obtain the fluorescence intensities of the (6,5)-SWCNTs which emit at ~ 1000 nm. Fluorescence emission of (7,6)-SWCNTs were detected with a > 1100 nm long pass filter.

SUPPORTING INFORMATION

Results and Discussion

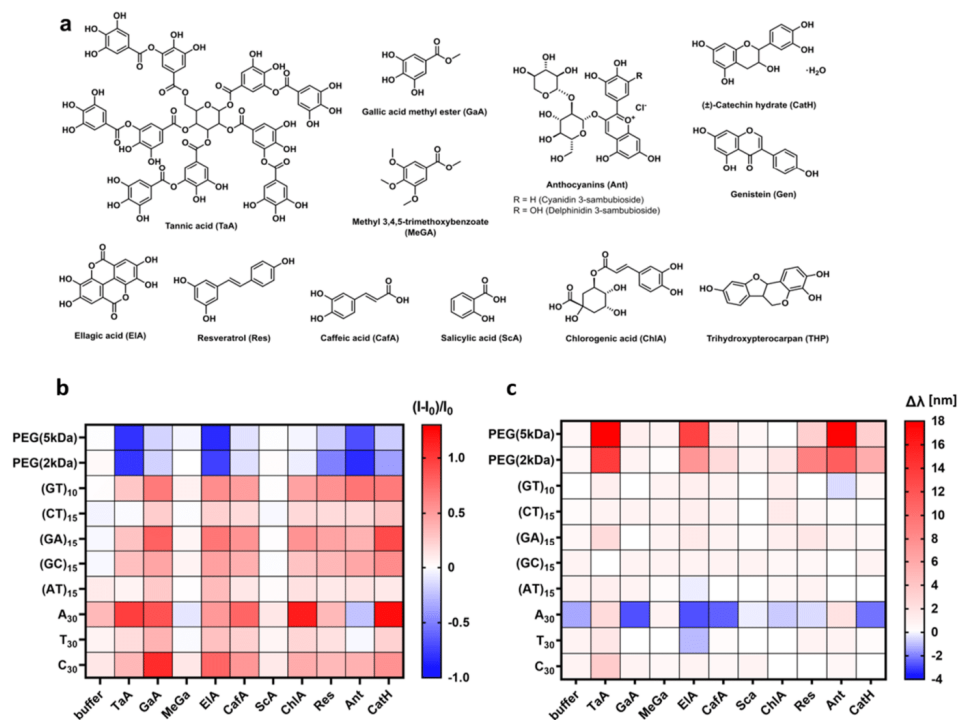


Figure S1: Sensor screening for plant polyphenol detection.

a) Chemical structures of the used polyphenolic compounds. b) Fluorescence changes ($I-I_0/I_0$) of all SWCNT-based sensors with different surface modifications, in response to different plant polyphenols summarized in a heatmap (mean, $n = 3$). Shades of blue indicate fluorescence decrease and shades of red fluorescence increase, within the indicated range. c) Emission wavelength changes ($\Delta\lambda$) of all SWCNT sensors after polyphenol addition. Shades of blue indicate hypsochromic shift and shades of red bathochromic shift, within the indicated range (polyphenol concentration = 10 μM ; TaA = 1 μM).

ssDNA-SWCNTs responded with a general pattern of fluorescence increase, however, showing distinct differences in sensing magnitudes. PEG-PL-SWCNTs on the other side responded with a fluorescence decrease. Note: It is known, that A-rich ssDNA-SWCNTs exhibit decreased colloidal stability over time^[5], which affects aggregation/quenching state, biasing the total emission intensity and sensors response. Moreover, a variety of molecules can modulate their photoluminescence, which makes this particular ssDNA modification less suitable for further sensor design. For the sake of completeness, we showed these screening results, but furthermore excluded A_{30} -SWCNTs for final polyphenol sensor development. To exclude pH or ionic strengths related sensing effects^[14], all experiments were performed under buffered conditions. $(AT)_{15}$ -ssDNA surface modification seem less sensitive to the tested polyphenolic compounds, which would make them a suitable reference material for multichiral sensing.

SUPPORTING INFORMATION

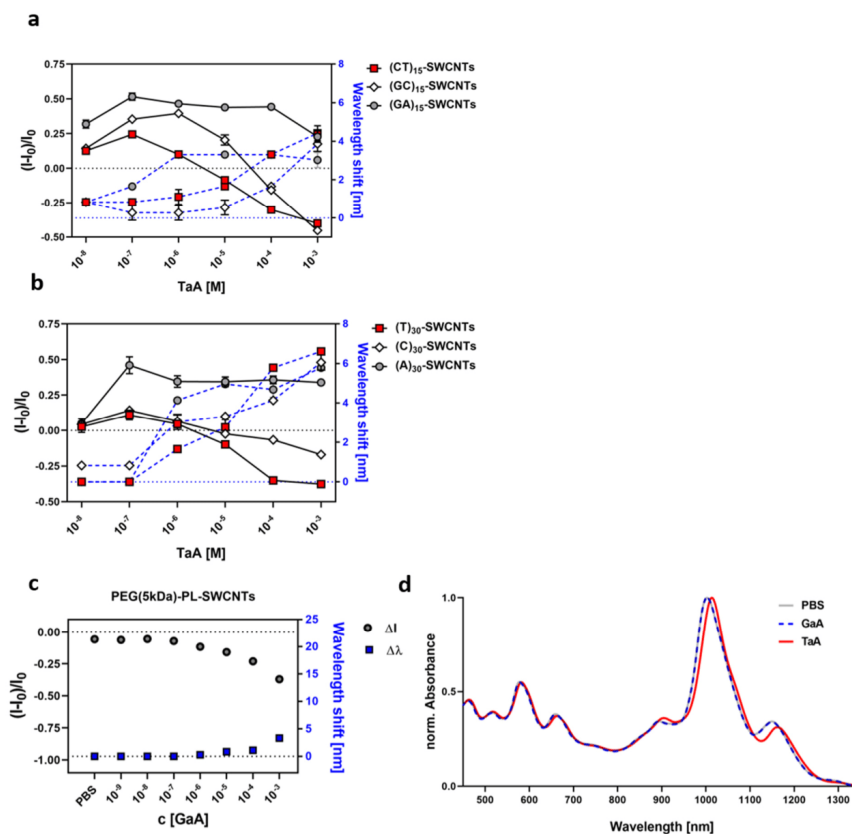


Figure S2: Sensing of tannic acid (TaA).

a) and b) Concentration dependent NIR fluorescence shifts of multiple ssDNA-SWCNTs in response to tannic acid. Intensity (black line) increases in the nM range, while higher concentrations lead to decreased fluorescence emissions, whereas wavelength shift (dotted blue line) increases with TaA concentration (mean \pm SD, $n = 3$). This observation could be the result of two different principles of interaction. The increase could be similar to the one known for dihydroxy group containing catecholamines[3] (like dopamine), so polyphenols could push the DNA-phosphate backbone closer to the SWCNT surface. At higher concentrations, polyphenol could lead to colloidal instability of the polymer-SWCNT complex, as known for PEG or protein precipitations[4], resulting in the fluorescence decrease. Since the fluorescence modulation from ssDNA-SWCNTs (e.g. (CT)₁₅- and (GA)₁₅-SWCNTs) were observed with quite different magnitudes, these types of interface modifications were excluded as further polyphenol-sensitive probes. c) GaA addition only slightly alternates the emission of PEG-PL-SWCNTs (mean \pm SD, $n = 3$), indicating that the three-dimensional architecture of structurally large polyphenols contributes significantly to the sensing mechanism. d) TaA interaction with PEG(5kDa)-PL-SWCNTs causes a ~ 10 nm bathochromic shift in E₁₁ absorbance maximum, while GaA does not cause a spectral shift (TaA, GaA = 10 μ M). The absorption at the excitation wavelength (E₂₂ transition), however, just showed a minor shift. Therefore, the observed shifts at the E₁₁ transition could correlate partly with the detected energy differences in fluorescence emission. However, we assume, that interaction of PEG-PL-SWCNTs with certain polyphenols will increase the local dielectric constant around the SWCNTs, thus causing the red-shifted emission features.

SUPPORTING INFORMATION

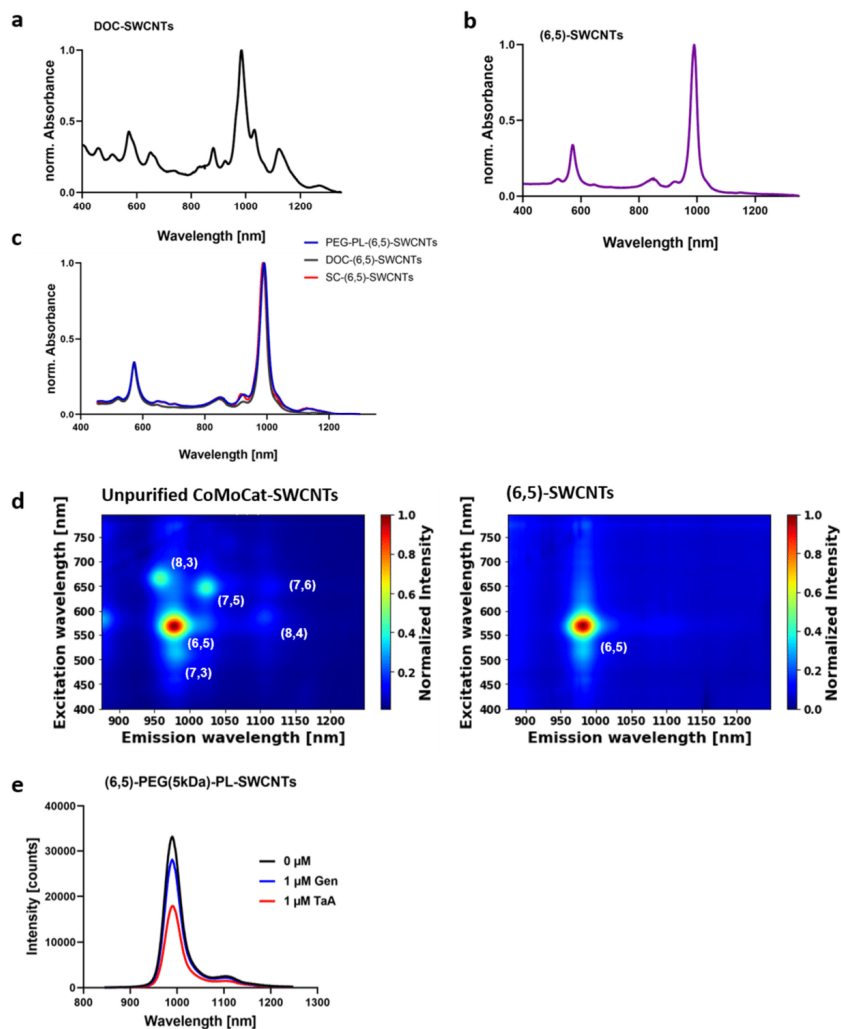


Figure S3: SWCNT purification to obtain monochiral PEG-PL-(6,5)-SWCNT sensors.

a) Normalized absorbance spectra of un-purified CoMoCat-SWCNTs dispersed in 1% DOC. b) Normalized absorbance spectra of purified (6,5)-SWCNTs, obtained by multiple step aqueous two-phase extraction (ATPE), following an approach described by Li et al.^[4] c) Normalized absorbance spectra of (6,5)-SWCNTs, exchanging the surface modification from sodium deoxycholate (DOC) to sodium cholate (SC) and to a biocompatible polyethyleneglycol-phospholipid (PEG-PL). d) Corresponding 2D photoluminescence spectra of the non-purified and the purified (6,5)-SWCNTs. e) Exemplaric fluorescence spectra of monochiral PEG(5kDa)-PL-(6,5)-SWCNTs before and after addition of tannic acid and genistein, showing a strong fluorescence decrease.

SUPPORTING INFORMATION

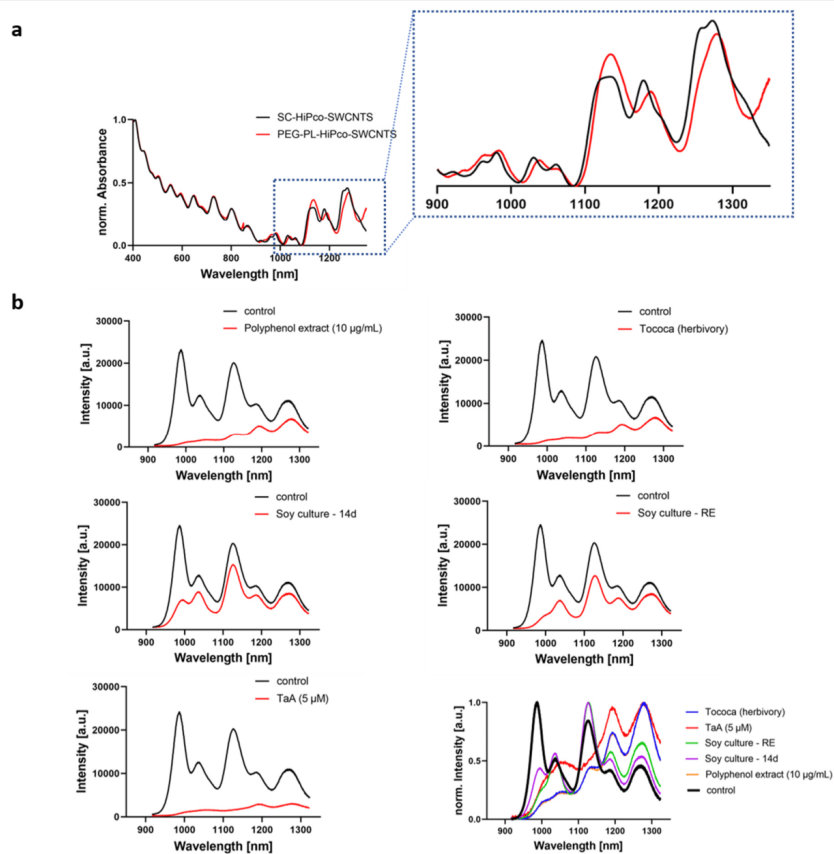


Figure S4: Polyphenol interaction with HiPco-SWCNTs.

a) Normalized absorbance spectra of SWCNTs dispersed in SC and after further surface exchange to PEG-PL. Additionally, a magnified E_{11} transition region is shown. b) NIR fluorescence spectra of PEG-PL-HiPco-SWCNTs before (black spectra) and after (red spectra) the addition of polyphenol containing plant extracts or TaA (*Tococa* polyphenol extract and MeOH extract from herbivory treated plants). Strong photoluminescence modulations are visible with certain differences between SWCNT chiralities, which could point towards a chirality dependent effect regarding the polyphenol composition (see last plot, compared as normalized fluorescence emissions).

SUPPORTING INFORMATION

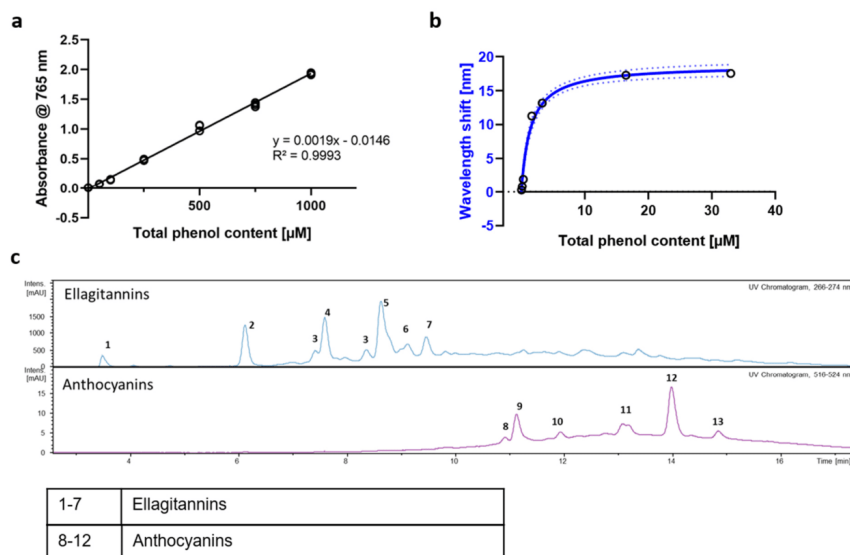


Figure S5: Total phenol content quantification and analysis of *Tococa spp.* polyphenol extract.

a) Calibration curve (linear regression) for the colorimetric assay^[13] used to assess the total phenol content. Known concentrations of gallic acid are challenged with the Folin–Ciocalteu reagent, while quantifying the absorbance at 765 nm ($n = 3$). The resulting calibration, expressed as gallic acid equivalents, shows a linear trend in the μM regime. b) Corresponding plot similar to Figure 3c. It shows the PEG-PL-SWCNT response to purified polyphenol extract from *Tococa spp.*, expressed as the total phenol content vs. wavelengths emission shifts (mean \pm SD, $n = 3$, blue line = hyperbolic fit). Compared to the classical Folin–Ciocalteu assay, the sensors display a highly dynamic response in the low μM range with a K_d of 1.5 μM . c) HPLC-UV-Vis chromatogram of the used *Tococa spp.* sample, containing all extractable leaf polyphenols with a predominantly high ellagitannin content, as seen from the counts in the UV trace (266–274 nm). Substance assignment as ellagitannins and anthocyanins were further confirmed by high resolution mass spectrometry and comparison of the LC-MS results to literature.^[15–17] As the sensors probe the total phenol content and the response depends pairwise on the polyphenol profile, it would be likely most accurate to create a sensor calibration curve for each plant species/genus of interest.

SUPPORTING INFORMATION

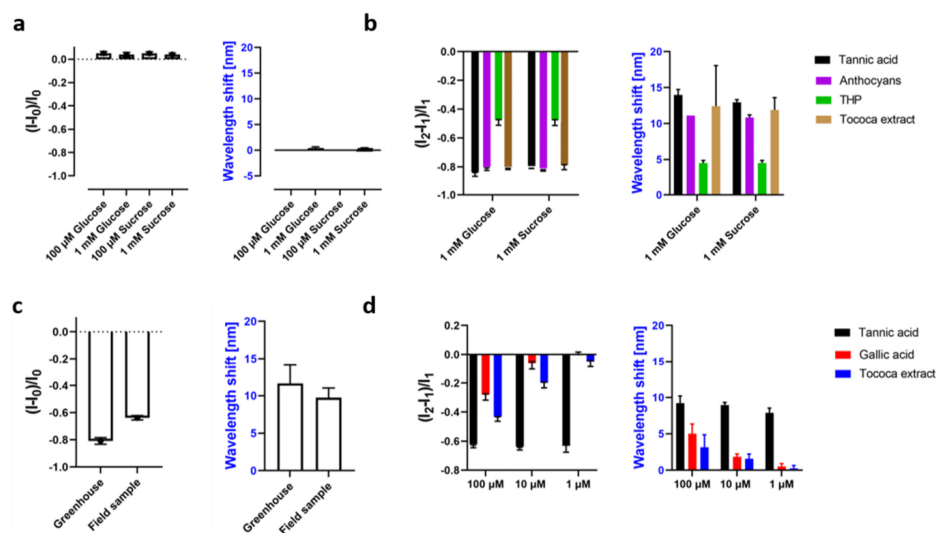


Figure S6: Polyphenol sensing with sugar and leaf extract background.

a) Polyphenol sensing with mono- and disaccharide background. Addition (I_1) of up to 1 mM glucose or sucrose is not changing the nanosensors responses. b) Further addition (I_2) of polyphenols leads to a similar sensor response, as seen in previous experiments in PBS (10 μM polyphenol concentration, 10 $\mu\text{g/ml}$ extracted polyphenol fraction for the Tococa extract (similar to Figure 3c and S5), mean \pm SD, $n = 3$). However, it should be mentioned, that the intensity changes of the sensors were unbiased, compared to similar experiments in the absence of saccharides, while the detected shift in emission wavelength was slightly reduced (e.g. Tococa extract shifted nanosensor emission by 17 nm w/o saccharides and \sim 12 nm with glucose/sucrose background). Since 2 μL leaf extract is added to 180 μL sensor solution, such unphysiological high background concentrations of sugars would not be expected in primary samples. c) Polyphenol sensing with a Tococa leaf extract background. Addition (I_1) of 2 μL Tococa leaf extract, ether from a 'field' or 'greenhouse sample' (see materials and methods), leads to a strong sensor response. d) Further addition (I_2) of polyphenols to e.g. 'field sample' can still be sensed in a concentration dependent way, illustration the principle of a standard addition in a chlorophyll (and polyphenol) containing background (mean \pm SD, $n = 3$). Similar results were obtained, when spiking the 'greenhouse sample', showing slightly smaller responses. Note that wavelengths shifts in (d) are compared to the addition (I_1) of totoca extracts, so overall shifts to the starting conditions (I_0) would be e.g. for tannic acid close to 20 nm.

SUPPORTING INFORMATION

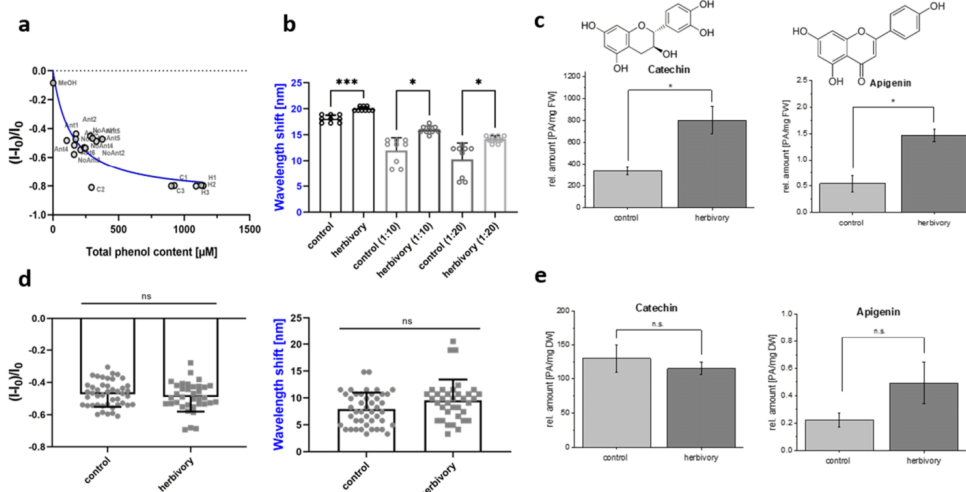


Figure S7: Analysis of crude *Tococa* spp. leaf extracts.

a) Correlation of the intensity changes against the total phenol content from multiple *Tococa* leaf MeOH-extracts (corresponding plot to Figure 3d, 2 μ L undiluted MeOH extract was added to the nanosensors). It should be mentioned, that first unknown *Tococa* extracts were analyzed by the nanosensors and then correlated with the established Folin–Ciocalteu assay. For such a species-specific calibration fit, a dynamic response in the μ M range of total phenols is observed (expressed as gallic acid equivalents) (mean \pm SD, N = 1, n = 3, blue line = hyperbolic fit). b) When diluting the plant extract from herbivore treated *Tococa* plants from the greenhouse, the phenol concentration is shifted to the dynamic response region of the nanosensors. This increases the mean difference in emission wavelength shift, which is hereafter still significantly different (complementary to Figure 3e, mean \pm SD, N = 3, n = 3). c) HPLC-MS quantification of catechin and apigenin as two prominent examples show as well a significant increase after herbivore treatment. d) Nanosensor responses of different extracts from wild *Tococa* plants show no significant difference in polyphenol levels after herbivore attack, which was carried out as described in the MM section. Hereby, a strong variation in the total phenol concentration is detected, pointing towards more complex interactions in the wild plants (e.g. previous pathogen / herbivore attack mediated a constant increase in polyphenol levels) (mean \pm SD, N = 6, n = 3). e) HPLC-MS quantification confirmed those results, by showing no significant differences in the most prominent flavonoid compounds (note that apigenin levels show a slight increase, not effecting the overall total phenol concentration, as seen from magnitudes higher, not varying catechin levels). (nanosensor analysis: ***P<0.001; *P<0.03; ns = not significant; unpaired t-test; PA = peak area, FW = fresh weight, DW = dry weight)

SUPPORTING INFORMATION

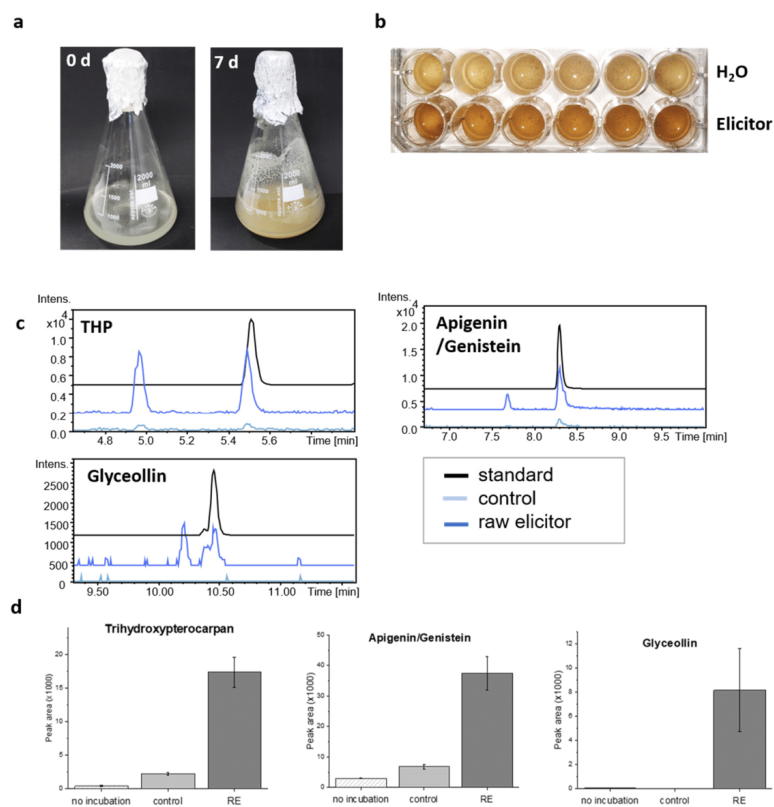


Figure S8: Characterization of polyphenols from soybean cell cultures.

a) Pictures of the soybean cultures show a clear browning after 7 days, indicating a release of polyphenols during growth and maturation. b) Six soybean culture replicates, stimulated with 0.5 mg/mL raw elicitor (lower row) or with H₂O (upper row) as a control. Again, a clear browning of the induced cultures is visible, which indicates accumulation of phenolic compounds.^[18] c) Extracted ion chromatograms (EIC) of the most abundant *m/z* values of the respective standards are shown. Comparison of these signals in samples from raw elicitor (RE) treated and control cultures shows that these compounds are accumulating after stimulation with RE. d) Peak areas of these EIC signals were used for relative quantification of the compounds. A drastic increase in flavonoids after raw elicitor treatment was detected.

SUPPORTING INFORMATION

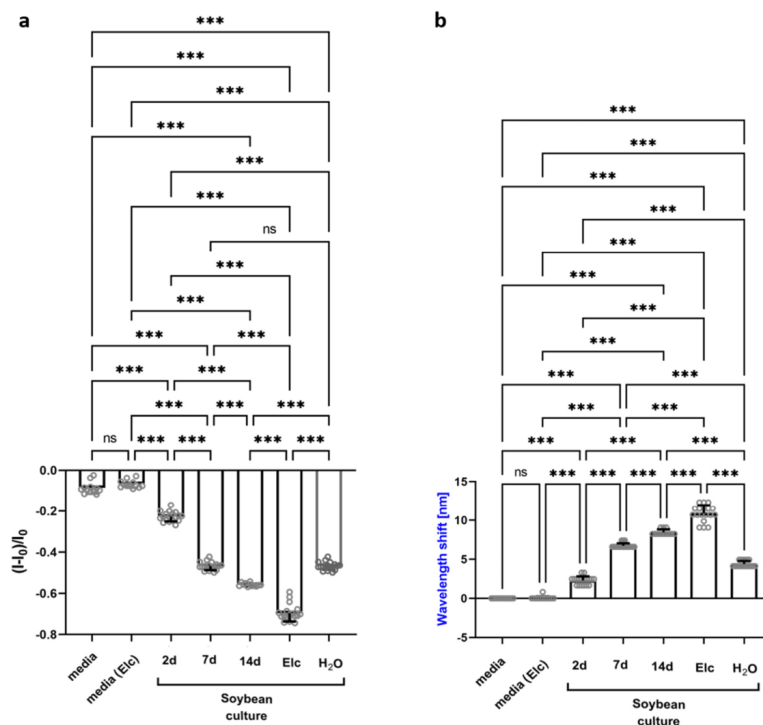


Figure S9: Sensor response to soybean cell cultures.

a) and b) Full statistical analysis (one-way ANOVA) for the shown sensor responses in Figure 3f and 3g. Here, soybean cell cultures (as cell-free supernatants) are added to the PEG-PL-SWCNT nanosensors, which react with a fluorescence decrease and emission wavelengths shift to the age and stimulus (elicitor, Elic) dependent polyphenol content (mean \pm SD, N = 6, n = 3; nanosensor analysis: ***P < 0.001; ns = not significant).

SUPPORTING INFORMATION

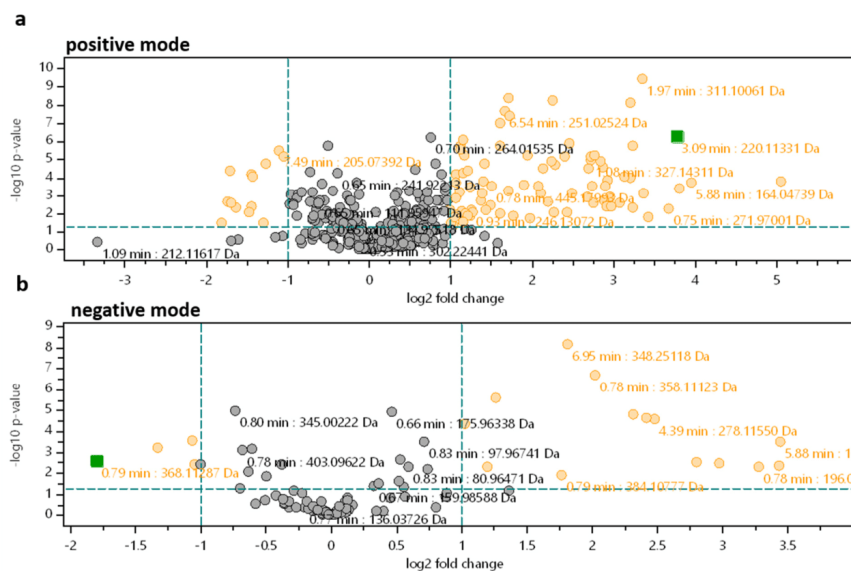


Figure S10: Volcano plot comparing feature abundance in control and elicitor induced soybean cell cultures.

LC-MS analysis of control and elicitor induced soybean cell cultures was conducted with the mass spectrometer operating in positive (a) and negative (b) ionization mode to compare the relative abundance of the extracted features. The volcano plot visualizes the metabolic differences (orange features, $p < 0.05$, fold change > 2) and non-affected features (grey) upon raw elicitor treatment. Green color marks the selected feature, which is not relevant for this result.

SUPPORTING INFORMATION

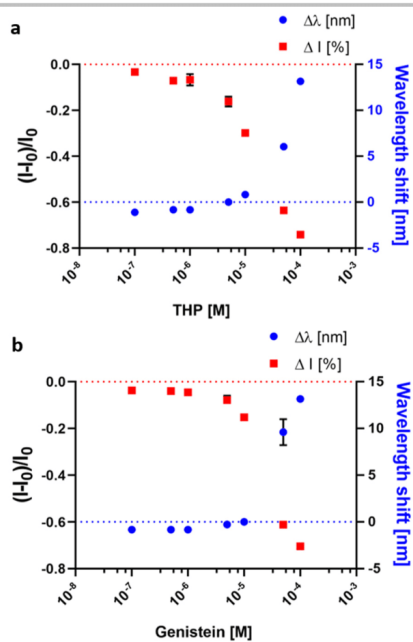


Figure S11: Sensor response to prominent soybean polyphenols.

a) Trihydroxypterocarpan (THP), an important compound released after pathogen (elicitor) stimulus and b) genistein, which is released during maturation, quench and shift the nanosensor fluorescence in a similar concentration dependent manner (mean \pm SD, n = 3).

SUPPORTING INFORMATION

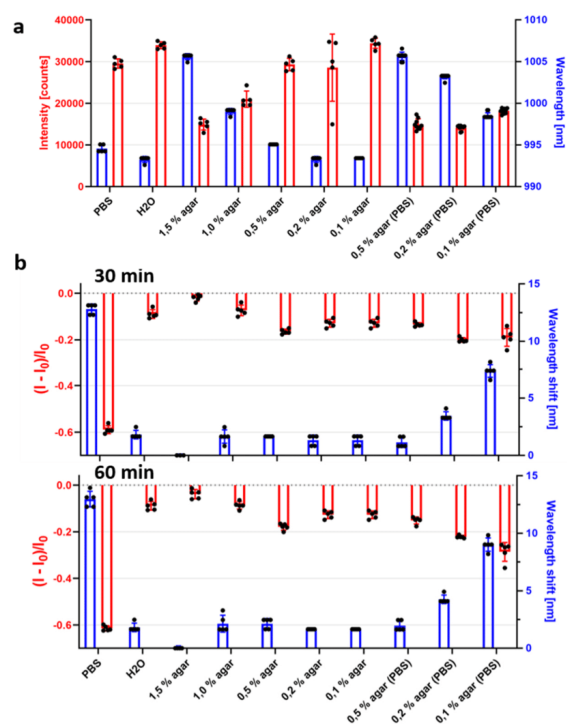


Figure S12: Tuning the nanosensor incorporation into functional agar medium.

a) Photoluminescence properties (intensity and emission wavelength) of PEG-PL-SWCNTs in different environments. 90 μ L SWCNT solution was placed in a 96-well plate and analyzed. Increasing agar concentration decreases the emission intensity and redshifts the maxima (mean \pm SD, $n = 5$). b) Sensing of polyphenols, here genistein with a final concentration of 100 μ M, seems to be strongly affected by a higher agar concentration, as well as by the ion concentration (agar system in H₂O or in PBS) (mean \pm SD, $n = 5$).

SUPPORTING INFORMATION

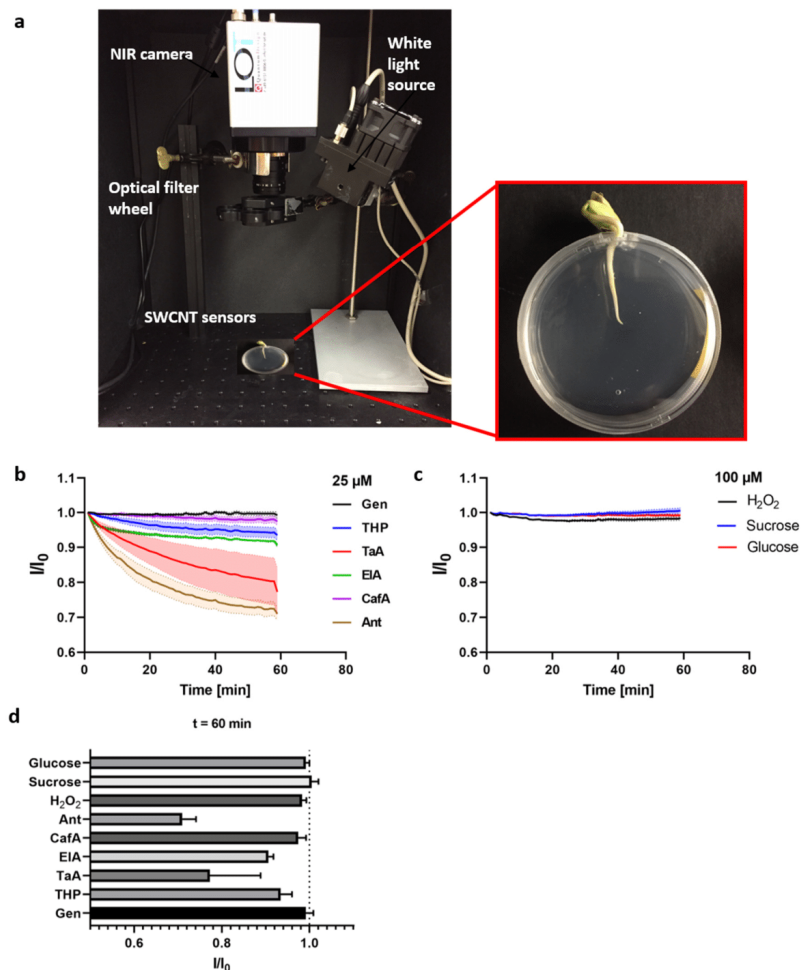


Figure S13: Imaging of sensor response during agar diffusion. a) Picture of the NIR stand-off imaging systems. A specialized InGaAs-Camera detects the fluorescence emission of the SWCNT sensors, incorporated into a agar medium (see close up image). b) PEG-PL-SWCNTs in 0.4 % culture medium agar (Murashige-Skoog-Medium) were challenged with different prominent polyphenols or possible interfering substances during NIR stand-off imaging. Nanosensor responses to 25 μM of different polyphenol compounds (line = mean, SD = pale boundaries, $n = 3$). c) Sensor response to potential interfering substances such as H_2O_2 , mono- or disaccharides. Four times higher concentrations with 100 μM did not change the nanosensors (line = mean, SD = pale boundaries, $n = 3$). d) Plotted NIR-fluorescence changes of the PEG-PL-SWCNTs agar after 60 min (mean \pm SD, $n = 3$). The sensors response to large (for rhizosphere conditions even unphysical high) H_2O_2 concentrations is within a range of $\sim 3\%$, far less than the detected polyphenol secretion after elicitor stimulus. However, a small contribution of released H_2O_2 on a short timescale can not be excluded, but should not affect the overall sensing outcome (as seen in Figure 4 e,f).

SUPPORTING INFORMATION

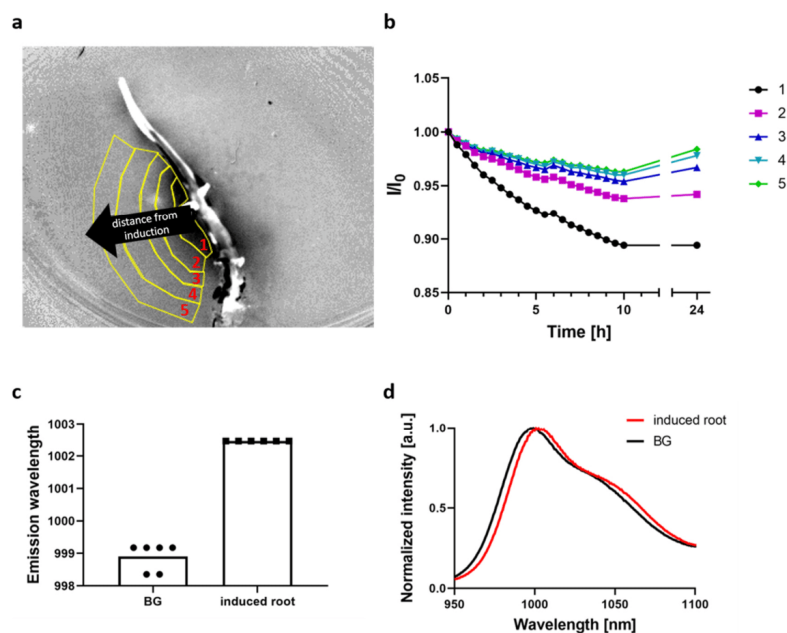


Figure S14: Elicitor induced polyphenol release from soybean seedlings. a) NIR fluorescence image of the *G. max* seedling shown in Figure 4d (10 h after induction). Different regions of interests (ROI) in the nanosensor-agar are marked, with an increasing distance from the induced root position. b) Mean intensity changes (I/I_0) of the associated ROI 1-5 are plotted over time, suggesting a constantly increasing release of polyphenols for 5-8 h after stimulus. c) Measuring the photoluminescence of the nanosensors at six random spots in the background (BG) and close to the induced region (ROI 1, labeled as 'induced root'), a clear redshift of the nanosensor emission becomes visible (mean, $n = 6$). d) Normalized mean fluorescence spectra of the described positions in (c) visualize the redshifted maxima. The fluorescence reduction during NIR stand-off imaging correlates therefore also with a shift in the emission spectra, as expected from polyphenol – nanosensor interaction. Moreover, with specialized optical systems also spectral-resolved imaging^[19] would be possible, likely increasing sensitivity of the presented approach. However, implementation of this technique for scientific of agricultural research and crop production would be more straightforward with the simple NIR imaging system we presented. In general, Polyphenol concentrations in the soil depend on several abiotic and biotic factors. The amounts can change with the season^[20], plant age^[21] and nutrient supply^[22]. These factors, however, are predictable and the changes are bound to occur slowly with an overall low fold change (≤ 2).^[20] Induction after pathogen attack on the other hand leads to a drastic increase of defensive compounds within 4-72 h. So, soybean root cell cultures exposed to fungal pathogen (*Fusarium*) showed 30x increase in glyceollin concentration.^[23] Overall, the sensor response from pathogen-mediated fast and drastic increase in polyphenol levels should not be biased by other factors. These findings and visualization of spatiotemporal polyphenol release are therefore in agreement with previous studies, which measured the bulk accumulation of glyceollin and THP over the course of 32 h^[24] or *via* radioimmunoassay analysis.^[18]

SUPPORTING INFORMATION

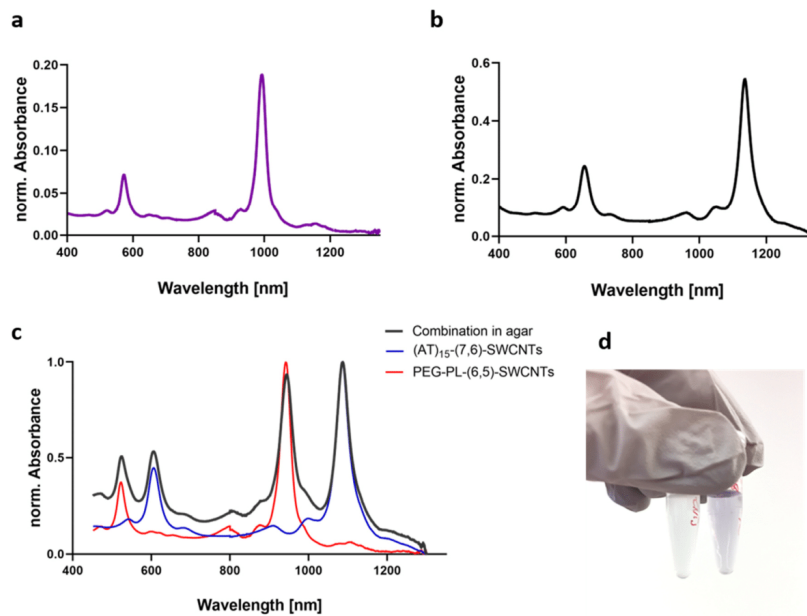


Figure S15: Separated SWCNT fractions for hyperspectral sensing. a) Absorbance spectra of PEG-PL-(6,5)-SWCNTs. b) Absorbance spectra of (AT)₁₅-(7,6)-SWCNTs. c) Normalized absorbance spectra of the purified and specifically modified SWCNT chiralities, measured independently and combined in agar. d) Photograph of Eppendorf tubes, containing (AT)₁₅-(7,6)-SWCNTs (left) and PEG-PL-(6,5)-SWCNTs (right).

SUPPORTING INFORMATION

References

- [1] R. Nißler, F. A. Mann, P. Chaturvedi, J. Horlebein, D. Meyer, L. Vukovic, S. Kruss, *J. Phys. Chem. C* **2019**, *123*, 4837–4847.
- [2] K. Welsher, Z. Liu, S. P. Sherlock, J. T. Robinson, Z. Chen, D. Daranciang, H. Dai, *Nat. Nanotechnol.* **2009**, *4*, 773–780.
- [3] F. Schöppler, C. Mann, T. C. Hain, F. M. Neubauer, G. Privitera, F. Bonaccorso, D. Chu, A. C. Ferrari, T. Hertel, *J. Phys. Chem. C* **2011**, *115*, 14682–14686.
- [4] H. Li, G. Gordeev, O. Garrity, S. Reich, B. S. Flavel, *ACS Nano* **2019**, *13*, 2567–2578.
- [5] R. Nißler, L. Kurth, H. Li, A. Spreinat, I. Kuhlemann, B. S. Flavel, S. Kruss, *Anal. Chem.* **2021**, *93*, 6446–6455.
- [6] R. Nißler, O. Bader, M. Dohmen, S. G. Walter, C. Noll, G. Selvaggio, U. Groß, S. Kruss, *Nat. Commun.* **2020**, *11*, 1–12.
- [7] R. Bergomaz, M. Boppre, *J. Lepid. Soc.* **1986**, *40*, 131–137.
- [8] J. Fliegmann, G. Schüler, W. Boland, J. Ebel, A. Mithöfer, *Biol. Chem.* **2003**, *384*, 437–446.
- [9] C. Grajeda-Iglesias, M. C. Figueroa-Espinoza, N. Barouh, B. Baréa, A. Fernandes, V. De Freitas, E. Salas, *J. Nat. Prod.* **2016**, *79*, 1709–1718.
- [10] A. Mithöfer, A. A. Bhagwat, M. Feger, J. Ebel, *Planta* **1996**, *199*, 270–275.
- [11] A. Mithöfer, A. A. Bhagwat, D. L. Keister, J. Ebel, *Zeitschrift für Naturforsch. - Sect. C J. Biosci.* **2001**, *56*, 581–584.
- [12] N. D. Lackus, A. Müller, T. D. U. Kröber, M. Reichelt, A. Schmidt, Y. Nakamura, C. Paetz, K. Luck, R. L. Lindroth, C. P. Constabel, S. B. Unsicker, J. Gershenzon, T. G. Köllner, *Plant Physiol.* **2020**, *183*, 137–151.
- [13] E. A. Ainsworth, K. M. Gillespie, *Nat. Protoc.* **2007**, *2*, 875–877.
- [14] D. P. Salem, X. Gong, A. T. Liu, V. B. Koman, J. Dong, M. S. Strano, *J. Am. Chem. Soc.* **2017**, *139*, 16791–16802.
- [15] J. Moilanen, J. Sinkkonen, J. P. Salminen, *Chemoecology* **2013**, *23*, 165–179.
- [16] D. M. O. Serna, J. H. I. Martínez, *Molecules* **2015**, *20*, 17818–17847.
- [17] D. Fracassetti, C. Costa, L. Moulay, F. A. Tomás-Barberán, *Food Chem.* **2013**, *139*, 578–588.
- [18] M. G. Hahn, A. Bonhoff, H. Grisebach, *Plant Physiol.* **1985**, *77*, 591–601.
- [19] D. Roxbury, P. V. Jena, R. M. Williams, B. Enyedi, P. Niethammer, S. Marcet, M. Verhaegen, S. Blais-Ouellette, D. A. Heller, *Sci. Rep.* **2015**, *5*, 1–6.
- [20] T. Sosa, C. Valares, J. C. Aliás, N. C. Lobón, *Plant Soil* **2010**, *337*, 51–63.
- [21] S. Cesco, T. Mimmo, G. Tonon, N. Tomasi, R. Pinton, R. Terzano, G. Neumann, L. Weisskopf, G. Renella, L. Landi, P. Nannipieri, *Biol. Fertil. Soils* **2012**, *48*, 123–149.
- [22] S. Cesco, G. Neumann, N. Tomasi, R. Pinton, L. Weisskopf, *Plant Soil* **2010**, *329*, 1–25.
- [23] V. V. Lozovaya, A. V. Lygin, O. V. Zernova, S. Li, G. L. Hartman, J. M. Widholm, *Plant Physiol. Biochem.* **2004**, *42*, 671–679.
- [24] P. Moesta, H. Grisebach, *Nature* **1980**, *286*, 710–711.

Author Contributions

R.N. and S.K. designed and conceived the research with input from J.P.G. S.K. coordinated the project. R.N., F.D. and L.K. performed chemical sensing experiments and separated (6,5)-SWCNTs. A.T.M., E.G.C. and A.M. performed plant cultivation, extraction and related analysis experiments. H.L. and B.S.F. performed (7,6)-SWCNT separation. All authors contributed to the writing of the manuscript and analysis of data. All authors have given approval to the final version of the manuscript.

10.3 Supplemental data of the thesis

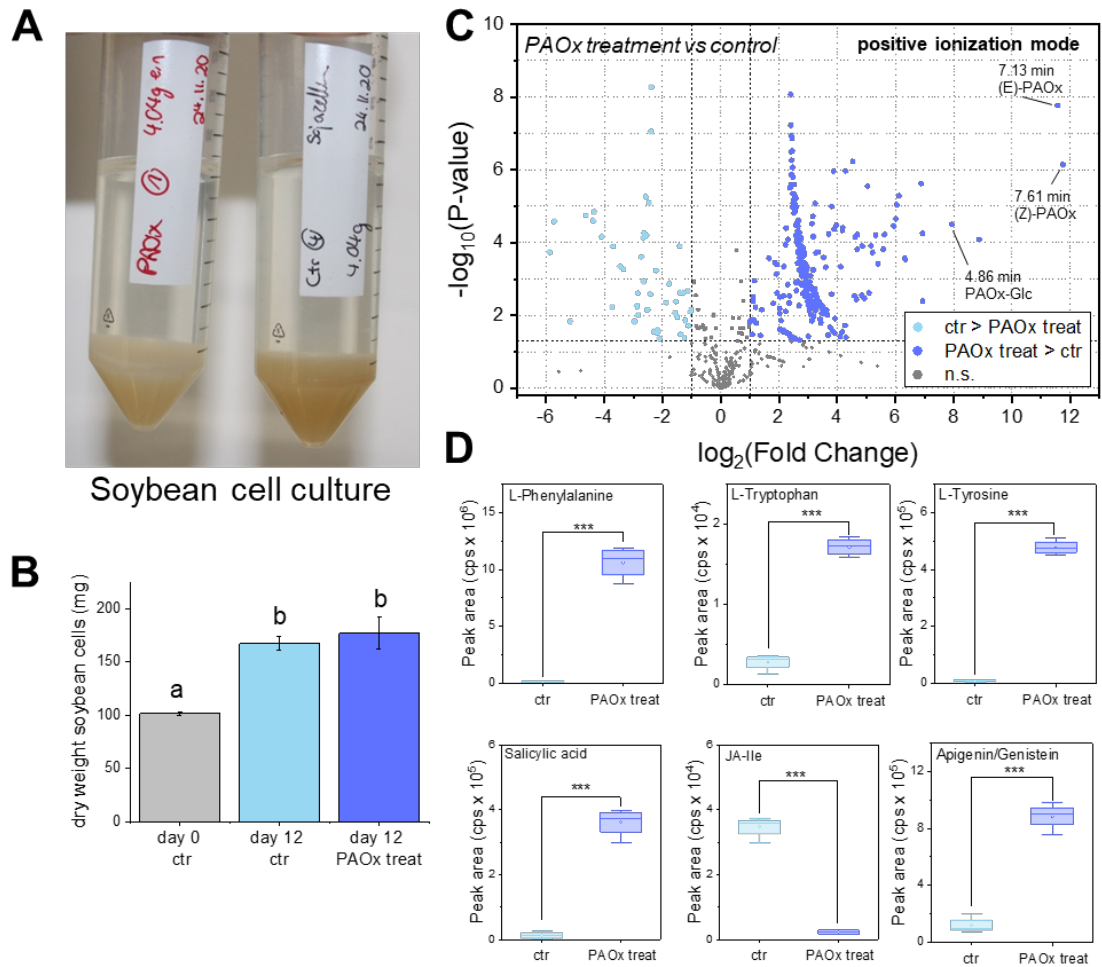


Figure S1: Phenylacetaldoxime (PAOx) affects metabolism of soybean cell culture. Soybean cell cultures were grown for 12 days with 1 mM PAOx ('PAOx treat') or with the same amount of ethanol (ctr) added to the medium. **A:** Cell cultures with and without PAOx treatment were visually different. **B:** In both treatments, cells were growing within the time span, and no difference in growth rate was observed. Kruskal-Wallis-test: χ^2 : 7.42, $p = 0.024$ followed by Dunn's test. Significant different groups are marked by different letters. $n=4$. **C:** The supernatants of the cell cultures were analyzed with high-resolution LC-qTOF-MS operating in positive ionization mode and the relative abundances of the features were compared. The volcano plot visualizes the metabolic differences, where the dark blue color marks features that accumulate in PAOx treated cell cultures, whereas the dots of light blue color represent down-regulated features as compared to control treatment (fold change >2 , $p < 0.05$, $n=4$). **D:** Furthermore, targeted LC-MS/MS was performed for some metabolites of interest. Statistical analysis via Student's t-tests, *** = $p < 0.001$, $n = 4$. cps: counts per second.

Methods Figure S1: *Glycine max* cell suspension cultures were maintained as described in **manuscript III**. For the actual experiment, soybean cell suspension cultures were sub-cultured in fresh medium (4 g cells in 40 mL medium) and 600 μL PAOx (9 mg/mL in EtOH:ddH₂O 2:1 v/v) or 400 μL EtOH as control were added to the cells. The flasks were kept in the dark under shaking conditions (100 rpm, RT) for 12 days. Then, the suspensions were transferred to suitable tubes for centrifugation, cells were removed (3600 rpm, 10 °C, 30 min) and the supernatant transferred to a new vial for subsequent

chemical analysis, while the cells were dried in an oven (60 °C) for 10 days until stable weight was reached. Then, the dry weight of the cultures was determined. The supernatant was used without further processing for LC-MS analysis. Untargeted metabolomics was performed as described in **manuscripts I and II**, whereas targeted metabolite analysis was performed according to **manuscript I** (phytohormones and amino acids) and **III** (apigenin). Data for the volcano plot were calculated with R using the package MetaboAnalyst (Pang et al., 2021) and Pareto scaling after preprocessing the data with MetaboScape (Bruker Daltonics). All other statistics were also performed using R. The results of the statistical analysis were visualized with OriginPro, Version 2019.

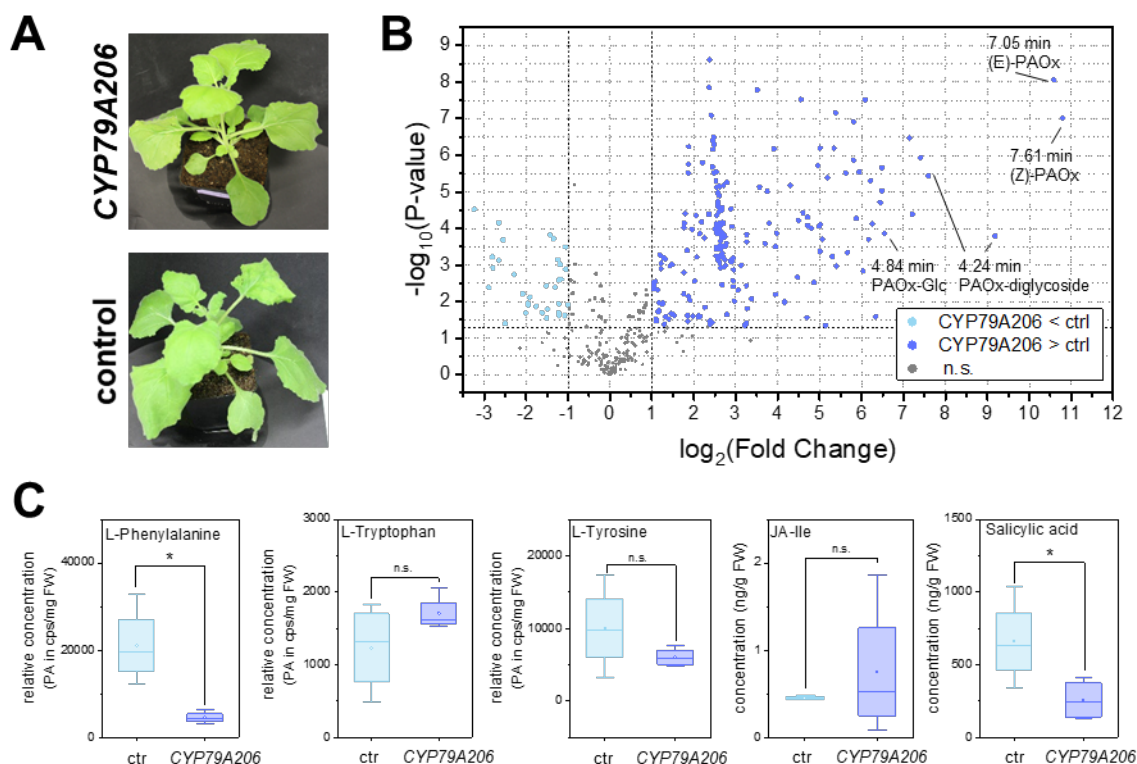


Figure S2: Phenylacetaldoxime (PAOx) affects metabolism of *Nicotiana benthamiana*. *N. benthamiana* leaves were transformed with *Agrobacterium tumefaciens* strains containing plasmids with *CYP79A206* or *eGFP* as a control treatment. Plants were grown for 5 days before leaves were harvested (**A**) and extracted with methanol. **B**: These extracts were analyzed with high-resolution LC-qTOF-MS-MS operating in positive ionization mode and the relative abundances of the features were compared. The volcano plot visualizes the metabolic differences, where the dark blue color marks features that accumulate in *CYP79A206* overexpressing plants, whereas the dots of light blue color represent down-regulated features as compared to control treatment (fold change >2, $p < 0.05$, $n=4$). **C**: Furthermore, targeted LC-MS/MS was performed for some metabolites of interest. Statistical analysis via Student's t-test or Mann-Whitney Rank Sum Test (JA-Ile), * = $p < 0.05$, $n = 4$, n.s.: not significant, cps: counts per second.

Methods Figure S2: *Nicotiana benthamiana* plants were grown and transformed as described in Irmisch et al., 2013 and **manuscript II**. Briefly, the coding region of *CYP79A206* was cloned into a suitable vector, *Agrobacterium tumefaciens* strain was transformed with either this or an *eGFP* construct. For the *N. benthamiana* transformation, transformed *A. tumefaciens* were grown in liquid culture, and the cells harvested and resuspended in infiltration buffer before four leaves of each 3-week-old *N. benthamiana* plant were transformed by syringe infiltration with the respective bacteria. Leaves were harvested five days after transformation, pooled for each plant and grinded in liquid nitrogen. As described in **manuscript II**, 100 mg leaf powder were extracted with 1 mL MeOH containing internal isotopically-labeled phytohormone standards by mixing and subsequent removal of the solid particles by centrifugation. Untargeted metabolomics was performed as described in **manuscript II** and Rizwan et

al. (2021) whereas targeted metabolite analysis was performed according to **manuscript I** (phytohormones and amino acids). Data for the volcano plot were calculated with R using the package MetaboAnalyst (Pang et al., 2021) and Pareto scaling after preprocessing the data with MetaboScape (Bruker Daltonics). The results of the statistical analysis were visualized with OriginPro, Version 2019.